Monkey Hear: A Morphometric Analysis of the Primate Auditory Ossicles

By

Yasmin Carter

A Thesis Submitted to the Faculty of Graduate Studies,

University of Manitoba

In partial fulfilment of the degree

MASTER OF ARTS

Department of Anthropology

University of Manitoba

Winnipeg

THE UNIVERSITY OF MANITOBA

FACULTY OF GRADUATE STUDIES

*****

COPYRIGHT PERMISSION

Monkey Hear: A Morphometric Analysis of the Primate Auditory Ossicles

BY

Yasmin Carter

A Thesis/Practicum submitted to the Faculty of Graduate Studies of The University of Manitoba in partial fulfillment of the requirement of the degree

MASTER OF ARTS

ABSTRACT

Hearing plays a vital role in the life of primates and an understanding of the anatomy of the auditory ossicles is necessary for analyses of hearing sensitivity. Morphometric studies conducted on the auditory ossicles of primates are rare and those few have tended towards simple magnitude and anatomical length measures. To address this issue, a landmark analysis based on Schmidt *et al.* (2009) was conducted on ultra-high resolution computer tomography (UhrCT) scans of twenty-six primate auditory ossicle chains. The resulting data were subjected to Euclidean distance matrix analyses (EDMA) in order to discuss differences between morphology between the species represented. A percussive forager, *Daubentonia,* was included to investigate whether its unique 'hunting' style affected its ossicular morphology. Two representatives of the non-primate family Cynocephalidae were also included as an outgroup to the primates in order to provide a non-primate comparison for the morphometric and taxonomic analyses.

The results of these investigations demonstrate that the greatest variable in ossicle morphology is size. In the shape analyses, the greatest differences occurred between the landmarks measuring the maximum length of the malleus, the maximum length of the incus and the maximum width of the ossicular chain bodies. The haplorrhine–strepsirrhine split is well reflected in ossicle morphology. Clustering into biological families was strong and the scaled data reflected the accepted taxonomy, although the hierarchy within families tended to be out of order compared to the cladogram. The results of the cluster analyses indicate that although diet and activity patterns may be relevant when discussing the morphology of a specific species, the grouping is not strong enough to suggest that these patterns are an important factor in adaptation. The auditory ossicles of the percussive forager are unusual in form and are the largest of all the

species represented. *Daubentonia*'s unique method of 'hunting' would seem a likely cause of the outstanding shape differences, although this remains impossible to prove with out further study. The Cynocephalidae have a unique ossicular morphology within the context of this study. Morphological evaluation of the Cynocephalidae auditory ossicles demonstrates a lack of concordance with the majority of phylogenetic hypotheses and highlights the issues with using cluster analyses to make phylogenetic-morphological assumptions. The EDMA method provided unanticipated information regarding the articulation angles of the ossicular chains, particularly that of *V.v. variegata*. The results provided by this study present opportunities for future research and suggest many new questions on the morphology of primate auditory ossicles.

ACKNOWLEDGEMENTS

This thesis would not have been possible without the guidance, support and patience of my committee: Dr Rob Hoppa, Dr Mary Silcox and Dr Tom Klonisch. Special thanks go to Dr Robert Hoppa, for being more than an advisor but a mentor who has taught me to prioritise the important things in my life. All that I am as an academic and in the future, a teacher, is a reflection of you. I hope to do you proud. My sincere gratitude goes to Dr Mary Silcox without whom this study would not have been possible; I am forever indebted to her for sharing her research, her inspiration and her ears. Challenging me to try the untested path and her continued support when I stumbled. I would also like to thank Jodie Schmidt for assistance and advice on landmarks. My sincerest thanks to Heather and Lynne for listening to my rants and rambles, providing advice, support and a heads up every time there was free food. Without them not only would the department cease to function but I would have too. Dr Valerie DeLeon for providing moral support, as well as insightful and inspiring comments pulling me through the quagmire of Euclidean distance matrix analyses. Any and all mistakes are my own doing. I am grateful to my fellow students who took time out of their own busy lives for chats and encouragement. Their willingness to share their invaluable knowledge and experience made this journey easier. Lastly I dedicate this work to my family Georgena, Peter and Elaine we share more than a last name, we share a belief in the power of our dreams. Thank you for your support and for teaching me that anything is possible if you take it in bite size pieces.

I gratefully acknowledge the financial support of the Canadian Research Chairs program, the Manitoba Graduate Scholarship, the Anthony Arnhold Fellowship and the University of Manitoba Department of Anthropology.

Table of Contents

LIST OF TABLES

LIST OF FIGURES

CHAPTER I – INTRODUCTION

Hearing, as one of the five senses, is vital to the life of any animal, playing a role in communication, predator detection, as well as sourcing prey for omnivores and carnivores. As an integral part of the auditory system, the ossicular chain of primates has received much study focusing mainly on human evolution, functional analyses and to a lesser degree variation and morphometrics. The precise nature of the function and movement of these three tiny bones is as yet undefined. The introductions of relatively recent technology to the field, including computed tomography, with resolution sufficient to view the auditory structures, allow a return to the anatomical foundations of functional and evolutionary studies. This in turn allows examination of the tiny bones of a number of species for variation and similarities, which may suggest common descent or adaptation. It is this opportunity that has led to the current study.

Analyses of the morphology of non-human primate auditory ossicles are rare but not without precedent and this current work builds largely on the studies of Masali and colleagues (e.g. Masali, 1964; Masali and Chiarelli, 1967; Masali, 1968; Masali, 1968; Masali, 1971; Siori and Masali, 1983; Masali 1992; Masali *et al.*, 1992). Previous morphometric studies have mainly been restricted to simple measurements such as anatomically relevant lengths and weights, largely due to constraints placed by the bones themselves, they are small as well as notoriously difficult to recover and measure. The current study is freed, to an extent, from these restrictions by the use of ultra-high resolution computed tomography (UhrCT) of *in situ* ossicular chains.

The current study has four main goals. First, to evaluate and validate the methodological frameworks specifically used for the measurement of primate auditory ossicles set out by

Schmidt *et al.* (2009). Second, to use the data gained to determine if there are any measurable differences in auditory ossicle morphology between primates at the suborder, family and species level. The third aim was to examine *Daubentonia madagascariensis* to determine what, if any, variation exists between percussive and non-percussive foragers, as percussive foragers have a unique 'hunting' style, which relies to an extent on hearing. The final goal focused on the inclusion of representatives of the order Dermoptera, specifically *C. volans* and *G. variegatus*. The Dermoptera specimens are the only non-primates in the study and they were included as an outgroup to the primates in order to provide a comparison for the morphometric and taxonomic analyses. Finally, the study conducted hierarchical analyses and compared the resulting phenograms, based on ossicular morphology to the currently accepted phylogeny.

The second chapter provides an overview of the functional anatomy of the primate auditory system with emphasis on the development and structure of the ossicles. A discussion of previous studies conducted on the auditory region is included, focusing on mechanics, evolution and functional analyses as well as morphometrics and variation. The debates surrounding the species of Dermoptera and *Daubentonia* are considered as well as their importance in this study. The third chapter outlines the materials and techniques used in the study as well as the approach taken. The first section gives a brief summary of the non-human primate sample set as well as the imaging and post-processing techniques used to generate the data. In the discussion of data collection and landmarking, the intra-observer error study is outlined along with the techniques used in the full morphometric analysis. The choices of data analysis are considered and a discussion of the methods used to explore and test the results follows.

The fourth chapter reviews the results of the intra-observer error trial before exploring the results of the morphometric analysis including the principal coordinate, cluster and phylogenetic

analyses. The fifth chapter discusses the implications of the study and examines the auditory ossicle morphology evidence for non-human primate taxonomy. The sixth chapter discusses the conclusions that can be drawn from the study and outlines possible directions for future studies.

CHAPTER II – LITERATURE REVIEW

Introduction

Most studies of mammalian and primate ossicles tend to focus solely on case studies rather than broader taxonomic trends or themes. This chapter brings together our current knowledge and provides a background to the study of the primate auditory structures, specifically the ossicles. The history of the study of the auditory system will be presented, as well as a description of the function of the outer, middle and inner ear anatomy with particular focus on the ossicles as well as potential problems. Modelling and prediction of the mechanics of the auditory system will be discussed as well as the potential for understanding primate hearing. The ossicle's place in evolutionary and comparative anatomy research is also reviewed. Finally, previous research on ossicle morphology, metrics and variation is discussed.

Functional Anatomy

The following sections present an overview of the auditory system of primates where possible and more generally the mammalian system where not. The ear is comprised of a series of complex structures each playing their role in the conduction of sound. To understand changes in the morphology of the auditory ossicles their place in the wider context of auditory functional anatomy must first be determined. The function of the mammalian external and middle ears appear quantitatively similar. The external ear collects sound in the form of pressure waves and transfers the collected waves to the middle ear. The middle ear then transmits this power to the inner ear via the motion of the tympanic membrane and auditory ossicles (Rosowski, 1994). The main inter-specific differences then, lie in morphology rather than function.

The Outer Ear

The outer ears of primates demonstrate considerable diversity in both mobility and morphology, which frequently follows phylogenetic patterns (Coleman and Ross, 2004). The outer ear is unique to mammals and can be broken into primary subdivisions of: the pinna flange (also called the auricle), the concha and the external auditory meatus (EAM), although the transition between these divisions may not be as obvious in other mammals as it is in primates (Shaw, 1974).

The pinna flange or 'ear' is the cartilaginous and sometimes mobile, flap-like soft tissue structure that protrudes from the head. In humans, the pinna flange is separated into the helix, tragus and lobule as well as a varying number of folds and furrows (Figure 2.1). Primate pinnae are highly variable in size and complexity (Coleman, 2007).

Figure 2.1 - Photo of human outer ear labeled with terminology

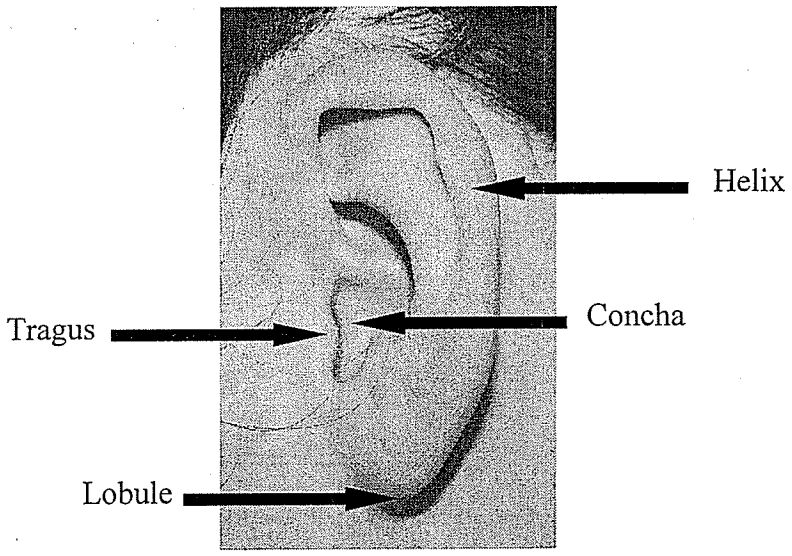

Although little is known about sexual dimorphism in pinnae size, in humans there is a 9% difference in linear dimensions roughly paralleling total body size dimorphism (Shaw, 1974). An index of ear size versus head size was calculated for over one hundred primate species by Schultz (1969; 1973), who found the majority of prosimians have relatively larger pinnae than all anthropoids. The degree of pinnae movement appears to be correlated with the development of the outer ear musculature, which follows similar phylogenetic patterns as differences in the overall morphology of the outer ear. There also appears to be a gradual decrease in the differentiation and development of intrinsic and extrinsic musculature as one proceeds from prosimians to hominids (Coleman, 2007).

The concha is a funnel-like structure that connects the opening of the pinna flange to the narrower external auditory meatus (Rosowski, 1994). Although it is often included in the literature as part of the pinna flange, they are anatomically separate structures and appear to have differing functional qualities (Dallos, 1973). The external auditory meatus, commonly known as the 'ear canal,' is a tubular structure that provides restricted entrance to the middle ear, serving to protect it from external injury whilst still allowing the conduction of sound waves (Rosowski, 1994). Extant primates have an EAM that consists of a medial bony section and a lateral cartilaginous section with inter-specific variations of the ratio of each. The EAM of ceboids, lemuroids and most lorisoids are almost entirely cartilaginous, while that of cercopithecoids, tarsoids and hominoids are comprised mostly of bone (Coleman and Ross, 2004). In humans the EAM is approximately 30mm long with a diameter of 7mm (Dallos, 1973). In mammals the EAM is terminated by the middle ear border, consisting of the tympanic membrane (Rosowski, 1994).

The Middle Ear

The relationship between middle ear structure and performance is not completely understood, however, the main function of the middle ear appears to be to translate vibrations passed from the outer ear into pressure waves in the fluid-filled inner ear, while matching impedances between this fluid and the air. The architecture of the middle ear therefore can be assumed to reflect this purpose (Wilson, 1987).

Located within the air-filled tympanic cavity, the middle ear system of terrestrial mammals is composed of several basic elements. Firstly, the tympanic membrane for reception of sound, three ossicles coupled and supported by various ligaments, the Eustachian tube to and to equalise pressure in the cavity and the middle ear muscles that tense the tympanic membrane and ossicular chain resulting in alterations in the sound transmission (Amin and Tucker, 2006).

The tympanic cavity extends from the termination of the EAM on its lateral border to the bony cochlear wall on its medial extreme. It communicates with the inner ear via two openings in the bony wall: the oval window (*fenestra ovalis*) and the round window (*fenestra rotunda*). The Eustachian tube merges with the nasopharynx, remaining closed except during swallowing or yawning (Dallos, 1973). The bones that surround the cavity come from as many as eight different sources including the: petrosal, squamosal, ectotympanic and entotympanic (Rosowski, 1994). The floor of the tympanic cavity is unique in extant primates, in that it is almost exclusively composed by the petrosal element of the temporal bone. The rigidity this provides prevents adjacent soft-tissue structures from compressing the cavity during head movements such as mastication, which may alter sound transmission and therefore acoustic properties (Henson, 1974).

The morphology of the tympanic membrane and auditory ossicles vary greatly amongst species as do the volume, structure and number of compartments of the tympanic cavity, as well as the relative dimensions of the middle ear muscles. No correlation is apparent between the areas of the middle ear and hearing thresholds (Rosowski, 1994). Studying the inter-specific variation of the placental mammal middle ear, Nummela (1995) showed that overall middle ear size is negatively allometric to skull size. The middle ear structures, however, scale isometrically with each other thorough a wide range of species (Hemilä *et al.*, 1995). Generally the linear dimensions of the ossicles vary with body size, the larger the mammal the larger the ossicles.This scaling is not universal, however, and some mammals such as the golden cape mole have prodigious ossicles compared to their body size (Rosowski, 1994).

Soft Tissue

The soft tissue component of the primate middle ear comprises two intratympanic muscles and numerous ligaments (Hüttenbrink, 1992). The internal carotid artery and numerous nerves also commonly course through the middle ear region (Coleman, 2007). The entire ossicular chain is covered in a mucosal lining of the same type that lines the walls of the tympanic cavity (Dallos, 1973). The middle ear contains two muscles: the *tensor tympani* and the *stapedius*, the function of which can be interpreted as preserving the intact cartilage of the ossicular joints (Hüttenbrink, 1992). In anthropoids and strepsirrhines, the stapedius muscle arises from a sulcus or canal in the posterior wall of the middle ear cavity, while in tarsiers and tree shrews the muscle originates outside the tympanic cavity on the side of the skull (MacPhee, 1981). Both muscles are of the striated pinnate type, highly enervated, generating substantial tension with minimal displacement. These muscles are the effectors of the middle ear muscle reflex, which forms one of the vital auditory feedback mechanisms (Dallos, 1973). When contracted the stapedius pulls the head of the stapes posteriorly, almost at right angles to the

ossicular plane of rotation. The *tensor tympani*, the larger of the two, draws on the manubrium of the malleus anteriomedially, again roughly perpendicular to the plane of rotation (Dallos, 1973). Even though they are functionally synergists, the two muscles exert their force in opposing directions acting as anatomical antagonists (Fleischer, 1978).

Contraction of both these muscles results in stiffening of the ossicular chain, the exact purpose of which is debated. Dallos (1973) proposes that this stiffening results in a decrease in low-frequency sensitivity while providing a slight, less than 10dB, increase in the mid- to high-ranges. The contraction of these muscles usually occurs at higher sound pressures, with many advocating a protective mechanism to the stiffening, Fleischer (1978) disagrees with this hypothesis noting that a number of biological arguments can be made against this theory. Firstly, by the time the muscles react to the loud sound it has already occurred and the damage has been done. It is also difficult to imagine a typical situation where a primate would require such protection against excessive noise. Loud noises over 120dB are rare in nature and occur more commonly in recent industrialised human societies, hardly likely to have led to the evolution of a protective mechanism.

In humans the ossicular chain is suspended within the middle ear cavity by five ligaments, the number and morphology of which vary between primate species, although with similar functions. Three of these attach to the malleus, one to the incus and one, the so-called annular ligament, fixes the stapedial footplate to the oval window (Dallos, 1973).

The lateral border of the middle ear is comprised of the tympanic membrane (*membrana tympani*), commonly called the 'ear drum.' This cone-shaped membrane is attached to the ectotympanic ring by its own fibrous border, the annulus, either on the inner border of the *sulcus*

tympanicus or its medial crest (*crista tympanica*) (Dallos, 1973). The outermost ossicle, the malleus, attaches to the apex of the tympanic membrane known as the *umbo*. The membrane is comprised of three layers; the outermost layer is continuous with the lining of the EAM, while the innermost is continuous with the lining of the tympanic cavity (Dallos, 1973). The middle layer consists of two groups of fibres, one radially orientated and the other concentrically arranged. These fibres result in the majority of the membrane being taut, giving its characteristic shape and structural stability, and consequently are named the *pars tensa* (Coleman, 2007). Helmholtz (1885) in his work on hearing proposed that the tympanic membrane is curved so that, when straightened, the fibres could force the *umbo* to move against a large force and therefore magnify small acoustic pressures sufficiently to displace the ossicles.

The Ossicles

The ossicular chain is comprised of three bones: the malleus, incus and stapes (Figure 2.2). This chain links the tympanic membrane with the inner ear. Together these bones form a functional unit with the joints between adjacent bones being relatively firm. In some mammals, notably the chinchilla and house mouse, the malleus and incus are so tightly bound as to appear fused (Rosowski, 1994). The ossicle joints are unique as they are constantly in motion and cannot be voluntarily controlled (Masali and Cremasco, 2006). With the exception of the stapes, these skeletal elements are unique to mammals and derive from the first branchial arches (Amin and Tucker, 2006).

Figure 2.2 - Diagram of Auditory Ossicle Chain terminology (*Loris tardigradus* pictured)

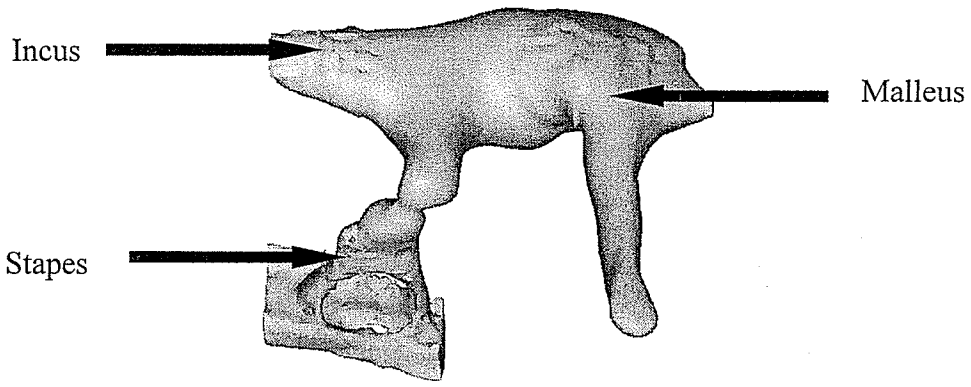

Early anatomical knowledge of the organisation of the ear was limited to those structures that were readily visible. According to O'Malley and Clarke (1961), Allessandro Achillini first noticed the presence of the bones of the human middle ear in the second half of the fifteenth century. It was not until the publication of *The Fabrica* by Vesalius of Padua in 1543, however, that the malleus and incus were identified and named for the first time. The discovery of the stapes is generally attributed to Giovanni Filippo Ingrassia of Naples. Cassebohm, in 1730 was probably the first to take measurements of the ossicles. Carus (1818) and Meckel (1821) studied the embryology and comparative anatomy of the auditory ossicles in the early nineteenth century (Arensburg *et al.*, 1981). The study of ossicle development and embryology was taken up again in the early twentieth century, and detailed descriptions of numerous species including primates soon followed. The literature now contains a solid description of the ear morphology of most major taxonomic groups (Hyrtl, 1845; Doran, 1878; Parker, 1886; van Kampen, 1905; Cockerell

et al., 1913; Schultz, 1969; Hinchcliffe and Pye, 1969; Lay, 1972; Fleischer, 1973; 1978; Henson, 1974; Hershkovitz, 1974; 1977; Hunt and Korth, 1980).

The primate malleus (Figure 2.3) is the largest and most external of the ossicles, consisting of a head (*capitulum mallei*), three processes: the manubrium (*manubrium mallei*), the anterior process (*processus gracilis*), the lateral or short process (*processus brevis*) and sometimes a neck (*collum mallei*). It is commonly referred to as the 'hammer' (Dallos, 1973).

Figure 2.3 - Diagram of malleus terminology (*Macaca nigra* 1 - LACM 90765 pictured. Illustration by Yasmin Carter)

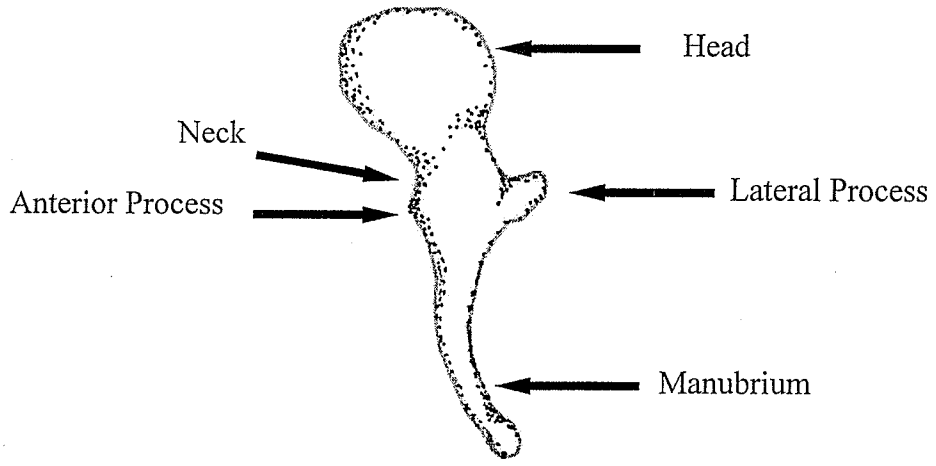

The head of the malleus is enlarged and rounded and incorporates the articular surface that connects with the matching facet of the incus, forming the stiff malleoincudal joint (Dallos, 1973). The articular surface is commonly divided into a pair of medial and lateral facets, separated by a small ridge. The malleus attaches to the umbo via the manubrium, commonly known as the handle. Excluding humans and most hylobatids, many primates have a short

tubercle situated midway along the manubrium for attachment of the tensor tympani muscle (Coleman, 2007). The head is connected to the roof of the tympanic cavity by the delicate superior ligament (Dallos, 1973).

All catarrhines and some prosimians posses a constricted area of the manubrium located between the head and lateral process known as the neck (Coleman, 2007). The neck is absent in nearly all platyrrhines, except for a few species of *Callithrix*, who also demonstrate a spherical protuberance (*orbicular apophysis*), on the posterior side of the manubrium, which is rare in primates but commonly seen in bats, rodents, marsupials and insectivores (Hershkovitz, 1977).

Manifest in all primates, the anterior process extends anteriorly from the inferior angle of the head, providing attachment for the anterior ligament (Dallos, 1973). The anterior process is one of the most variable ossicular structures. In humans, the adult form is a small tubercle; in children it is a longer process, which may even form a short synarthrosis with the tympanic bone. The most prominent anterior process seems to occur in bats and shrews. In non-human primates the anterior process varies from a small tubercle to nearly absent (Rosowski, 1994). Associated with variations in the prominence of the anterior process are variations in the orientation of the manubrium relative to the horizontal plane and the long crus of the incus, known as the axis angle (Fleischer, 1973; 1978). In mammalian species with a reduced anterior process, the manubrium and long process of the incus are nearly parallel and both are perpendicular to the horizontal plane (Rosowski, 1994). Fleischer (1978) proposed that the anterior process is a distinguishing functional feature, since mammals with prominent anterior processes tend to be insensitive to sounds below 1kHz and more sensitive to sounds at higher frequencies. Projecting from the root of the manubrium, the lateral process is absent in all platyrrhines but well

developed in prosimians and catarrhines, reaching its maximum development in hominoids (Hershkovitz, 1977)

Intermediately positioned, the incus (Figure 2.4) is comprised of a body (*corpus incudis*) and two crura (processes): the long crus (*crus longum*) and the short crus (*crus breve*) (Dallos, 1973). The body bears the medial and lateral facets for articulation with the malleus. The articular surfaces of the malleoincudal joint are complex and best described as saddle-shaped (Wever and Lawrence, 1954). In the few primates examined this joint appears to be of the synovial variety (Hinchcliffe and Pye, 1969).

Figure 2.4 - Diagram of incus terminology (*Macaca nigra* 1 - LACM 90765 pictured. Illustration by Yasmin Carter)

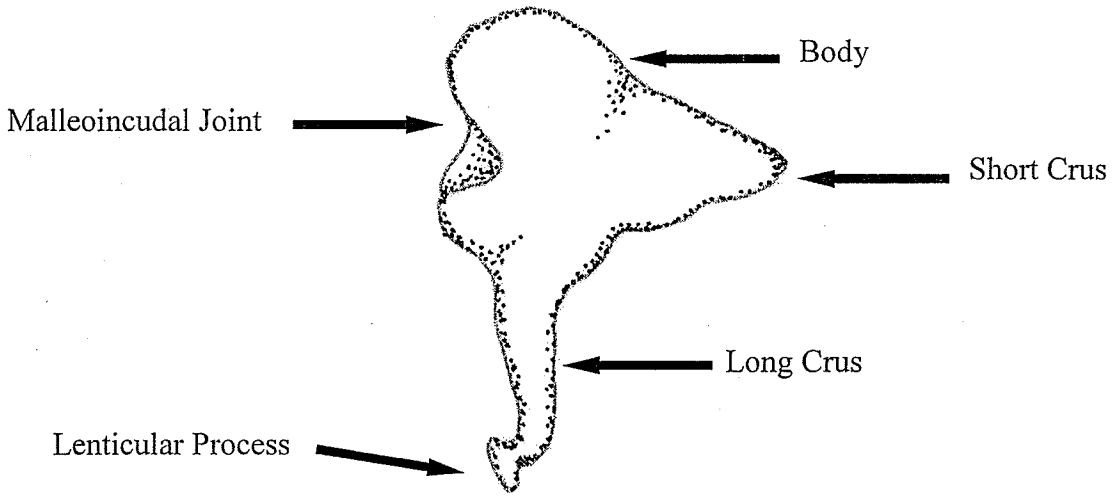

The two crura emerge from the body at approximately right angles and vary as much in function as morphology (Coleman, 2007). The short crus is conical in shape and is anchored in the tympanic cavity by the posterior incudal ligament (Dallos, 1973). Parallel to the manubrium of the malleus is the long crus. It is generally slightly longer and has a slender profile. The long crus

may be grooved along its length by the *sulcus incudis*, and terminates at the inferior extremity in a globular projection, the lenticular process (*processus lenticularis*) (Coleman, 2007). The lenticular process articulates with the stapes in the ball and socket-like incudostapedial joint, which also appears to be of the synovial type (Hinchcliffe and Pye, 1969), although in other mammal species with increased sound frequency sensitivity, such as bats, this joint is fibrous (Lombard and Hetherington, 1993).

The most medial bone in the ossicular chain, the stapes (Figure 2.5) is also the smallest bone in the body and consists of a head (*caput stapedis*), a neck, and two crura: anterior (*crus anterius)* and posterior (*crus posterius*) as well as a footplate (*basis stapedis*) (Dallos, 1973). The head of the stapes articulates laterally with the lenticular process of the incus and is medially constricted to form a neck (Dallos, 1973). Diverging from the neck, the crura are normally hollow and connect at their medial extremities to the footplate (Dallos, 1973). The bifurcating crura of the stapes produce the intercrural or obturator stapedial foramen. In species where the adult individual lacks a stapedial artery, this foramen may be obstructed along the dorsal aspect by a thin lamina of bone (Coleman, 2007).

The oval-shaped footplate is fixed along its circumference into the oval window by the annular ligament, a belt of radially orientated fibres, creating the stapediovestibular joint (Coleman, 2007). No vessels of any kind enter the shafts of the crura or the central region of the footplate (Rosowski, 1994). Together these bones form a vital part of the auditory system, changes in one component can lead to changes in its overall efficiency (Matshes *et al.*, 2004).

Figure 2. 5 - Diagram of stapes terminology (*Macaca nigra* 1 - LACM 90765 pictured. Illustration by Yasmin Carter)

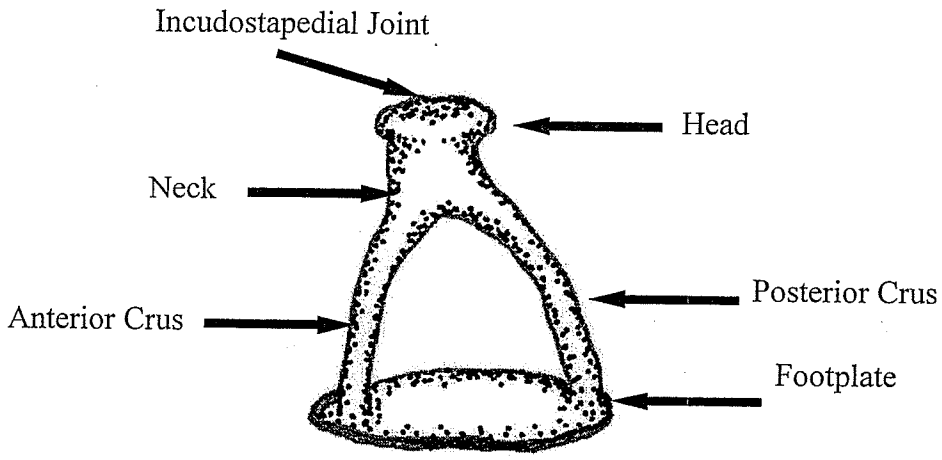

Studies of the embryological development of the primate auditory ossicles tend to focus on a single species e.g. humans (O'Rahilly, 1983) or macaques (Wilson *et al.*, 1975) and a number of these studies result from examinations of tetragenic effects on embryological development and staging (Newman and Hendrickx, 1981; Merker *et al.*, 1988). Inferences on auditory ossicle development in non-human primates can be reliably based on human studies (O'Rahilly, 1983). Ossification of the auditive chain begins in the fourteenth week intrauterine via a primary centre located in the long process. Malleal endochondral ossification begins at sixteen weeks, and the stapes between the eighteenth and nineteenth week (Whyte *et al.*, 2008). The ossicular joints express defined characteristics during the twentieth week intrauterine but with limited mobility, mostly as a reaction to swallowing (Whyte *et al.*, 2002). Research by Olszewski (1990) demonstrated that development of the human auditory ossicles is not completed during foetal life as previously believed (Heron 1923; Bouchet and Giraud, 1968; Masali and Cremasco, 2006), but during the fourth year post-natal. The stapes undergoes an erosive thinning process and a loss of substance shortly after its ossification, so that the adult stapes in thinner and more gracile that

the neonatal bone (Qvist and Grøntved, 2000). *Macaca* ossicles were found to experience changes in weight, becoming heavier after birth (Parzek and Varacka, 1967).

There has been little examination in the literature of the microstructure of non-human primate auditory ossicles. It can, however, be said that they demonstrate great diversity of bone density (Sarrat *et al.*, 1992). Again, to use the human ossicles as the exemplar, they are histomorphologically unique compared to other human lamellar bone. They are almost completely solid (Walker *et al.*, 2006), although finite element analysis has demonstrated that the ossicles can be treated as rigid bodies only in a restricted frequency range from 0 to 3.5 Hz (Beer *et al.*, 1999).

In any dynamic system, such as exists within the ossicular chain, the organisation of the microarchitecture of the trabeculae is not random but is arranged along 'force lines,' to transmit pressures and tractions better (Whyte *et al.*, 2008). The human malleus is a compact bone, covered by a thick layer of hyaline cartilage. The head consists of dense bone, with tight lamellae and small lacunae, haversian canals and resorption spaces (Sarrat *et al.*, 1992). The neck demonstrates a high condensation of fuchsinophil lamellae bundles, which extend to the manubrium. The manubrium has a lamellae structure, with three dense areas of force transmission. The osseous structure becomes weaker, towards the end of the manubrium becoming almost completely cartilaginous (Sarrat *et al.*, 1992).

The incus is also covered with a thick cartilaginous layer. In the body, lamellar bone bundles point towards the long crus and concentrate in the lenticular process. The short crus consists of less compact bone with a significant number of cartilaginous inlets (Sarrat *et al.*, 1992). The stapes is a frangible bone, with the head and tips of the crura the most compact structures. The

head demonstrates large lacunae with lamellar bone bundles originating there, passing through the crura and terminating at the footplate (Sarrat *et al.*, 1992). The footplate consists of a thin and irregular layer of compact osseous tissue, covered on the vestibular side with cartilage. Due to its fragility, the footplate is highly susceptible to pathological conditions, which may alter, calcify and thicken or even completely obliterate the plate (Wever and Lawrence, 1954).

Burkert *et al.* (2002) used scanning acoustic microscopy (SAM) for quantitative examinations of the micro-mechanical properties of human auditory ossicles. They found statistically significant differences in the acoustic impedance within the discrete ossicles as well as between regions within individual ossicles, agreeing with the results of previous histological studies of force lines by Sarrat *et al.* (1992). Overall the ossicles consist of compact bone with some cavitations, few vascular channels, no real identifiable secondary osteons and eventual cartilaginous nodules. The degree of cavitation differs greatly between specimens, while bone lacunae increase with age (Sarrat *et al.*, 1992).

The majority of auditory research refers to typical or standard ossicles without considering morphological variation or damage in individual specimens. Deformities of the ossicle chain are very rare and human congenital ossicular abnormalities have a suggested incidence of less than one per 15,000 births (Raveh et al., 2002). Changes observed in the auditory ossicles can be divided into two categories: destructive and articular. Destructive alterations include and micro- or macroscopic modification of a destructive nature. Articular alterations are defined as aberrant arrangements of the articular elements of the ossicular chain (Mutaw, 1986). Common ossicular anomalies of the malleus include: fusion of the malleoincudal joint, deformation of the head, tripartite union of the manubrium with the long crus of the incus and the head of the stapes and complete absence. Incudal anomalies commonly include: fibrous union of the incudostapedial

joint either bony or fibrous, absence of the incudostapedial joint, shortening or malformation of the long crus, bony fusion of the short crus to the tympanic cavity wall and absence. The most common change is stapedial footplate fixation. Also common are fusion of the stapedial head to the promontory, absence of the head of crura, small or foetal form and complete absence (Lindsay, 1971).

These changes are caused by many factors including pathology, mechanical damage, congenital defects and anatomical variation. Little research has been conducted on these factors in nonhuman primates so it is difficult to judge the level of impact they will have on this study. Being such frangible bones, alteration of the ossicles can easily result from taphonomic changes as well as rough handling during the collection phase (Hüttenbrink, 1992).

Examples of nonhuman primate middle ear disease are rare in the literature. Most paleoanthropological studies are case reports, written when an aberrant specimen was chanced upon (Spoor *et al.*, 1998; Quam and Rak, 2008). A few larger studies of pathological changes have been conducted on archaeological populations (Holzheuter *et al.*, 1965; Birkby and Gregg, 1975; Mutaw, 1988; Bruintjes, 1990; Arensburg *et al.*, 2005; Flohr and Schultz, 2007; Qvist and Grøntved, 2000) and the vast majority on modern humans from a medical and surgical perspective on deafness (see Wever and Lawrence, 1954 for a comprehensive overview).

Notwithstanding the effects of pathology, the ossicles were thought not to change significantly during life (Masali and Cremasco, 2006). Recent research by Lannigan *et al.* (1993; 1995) demonstrated erosive resorptive changes in the human incus throughout life in a symmetrically and possibly sex-related way, contrary to studies by Anson and Bast (1959) who found remodelling of the incus to normalise with deposition equal to the resorption rate. These changes

appear frequently in histological examinations of the long crus with depressions visible in a study by Ghorayeb and Graham (1978) in 81.2% of the samples. Lannigan *et al.* suggest mechanical fatigue as a contributing factor. Possible destructive alterations caused by biomechanical stress may be confused with pathologies but other than confusion of etiology, appear to have little to no effect on hearing (Ghorayeb and Graham, 1978).

Congenital ossicular disruption is common and well examined in humans although differentiation of genetically determined changes from those with an acquired congenital origin presents difficulty (Raveh *et al.*, 2002). One of the most common congenital defects after footplate fixation, is absence of either the oval or round windows (Richardson *et al.*, 1997).

Anatomical variations in humans are common and it is important to note that they may also occur in nonhuman primates. One of the most common variations is a change in the inclination angle of the malleal head and neck in relation to the manubrium. This angle is also used in discussions of the effect of bipedalism on the basicranial morphometry (Sarrat *et al.*, 1988). Ageing may also be a factor, with ossification of ligaments and resorption of bone. In older *Lemur* specimens, the annulus membrane may become ossified so that the tympanic ring is attached to the bulla by bone instead of cartilage, as well as changing morphology these anomalies may also have effected hearing (Cartmill, 1975).

The relative frequencies of middle ear damage are unknown; a radiologic analysis of an archaeological population by Gregg *et al.* (1965) showed that 50% of Native American crania had evidence of middle ear and mastoid damage. Guild (1944) found the clinical incidence of stapedial footplate fixation among Caucasians to average 1%, Dalby *et al.* (1993) concurs with an incidence finding of 0.9%. Congenital bony fixation of the malleus occurs at a rate of 1.4%

(Subotic *et al.* 1998). The effects of these bony changes on hearing sensitivity remain unresolved. In many human hearing disorders the malleus and incus are malformed and/or fused, yet animals such as the chinchilla have very sensitive hearing while their malleoincudal joint have coalesced (Amin and Tucker, 2006). Even when ossicular conduction is impaired, sound can still be passed directly to the cochlea via sound-induced vibration of the skull (Wilson, 1987).

The Inner Ear

The vibrations of the medially located stapes are delivered to the inner ear, also called the vestibulocochlear organ, via the oval window (Dallos, 1973). Housed within the petrosal or petrous portion of the temporal bone, the inner ear is comprised of three main structures: the vestibule, the cochlear portion and the semi-circular canals (Rosowski, 1994).

The structures related to hearing are confined to the spiral-shaped cochlea. The cochlea is divided into three sub-compartments by the membranous cochlear duct: the *scala tympani*, the *scala vestibuli* and the *scala media* (Coleman, 2007). The size of the cochlea demonstrates only a loose relationship with the overall size of the individual animal (Wysocki, 2001). Within the cochlea the perilymph (extracellular fluid) transfers the vibrations to the cilia resulting in electrical stimulus to the brain; sound perception is a neurological event (Wever and Lawrence, 1954).

The auditory apparatus of primates is a complex system that selectively transfers acoustical input into nerve impulse output. In its performance of this function the entire auditory periphery is constrained by the size and structure of its varying components. Specialisations for a particular hearing pattern are likely to be reflected in all three regions of the ear (Coleman, 2007).

Although few specifics are completely understood, two key conventions can be acknowledged: ears that seem best at transferring high-frequency sound energy tend to be small and stiff, those that perform better at transferring low-frequencies are larger and more flexible (Coleman and Ross, 2004).

Mechanics

This section examines the biomechanical operation of the ear. Firstly considering the mechanical theories used to explain and predict how the ossicles move, and secondly, how these mechanical theories can be used to model sound sensitivity, frequency and levels.

The function of the auditory system can be viewed as a cascade of interdependent acoustical and mechanical processes, with outputs that act as inputs to the subsequent stages (Rosowski, 1994). Input to the first stage, the outer ear, is a uniform plane wave of sound pressure. The pressure and volume velocity at the entrance of the external auditory meatus are transformed by the EAM into a pressure and volume velocity at the tympanic membrane. The membrane then transfers these units into a force on and subsequent movement of the manubrium of the malleus. The middle ear ossicular system converts motions of the umbo into motions of the stapes (Rosowski, 1994).

This transformation from acoustic variables (pressure and volume) to mechanical variables (force and velocity) can be mathematically approximated to create bivariate plots of threshold values known as audiograms, with frequency measured in hertz (Hz) and amplitude in decibels (dB) (Wever and Lawrence, 1954). Discussion of the auditory mechanics of the outer and inner ears in the academic literature are vast and will be discussed only briefly, as emphasis is placed on the middle ear.

Soon after the auditory structures were first discovered and described, mechanical engineering theory was applied in order to understand the movements of the various components and the forces generated during this process (Wever and Lawrence, 1954). The arrangement and degree of flexibility of the middle ear is thought to affect the hearing range. Fleischer (1973; 1978) proposed three classifications of mammalian middle ear types based on this degree of stiffness: the microtype, the transitional type and the freely-mobile type. The microtype is characterised by a malleus that is fused to the tympanic bone via the gonial process resulting in high torsional stiffness. This type is restricted to small mammals including bats, shrews and many rodents, although possibly several species of the primate *Callithrix* may be placed in this category due to the presence of an *orbicular apophysis* (Hershkovitz, 1977). Fleischer advocated that the microtype is most similar to the 'ancestral type,' which will be discussed later.

The transitional type has an intermediate degree of torsional stiffness. This type is commonly found in horses, cats, squirrels, tree shrews and some galagos (Fleischer, 1978). At the far end of the spectrum is the freely-mobile type. Humans and some simians, including *Pan* and *Macaca* have a freely mobile middle ear whereby the malleus is not fixed in place to the tympanic ring but instead is linked to the tympanic membrane via a ligament and the centre of mass generally coincides with the rotational axis (Amin and Tucker, 2006).

Fleischer (1978) suggests that the type of ear is representative of the overall hearing capacity, with the microtype found in taxa with exceptional high-frequency sensitivity, for example bats. While the freely-mobile type is found in taxa with expanded low-frequency sensitivity, like the simian primates. Research by Rosowski (1992) into species representing the three ear types demonstrates significant differences in high- and low- frequency sensitivity between the types,

although with some considerable overlap. This research also supported Fleischer's hypothesis that the microtype represents the ancestral pattern.

The transmission of sound vibrations through the middle ear involves complex motions of the ossicular chain although until recently the exact plane of movement was poorly understood (Rosowski, 1994). The traditional view held that the malleus and incus rotate as a rigid unit about an axis (the rotational axis), which runs through the anterior process of the malleus and the long crus of the incus propelling the stapedial footplate in a piston-like motion at the oval window (Wever and Lawrence, 1954; Békésy, 1960). The malleoincudal joint, however, is not fixed in most animals, thereby allowing relative movements between the bones, furthermore the rotational axis has been shown in humans to vary considerably with frequencies above 1 or 2 kHz, therefore the traditional axis can only be considered a rough approximation (Decraemer *et al.* 1991; Decraemer and Khanna, 1995; 2004; Kelly and Prendergast, 2001). Studies have also demonstrated that the stapes only moves in a piston-like fashion at lower frequencies (Hüttenbrink, 1988; Willi *et al.*, 2002; Nakajima *et al.*, 2005).

A key purpose of the middle ear is as an impedance matching apparatus. One of the first studies, *On the Sensations of Tone* (Helmholtz, 1885) proposed three possible processes responsible for the increased pressure required in impedance matching: the conical lever action of the tympanic membrane, the areal convergence theory and the ossicular lever hypothesis.

The tympanic membrane conical lever theory proposes that the interaction of the radial and circular fibres of the membrane causes the surface to curve convexly, despite the overall concave shape created by the attachment of the umbo to the malleus. Helmholtz (1885) suggested this reflex curve determined that vibrations of large amplitude but smaller force occurring in the

middle radial fibres will be transformed into vibrations of smaller amplitude but greater force at the ends of the fibres. Because the umbo is at one end of the fibrous membrane the forces transferred to the malleus will be greater than the original force on the membrane creating an increase in the signal strength.

Although experimental research by Békésy (1941) and Wever and Lawrence (1954) found no support for the theory, more recent research on cats and humans found a limited number of results did corroborate Helmholtz's theory (Tonndorf and Khanna 1970; 1972; Khanna and Tonndorf, 1972). Nevertheless, the theory has received little attention among auditive scientists.

Helmholtz also advocated the areal convergence theory which states that the increased signal pressure is caused by a hydraulic action resulting from the smaller surface area of the stapedial footplate compared to that of the tympanic membrane, producing a mechanical advantage. Helmholtz suggested that in humans this gain would be between 15:1 and 20:1, subsequent research has confirmed this (Henson, 1974; Roswoski 1992; Rosowski and Graybeal 1991). The problem with determining the true effect of this advantage lies in determining the vibrational patterns of the tympanic membrane. Several studies have attempted to reveal the exact modes of vibration but with conflicting results (Békésy, 1941; Wever and Lawrence, 1954, Tonndorf and Khanna, 1970).

The theory of impedance matching most commonly adopted by auditive scientists is the ossicular lever hypothesis (Wever and Lawrence, 1954; Békésy, 1960; Dallos, 1973). Helmholtz (1885) described the middle ear as a hydraulic and mechanic lever system which gains signal strength due to the uneven lengths of the manubrium of the malleus, considered the effort arm, and the long crus of the incus, the resistance arm, transforming small forces of low magnitude and high

displacement at the tympanic membrane into small displacements with high force at the incudostapedial joint. The lever action of the ossicles, however, is not as significant as expected, providing a force gain in humans of only x1.3 (2dB) and x2 in many other non-human primates (Wilson, 1987).

The effective lever arms are determined by measuring the perpendicular distance from the axis of rotation to the point of operation of the force, traditionally considered to occur at the umbo. Khanna and Tonndorf (1972), however, suggest that in some species because the manubrium is embedded in the tympanic membrane for almost its entire length, the forces applied will be transferred along its length and therefore each point along the manubrium will have an associated effort lever arm, substantially reducing the total effective leverage. Testing this hypothesis in cats they found an actual lever arm ratio of 1.15:1 compared with a 'full-length' value of 2.35:1. This finding is less relevant for primates as the majority have a strong attachment only at the umbo and lateral process (Graham *et al.* 1978).

The major difficulty in applying this lever mechanics approach is determining the axis of rotation, which as previously demonstrated changes with frequency (Decraemer *et al.*, 1991) and indeed does not simply rotate but moves in a complex pattern of bending, compression and flexion. Non-ideal ossicular motions are more significant above 5kHz (Rosowski, 1994). At 120dB or above, as is the case with great sound intensities, the malleoincudal joint becomes increasingly elastic (Cancura, 1980). This supports Hüttenbrink's (1988) hypothesis that the degree of motion possible in the ossicular joints is a protection mechanism against loud sounds. Whether this function is instead of or as well as the previously mentioned middle ear muscle tension defence is unknown. Kelly and Prendergast (2001) using finite element analysis modelling found that the axis of rotation at any one point in time changed depending on the

frequency applied and calculated that the lever arm ratio for humans rarely exceeded 1:1, suggesting that in fact the function of the ossicles is not to provide mechanical leverage.

This straightforward transfer-function based description of the ear as a vibratory system, is only valid if the system is linear (Dallos, 1973). The question of linearity is vital to any physical system. In a linear system the output is proportional to the input and therefore predictable and this transfer-function or ratio is independent of level. Experiments with several mammalian species, however, strongly suggest that the middle ear is linear only for sound pressure less than 130dB (Rosowski, 1994).

Once estimates of the mechanical advantage provided by the various auditory structures have been determined it is then possible to calculate an overall ratio of the transformed sound pressures. Two major sets of models have been used to determine these transformer ratios: the so-called ideal transformer models and the peripheral hypothesis, both are transfer functions, predicting the ratio of output to input.

The ideal transformer model was first defined by Wever and Lawrence in their seminal work *Physiological Acoustics* (1954) building on previous mechanical studies of the auditory system. Currently, two ratios built on the ideal transformer models have been defined: the pressure transformer ratio (PTR) and the impedance transfer ratio (ITR).

The PTR was initially popular due to early views of the ear as essentially functioning as a pressure detector (Békésy, 1960). Subsequent research has demonstrated that the transformer action does not increase hearing sensitivity in direct proportion to pressure. This knowledge has lead to the widely accepter notion that the middle ear functions primarily as an impedance

matching device (Dallos, 1973). Since then more emphasis has been placed on the impedance transfer ratio. The PTR is reached by multiplying the areal convergence ratio by the ossicular lever ratio, essentially measuring the greatest degree of pressure attainable by the middle ear. The ITR focuses more on the ossicular lever ratio although the areal convergence ratio is still the most important factor in both equations (Nummela and Sánchez-Villagra, 2006). The ITR predicts a direct correlation between the tympanic membrane area and the power available to the middle ear (Rosowski, 1994). Several researchers have demonstrated a lack of association between the ideal transformer models and measurements of hearing sensitivity (Lay, 1972; Rosowski and Graybeal, 1991; Rosowski, 1994).

The main problem with the ideal transformer models is that they assume 'ideal' function. The hypothesis on which they are based is a simplification. It ignores many extraneous factors including variance in ossicle stiffness, mass, flexibility of the ossicular joints as well as the mechanical and acoustical properties of the outer, middle and inner ear structures themselves (Rosowski, 1994). All vibrating bodies are constrained by the limitations of their movements as defined by their 'mechanical impedance'. This impedance is controlled by three factors: mass, stiffness and frictional resistance (Wever and Lawrence, 1954). The stiffness of the middle ear plays a large role in the measurement of function. It is worth noting that this relationship of size and stiffness is unique to mammals; birds and reptiles have similar tympanic membrane areas but their middle ears are far more flexible (Roswoski, 1994). These factors need to be included to accurately model and predict audiogram shapes and therefore hearing sensitivity.

Alternatives to the ideal transformer models are the peripheral filter hypotheses. These hypotheses not only take the mechanical and acoustic properties of the auditory structures into account, but also contend that it is these factors that determine the shape of the audiogram

(Roswoski, 1994). There are three basic types of peripheral filter hypothesis: isostapes motion theories, isocochlear pressure theories and isopower theories. Isostapes motion theories correlate the plane wave sound pressure needed to produce constant motion (velocity) of the stapes with the auditory threshold at various frequencies (Dallos, 1973; Zwislocki, 1975). Isochoclear pressure theories relate the auditory thresholds to the plane wave sound pressure required to produce constant sound pressure within the cochlea (Lynch *et al.,* 1982; Décory, 1989).

The most widely applied of the three basic types are the isopower theories. These theories correlate the audiological threshold with the sound pressure required to produce specific sound powers at the cochlea entrance (Khanna and Tonndorf, 1972; Rosowski, 1991). Isopower theories have several advantages over the motion and pressure theories, namely that they account for inter-specific variations in inner ear impedance. The variances produce uncertainties and greatly complicate taxonomic comparisons (Rosowski, 1994). Unlike the others, the isopower theories are conceptually linked to the notion of the auditory system as an impedance matching mechanism, transferring sound energy from the air to the cochlea but unlike the ideal transformer models, isopower theories allow for significant frequency-related losses between the external sound wave power and the power that reaches the inner ear (Rosowski, 1994). Data suggest that more than half of the sound power that enters the middles ear is absorbed with only a fraction of the original power transmitted to the cochlea (Rosowski, 1994). The power theories have been shown to adequately predict the audiogram shape of a limited number of mammalian species (Dallos, 1973; Zwislocki, 1975; Lynch *et al.*, 1982; Rosowski, 1991).

Despite the growing awareness that all of the structures of the middle ear and their relative motions, mass, elasticity etc. must be included in auditory studies, a number of investigation still use impedance transfer models as direct measures of hearing performance (Wever and Lawrence,

1954; Hunt and Korth, 1980; Masali *et al.*, 1992). Coleman and Ross (2004) found that the greatest departures from expected theoretical results came from those measures using areal convergence ratio, lever arm ratio, ITR and PTR, where a higher transformer ratio was associated with a decrease in actual sensitivity. This suggests the auditory system is more complex than the current functional models allow for.

The results of these mechanical and functional hypotheses can be evaluated against audiograms obtained through direct behavioural testing. Although absolute auditory thresholds are considered the fundamental evaluation of audition, auditory testing can include temporal or frequency difference limens, localisation acuity and amplitude (Stebbins, 1975). Compared with some other mammalian orders, primates have fairly standard middle ear transmission properties (Colman and Ross, 2004). References to primate hearing in the literature abound. To outline the concepts only a few are given here.

The squirrel monkey (*Saimiri scuireus*) and the macaque (*Macaca sp.*) are perhaps the most widely used nonhuman primates for auditory studies. According to Beecher (1974a) both function so similarly that he advocates the ability to refer to 'monkey auditory function' without specifying a particular species, an oversimplification at best. Among vertebrates high frequency hearing ability is only found in mammals (Nummela and Sánchez-Villagra, 2006). Monkeys are more sensitive than humans to the higher frequencies, above 16kHz. Studies have demonstrated that many Old and New World monkeys have a W-shaped audiogram, meaning they are sensitive to 1kHz and below as well as above 8kHz but lose sensitivity between 2-4kHz. Humans do not lose sensitivity in this range; in fact they are most sensitive to this range, showing a U-shaped audiogram. Interestingly, sounds with frequencies less than 4kHz are often used in human speech (Kojima, 1990). Similar to monkeys, chimpanzees also show loss in the 2-4kHz

range. They appear to be more sensitive than humans to high-frequency tones but not as much as monkeys (Kojima, 1990).

It can thus be suggested that humans have evolved sensitivity to low- and mid-frequency ranges as a specialisation of auditory functionality, perhaps even speech (Kojima, 1990). The high-frequency specialisation of some apes and monkeys has been suggested as related to sound localisation (Masterton *et al.*, 1969), although loud stimulus rather than high-frequencies are most easily and accurately located (Stebbins and Moody, 1994). Superior high-frequency hearing, like that used by bats and many smaller mammals, enables precise echolocation and provides an opportunity for communication outside the hearing range of larger predators (Heffner and Heffner, 1985). It has also been proposed that the high-frequency hearing limitations are largely determined by the cochlea due to the constraints of the auditory nerve fibres (Ruggero and Temchin, 2002). Hence the cochlea appears to have a significant effect on the upper and lower boundaries of the primate audiogram. The reactive component of cochlear impedance is thought to decrease low-frequency sound sensitivity (Lynch *et al.*, 1982).

Although intuitively it might seem advantageous for primates to maximise their hearing sensitivity to as wide a range of frequencies as possible, in reality this is not necessarily beneficial. For example a primate species that relies heavily on high-frequency reception for survival may find it advantageous to avoid perception of low-frequency sounds, which may mask more vital ones (Coleman and Ross, 2004). Difference in auditory sensitivity may be largely controlled by their intended use, with factors such as group communication, prey detection and predator avoidance playing vital roles. In this way primate auditory perception is closely linked to the animal's natural ecology, which can vary depending on the species (Stebbins, 1975; Stebbins and Moody, 1994).

Numerous researchers advocate that primate communication within their natural habitat occurs within 'sound frequency windows.' These specific frequency channels are supposed to increase vocal propagation and reduce extraneous sound interference (Waser and Brown, 1984). There are a few Old World monkey species that demonstrate unusual acuity within their vocal frequency range, these differences are large enough (18dB) to be considered related to communication within their specific habitat (Stebbins and Moody, 1994).

Examining blue monkeys (*Cercopihecus mitis*), Brown and Waser (1984) found specialisations for low-frequency vocal production and low-frequency hearing work together to increase the effective distance of their long-range acoustic communication within the forest canopy by up to four times. Owren *et al.* (1988) found similar vocal specialisations in de Brazza's monkeys (*Cercopithicus neglectus*), without the enhanced low-frequency hearing. The authors suggest this is due to differences in their respective habitats, as de Brazza's monkeys are found mainly in African wetlands while blue monkeys are found in evergreen forest canopies.

Interestingly, comparisons of the nocturnal owl monkey (*Aotus lemurimus*) with the diurnal squirrel monkey, which are a similar size and live in similar habitats, found no strong differences in auditory function suggesting that there is not a specialisation for nocturnal hearing (Beecher, 1974b). Habitat sound propagation is shown to be influenced by signal frequency, sound source height and time of day (Morton, 1975; Marten *et al.*, 1977; Waser and Waser, 1977).

In a study of three tropical environments commonly inhabited by primates: rainforest, riverine forest and savannah, Waser and Brown (1986) found markedly different obstacles to acoustic communication in each. Examples included high ambient noise disruption caused by wind and

reverberation which constrains vocal communication even over short distances. A recent study by Coleman *et al.* (2009) examined primate vocalisation and ambient acoustics in the Ecuadorian jungle. Preliminary results show a ground level frequency window for communication and suggest distinct and more complex differences between audition in South American and African environments. So it would seem that any discussion of primate hearing must take into account external factors such as ecology as well as the sensitivity of the physiological system.

It would appear that these functional auditory characteristics evolved relatively slowly in response to persistent selective pressures extending over a long time. This in turn implies that variation in auditory characteristics between primate species may be due to differences in their ancestral lineages rather than to differences in their present habitat (Heffner and Masterton, 1970). The interaction between form, function and habitat can be viewed as an 'adaptive triangle' where each factor influences the other and the affectations of each depend on the circumstances (Coleman and Ross, 2004). Overall, it is difficult to disentangle the function of any one separate piece of the auditory puzzle from its influence on the others. The aim of these mechanical and functional theories is to accurately postulate the actual hearing performance of an individual or species, which can then be used to make inferences about primate hearing levels, communication and evolution.

Evolution

The origin and development of the mammalian middle ear from elements of the jaw apparatus in non-mammalian cynodontsis a classic example of evolutionary change. Although examples of preserved auditory systems are rare, in that only a fraction of the original population is represented, discussions of mammalian and primate hearing evolution abound in the literature

(Allin, 1975; Rowe, 1996). The majority are based on measurements of the structures and cavities of the system, the discussion following will concentrate on the ossicles.

Discussions of auditory evolution frequently rely on the scant primary evidence of fossils. To allow reconstruction of locomotor, sensory and behavioural patterns of extinct species, analogies are made by comparison with living forms and by biomechanical analyses such as have been previously discussed (Walker *et al.*, 2008). Ossicles are among the rarest bones in the fossil record (De Ruiter *et al.*, 2008). They are recovered infrequently both due to their small size and because they are frequently lost from the tympanic cavity before fossilisation could occur (Silcox and Bloch, 2004).

Terrestrial hearing can be examined as far back as 410 million years ago when the first aquatic animals, the tetrapods, moved on to land. Their 'hearing' sense was limited to ground-borne vibrations much as in many extant snakes and newts (Prendergast, 2002). The first 'ossicle', a proto-stapes, appeared in the early reptiles that had still not evolved 'air-sensitive' hearing, this was to come with the more mammal-like reptiles and archosaurs, a group which includes dinosaurs (Clack, 1997). Archosaurs evolved a tympanic membrane to accompany their one ossicle, which likely provided a considerable selective advantage. The single ossicle middle ear apparatus was passed on to the dinosaurs and their descendants including the extant birds and crocodiles who maintain it (Clack, 1997).

The three-ossicle pattern evolved between the tetrapods and today's mammals, perhaps with the morganucodontids of the Mesozoic, approximately 210 million years ago (Ross and Graybeal, 1991). The fossil record demonstrates that as the mammalian mandible developed, a group of four bones detached from the jaw to form the ossicular chain and supporting bone for the

tympanic membrane (Nakajima, 2005). Structural changes appear to be correlated with alteration in function, over the 100 million year span of premammalian history, the ossicles gradually reduced, reflecting a specialisation for increasing high-frequency sensitivity (Rowe, 1996).

As previously mentioned, Fleischer (1973; 1978) equated the microtype stiff ear with an 'ancestral type' which he proposed all extant mammals developed from. The ancestral type is characterised by a U-shaped malleus with one arm connected to the circumference of the tympanic membrane. A later type then followed this, where one arm of the U-shaped malleus became a ligament slowly reducing in size to the current attachment for the anterior mallear ligament. Comparative morphological studies on early mammals and cyndonts support the premise that the attached malleus represents the early or ancestral mammalian condition (Hunt and Korth, 1980).

If as Fleischer predicted, the auditory ossicles function primarily as a lever system, then the evolution should trend towards improved lever-ratio adaptations, a contention not supported by the anatomical evidence (Prendergast, 2002). Prendergast (2002) proposed a model of mammalian evolution based on increasing inertial mass of the ossicles, with future experiments planned to test this hypothesis. These debates then beg the question of what drove the biomechanical force behind mammalian and primate middle ear evolution.

Studies of primate auditory evolution have focused on these divergent points in an attempt to ascertain the genera and circumstances under which major adaptations in the auditory system occurred. What ancestral primates could hear has been a subject of much discussion (Nummela and Sánchez-Villagra, 2006). Among vertebrates, high-frequency hearing occurs only in mammals but when this trait evolved is currently unknown (Masterton *et al.*, 1969; Fleischer,

1973; 1978). A number of studies have focussed on the auditory ossicles of the Plesiadapiformes, late Palaeocene primates. A malleus and incus were virtually reconstructed from a micromomyid, from the most primitive plesiadapiform cranium currently known (Silcox and Bloch, 2004). Coleman (2007) included two plesiadapid species in his study of primate auditory systems and sensitivity modelling. Anatomical evidence from extant mammals and mammaliaforms (*Morganucodon*) suggest the last common ancestor of the crown-clade Mammalia had high-frequency sensitivity; sensitivity to low-frequencies appears to have evolved later (Rosowski and Graybeal, 1991).

The evolution of the hominid auditory system has received a great deal of attention. A few australopith ossicles have been described in the literature (De Ruiter *et al.,* 2002; Moggi-Cecchi and Collard, 2002; Rak and Clarke, 1979a; 1979b) as well as Neanderthals and remains from the Middle-Pleistocene (Angel, 1972; Arensburg *et al.,* 1981; Martinez and Arsuaga, 1997; Martinez *et al.*, 2004). These studies are important for the evaluation of the evolution of primate communication. Speech as a form of communication was a critical step in human evolution. It must have been a powerful agent of natural selection and the point at which it occurred is a subject of much controversy (Arensburg and Tillier, 1991). The degree to which the evolution of hearing sensitivity impacted the development of speech is unknown, it has been suggested that human speech evolved from a vocal communication similar to the short-distance relatively soft calls of apes (Kojima, 1990). Although the primate middle ear has changed drastically throughout its evolution both in morphology and function, much work remains to fully understand its influence on audition and the impact it had on the evolution of primates in general.

Goal-Driven Species Inclusion

Phylogenetics play a major role in the objectives of this investigation not only looking for measurable differences in auditory ossicle morphology between primates at the suborder, family and species level as well as between percussive and non-percussive foragers. Representing percussive foragers in the sample set, *Daubentonia madagascariensis,* commonly known as the aye-aye, is the only extant member of the family Daubentoniidae and is the largest nocturnal lemur (Quinn and Wilson, 1994). It has a mean body mass of 2.5kg and is distinguished from other lemurs by its long bushy tail, prominent triangular pinnae and elongated digits with curved claws (Feistner and Sterling, 1995). It is widely distributed throughout Madagascar but with a low population density. The species is considered endangered with an estimate of between 1,000 and 10,000 individuals in the wild (Quinn and Wilson, 1994).

The family Daubentoniidae is classified among strepsirrhine primates and consists of the extant *Daubentonia madagascariensis* and the extinct late-Holocene *Daubentonia robusta. D. madagascariensis* has incisors that grow continuously like those of a rodent, a feature that contributed to its initial misclassification as a squirrel (Sterling, 1994). Chromosomal and DNA investigations (Dene *et al.*, 1980; Rumpler *et al.*, 1988; Del Pero *et al.*, 1995; Porter *et al.*, 1995) indicate that *Daubentonia* is a sister group to the lemuriformes. Alternative morphological studies (Groves, 1989; Jablonski, 1986) as well as mitochondrial DNA analyses (Adkins and Honeycutt, 1994) suggest that *Daubentonia* may be a sister group to both Lemuriformes and Lorisformes.

Daubentonia is strictly nocturnal with activity beginning thirty minutes before sunset and continuing till three hours after. The rest of the day is spent nesting high in the trees (Quinn and Wilson, 1994). *Daubentonia* spend 25% of its time on the ground (Glander, 1994) and frequently clings upside down, resting in a horizontal or vertical position. Quadrupedal walking and leaping

between trees occurs and individuals may descend a vertical support either head or tail first (Ancrenaz *et al.*, 1994).

Daubentonia occupy a wide variety of habitats including primary and secondary low- to mid-altitude rainforests, deciduous forests, dry scrub forests, mangrove swamps and occasionally cultivated areas such as lychee or coconut plantations (Oxnard, 1981). Female ranges (30-50 ha) are smaller than male ranges (100-200 ha). Male ranges may overlap by 40-75% (Sterling *et al.*, 1994). *Daubentonia* males and females are generally solitary, although foraging associations of two to three individuals commonly form (Quinn and Wilson, 1994). As they are non-gregarious and nocturnal animals, they have only a small number of vocalisations; these serve affiliative, aggressive and informative functions. The 'hai-hai' vocalisations from which *Daubentonia* derive their common name are emitted during capture attempts (Stanger and Macedonia, 1994).

Daubentonia is morphologically unique amongst living primates, with an elongated third finger, which manoeuvres independently of the other digits, used in feeding and delicate grooming (Quinn and Wilson, 1994). They are also the most highly encephalised of the strepsirrhines (Kaufman *et al.*, 2005) with a more globular and heightened skull (Oxnard, 1981). The auricular, masticatory and caudal muscles are strongly developed (Quinn and Wilson, 1994). Along with galagos, *Daubentonia* have the largest relative outer ear size among primates (Schultz, 1969; 1973).

The *Daubentonia* diet consists of xylophagus insect larvae, fruits, nuts and plant exudates (Quinn and Wilson, 1994). To obtain the larvae portion of their diet, *Daubentonia* use a distinctive technique known as 'percussive foraging.' Hunting in almost total darkness, the animal taps its middle digit against the wood surface repeatedly in an activity designated 'tap-scanning,'

apparently to generate auditory cues, which reveal the location of prey in empty cavities (larvae mines). When a subsurface larval mine is located, the surface is gouged away with the incisors and the third digit used for extraction (Erickson, 1994; 1995).

Daubentonia tap-scans with its large pinnae bent down and forward apparently interpreting acoustical reverberations (Erickson, 1994). Erickson (1991) determined that visual and olfactory cues are not necessary for cavity location, but precisely what the animal is 'listening' to remains undetermined. It is likely that they locate prey by hearing their subsurface activities and experiments with captives showed hollows with moving prey were excavated most frequently (Erickson, 1995). It is likely that in some circumstances the tapping behaviour stirs subsurface prey into audible activity (Erickson, 1994), although, it appears the cavities themselves are of some auditory interest to the animal. A recent series of studies revealed that backfilled chambers were still excavated although not as frequently as empty ones, suggesting that any break in the natural integrity of the wood's inner structure elicits excavation (Erickson 1998; Erickson *et al.* 1998). Differences in arrival time, timbre, phase and intensity of sound when combined with movements of the pinnae and head can foster great accuracy. It is possible that the auditory cues provided by repeated tap-scanning allows the individual to construct a mental representation of the subsurface configuration (Erickson, 1994).

Daubentonia has several morphological features that are clearly adapted for percussive foraging: large mobile outer ears, perpetually growing incisors and an elongated probe-like digit (Erickson, 1991). It seems likely that the auditory cues perceived by *Daubentonia* are numerous and whether the ossicles are equally well adapted for these stimuli remains undetermined. One important aim of this thesis was to examine the degree of difference between *Daubentonia* ossicles and those of other primate taxa to allow inferences on hearing specialisation.

Other unusual taxa relevant to the objectives of this project are the Dermoptera. As previously stated the fourth goal of this study was to compare the auditory ossicle morphology of the order Dermoptera with to that of the primates in order to facilitate comparative studies. The order Dermoptera contains a single family, the Cynocephalidae. Known alternatively (colloquially) as 'colugos,' 'flying-lemurs' or 'mitten-gliders.' The two extant species are now placed in separate genera: *Cynocephalus volans*, the 'Philippine flying lemur' and *Galeopterus variegatus*, (formerly known as *Cynocephalus variegatus*) 'the Malayan or Sunda flying lemur' (Stafford and Szalay, 2000). These divisions are mostly based on dental morphology (Wilson and Reeder, 2005). Stafford and Szalay (2000) suggest further distinction at the subspecies level for *G. variegatus* based on geographic as well as biologic distinctions. Both species are geographically confined to Southeast Asia and the East Indian Islands (Wilson and Reeder, 2005).

These so-called flying lemurs are inaccurately named as they neither fly nor are they lemurs; they are however, gliders. Entirely arboreal living in large multi-layered rainforests, the Dermoptera glide from tree to tree using their extensive patagium, membranous folds of skin stretched between their appendages. Their diet consists of tree leaves, buds, flowers and seed-pods (Wilson and Reeder, 2005). They are crepuscular and nocturnal seeking refuge during the day in the large hollows of trees, their chief predators would appear to be carnivores, snakes and more recently, man (Hunt and Korth, 1980).

The general structure of the auditory region is said to be uniform between the genera (Hunt and Korth, 1980). Extensive anatomical investigation and description of *Cynocephalus volans* was undertaken by Hunt and Korth (1980). The ossicles however, were almost entirely omitted from the study, except to confirm that they were neither developed abnormally in size or mass, with no

evident morphological specialisations that would suggest unusual mass distribution, excessive stiffness or strong frictional resistance.

The determination of higher-level relationships among placental mammals has proven remarkably difficult (Martin, 2008). The correlation of Dermoptera to fossil and other extant mammals has been hotly debated with hypothesised relationships first based on morphological features and later on molecular and chromosomal investigative techniques (Silcox *et al.,* 2005). The living Dermoptera have a limited fossil record (Silcox *et al.,* 2005). Dermoptera was first recognised as a distinct order by Gregory (1910). This allocation has been accepted by virtually all subsequent authors (Hunt and Korth, 1980).

Subsequent molecular evidence indicates that Dermoptera, Scandentia (tree-shrews) and Primates cluster together on the mammalian phylogenetic tree however, the exact relationship of these groups and their relative importance in primate evolution is still unresolved (Martin, 2008). Some studies, based on Mitochondrial DNA (mtDNA) sequences and Amino Acid (AA) composition have challenged the monophyly of primates, grouping Dermoptera and Primates on a common branch with Dermoptera falling as a sister group to the higher primates (Anthropoidea) to the exclusion of the Prosimians (Arnason, 2002; Janeka *et al.*, 2007; and Murphy, 2001). There are morphological arguments for placing the Primates and Dermoptera as sister groups, particularly based on craniodental morphology and the structure of the tarsus (Stafford and Szalay, 2000).

Schmitz *et al.* (2003) used short interspersed nuclear elements (SINEs) to contradict this phylogentic (2003) positioning, supporting primate monophyly; this research was further validated by later chromosomal comparison studies by Nie *et al.* (2008). However, Schmitz *et al.*

were unable to resolve the Dermoptera, Scandentia, Primate trichotomy due to the limited genomic data available of the Dermoptera.

A general problem with the majority of these studies has been the inclusion of only one Dermoptera species, specifically *G. variegatus*. Due to long-branch attraction, misleading results can be generated when only a single representative species is used (Martin, 2008). Janeka *et al.* (2008) has been the only study to use both *Cynocephalus volans* and *Galeopterus variegatus.* In doing so this alleviated the affects of long-branch attraction and enabled them to demonstrate a surprisingly deep divergence between the two genera, at approximately twenty million years ago, thereby supporting the division of the Dermoptera at a generic rather than species level.

The choice for the study of Dermoptera as an outgroup to the primates rather than the more traditional use of Scandentia is supported by the molecular evidence of Janecka and colleagues (2007). They found that the Dermoptera represented the closest living relatives of primates with this divergence indicated to have occurred during the Cretaceous. For this analysis the Dermoptera representatives provide ossicular morphology that is closely related to the primates in the study but not as closely related as any of the primates are to each other, this will facilitate discussions of the taxonomic layout of the groups in clustering analysis. As noted by both Nie *et al.* (2008) and Janeka *et al.* (2007), true comprehension of the genomic and morphologic evolution of primates requires identification of sister groups and clarification of the phylogenetic tree, for both, Dermoptera stand as excellent candidates for study.

Morphometric Studies

Studies focusing on the morphometrics of primate ossicles are relatively rare, compared to most other bones, with more emphasis on the previously mentioned evolutionary studies. The

first morphometric studies of primate auditory ossicles involved simple measurements such as length and weight (Hyrtl, 1845; Arione, 1923; Werner, 1956; Parizek and Varacka, 1967). Werner (1956) noted that ossicular morphology is variable among taxonomic groups. Human morphometric studies have focused on applications of auditory ossicles in osteological aging, sexing and population affinities (Mutaw, 1986; Sakaliskas, 1995; Unur, 2002; Flohr, 2006).

Morphometric-based taxonomic studies including nonhuman primates are slightly more common. Masali and Chiarelli (1967) saw the first English publication of the standardised 2D morphometric measurement technique for human ossicles proposed by Masali (1964). These techniqueswere not described in any detail until 1968 (Masali, 1968). Both the 1967 and 1968 publications include diagrams but no definitions or landmark instructions. Due to the small size of the ossicles and the impossibility of accurate measurements using normal devices such as callipers, Masali recommended the use of indirect observations and measurements taken on enlarged single plane projections. These measurements include: length between the perpendiculars of the malleus, malleus body length, chord of the manubrium arch, incudal length, incudal breadth, incus crural length, incus crural arch chord, stapedial crura length and stapes base length.

Masali and Chiarelli (1967) began their taxonomic study of 10 representative sets of human and nonhuman Old World primates with a visual comparative overview, which suggested common traits in the different genera. Masali and Chiarelli (1967) found the main features of the ossicles are fairly constant among humans. The measures obtained for the human sample in this paper were used as the raw data in subsequent publications (Masali, 1968; Masali, 1971; Siori and Masali, 1983; Masali 1992; Masali *et al.*, 1992). The ossicles of humans and true apes (*Gorilla, Pan* and *Pongo*) were found to be the same general size while the others were smaller. The

malleus of *Gorilla* and *Pan* is similar to the human morphology although the manubrium appears more slender and longer, particularly in *Gorilla.* The head has almost equal transverse dimensions in humans, while in *Gorilla* and *Pan* it appears flattened and asymmetrical. The malleus of *Pongo* is differentiated from humans and other apes by its unnaturally thin features. This attenuation is demonstrated in the poor differentiation of the head, neck and manubrium. The malleus of *Hylobates* is clearly smaller than true apes and appears the same size as the other primates studied. The other primate species studied demonstrate an obvious tubercle on the convex edge of the manubrium, said to be a fairly constant feature of Old World monkeys.

The incus demonstrates more variability than the malleus, although the differences between the genera are more dimensional than morphological. The human incus shows greater distinction of the two crura. *Gorilla* and *Pan* have less distinct crura that are shorter and closer together. Again the incus of *Pongo* is attenuated, with crura that are barely distinguishable from the body. No *Hylobates* incus was available for study. The incudi of the other Old World primates are distinguishable from those of the Hominidae by a proportionally thicker body. The crura are more similar, cylindrical and straight. Only a few stapes were available for study although Masali and Chiarelli (1967) infer that the stapes is less variable in morphology with no appreciable difference between *Homo* and *Pan.* In other Old World primates the crura are straight and the stapedial footplate is reduced.

The linear metrics taken using Masali's method generally agrees with the traditional taxonomy with some informative deviations (Masali and Chiarelli, 1967). *Hylobates* is at the lower end of the scale. *Papio* falls in the middle range within the limits of human standard deviation. The arch chord of the malleal manubrium (essentially the manubrium length) shows *Hylobates* at the short end of the spectrum with the longest being *Gorilla.* Humans sit between the great apes and

monkeys. In most of the incudal measures, *Homo* is much larger than other apes by up to two standard deviations. The crural arch chord has very high variability due to the features of the crura.

The differences in dimension allow clear separation on one side of *Gorilla, Pan, Pongo* and *Homo* with *Hylobates* and the other Old World primates on the other. Aspects of the malleus and incus allow differentiation of *Pongo* from *Homo* and the African apes. *Homo* differs from *Gorilla* and *Pan* by some incudal features. *Gorilla* is distinct from *Homo* and *Pan* by the length and proportion of the malleal manubrium (Masali and Chiarelli, 1967) .

Masali's 1968 publication examining taxonomic and postural distinctions in Old World primates saw one slight change to the linear metric schema for nonhuman primates. The definition of incudal crural length, which is taken from the perpendicular that intersects the inter-crural arch at its deepest point, was changed to account for the previously mentioned inconsistencies in the crura morphology.

This study also introduces for the first time, indices independent of dimension in order to compare homologous elements of varying sizes. Also included are discussions of angular value, relevant to discussions of the relationship between the positions of the tympanic membrane and the ossicles. The smallest angles (121°) occur in *Gorilla*, humans and other Old World primates follow with the largest belonging to *Hylobates* (146°). Possible causes of the inter-specific variations are discussed including: the position, inclination and concavity of the tympanic membrane, evolutionary changes in the temporal bone due to posture and the relative size of the adult skull.

The ossicles of New World monkeys are examined for the first time in Masali's 1971 publication. In terms of morphological variability New World primates appear the most differentiated. These differences are not simple anatomical variation because the vestigiality or lack of some features is common. New World primate ossicles are generally smaller than Old World primates, which may be related to differences in general body dimensions. The largest ossicles are found in *Ateles* and *Lagothrix*, which reach dimensions found in the Cercopithecinae. The lack of an extended external auditory meatus is a common characteristic of New World primates (Werner, 1956) and it is suggested that this influence has lead to the aberrant morphology of the malleus (Masali, 1971).

The New World primate's malleus lacks a lateral process and commonly lacks an anterior process. This leads to complications in measurements particularly the length of the manubrium, which is usually measured to the tip of the lateral process. The measurement of malleus length tends to be a little longer due to the wider axis angle found in New World primates. The incus is less differentiated than the malleus. Overall, New World primates as a group, metrically appear fairly homogenous and clearly differentiated. This differentiation seems to indicate a dichotomic system of evolution, which with further research may inform the issue of New versus Old World taxonomy (Masali and Siori, 1979).

The osteological material to this point was too scarce to permit an extensive statistical review. This changes with Siori and Masali's 1983 publication. The availability of new ossicle data allowed for a larger-scale multivariate analysis, including previously published data. A single malleus and incus was chosen to represent each species. The results of this work tended to support the traditional taxonomy, presenting the separation of the Old and New World primates

both in raw data and measures converted to "shape variables," although more so when overall size was included.

Masali 1992 and Masali *et al.*, 1992 presents the previously published morphometric data and uses them to create a biomechanical lever model of primate auditory sensitivity as discussed earlier. Nearly forty years of ossicle research are reviewed in Masali and Cremasco's seminal paper *Hoc alterum auditus organi ossiculum est: ear ossicles in physical anthropology* (2006). Generally, primate auditory ossicles can be classified morphometrically into two distinct groups: the Old World primate type and the New World and prosimian type. The malleus shows large inter- and intra-specific differences in morphology. The stapes appears least variable, although few have been studied and due to its anatomical function small differences may produce important effects. This decreasing variability from the external ossicle to the most medial has been explained by the phylogenetic age of the ossicles, with the stapes the oldest and therefore most stable (Masali and Cremasco, 2006).

Summary

The study of primate auditory ossicles presents an opportunity to conduct new research, which will have significant contributions not just to the field of primatology but also to paleoanthropologists examining broader questions of primate evolutionary anatomy. Morphological variance may be used in the analysis of taxonomic differences as well as inform debates on primate auditory sensitivity. The following chapter details the materials and methodology of the current study, which aims to answer some of the questions raised by previous research.

CHAPTER III – MATERIALS AND METHODS

Introduction and Objectives

The aims of the current study are to evaluate and validate the methodological frameworks specifically used for the measurement of primate auditory ossicles, and then use these to determine if there are any measurable differences in auditory ossicle morphology between primates at the suborder, family and species level as well as between percussive and non-percussive foragers. Specimens of Dermoptera were also investigated to provide context for phylogenetic comparison discussions of primate ossicular morphology. Finally, the study aimed to employ any morphological differences discovered, in the context of primate phylogeny. In order to achieve the first objective, an error measurement study was completed to test the repeatability of the auditory ossicle landmarks set out by Schmidt *et al.* (2009). The main study focused on answering questions of morphology and metrics. Ultra-high resolution X-ray computed tomography scans of primate auditory ossicles were landmarked and the resulting measurements tested using Euclidean distance matrix analyses to examine the implications of these results in a phylogenetic context.

Sample

The non-human primate and Dermoptera samples used in this study consist of ultra-high resolution X-ray computed tomography (UhrCT) scans of twenty-six individuals representing twenty-one species (Table 3.1) collected for a study of the semi-circular canals (Spoor et al., 2007). The number of scans available for study restricted the number of samples and species represented. The scans were taken at the Center for Quantitative X-Ray Imaging (CQI) at Penn State University on an HD600 (OMNI-X) industrial high resolution x-ray computed tomography and at the High Resolution X-Ray CT Facility at the University of Texas, Austin. The original uncropped datasets were typically 1024 x 1024 pixels and 200-500 slices. The datasets had previously been cropped and the ossicles segmented from their surrounding tissues using Image J (Rasband, 1997), to isolate them for easier measurement. Although ossicles from the left and right side of the body are not significantly different (Arione, 1923; Bouchet and Giraud, 1968; Heron, 1923; Masali, 1964), where possible scans of the right auditory ossicles were used. Specimens with damaged or incomplete ossicular chains were excluded from the study.

The twenty-one species in the sample represent many of the major branches of the phylogenetic tree based on Purvis (1995). This includes one species representing Tarsii, two Platyrrhini and one Catarrhini. The Strepsirrhini include nine examples of Lorisformes and six of Lemuriformes, including the percussive forager *D. madagascariensis*. As an outgroup for comparison, two specimens of non-primate Cynocephalidae were included.

Table 3.1 - Species studied in this analysis. The specimen accession number follows.

FAMILY	SPECIES
Cercopithicidae	*Macaca nigra* (1) – LACM 90765 *Macaca nigra* (2) – LACM 90766
Cheirogaleidae	*Cheirogaleus medius* (1) – 034 (1010) *Cheirogaleus medius* (2) – 0142 (1285)
Daubentoniidae	*Daubentonia madagascariensis* – Hylaex specimen
Galagidae	*Galago alleni* – CM 16090
	Galago elegantulus – UM 3901
	Galago moholi (1) – CM 6982 *Galago moholi* (2) – CM 57105
	Galago senegalensis – CM 57950
	Galagoides demidoff – CM 2942
	Otolemur crassicaudatus – 024 (1001)
	Otolemur garnettii – 105 (1100)
Lemuridae	*Eulemur fulvus albifrons* – 0100 (4580)
	Eulemur fulvus rufus – 010 (1153)
	Hapalemur griseus – FHNM 57631
	Lemur catta – BMOC Uncat.
	Varecia variegata variegata – UM-APC 210
Lorisidae	*Arctocebus calabarensis* – CM 16188
	Loris tardigradus (1) – UM-APC 70 *Loris tardigradus* (2) – FMNH 17096

Pitheciidae	*Callicebus moloch* – CM 2740
	Callicebus torquatus – FMNH 70695
Tarsiidae	*Tarsius bancanus* - 045
Cynocephalidae	*Cynocephalus volans* – NMNH 144660
	Galeopterus variegatus – NMNH 255716

Imaging

Recent developments in imaging modalities in combination with increasingly sophisticated computer graphics software have opened up a range of opportunities for qualitative and quantitative investigation of morphology, particularly with the application of morphometrics in the virtual environment.

Since its inception and development in the 1970's, X-ray computed tomography (CT) scanning has superseded conventional radiography as the preferred imaging modality for the investigation of complex skeletal morphology. The production of cross-sectional images in CT overcomes the superimposition of structures problematical to conventional radiography. Uses of CT are mostly limited to bone due to the high differential contrast. Soft tissue is better-visualised using magnetic resonance imaging (MRI) modalities (Zollikofer and Ponce de León, 2005).

CT scanners work in a similar way to conventional X-ray radiography, utilising a source and detector mechanism. In medical CT scanners an X-ray source and array of detectors rotate around the specimen measuring fan-beam attenuation within the confines of a slice shaped volume in a multitude of directions. Digital cross-section images are calculated from these beam measurements and are displayed on a computer in grey-scale with black representing the lowest and white the highest density. This density is measured in Hounsfield units (Hu), the Hounsfield scale is defined by values that represent the attenuation of the X-ray beam through a vacuum, practically valued as air –1000Hu and that of water 0Hu (Zollikofer and Ponce de León, 2005).

Like any digital image, each CT scan slice consists of a specific number of image elements or pixels. Different to a photo, however, each slice has a third dimension, thickness. Therefore each element is a volume element known as a voxel i.e. 3-D pixel. The voxel size is limited by the

scanning machine's capabilities and operational selections. The spatial resolution, or quantitative measure of the ability to visualise small details separately is not as good in CT as in traditional radiography. The contrast resolution, however, is superior in CT so that small density differences can be visualised such as those between air and bone or structures of differing thicknesses (For an in-depth discussion of the mechanics of imaging modalities see: Spoor *et al.*, 2000; Zollikofer and Ponce de León, 2005).

Unlike medical CT scanners, dedicated industrial and research ultra-high resolution CT (UhrCT) scanners have been developed, which provide images with thinner slices and significantly higher spatial resolution allowing much smaller structures to be visualised (Bloch and Silcox, 2006). While medical CT scanners are calibrated to the dimensions and material properties of the human body with scan times in the order of seconds per slice to reduce *in vivo* radiation exposure, typically in UhrCT radiation intensity is not a concern, allowing slice times in minutes. This difference in industrial tomography allows options of higher-intensity X-rays, smaller detector apertures, adaptable source/ detector geometry and longer sampling intervals, which can improve spatial and contrast resolution. These scanners also differ in that it is the specimen, on a turntable, that rotates rather than the source/detector apparatus (Spoor *et al.*, 2000). In addition CT does not generally require extensive specimen preparation although this depends largely on gantry size, a significant limiting factor in UhrCT (Spoor *et al.*, 2000).

Interest in the application of CT scanning modalities to the study of the middle ear has been high since the first commercial high-resolution scanning system was introduced by EMI in 1978 (Lloyd *et al.*, 1979). CT scans of the temporal bone have been shown to demonstrate both normal middle ear anatomy and pathology with accuracy and high sensitivity (Chakeres and Speigel, 1983) making this an excellent tool for the study of primate middle ear morphology.

The benefits of virtual imaging techniques are also expressed in specimen preservation. As previously noted, when examining *ex vivo* or fossilised specimens auditory ossicles are frequently lost. Even if the ossicles remain it may be impractical or impossible to remove them, making imaging modalities the only available option (Silcox and Bloch, 2004). There are, however, some limitations to CT scanning. One of the primary restrictions in the resolution of small structures like those in the middle ear is partial volume averaging (PVA) (Chakeres, 1983). The Hu and hence the grey-scale representation of each individual voxel is determined by averaging the densities of the materials occupying the volume space to produce a single attenuation coefficient. In areas where contrasting materials like a structure's edge occupy the same voxel then the Hu number is a combination of these represented materials, so small structures such as the stapedial footplate are poorly visualised (Spoor *et al.*, 2000). PVA also leads to complications in the thresholding process that will be discussed shortly.

Image Processing

Once the scan has been obtained it is opened using specialist software determined by the requirements of the study. The processing software used for this project, MIMICS v12.0, is an image processing software package developed by Materialize. MIMICS provides a selection of tools for importing CT scans, segmenting, incorporating many of these tools allowing voxel-by-voxel selection of threshold areas, 3D volume rendering and morphometric measurement and was used to edit, measure and analyse the ossicle UhrCT scans.

Series of contiguous or overlapping CT slices can be stacked to provide a 3-D dataset of the object, which can be visualised and analysed in numerous ways using multiple pieces of software. The two most common ways of visualising the 3-D data set are surface rendering, in

which only the surfaces of selected tissues are extracted from the data volume and rendered into an image, and volume rendering, in which all of the data volume contributes to the image (Spoor *et al.*, 2000). Both processes generally involve three steps: segmentation, rendering and creation of a virtual environment.

The first step, segmentation, is to isolate the specific data representing specific structures or materials to be included in the 3-D reconstruction. This process is most commonly performed by thresholding for the range of Hu characterising the relevant structure. In some software programs segmentation is a single step with a single threshold value applied to the scan slices of interest. This is problematic as one Hu range rarely encompasses all of the desired structure without including extraneous information (Coleman and Colbert, 2007). The precision of the segmentation process can be improved by manually designating regions of interest to exclude unwanted values and areas based on the operator's knowledge of the surrounding anatomy. This is achieved using specialised region growing and edge detection software tools to complement the operator's skills. Although time consuming this is useful as it puts the emphasis back on the operator.

In the second step, rendering, the highlighted thresholds are combined to create a 3-D model. Depending on the software used this option often involves interpolation between slices to create a smooth surface (Spoor *et al.*, 2000). The final step is heavily dependant on operator choice and software constraints. The creation and adaptation of the virtual environment allows the reconstruction to appear 3-D while projected on a 2-D surface (computer monitor) (Zollikofer and Ponce de León, 2005). Changes can be made in background as well as object colouring and shading and illumination by one or more multidimensional virtual light sources. These changes also allow better discrimination of surface detail. 360° rotation and zoom features allow better

visualisation, vital for further morphological and metric analyses (Spoor *et al.*, 2000). Metric analyses can be conducted on CT scans without conversion to a 3-D rendering. In this project the morphometric analyses requires visualisation of extremal points and identification of the ossicle surface; 3-D rendering greatly facilitates these operations.

Increasingly with developments in software engineering, 3-D renderings can appear exceptionally realistic but the extent to which these renderings reflect reality primarily depends on limits inherent to the imaging modality. Accuracy is limited by spatial resolution within the scan plane and by voxel size (Spoor *et al.*, 2000). As previously mentioned this is alleviated to a degree by the use of UhrCT. These voxel limitations may not be obvious on the final 3-D rendering because of the surface smoothing resulting from sophisticated interpolation algorithms in the rendering software (Spoor *et al.*, 2000).

Segmentation is another important process affecting the accuracy of the 3-D rendering. Because boundaries between adjacent structures e.g. bone and air are not clearly defined and are displayed as a continuum of grey-scale density values, it is particularly difficult to segments a specific structure or surface precisely to its edge. Some techniques developed to combat this include snake thresholding, balloon thresholding and other software algorithms (Coleman and Colbert, 2007). In this study thresholding boundaries are less of a problem due to the spatial resolution of the UhrCT scans and the voxel-by-voxel threshold selection available in the MIMICS program. All of the scans were thresholded by a single observer with anatomical knowledge of the areas involved, a base threshold was used to identify the relevant bones, the voxel-by-voxel thresholding technique was then used to visualise small structures or those obstructed by otherwise unnecessary tissue.

Data Collection and Landmarks

The 3-D rendering will be utilised for morphometric analysis to determine the extent, if any, of difference between the species of primate ossicles. Geometric morphometrics have been shown to be a great methodological advance in the analysis of phenotypic variation (Hallgrimsson *et al.*, 2008). Morphometric analyses are based on the quantification and visualisation of form. Traditional morphometrics as defined by Bookstein (1991) is the multivariate statistical analysis of linear distance, areas, volumes and angles.

The morphometric technique used in this study collects data based on anatomical landmarks, visualised and measured on the 3-D render and 2-D scan slices within the virtual environment. Each set of landmarks was collected twice and then checked for measurement error. If significant differences were found a third set would have been taken and the results averaged. There are numerous definitions of landmarks. Richtsmeier *at al.* (1995) define anatomical landmarks as biologically meaningful loci that are unambiguously defined and able to be located repeatedly with a high degree of precision. Landmarks provide a morphological point of reference on which correspondence between specimens can be established (Valeri *et al.*, 1998) i.e. they have to mean the same thing across groups or species depending on the research protocols (Bookstein, 1991).

There are a number of landmark types, of which Bookstein's (1991) classification is undoubtedly the most renowned. The landmarks used in this study, defined in Tables 3.2, 3.3 and 3.4, are mostly fuzzy landmarks as established by Valeri *et al.* (1998), except for the landmark representing the articulation of the stapes with the incus (ARI) which refers to a specific point. All other definitions of landmarks and landmark classes, including Bookstein's typography, share the concept of the landmark as a point location. Fuzzy landmarks define the centroid of

areas which are void of single-point features but which have topographic characteristics of interest.

A fuzzy landmark " ...represents a biological structure that is precisely delineated and that corresponds to a locus of some biological significance, but occupies an area that is larger than a single point" (Valeri *et al.,* 1998: 114). To determine the location of these landmarks Valeri and colleagues recommend viewing the structure in question from many different perspectives to ensure the most accurate placement possible, it is also for this reason that the landmarks used in this study were visualised using the 3-D renderings as well as the 2-D scan planes as not all of the landmarks are visible on the render.

Table 3.2 – Malleus Landmarks. Adapted from Schmidt *et al.* (2009)

Number	Abrev.	Name	Description
1.	MAN	Apex of the Manubrium	Placed at the apex of the manubrium of the malleus. It can be used in defining the functional length of the malleolar lever arm.
2.	LAT	Lateral Process of the Malleus	The apex of the lateral process of the malleus. This landmark can be used in defining the axis of rotation for determining the length of the malleolar lever arm.
3.	HEA	Superior Point on the Head of the Malleus	Found at the most superior point on the surface of the head of the malleus in line with MAN. This landmark can be used to calculate the conventional, maximum

			length of the malleus.
4.	ART	Most Invaginated Point of the Malleolar-Incudal Articulation	Defines the most invaginated point on the malleus in the malleolar-incudal articulation. It is not visible on the exterior surface of the 3D image and is viewed in sagittal section. The malleolar-incudal articulation has a complicated 3D morphology and therefore three points are defined here to characterize its shape (ART, IAR, SAR).
5.	IAM	Interior Arch of the Malleus	Placed at the midpoint of the interior arch of the malleus (i.e., the area of connection medially between the malleus and the rest of the bone). It can be used to help characterize the shape of the malleus.

Table 3.3 – Incus Landmarks. Adapted from Schmidt *et al.* (2009)

Number	Abrev.	Name	Description
1.	LCR	Apex of the Long Crus	Located at the most inferior point on the long crus of the incus. It can be used in defining the functional length of the incudal lever arm.
2.	SCR	Apex of the Short Crus	Located at the apex of the short crus of the incus. It can be used in defining the axis of rotation for determining the length of the incudal lever arm.

3.	IAR	Most Inferior Aspect of the Malleolar-Incudal Articulation	The most inferior point on the incus in its articulation with the malleus. It can be viewed in both coronal and sagittal sections as well as on the inferior surface of the 3D image.
4.	SAR	Most Superior Aspect of the Malleolar-Incudal Articulation	The most superior point on the incus in its articulation with the malleus. It can be seen in both coronal and sagittal sections.
5.	MAH	Superior Point on the Head of the Incus	Found at the most superior point on the surface of the incus in line with LCR. This landmark can be used to measure the traditionally defined maximum length of the incus.
6	IAI	Interior Arch of the Incus	Placed at the midpoint of the interior arch of the incus (i.e., the area of connection laterally between the long crus and the rest of the bone). It can be used to help characterize the shape of the incus.

Table 3.4 – Stapes Landmarks. Adapted from Schmidt *et al.* (2009)

Number	Abrev.	Name	Description
1.	ARI	Articulation with	The point of articulation between the stapes and the

		the Incus	incus. It is not visible on the exterior surface of the 3D image and is viewed in sagittal section.
2.	MFP	Medial Aspect of the Footplate	Placed at the medial extent of the oval window, and can be used to provide an estimate of the size of the stapedial footplate, a functionally significant measurement.
3.	LFP	Lateral Aspect of the Footplate	Placed at the lateral extent of the oval window, and can be used to provide an estimate of the size of the stapedial footplate, a functionally significant measurement.
4.	SFP	Superior Aspect of the Footplate	Placed at the superior extent of the oval window, and can be used to provide an estimate of the size of the stapedial footplate, a functionally significant measurement.
5.	IFP	Inferior Aspect of the Footplate	Placed at the inferior extent of the oval window, and can be used to provide an estimate of the size of the stapedial footplate, a functionally significant measurement.

Intra-Observer Error Study

A limited number of studies have examined the precision, repeatability, and validation of anthropometric landmarks digitised from computed tomography (CT). All were found to be highly repeatable (Ross and Williams, 2008). An earlier study by Schmidt *et al* (2009) found the sixteen auditory ossicle landmarks in use in the study to be highly repeatable with both between- and within-observers. Nonetheless, the first step before beginning the full-scale study was to undertake a measurement error analysis to quantify the repeatability of proposed landmarks. This trial consisted of three sets of sixteen landmarks taken by a single observer on three specimens. The three specimens (*Callicebus moloch* 1 (CM 2740); *Loris tardigardus* 1 (UM-APC 70); *Tarsius bancanus* (045)) were selected for this study based on the visibility of all sixteen landmarks as previously discussed in Chapter 2. Each specimen underwent two separate landmark placement sessions by a single observer, one week apart. Because the landmark data were collected from objects in a fixed coordinate system, measurement error analysis is relatively straightforward (Valeri *et al.*, 1998).

The palaeontological statistical program PAST (Hammer and Harper, 2006) was used to calculate the Euclidean distance between the pairs of repeated digitized x/y/z landmark coordinates from each species. These inter-landmark linear distances or ILD's allow for simplified multivariate analysis of distance data as they are not sensitive to rotation or translation (Ross and Williams, 2008).

Statistical analyses of the resulting ILD's were performed using SPSS® 17.0 (SPSS, Inc., Chicago, IL). Repeatability, defined here as the between-session variation, was tested with a one-sample t-test to determine if the average deviation for that landmark was zero. With ideal replicability, theoretically the average distance should be not statistically significantly different

from zero. Specific species or landmarks that seem to have the higher magnitude of error are of particular interest, as this would suggest they are less reproducible to the same coordinates. A mixed model analysis of variance (ANOVA) was used to examine all the forty-eight distances for variation in error between-landmarks compared to within-landmarks, grouped by species.

Data Analysis

Once collected, the landmark data in the larger study were subjected to EDMA form comparison utilising WinEDMA software (© 2002 T.M. Cole). Morphometric analyses based on anatomical landmarks, such as EDMA gather data on form. Form refers to the size and shape of an object; these data then invariably contains differences in scales and rotation (Hallgrimsson *et al.*, 2008). Morphometric techniques provide an excellent basis for comparative studies in many contexts, but they have three fundamental limitations that must be considered as part of a research design (Hallgrimsson *et al.*, 2008). Firstly, size and shape represent properties of the same form and can be difficult to separate for analysis, a requirement of many geometric morphometry techniques. Secondly, spatial relationships among measurements are almost always lost in the measurement process. Following this the third limitation finds that the results do not always lend themselves to biologically meaningful visualisation (Hallgrimsson *et al.*, 2008).

To deal with these biases two opposing solutions have been proposed. The first is superimposition-based morphometrics and the other is Euclidean distance matrix analysis (EDMA). Superimposition is used in morphometric analyses solely concerned with shape. To get to this descriptive data the other factors of form such as size, rotation and location, must be removed (Slice, 2005). Various techniques have been developed for reaching shape only data. Bookstein registration was traditionally applied but requires fixed coordinates. More commonly

used is Procrustes Superimposition; a least-squares approach (Slice, 2005). The Procrustes Superimposition method begins by centering shapes at a standard origin and scaled to a common size, the shapes are then rotated to minimise the differences between landmarks. Usually Procrustes Superimposition begins with Principal Component Analysis (PCA) to correct for these factors. PCA is a mathematical approach that transforms a number of possibly correlated variables into the least number of uncorrelated variables known as principle components. These components can then be analysed with multivariate and covariate statistical analyses. Resulting deviations are commonly visualised using thin plate spline deformation (Hallgrimsson *et al.*, 2008).

Leading the charge against superimposition methods, Lele and Richtsmeier (Lele and Richtsmeier 1991; 2001; Richtsmeier *et al.*, 2002) extensively criticised the method on the grounds that the associated variance-covariance matrix becomes inestimable following the superimposition step. They argue that the orientation of an object cannot be accurately determined solely from landmark data yet superimposition theory dictates all specimens must be orientated to a common arbitrary coordinate system. Lele and Richtsmeier (2001) instead suggest the use of EDMA.

EDMA is a linear-distance method based on pair-wise interlandmark chords, essentially all possible distances between all landmarks in sets of two. By comparing distances between landmarks rather than landmark coordinate data, EDMA does not require the a priori assumptions of superimposition techniques. EDMA can examine form, both size and shape or post scaling for common size it can be used to exclusively examine shape (Lele and Richtsmeier, 2001). The ability to analyse both the size and shape of objects statistically is the reason this project used EDMA based methods. Relative changes in the size of the primate auditory ossicles

may have a diagnostic value and are an important variable in this study. The value of this approach to the quantification of morphology has been demonstrated in its previous application in studies of fluctuating asymmetry (Richtsmeier *et al.*, 2005) and temporal bone pneumatisation (Hill and Richtsmeier, 2008) among others.

Although critics of EDMA-based approaches cite the unnecessary production of a large number of variables that inflate the degrees of freedom as a deterrent to the use of this method (Rohlf 2000). The lack of required specific assumptions about common fixed coordinates and the ability to include the size variable make EDMA the most valid approach to quantify and analyse morphological variation in this study of primate auditory ossicles. EDMA does not produce the graphical visualisations of shape difference common to the other analytical techniques (e.g. thin plate spline deformation) but instead provides summary statistics of differences in form as well as confidence intervals for individual linear distances (Richtsmeier *et al.*, 2002). These results were then manually converted to simple graphs in order to illustrate linear-distance changes.

Issues with Landmarks

Due to differences in the scan quality, the internal structures of twenty of the twenty-six samples (see Appendix 1) featured in this study were not visible. This obliteration meant that one landmark, ART, the most invaginated point of the malleolar-incudal articulation could not be visualised or a point placed for further morphometrics (Figure 3.1 and Figure 3.2). Although the ART landmark is important for functional analyses, to determine the effects of its inclusion in the taxonomic analysis, two trials were run using the Ordination procedure of the WinEDMA program. The first trial included the six specimens with all sixteen landmarks visible, the second trial used these same six specimens but did not include the ART landmark. The resulting principal coordinate graph plots were compared for changes in species clustering.

Figure 3.1 – Example of visible malleolar-incudal articulation (*Loris tardigradus* pictured)

Figure 3.2 – Example of incudal obliteration pictured)

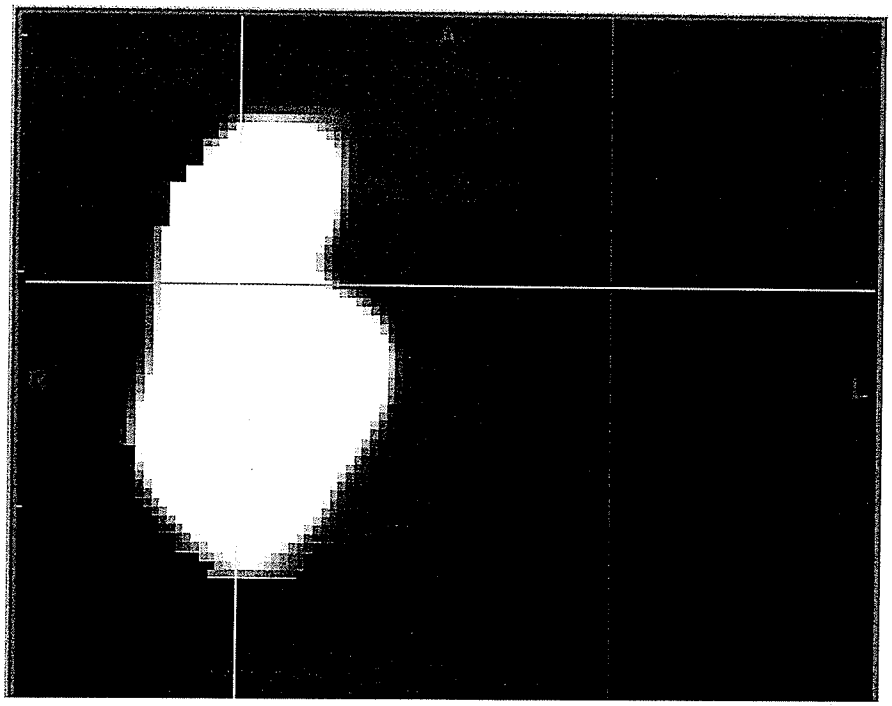

malleolar-articulation (*Arctocebus calabarensis*

Four separate EDMA trials were conducted to obtain comparable data output. The first trial included all twenty-six specimens each with fifteen landmarks. As the WinEDMA software does not allow for gaps in the data, the six specimens that also had the sixteenth landmark, discussed earlier, were included in a separate smaller investigation. Both of these trials were then scaled to by the geometric mean to investigate the effect of size as a variable.

Cluster Analysis

The EDMA based approach was used to explore the data for clustering and ordination, which is the spreading out of the individual specimen forms as points in Euclidean space (Lele and Richtsmeier, 2001). The ordination component of the WinEDMA software was used as the basis for the study. The output of this included the pair-wise distances between all landmarks, Eigenvalues (sometimes called latent root), Eigenvectors, also known as principal coordinate scores and, where applicable, scaling factors.

From the Euclidean pair-wise distances calculated, a square symmetric matrix, known as a matrix of dissimilarity, was created where each row and column corresponds to an individual and the diagonal elements are equal to zero as the dissimilarity between an individual and itself is always zero (Lele and Richtsmeier, 2001). These output were then subjected to Principal Coordinate Analysis (PCoA), cluster analysis and phylogenetic analysis.

Principal Coordinate Analysis, also known as metric multidimensional scaling, results in a similar graphical output to Principal Component Analysis (PCA) but whereas PCA is based on variance- covariance matrices, PCoA is based on dissimilarity matrices. PCoA is an ordination technique used to graphically project a multivariate dataset into two or three dimensions to allow for visualisation of trends and groups and to reduce the overall difference to a few variables (Lele and Richtsmeier, 2001). As with the more commonly applied PCA, each principal coordinate axis has an Eigenvalue associated with it, expressing the relative proportion of overall variation in the data explained by that axis. The first axis is aligned with the greatest dimension of overall variation; the second axis is the next greatest perpendicular, however, to the first. Each subsequent axis explains progressively smaller amounts of variation.

The principal coordinate scores are the values for the individuals along these axes. In PCoA the Euclidean distance in the low-dimensional space (i.e. two or three) should reflect the original distances as measured in multidimensional space e.g. if two samples are similar they should appear close together on a PCoA graph plot. Some Euclidean distance measures can produce negative Eigenvalues, these are mostly connected to the least relevant axes and can be disregarded, however, when large negative values occur the PCoA should be considered suspect (Lele and Richtsmeier, 2001).

The Eigenvectors, after standardising by division by the square root of their corresponding Eigenvalue, are output as the principal coordinate axis. In other words, Eigenvectors give the principal coordinates and Eigenvalues relate the proportion of total variance accounted for. If there are *x* landmarks (variables) and *n* species there will be *n*-1 principal coordinates, as the last Eigenvalue is always zero. If *x* is less than *n* only the first *x* principal coordinate axes will be relevant and the rest will have Eigenvalues close to zero. Principal coordinate axes are rarely easily interpretable in PCoA and tend to demonstrate where individuals fall rather than why (Lele and Richtsmeier, 2001). In order to compare the affect of size on the dataset, PAST, was used to calculate the centroid size for each specimen (Hallgrimsson *et al.*, 2008). Centroid size is defined as the square root of the sum of the squared Euclidean norm of the distances from each landmark to the centroid. Centroid size was chosen as a secondary scaling factor, because this dataset consists of landmark positions and centroid size analysis takes into account all landmarks. After cluster analysis to look for specific families and suborders, the datasets were clustered according to the primates' activity cycles, diet and habitat interaction, in order to discuss possible causes of variation and adaptation.

Data Exploration

The PCoA looked at the equalities and dissimilarities in overall form or shape, however, there may be regions or loci where the forms are different but they may also share similar specific features, as defines by their principal axis scores and landmark distances and to understand this, more in-depth analytical approaches are required (Lele and Richtsmeier, 2001).

This "data exploration" localises form difference to those parts of the ossicle that significantly contribute to the differences observed in the dissimilarity matrices, but they also look for differences in specific loci in forms that are seemingly similar (Richtsmeier *et al.*, 2002). This

also allows for ranking the parts of the shape-form in terms of their relative contribution to the observed dissimilarity. For this study, correlation matrices were created which chart the correlations between distances and principal coordinate axis scores. Each element represents the association of a specific Euclidean linear distance between pair-wise landmarks with the position of specimens along that axis. These correlations were then used to discuss the landmark specific similarities and differences between the samples.

Hierarchical Analyses

To further the objective of using phenogramss to compare the morphological evidence to phylogenetic relationships, the EDMA analysis of the morphological variation of primate auditory ossicles was used to examine similarities and differences between and, where possible, within the species. In order to understand the natural world, biologists classify extinct and living organisms, according to the similarities of their features. Phylogenetics is the scientific field concerned with determining the evolutionary development and diversification of a species, group of organisms or of a particular feature of an organism (Stanford *et al.*, 2009). The description of these phylogenetic relationships is based on hierarchically nested sets of ranks; the taxonomic name indicates common membership to a group and forms the basis of biological classification (Martin, 1990).

At present there is virtually no aspect of primate phylogeny on which all authorities agree (Cartmill, 1975) but the tools used for such analyses are more readily accepted. Data on the relative lengths of skeletal elements have been utilised by many researchers as indicators of taxonomic affinity among primates (Delson and Andrews, 1975). The auditory region contains numerous structures that have proven useful phylogenetic criterion for advancing hypotheses on relationships among various extinct and extant taxa (Masali, 1968; 1992; Cartmill, 1975; Szalay,

1975; MacPhee, 1981; Wible and Covert, 1987), suggesting that a repeatable and in-depth study of the auditory ossicles can provide relevant and useful data for discussions of primate phylogenetic relationships.

The phylogenetic relationships used in this study (Figure 3.3) were based on Purvis (1995), which presents a composite estimate of the phylogeny of all 203 primate species. Although accepted by the author to be incomplete and include as yet unknown inaccuracies, it represents the first attempt to systematically combine the evidence that has accumulated on the whole order. Relationships between the species are visually represented with dendrograms, tree-like diagrams, which indicate how distantly or closely related the groups are. Although traditionally this classification was achieved by comparing observable traits, scientific advancements over the last 30 years in the field of molecular genetics have allowed these methods to take an important role in phylogenetic analysis (Stanford *et al.*, 2009). These phylogenetics trees are not precise reconstructions of relationships or evolutionary events, rather they represent hypotheses about associations of each component inferred from genetic or characteristic data collected from living or extinct populations (Silcox, 2007).

Figure 3.3 - Dendrogram of species relationships, after Purvis (1995).

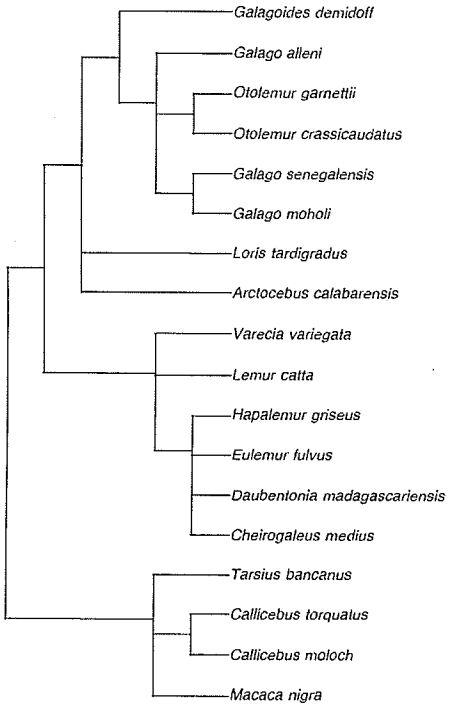

The goal-driven inclusion in the study, of *Daubentonia madagascariensis* and two species of Dermoptera were used to examine the current evidence for placement of *Daubentonia* within primates and to facilitate cluster analyses.

In order to compare morphology-based phenograms with the currently accepted primate phylogeny, the dissimilarity matrices for both form and shape were analysed using clustering methods. It must be noted, however that inconsistencies between the phenogram and the cladogram representing primate phylogeny do not suggest alternative phylogenetic hypotheses but instead represent areas of morphological divergence which may be related to other factors such as adaptive traits. When comparing morphological classifications with a genealogical hypothesis, the comparison is one of hierarchical relationships (Lele and Richtsmeier, 2001). The first step then, is to determine whether or not a hierarchical structure exists within the data.

There are a number of algorithms available for constructing hierarchical clusters and these may yield differing results even when based on the same dissimilarity matrices. The correct method to use then is the one that introduces the least distortion and provides the fullest summary of the information contained within the matrix (Lele and Richtsmeier, 2001). The measure of accuracy used in this study is the cophenetic correlation, which compares the correlation between the elements of the dissimilarity matrix and those implied by the hierarchical clustering, the closer the cophenetic correlation is to 1.0, the "better" an algorithm is considered to be.

In this study three different algorithms were tested. First, unweighted pair-group average (UPGMA) where groups are based on the average distance between all members in the cluster. Second was the single linkage method, also known as the nearest neighbour method, where groups are joined based on the smallest distance between clusters and lastly, Ward's method where groups are clustered to reduce within-group variation. The resulting diagram of hierarchical structure, known as a phenogram, of the highest cophenetic correlation method was then subjected to bootstrap analysis to test the strength of the clusters.

Felsenstein first used bootstrapping in phylogenetic analysis in 1985 (Lele and Richtsmeier, 2001) and almost all subsequent analyses have included it. In bootstrapping, the dissimilarity matrix is resampled using an algorithm that randomly selects columns for replacement, constructing a new bootstrap tree each time. Once a large number of bootstrap trees have accumulated, each node in the phenogram is assigned a bootstrap proportion representing the portion of resamplings where the included specimens were grouped together in the bootstrap trees. The closer the probabilities are to 100%, the stronger the likelihood of the morphological relationship being repeated, a probability closer to 0% suggest little or no repeatable relationship

because the clusters are unlikely to be reproduced during resampling. The bootstrap results refer only to consistency within the datasets represented and do not infer that the clusters represent real-world groups. The bootstrapped morphometric phenogram was then compared to the cladogram based on Purvis (1995) to allow inferences and discussion of auditory ossicle morphology and taxonomic relationships.

CHAPTER IV – RESULTS

Intra-Observer Error Trial

Table 4.1 shows the inter-landmark distances for all the repeated landmarks. To determine if the average landmark specific deviation was zero, a one-sample t-test was conducted for each landmark distance across the three species (Table 4.2). Only three landmark

coordinates showed statistically significant differences ($p<0.05$) and therefore may be less reproducible. The three significant error-prone landmarks were LAT ($p = 0.017$), MFP ($p = 0.011$) and SFP ($p = 0.013$); MAH was the least error-prone. The mixed model ANOVA of all forty-eight distances (Table 4.3) detected no significant error, suggesting there is no more variation in error between-landmarks than there are within-landmarks, although certain pairs of comparisons do show significant differences.

Table 4.1: Inter-landmark distances determined for the three species included in the error measurement trials. Measured using PAST software (Hammer and Harper, 2006).

Landmark Name	***Callicebus moloch* 1**	***Loris tardigradus* 1**	***Tarsius bancanus***
1. MAN	0.02	0.064807	0.043589
2. LAT	0.041231	0.064031	0.04899
3. HEA	0.27459	0.22672	0.073485
4. ART	0.11091	0.045826	0.083666
5. IAM	0.12124	0.022361	0.05099
6. LCR	0.064031	0.028284	0.089443
7. SCR	0.18682	0.08124	0.05099
8. IAR	0.24352	0.088318	0.22226
9. SAR	0.2161	0.086023	0.1118
10. MAH	0.5361	0.13638	0.098489
11. IAI	0.30561	0.05	0.3178
12. ARI	0.16523	0.07874	0.060828
13. MFP	0.10488	0.096954	0.13601
14. LFP	0.064807	0.15297	0.11489

15. SFP	0.057446	0.074833	0.05099
16. IFP	0.17916	0.071414	0.10677

Table 4.2: Results of one-sample t-test on inter-landmark distances determined for the three species included in the error measurement trials. Statistical analyses performed using SPSS® 17.0 (SPSS, Inc., Chicago, IL).

One-Sample Test

	Test Value = 0					
					95% Confidence Interval of the Difference	
	t	df	Sig. (2-tailed)	Mean Difference	Lower	Upper
MAN	3.307	2	.081	.04280	-.0129	.0985
LAT	7.683	2	**.017**	.051417333	.02262073	.08021394
HEA	3.159	2	.087	.19159833	-.0693657	.4525623
ART	4.246	2	.051	.08013400	-.0010611	.1613291
IAM	2.208	2	.158	.06486367	-.0615256	.1912529
LCR	3.415	2	.076	.060586000	-.01573837	.13691037
SCR	2.583	2	.123	.10635000	-.0707976	.2834976
IAR	3.802	2	.063	.18469933	-.0243231	.3937217
SAR	3.470	2	.074	.1379743	-.033122	.309070
MAH	1.836	2	.208	.2569897	-.345309	.859289
IAI	2.571	2	.124	.22447000	-.1511772	.6001172
ARI	3.152	2	.088	.10159933	-.0370871	.2402858
MFP	9.448	2	**.011**	.11261467	.0613299	.1638994
LFP	4.344	2	.049	.110889000	.00104672	.22073128
SFP	8.580	2	**.013**	.061089667	.03045516	.09172417
IFP	3.756	2	.064	.11911467	-.0173229	.2555523

Table 4.3: Results of ANOVA on inter-landmark distances determined for the three species included in the error measurement trials. Statistical analyses performed using SPSS® 17.0 (SPSS, Inc., Chicago, IL).

ANOVA

Distance

	Sum of Squares	df	Mean Square	F	Sig.
Between Groups	.187	15	.012	1.613	.125
Within Groups	.247	32	.008		
Total	.434	47			

Morphometric Analysis

The first step in the EDMA-based approach was to calculate the distance between all the landmarks in pairs for each specimen (Appendix 2). The number of distances measured can be calculated as $n(n\text{-}1)/2$ pair-wise distances per x individuals, with n the number of landmarks observed. For the studies containing sixteen landmarks, this equals one hundred and twenty pair-wise distances for each of the five individuals and one hundred and five pair-wise distances for the twenty-six individuals in the fifteen-landmark trial. It should be noted that these are dissimilarities between individuals, not to be confused with the inter-landmark distances used in the error study. The relative distances between forms were collected into dissimilarity matrices.

The dissimilarity matrices of the fifteen and sixteen landmark trials (Tables 4.4 and 4.5) are form difference matrices, in that they represent both size and shape. The two trials scaled for

geometric mean resulted in a shape difference matrix (Tables 4.6 and 4.7). Because the dissimilarity matrices are symmetrical, only the below diagonal elements are needed to record the distance difference. So the matrix is written as a triangle rather than a rectangle with a line of zeros in the middle and everything repeated above. The closer an entry in the matrix is to one the less distance difference exists between the relative positions of the corresponding landmark pair.

Table 4.4 – Dissimilarity matrix based on form for non-scaled fifteen-landmark trial

Acalabal	0.000																														
Cmolochl	3.797	0.000																													
Ctorquat	3.697	2.329	0.000																												
Cmediusl	3.180	2.935	3.277	0.000																											
Cmedius	2.963	4.333	4.727	2.090	0.000																										
Cvariega	3.957	3.213	3.497	3.031	3.894	0.000																									
Cvolans	3.809	3.250	3.632	2.338	3.238	2.177	0.000																								
Dmadagas	6.951	5.290	4.560	6.506	7.949	4.871	5.741	0.000																							
Efalbifo	4.833	3.280	2.967	3.959	5.391	2.976	3.919	3.714	0.000																						
Efrufus	4.493	3.404	2.907	3.447	4.831	2.770	3.515	4.070	2.523	0.000																					
Galleni2	2.304	2.489	2.921	1.468	2.349	2.800	2.319	6.184	3.744	3.373	0.000																				
Gelegan1	2.303	3.884	4.131	2.777	2.460	3.881	3.716	7.142	4.739	4.302	1.920	0.000																			
Gmoholi1	2.265	3.049	3.365	1.978	2.170	3.028	2.868	6.699	4.184	3.703	1.192	1.719	0.000																		
Gmoholi2	2.376	3.111	3.622	2.143	2.334	3.293	3.131	6.893	4.443	3.883	1.429	1.778	1.520	0.000																	
Gsenegal	2.740	3.009	3.392	2.105	2.626	3.352	2.825	6.473	4.272	3.646	1.410	1.878	1.320	1.887	0.000																
Gdemidol	3.733	5.053	5.649	3.295	2.232	4.993	4.548	9.020	6.284	5.691	3.214	2.546	2.806	2.585	3.150	0.000															
Hgriseus	3.186	2.825	2.636	2.290	3.383	2.109	2.488	4.883	2.878	1.880	2.072	3.119	2.548	2.637	2.684	4.549	0.000														
Lcatta2	4.183	2.890	2.562	3.143	4.594	2.368	3.207	3.988	1.865	1.145	2.933	3.948	3.374	3.470	3.363	5.416	1.671	0.000													
Ltardig1	2.580	3.228	3.530	1.912	2.160	3.309	3.357	6.698	4.149	3.607	1.684	1.811	1.630	1.652	1.800	2.790	2.533	3.280	0.000												
Ltardig2	2.616	3.770	4.348	2.577	2.202	3.955	3.396	7.548	5.120	4.489	2.098	2.293	2.231	1.659	2.375	2.724	3.140	4.165	2.128	0.000											
Mnigra1	5.197	3.582	2.917	4.878	6.255	3.729	4.725	3.941	3.063	2.904	4.592	5.754	4.840	5.100	5.136	7.157	3.611	2.937	5.078	5.774	0.000										
Mnigra2	4.979	3.226	2.304	4.548	6.025	3.726	4.484	3.790	2.891	2.928	4.272	5.525	4.661	4.862	4.912	7.011	3.379	2.796	4.900	5.615	1.246	0.000									
Ocrassil	3.978	2.521	1.908	3.450	4.883	3.135	3.771	4.212	2.519	2.316	2.968	4.025	3.356	3.578	3.294	5.671	2.506	1.914	3.387	4.280	2.801	2.356	0.000								
Ogarnett	3.281	2.498	2.482	2.795	3.910	2.715	3.244	5.016	2.691	2.857	2.094	2.889	2.557	2.625	2.590	4.561	2.273	2.084	2.360	3.308	3.895	3.568	1.919	0.000							
Tbancanu	4.132	4.411	3.966	3.307	4.080	3.685	3.816	5.912	3.807	2.819	3.358	3.721	3.646	3.542	3.729	4.701	2.622	2.840	3.249	3.871	4.631	4.657	3.968	3.497	0.000						
V.v.vari	5.640	4.074	3.370	4.541	6.148	3.527	4.348	3.450	2.686	2.114	4.606	5.728	4.078	5.234	4.011	7.021	3.430	2.222	4.888	5.055	2.825	2.808	2.962	3.711	4.040	0.000					

Table 4.5 – Dissimilarity matrix based on form for non-scaled sixteen-landmark trial

Cmolochl	0.000					
Ctorquat	2.437	0.000				
Ltardig1	3.382	3.781	0.000			
Mnigra2	3.369	2.409	5.209	0.000		
Tbancanu	4.553	4.120	3.437	4.920	0.000	
V.v.vari	4.180	3.414	5.169	2.942	4.246	0.000

Table 4.6 – Dissimilarity matrix based on shape for scaled fifteen-landmark trial

Acalabal	0.000																														
Cmoloch1	3.257	0.000																													
Ctorquat	2.628	2.237	0.000																												
Cmedius1	3.178	2.112	1.875	0.000																											
Cmedius	2.444	2.370	2.014	1.358	0.000																										
Cvariega	3.609	3.196	3.357	2.504	2.072	0.000																									
Cvolans	3.749	2.990	3.080	2.210	2.225	1.961	0.000																								
Dmadagas	3.925	3.696	3.311	2.903	2.872	2.606	2.713	0.000																							
Efalbifo	3.756	3.094	2.934	2.429	2.613	2.615	3.126	2.554	0.000																						
Efrufus	3.792	3.373	2.900	2.377	2.578	2.656	3.058	2.345	2.443	0.000																					
Galleni2	2.293	1.793	1.700	1.435	1.380	2.428	2.275	2.805	2.469	2.570	0.000																				
Gelegan1	2.175	2.784	2.407	2.694	2.282	3.068	3.428	2.976	2.835	2.913	1.650	0.000																			
Gmoholi1	2.259	2.201	1.926	1.977	1.550	2.451	2.744	3.183	2.697	2.668	1.129	1.611	0.000																		
Gmoholi2	2.349	2.083	2.088	2.125	1.927	2.632	2.955	3.219	2.861	2.722	1.304	1.733	1.507	0.000																	
Gsenegal	2.740	2.245	2.115	2.105	2.064	2.905	2.730	2.899	2.948	2.691	1.382	1.740	1.315	1.862	0.000																
Gdamidol	2.666	2.165	2.172	2.114	2.026	2.646	3.139	3.410	2.741	2.674	1.507	1.741	1.358	1.264	1.832	0.000															
Hgriseus	2.895	2.755	2.310	1.800	1.552	2.088	2.401	2.105	2.315	1.539	1.753	2.317	2.068	2.026	2.302	2.266	0.000														
Lcatta2	3.448	2.859	2.552	1.961	2.178	2.247	2.725	2.138	1.740	1.144	2.002	2.411	2.235	2.144	2.334	2.122	1.309	0.000													
Ltardig1	2.563	2.314	2.014	1.900	1.664	2.695	3.212	2.908	2.463	2.382	1.601	1.752	1.624	1.651	1.783	1.555	1.940	1.908	0.000												
Ltardig2	2.412	2.330	2.418	2.404	2.100	2.950	2.946	3.380	3.128	2.904	1.693	2.279	2.061	1.525	2.172	2.204	2.090	2.432	2.004	0.000											
Mnigra1	3.200	2.870	2.505	2.512	2.414	2.791	3.263	3.583	2.875	2.366	2.473	3.093	2.311	2.484	3.031	2.493	2.323	2.377	2.546	2.692	0.000										
Mnigra2	2.894	2.450	1.790	1.888	1.869	2.824	2.953	3.395	2.709	2.425	1.900	2.722	2.000	2.046	2.700	2.174	2.003	2.234	2.257	2.425	1.245	0.000									
Ocrassi1	2.839	2.379	1.899	1.910	1.982	2.911	3.126	3.007	2.506	2.285	1.500	1.909	1.610	1.705	1.672	1.731	2.039	1.868	1.398	1.971	2.477	1.988	0.000								
Ogarnett	2.864	2.473	2.271	2.230	2.136	2.715	3.110	2.836	2.273	2.739	1.580	1.672	1.857	1.748	1.995	1.746	2.257	1.936	1.404	2.030	2.990	2.592	1.508	0.000							
Tbancanu	4.099	4.171	3.374	3.252	3.442	3.515	3.812	2.774	2.849	2.088	3.345	3.496	3.583	3.432	3.686	3.508	2.492	2.151	3.146	3.557	2.939	3.031	3.254	3.324	0.000						
V.v.vari	4.202	3.643	3.159	2.387	2.842	2.702	3.040	2.840	2.583	1.613	2.033	3.501	3.040	3.208	3.076	2.907	2.404	1.720	2.700	3.530	2.807	2.885	2.702	3.006	2.384	0.000					

Table 4.7 – Dissimilarity matrix based on shape for scaled sixteen-landmark trial

Cmoloch1	0.000					
Ctorquat	2.336	0.000				
Ltardig1	2.362	2.141	0.000			
Mnigra2	2.552	1.882	2.405	0.000		
Tbancanu	4.312	3.509	3.301	3.286	0.000	
V.v.vari	3.711	3.186	2.801	2.929	2.562	0.000

Principal Coordinate Analysis

In order to conduct a principal coordinate analysis, principal coordinate axes (Eigenvectors) and Eigenvalues were determined for the four studies (Tables 4.8, 4.9, 4.10 and 4.11). For convenience the Eigenvalues have been converted into percentages of their sum. The principal coordinate axes have been given in order of diminishing proportion of overall variation. No negative Eigenvalues occur in any of the four studies also of note is that once scaled, the Eigenvalues are very similar suggesting that the greatest cause of variation is size. For the complete principal axis scores, see Appendix 3. To confirm that the first principal coordinate of the non-scaled data represents size, the positions of the specimens on this axis were compared to an ordered table of the species based on centroid size (Table 4.12). The results are very similar confirming size is the main variable affecting the non-scaled dataset.

Table 4.8 – Principal Coordinate Axes and Eigenvalues for non-scaled fifteen-landmark trial

Principal Coordinate Axis	Eigenvalue	% Explained	Cumulative
1	109.85427	60.76	60.76
2	17.06916	9.44	70.2
3	11.45538	6.34	76.54
4	9.43531	5.22	81.76
5	7.25500	4.01	85.77
6	4.99963	2.77	88.54
7	4.01192	2.22	90.76
8	3.79823	2.10	92.86
9	2.67026	1.48	94.34
10	2.08788	1.15	95.49
11	1.83988	1.02	96.51
12	1.72728	0.96	97.47
13	1.28788	0.71	98.18
14	0.80911	0.45	98.63

15	0.62638	0.35	98.98
16	0.44437	0.25	99.23
17	0.40043	0.22	99.45
18	0.27770	0.15	99.6
19	0.22337	0.12	99.72
20	0.16509	0.09	99.81
21	0.11062	0.06	99.87
22	0.09558	0.05	99.92
23	0.06685	0.04	99.96
24	0.05841	0.03	99.99
25	0.03923	0.02	100.01
26	0.00000	0.00	100.01

Table 4.9 – Principal Coordinate Axes and Eigenvalues for non-scaled sixteen-landmark trial

Principal Coordinate Axis	Eigenvalue	% Explained	Cumulative
1	19.72862	50.97	50.97
2	11.81470	30.52	81.49
3	3.53638	9.14	90.63
4	2.12668	5.49	96.12
5	1.49870	3.87	99.99
6	0.00000	0.00	99.99

Table 4.10 – Principal Coordinate Axes and Eigenvalues for scaled fifteen-landmark trial

Principal Coordinate Axis	Eigenvalue	% Explained	Cumulative
1	24.50904	30.23	30.23
2	11.51350	14.20	44.43
3	9.89531	12.21	56.64
4	7.32171	9.03	65.67
5	5.11594	6.31	71.98
6	4.30898	5.32	77.3
7	3.88315	4.79	82.09
8	2.82331	3.48	85.57
9	2.45775	3.03	88.6
10	1.88455	2.32	90.92
11	1.73293	2.14	93.06
12	1.48367	1.83	94.89
13	0.96214	1.19	96.08
14	0.79735	0.98	97.06
15	0.62527	0.77	97.83
16	0.43329	0.53	98.36
17	0.34184	0.42	98.78
18	0.27481	0.34	99.12
19	0.22292	0.27	99.39
20	0.15011	0.19	99.58
21	0.10636	0.13	99.71
22	0.09256	0.11	99.82
23	0.06020	0.07	99.89
24	0.03932	0.05	99.94
25	0.02956	0.04	99.98
26	0.00000	0.00	99.98

Table 4.11 – Principal Coordinate Axes and Eigenvalues for scaled sixteen-landmark trial

Principal Coordinate Axis	Eigenvalue	% Explained	Cumulative
1	11.90955	54.56	54.56
2	3.55416	16.28	70.84
3	2.78216	12.75	83.59
4	2.10116	9.63	93.22
5	1.48009	6.78	100
6	0.00000	0.00	100

Table 4.12 – Species sorted by ascending centroid size

Species	Centroid Size
Galagoides demidoff 1	3.84135
Cheirogaleus medius 2	4.28326
Galago elegantulus 1	4.65128
Loris tardigradus 2	4.67854
Galago moholi 2	4.90312
Loris tardigradus 1	4.9089
Galago moholi 1	4.91877
Arctocebus calabarensis 1	4.9198
Cheirogaleus medius 1	5.11904
Galago senegalensis	5.15687

Galago alleni 2	5.17755
Tarsius bancanus	5.47411
Cynocephalus volans	5.63872
Hapalemur griseus	5.93376
Otolemur garnettii	5.95082
Galeopterus variegatus	6.02035
Callicebus moloch 1	6.20466
Callicebus torquatus	6.55684
Lemur catta 2	6.64203
Eulemur fulvus rufus	6.78842
Otolemur crassicaudatus 1	6.79493
Eulemur fulvus albifrons	6.99904
Varecia variegata variegata	7.45403
Macaca nigra 2	7.57578
Macaca nigra 1	7.60457
Daubentonia madagascariensis	9.4346

Obliteration of the ART Landmark

The PCoA graph plots of the six-specimen sixteen- and fifteen-landmark trials (Figure 4.1) show little difference in spread, suggesting that the loss of the sixteenth landmark in the larger study does not greatly affect cluster analysis. These conclusions remain true when the two trials are scaled to a geometric mean (Figure 4.2).

Figure 4.1 – Principal Coordinate Analysis plots for the non-scaled sixteen- and fifteen-landmark trials

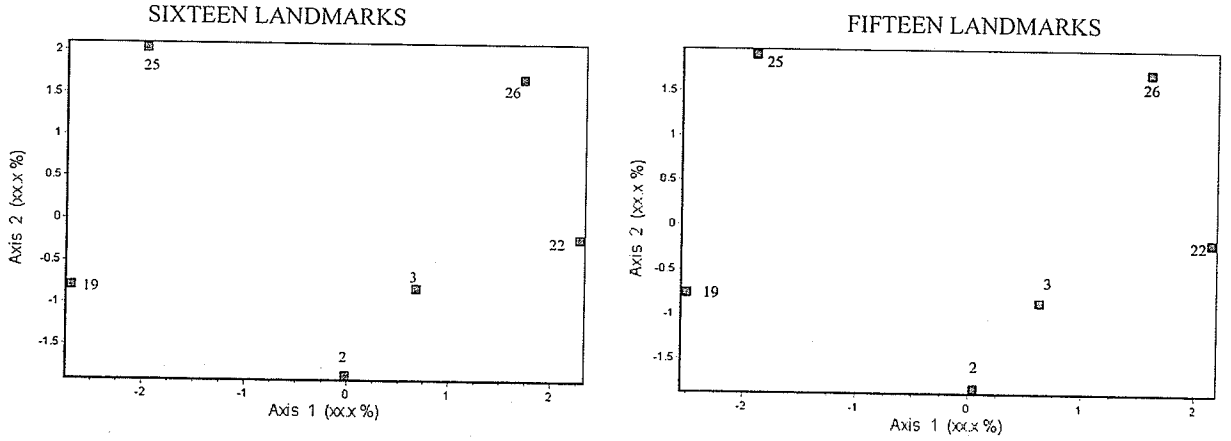

Legend - Six Specimen Trial

2	*Callicebus moloch* 1	22	*Macaca nigra* 2
3	*Callicebus torquatus*	25	*Tarsius bancanus*
19	*Loris tardigradus* 1	26	*Varecia variegata variegata*

Figure 4.2 – Principal Coordinate Analysis plots for the scaled sixteen- and fifteen-landmark trials

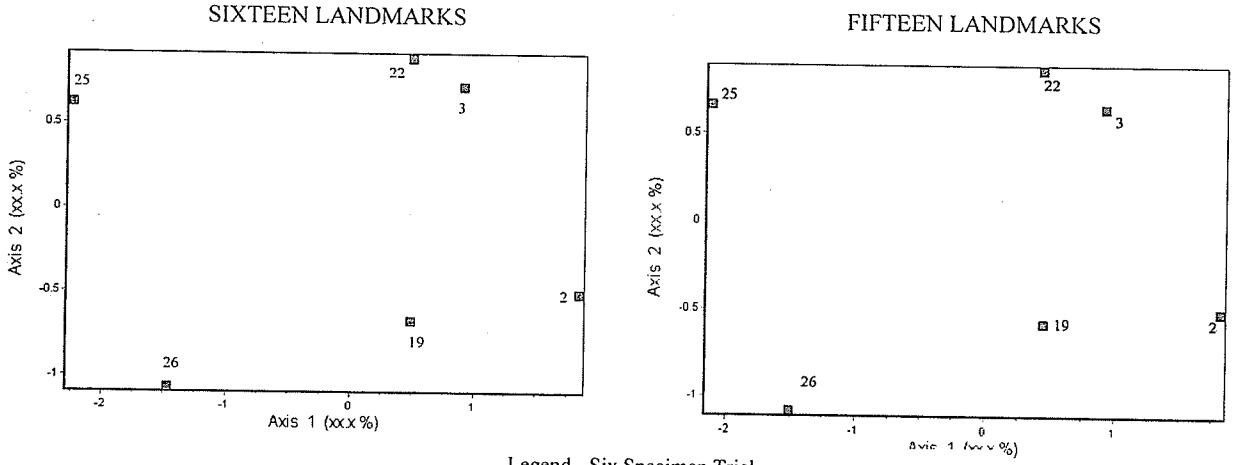

Legend - Six Specimen Trial

2	*Callicebus moloch* 1	22	*Macaca nigra* 2
3	*Callicebus torquatus*	25	*Tarsius bancanus*
19	*Loris tardigradus* 1	26	*Varecia variegata variegata*

Cluster Analysis

Viewed as a PCoA plot, the graphic nature of the data presentation lends itself to intuitive visualisations. When compared with the accepted dendrogram of the sample species (Figure 4.3) both the scaled and non-scaled PCoA plots are in good accordance with the expected phylogenetic relationships. This visual form of grouping analysis is productive as a preliminary step for understanding the data, as unlike the dendrogram, a PCoA plot does not enforce an artificial visual hierarchy upon the dataset, also the relative distances between the species are more evident.

Figure 4.4 shows a scatter plot of the non-scaled fifteen-landmark trial using the first two principal coordinates, which explain 70.2% of the overall variation in the distance matrix. Overall, the non-scaled trial has high variability (dissimilarity) in the PCoA plot but the species represented group well into their accepted phylogenetic relationships (Figure 4.5). After scaling for geometric mean to remove size as a variable, the first two principal coordinates of the fifteen-landmark trial (Figure 4.6) explain only 44.43% of the overall variation in the distance matrix. The specimens group much closer together on the plot (Figure 4.7), with less dissimilarity but do not cluster according to their phylogenetic relationships as well as when form is scored. These results suggest that size is the major factor affecting position along the first principal coordinate in the non-scaled analysis, making this an important grouping factor and suggesting that clustering of species into phylogenetic groups on the PCoA plot is less to do with shape and more related to the overall size of the ossicular chain.

When examined for primate suborders (Figure 4.8), again the separation into the haplorrhine and strepsirrhine clades is more evident in the non-scaled plot. This is particularly obvious with the

grouping of the Tarsiidae, Cercopithicidae and Pitheciidae families representing the haplorrhines, once scaled their principal coordinate scores become more dissimilar.

As expected the form (non-scaled) score of the percussive forager, *Daubentonia madagascariensis* is significantly different to the other groups lying separately in the PCoA plot. When scaled to a geometric mean, however, the *D. madagascariensis* specimen becomes more similar to the other primate groups. Opposite to the daubentonid specimen, the two representatives of Cynocephalidae were similar to the primate species, lying close to the Lemuridae, in the form plot but became significant outliers when the specimens were scaled to compare shape only difference. The unexpected outlier was *Tarsius bancanus*, which in both form- and shape- dissimilarity matrices was distinguishable from the other species.

Figure 4.3 - Dendrogram of species relationships After Purvis (1995).

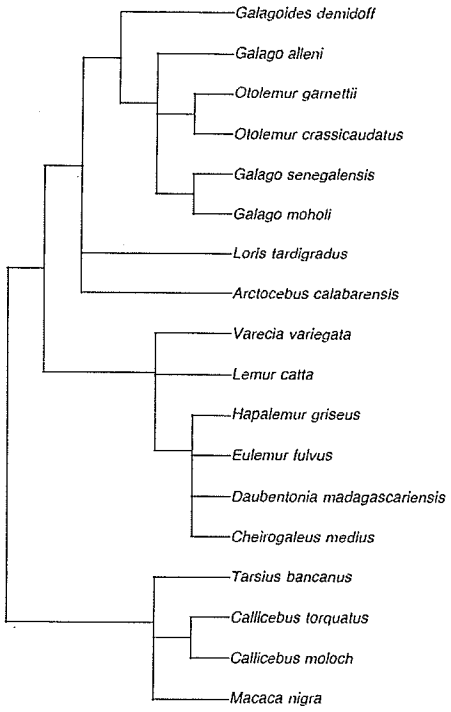

Figure 4.4 – Principal Coordinate Analysis plot for the non-scaled fifteen-landmark trial

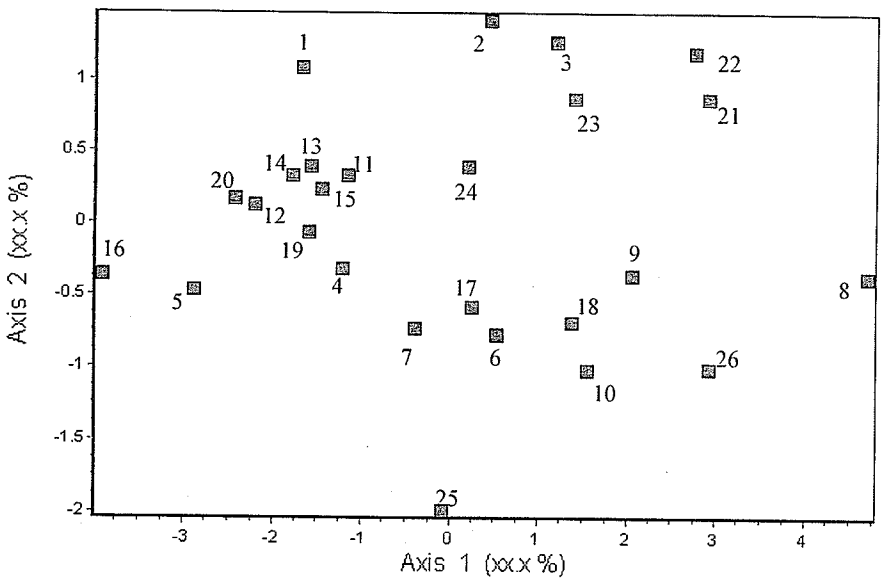

Fifteen-landmark Trial - Legend

1	*Arctocebus calabarensis 1*
2	*Callicebus moloch* 1
3	*Callicebus torquatus*
4	*Cheirogaleus medius* 1
5	*Cheirogaleus medius* 2
6	*Galeopterus variegatus*
7	*Cynocephalus volans*
8	*Daubentonia madagascariensis*
9	*Eulemur fulvus albifrons*
10	*Eulemur fulvus rufus*
11	*Galago alleni 2*
12	*Galago elegantulus* 1
13	*Galago moholi* 1
14	*Galago moholi* 2
15	*Galago senegalensis*
16	*Galagoides demidoff* 1
17	*Hapalemur griseus*
18	*Lemur catta 2*
19	*Loris tardigradus* 1
20	*Loris tardigradus* 2
21	*Macaca nigra* 1
22	*Macaca nigra* 2
23	*Otolemur crassicaudatus* 1
24	*Otolemur garnettii*
25	*Tarsius bancanus*
26	*Varecia variegata variegata*

Figure 4.5 – Principal Coordinate Analysis plot for the non-scaled fifteen-landmark trial showing primate family clustering

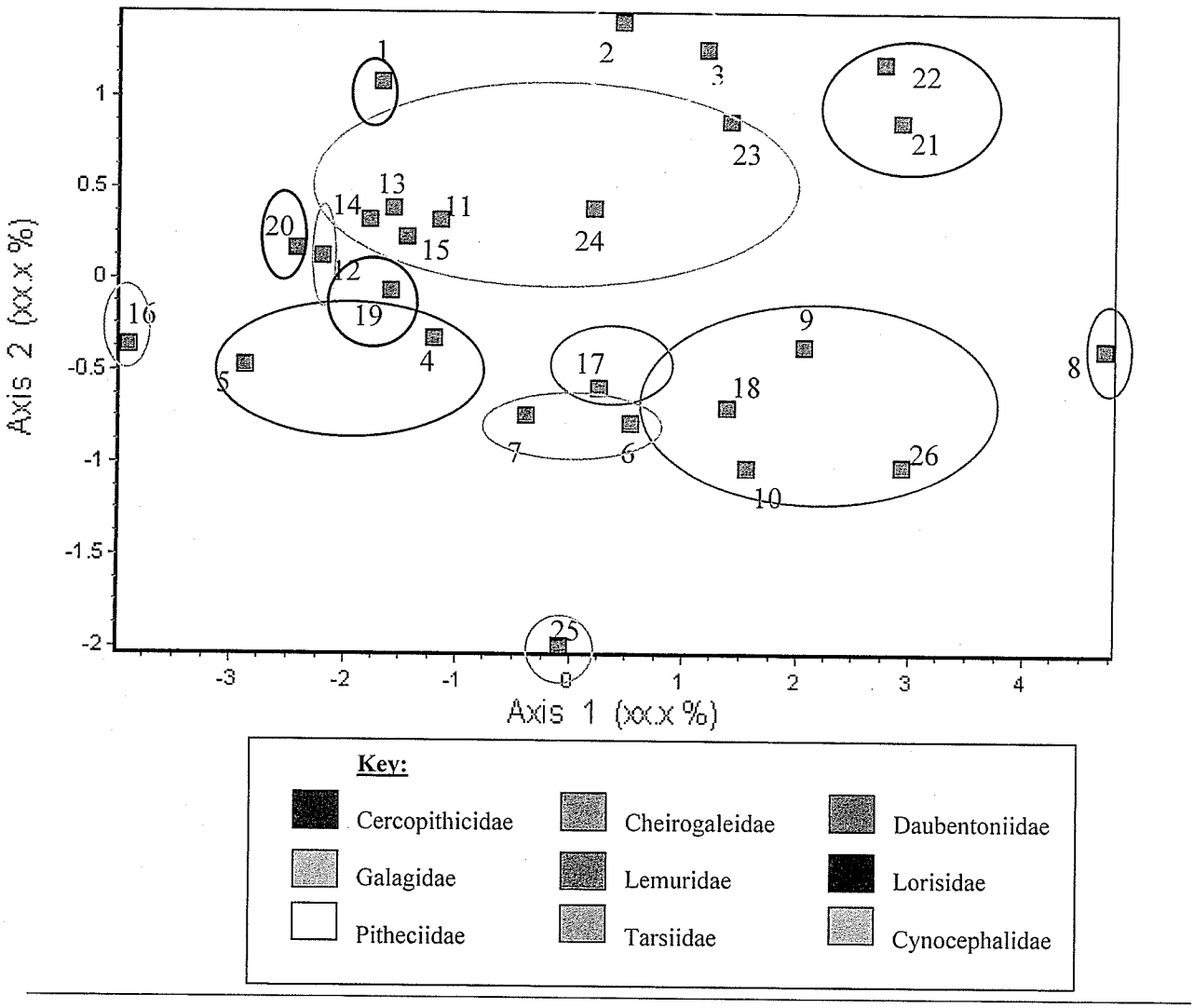

Figure 4.6 – Principal Coordinate Analysis plot for the scaled fifteen-landmark trial

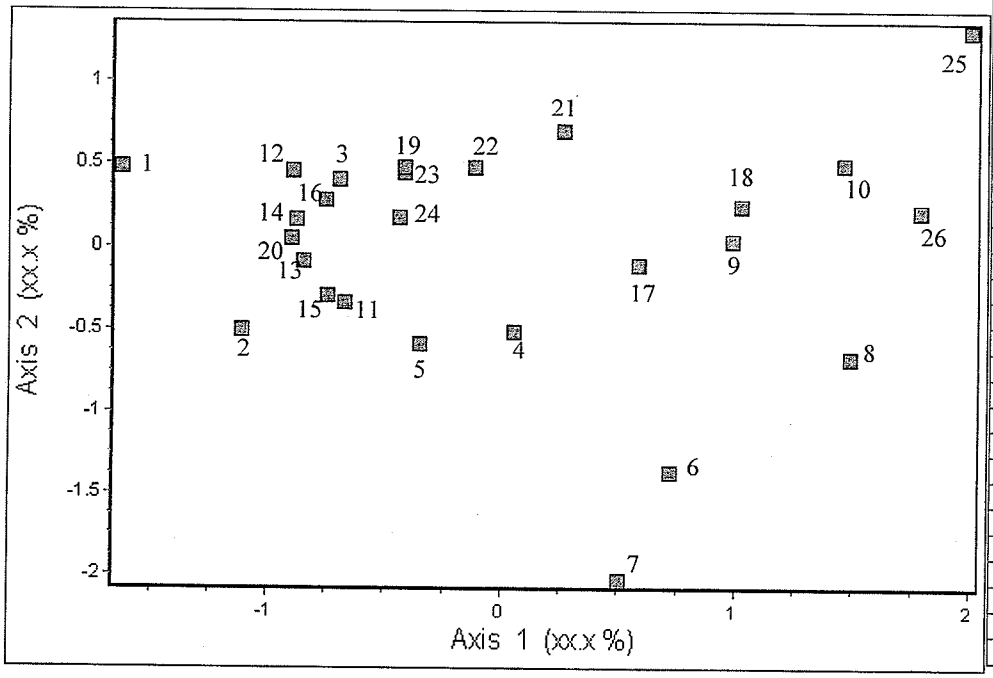

Fifteen-landmark Trial - Legend	
1	*Arctocebus calabarensis 1*
2	*Callicebus moloch* 1
3	*Callicebus torquatus*
4	*Cheirogaleus medius* 1
5	*Cheirogaleus medius* 2
6	*Galeopterus variegatus*
7	*Cynocephalus volans*
8	*Daubentonia madagascariensis*
9	*Eulemur fulvus albifrons*
10	*Eulemur fulvus rufus*
11	*Galago alleni 2*
12	*Galago elegantulus* 1
13	*Galago moholi* 1
14	*Galago moholi* 2
15	*Galago senegalensis*
16	*Galagoides demidoff* 1
17	*Hapalemur griseus*
18	*Lemur catta 2*
19	*Loris tardigradus* 1
20	*Loris tardigradus* 2
21	*Macaca nigra* 1
22	*Macaca nigra* 2
23	*Otolemur crassicaudatus* 1
24	*Otolemur garnettii*
25	*Tarsius bancanus*
26	*Varecia variegata variegata*

Figure 4.7 – Principal Coordinate Analysis plot for the scaled fifteen-landmark trial showing primate family clustering

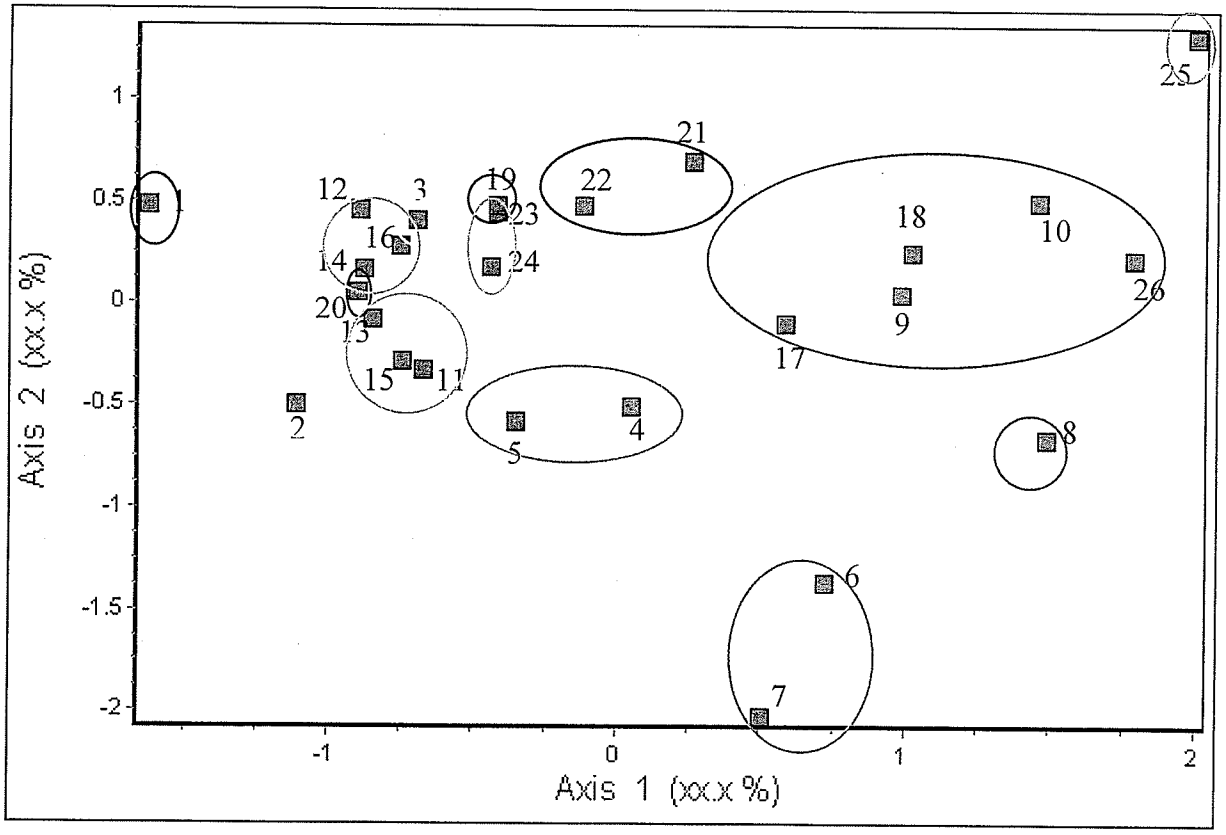

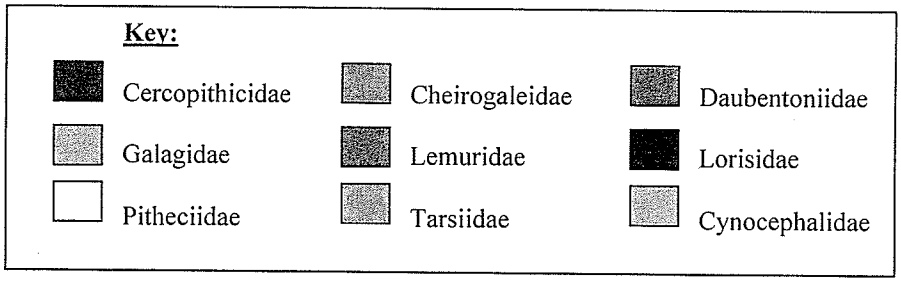

Figure 4.8 – Principal Coordinate Analysis plot for the non-scaled and scaled fifteen-landmark trial showing the relative clustering of the haplorrhine and strepsirrhine clades

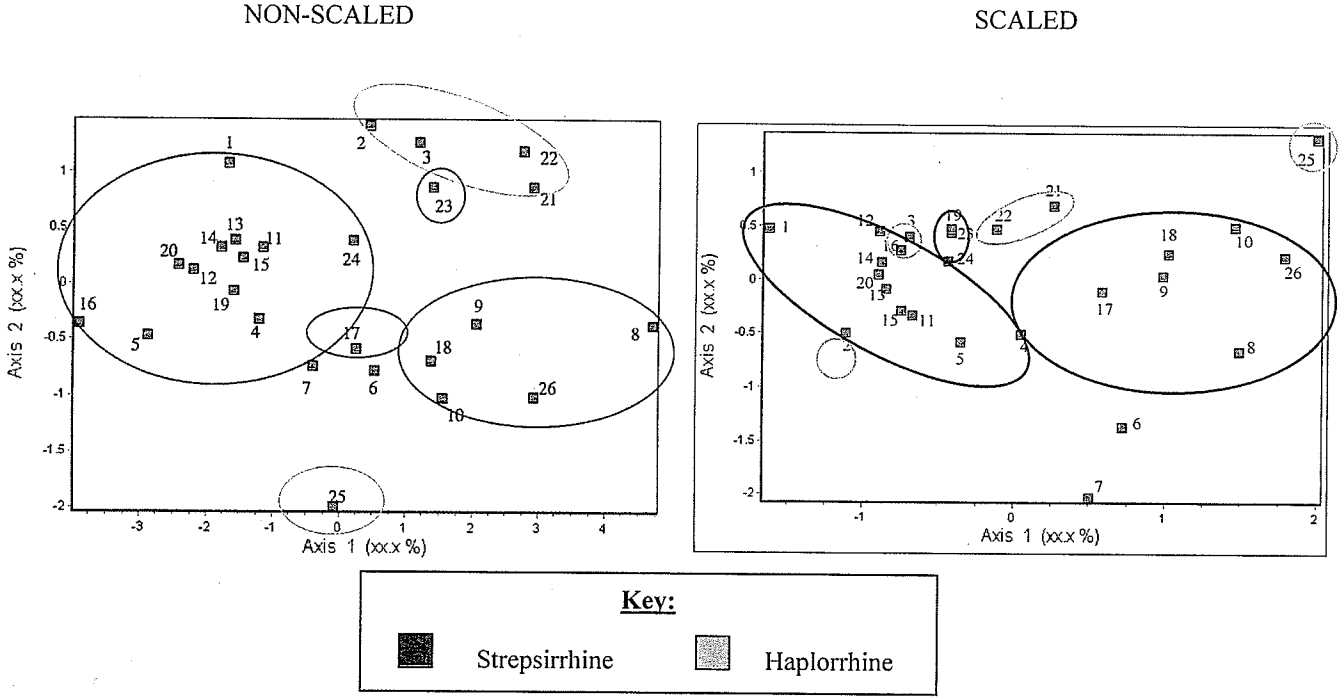

Classification Analyses

In order to examine possible causal factors of variation the species were grouped according to their activity cycles, diet and habitat interaction based on current knowledge of the living species (Wilson and Reeder, 2005). There is little visible clustering according to activity cycle. The classification of the principal coordinate axis scores into the diet-type groups was not strong. The results of the habitat interaction clustering do not group well; this is in part due to the small number of representatives of the terrestrial groups.

Figure 4.9 – Principal Coordinate Analysis plot for the non-scaled and scaled fifteen-landmark datasets clustered according to species activity patterns based on Wilson and Reeder (2005)

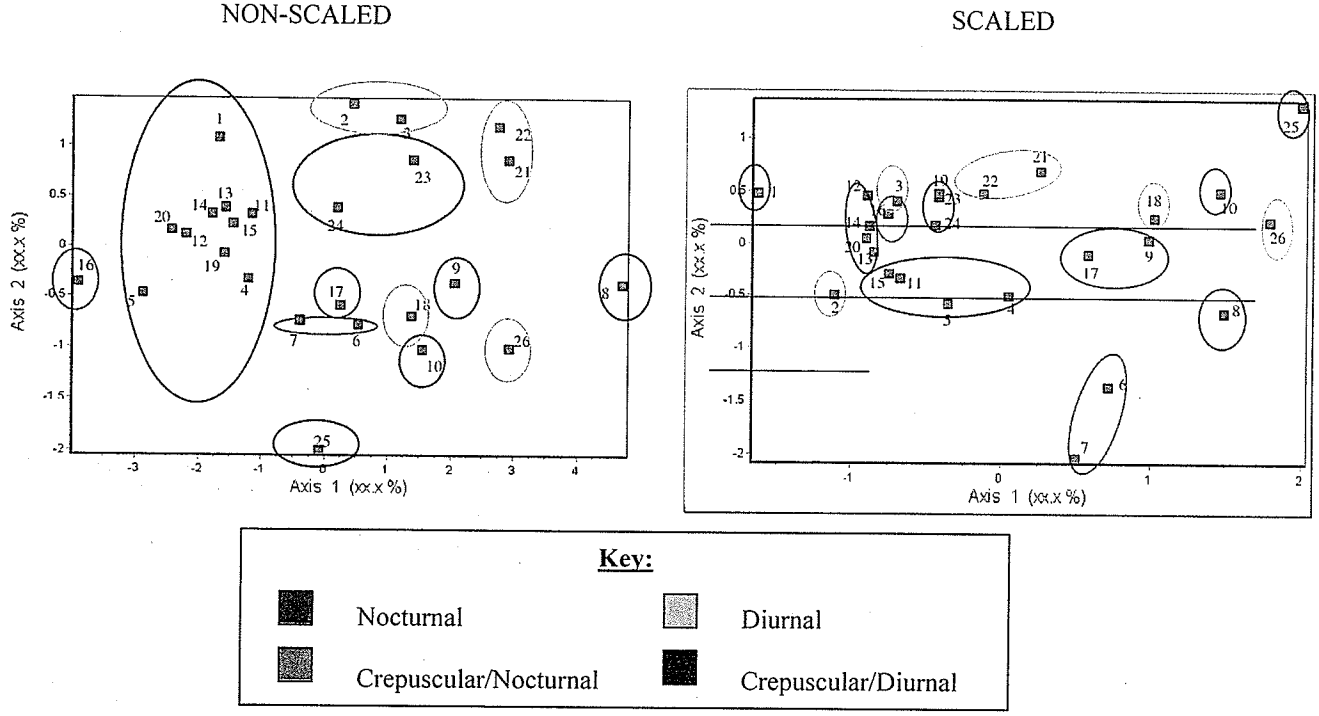

Figure 4.10 – Principal Coordinate Analysis plot for the non-scaled and scaled fifteen-landmark datasets clustered according to species diet based on Wilson and Reeder (2005)

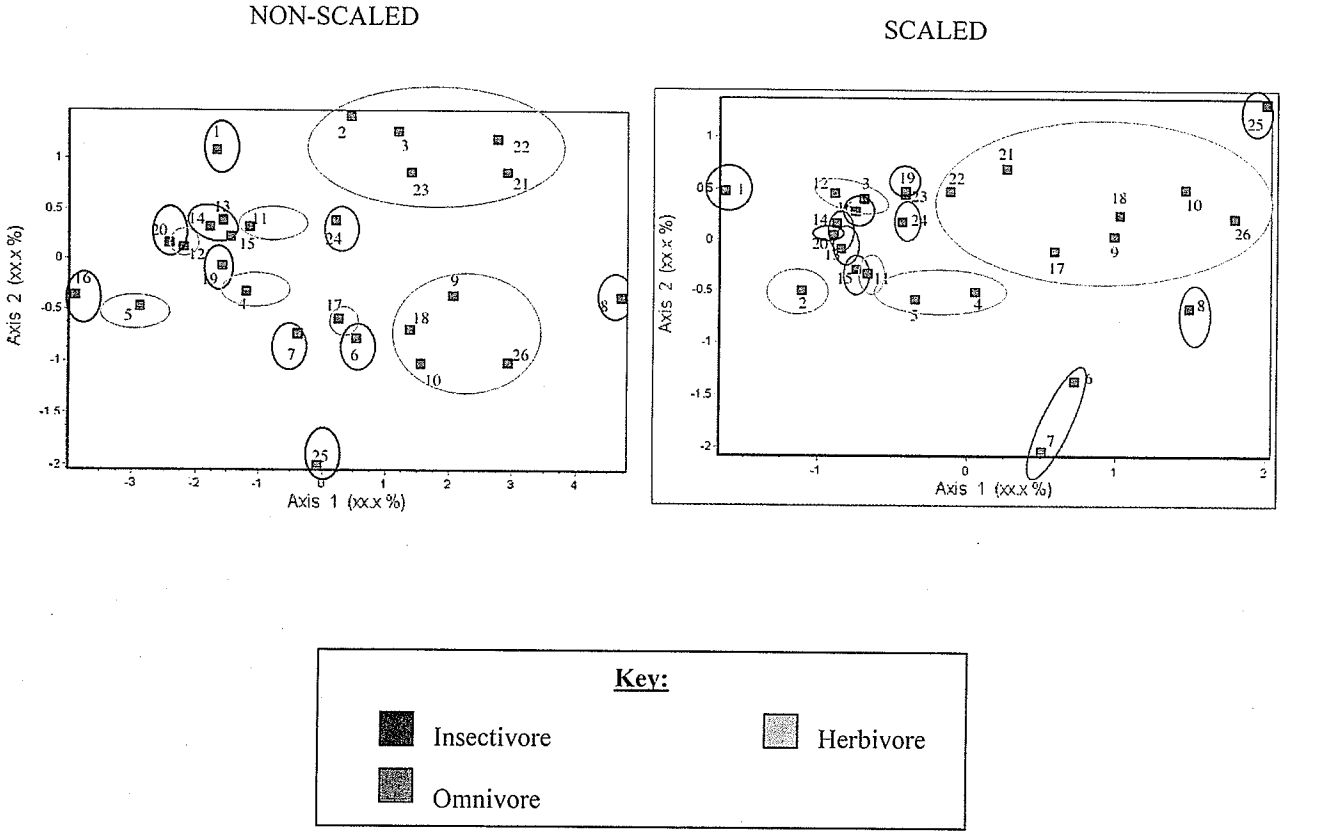

Figure 4.11 – Principal Coordinate Analysis plot for the non-scaled and scaled fifteen-landmark datasets clustered according to species habitat interaction based on Wilson and Reeder (2005)

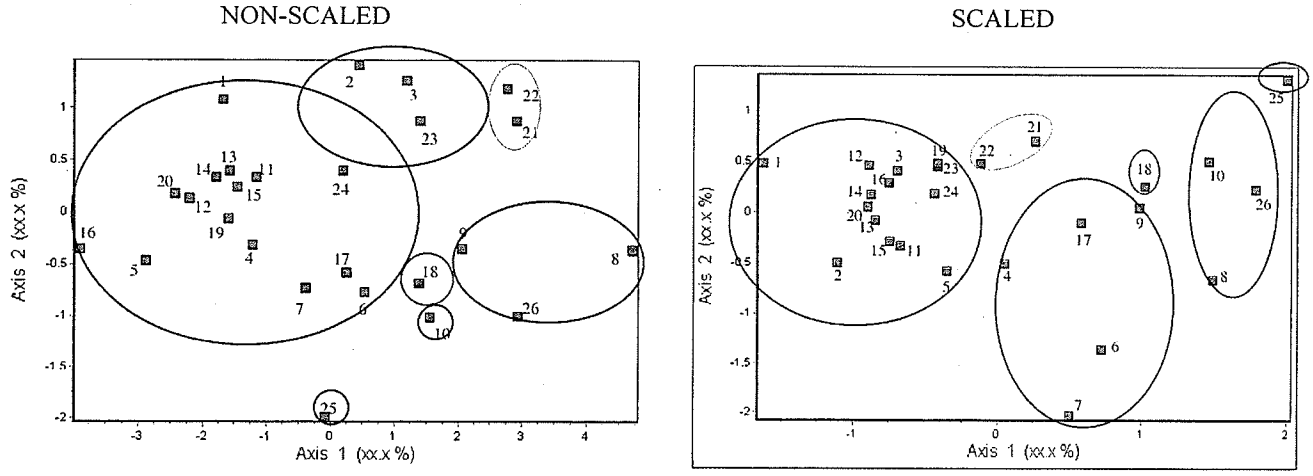

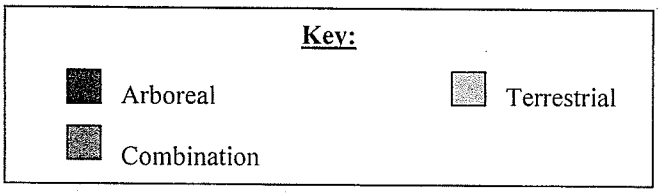

Data Exploration

The correlation matrices for the first axis, both non-scaled and scaled (Table 4.13), are used as examples here (see Appendix 4 for the complete list of correlation matrices). Positive scores in the correlation matrix mean that the linear distance measured is positively correlated with position on that particular axis. Negative correlation matrix scores mean that the linear distance is negatively correlated with position on the axis.

For example in the non-scaled matrix the linear distance MAN-HEA is positively correlated with position on the first axis (0.93) and SAR-MAH is negatively correlated with position on the first axis (-0.26). Because *Galagoides demidoff* is at the low end of axis one (Figure 4.4) this means that it has a relatively short MAN-HEA and a relatively long SAR-MAH. When scaled for geometric mean, these two linear correlations stay similar with MAN-HEA still positively correlated (0.72) and SAR-MAH negatively correlated (-0.73). *G. demidoff* is still on the low end of axis one but a number of other species are lower, i.e. *Arctocebus calabarensis*, suggesting that although *G. demidoff* has a relatively short MAN-HEA and long SAR-MAH, *A. calabarensis* is more so.

Table 4.13 – Correlation Matrix Examples

15-landmark non-scaled trial correlations between distances and axis 1 scores:

	MAN	LAT	HEA	IAM	LCR	SCR	IAR	SAR	MAH	IAI	ARI	MFP	LFP	SFP	IFP
MAN															
LAT	0.92														
HEA	0.93	0.67													
IAM	0.86	0.73	0.86												
LCR	0.65	0.86	0.94	0.53											
SCR	0.89	0.84	0.83	0.48	0.89										
IAR	0.84	0.86	0.88	0.46	0.64	0.70									
SAR	0.91	0.75	0.41	0.79	0.94	0.84	0.76								
MAH	0.90	0.62	0.01	0.85	0.95	0.89	0.84	-0.26							
IAI	0.85	0.77	0.87	0.02	0.72	0.92	-0.09	0.75	0.83						
ARI	0.66	0.88	0.93	0.64	0.66	0.89	0.70	0.93	0.95	0.77					
MFP	0.83	0.93	0.94	0.89	0.93	0.95	0.93	0.95	0.98	0.95	0.91				
LFP	0.76	0.91	0.93	0.94	0.90	0.96	0.95	0.93	0.96	0.93	0.90	0.82			
SFP	0.78	0.91	0.92	0.91	0.92	0.94	0.93	0.92	0.96	0.94	0.90	0.82	0.69		
IFP	0.79	0.92	0.93	0.89	0.90	0.94	0.93	0.94	0.97	0.91	0.87	0.76	0.71	0.61	

15-landmark trial correlations between SCALED distances and axis 1 scores:

	MAN	LAT	HEA	IAM	LCR	SCR	IAR	SAR	MAH	IAI	ARI	MFP	LFP	SFP	IFP
MAN															
LAT	0.56														
HEA	0.72	0.13													
IAM	0.56	0.32	0.60												
LCR	0.27	-0.45	0.01	-0.61											
SCR	0.52	-0.72	-0.67	-0.65	0.36										
IAR	0.43	-0.02	0.57	-0.06	-0.59	-0.65									
SAR	0.68	-0.00	-0.17	0.51	0.16	-0.63	0.52								
MAH	0.67	-0.63	-0.76	0.33	0.77	0.67	0.51	-0.73							
IAI	0.46	-0.69	0.12	-0.66	-0.06	0.00	-0.75	0.24	0.63						
ARI	0.30	-0.54	-0.05	-0.61	0.44	0.39	-0.60	0.09	0.76	-0.04					
MFP	0.42	-0.47	-0.20	-0.21	0.41	0.59	-0.20	-0.07	0.67	0.32	0.20				
LFP	0.32	-0.48	-0.00	0.11	0.22	0.57	0.02	0.09	0.52	0.25	0.02	0.25			
SFP	0.33	-0.62	-0.20	-0.22	0.18	0.46	-0.29	-0.10	0.49	0.16	-0.09	0.23	0.17		
IFP	0.29	-0.58	-0.19	-0.28	0.05	0.50	-0.38	-0.08	0.61	0.08	-0.17	0.25	0.15	0.20	

The non-scaled specimen's principal axis scores were analysed as they clustered together on the first axis. Six groups were identified (Table 4.14), Group 1 includes *G. demidoff* at –3.905, Group 2 ranges from –2.873 to –1.152, Group 3 covers –0.396 to 0.531, Group 4 from 1.195 to 1.376, Group 5 from 2.066 to 2.931 and Group 6 contains the outlier *D. madagascariensis* (4.720). It is important to remember these scores represent form differences i.e. difference in size and shape. When these grouped principal axis scores are compared with the correlation matrices, trends in the landmark linear distances can be seen.

Group 1: Has the shortest distance between MAN, HEA, MAH and almost all other landmarks except SAR-MAH. Group 1 also has the longest IAR-IAI and SAR-MAH distances of all the groups.

Group 2: Have relatively short MAN, HEA, MAH to almost all other landmark distances, except for SAR-MAH and IAR-IAI which are relatively long, although less so than Group 1.

Group 3: Have shorter MAN, HEA, MAH to almost all other landmark distances than Groups 4, 5 and 6 although longer than Groups 1 and 2 and longer SAR-MAH and IAR-IAI than Groups 4, 5 and 6.

Group 4: Have longer MAN, HEA, MAH to almost all other landmark distances than the earlier groups and shorter SAR-MAH and IAR-IAI than Groups 1, 2 and 3.

Group 5: Have relatively long MAN, HEA, MAH to almost all other landmark distances, compared to Groups 1, 2, 3 and 4. Except for SAR-MAH and IAR-IAI which are relatively short, although less so than Group 6.

Group 6: Has the largest distances between MAN, HEA, MAH and almost all other landmarks except SAR-MAH. Group 6 has the shortest IAR-IAI and SAR-MAH distances of all the groups.

Table 4.14 – Grouped non-scaled principal axis 1 scores.

Species	Principal Axis 1 Score	Group
Galagoides demidoff 1	-3.905	1
Cheirogaleus medius 2	-2.874	2
Loris tardigradus 2	-2.423	2
Galago elegantulus 1	-2.196	2
Galago moholi 2	-1.793	2
Arctocebus calabarensis 1	-1.678	2
Loris tardigradus 1	-1.591	2
Galago moholi 1	-1.573	2
Galago senegalensis	-1.460	2
*Cheirogaleus medius*1	-1.214	2
Galago alleni 2	-1.152	2
Cynocephalus volans	-0.396	3
Tarsius bancanus	-0.086	3
Otolemur garnettii	0.204	3
Hapalemur griseus	0.251	3
Callicebus moloch 1	0.438	3
Galeopterus variegatus	0.531	3
Callicebus torquatus	1.195	4
Lemur catta 2	1.376	4
Otolemur crassicaudatus 1	1.395	4
Eulemur fulvus rufus	1.562	4
Eulemur fulvus albifrons	2.066	5

Macaca nigra 2	2.757	5
Macaca nigra 1	2.916	5
Varecia variegata variegata	2.931	5
Daubentonia madagascariensis	4.720	6

The scaled principal axis scores were also grouped according to their position along the first axis (Table 4.15). Group 1 consists of the outlying *A. calabarensis* (-1.164), Group 2 ranges from –1.111 to –0.671, Group 3 ranges from –0.440 to 0.049, Group 4 from 0.264 to 0.724, Group 5 from 0.998 to 1.489 and Group 6 includes *V. variegata variegata* (1.791) and *T. bancanus* (2.001). Corrected for scaling, these results more accurately reflect shape differences.

Group 1: Has the shortest distance between MAN-HEA, LCR-MAH and MAH-IAI. Group 1 also has the longest HEA-MAH, LAT- SCR and IAR-IAI distances of all the groups.

Group 2: Have relatively short distances between MAN-HEA, LCR-MAH and MAH-IAI. HEA-MAH, LAT- SCR and IAR-IAI are relatively long, although less so than Group 1.

Group 3: Have shorter MAN-HEA, LCR-MAH and MAH-IAI distances than Groups 4, 5 and 6 although longer than Groups 1 and 2 and longer HEA-MAH, LAT- SCR and IAR-IAI than Groups 4, 5 and 6.

Group 4: Have longer MAN-HEA, LCR-MAH and MAH-IAI distances than the earlier groups and shorter HEA-MAH, LAT- SCR and IAR-IAI than Groups 1, 2 and 3.

Group 5: Have relatively long MAN-HEA, LCR-MAH and MAH-IAI landmark distances, compared to Groups 1, 2, 3 and 4. HEA-MAH, LAT-SCR and IAR-IAI are relatively short, although less so than Group 6.

Group 6: Has the largest distances between MAN-HEA, LCR-MAH and MAH-IAI. Group 6 has the shortest HEA-MAH, LAT- SCR and IAR-IAI distances of all the groups.

Table 4.15 – Grouped scaled principal axis 1 scores.

Species	Principal Axis 1 Score	Group
Arctocebus calabarensis 1	-1.624	1
Callicebus moloch 1	-1.111	2
Loris tardigradus 2	-0.901	2
Galago elegantulus 1	-0.896	2
Galago moholi 2	-0.877	2
Galago moholi 1	-0.850	2
Galagoides demidoff 1	-0.754	2
Galago senegalensis	-0.743	2
Callicebus torquatus	-0.699	2
Galago alleni 2	-0.671	2
Otolemur garnettii	-0.440	3
Loris tardigradus 1	-0.421	3
Otolemur crassicaudatus 1	-0.421	3
Cheirogaleus medius 2	-0.351	3
Macaca nigra 2	-0.119	3
Cheirogaleus medius 1	0.049	3
Macaca nigra 1	0.264	4
Cynocephalus volans	0.502	4
Hapalemur griseus	0.586	4

Galeopterus variegatus	0.724	4
Eulemur fulvus albifrons	0.988	5
Lemur catta 2	1.024	5
Eulemur fulvus rufus	1.463	5
Daubentonia madagascariensis	1.489	5
Varecia variegata variegata	1.791	6
Tarsius bancanus	2.001	6

Hierarchical Analyses

When subjected to hierarchical cluster analysis, the dissimilarity matrix of the non-scaled dataset produced cophenetic correlations of 0.8039 for the unweighted pair-group average (UPGMA) using the Euclidean distance index and 0.4994 for the user-specified dissimilarity index. The single linkage method resulted in 0.682 using the Euclidean distance index and 0.2968 for the user-specified dissimilarity. Ward's method has a Euclidean distance index inherent to the algorithm and resulted in a cophenetic correlation of 0.7158. This means that the UPGMA hierarchical clustering with a Euclidean distance index provides the least inaccurate phenogram for the non-scaled dataset.

The scaled dataset produced cophenetic correlations of 0.7983 for the UPGMA using the Euclidean distance index and 0.603 for the user-specified dissimilarity index. The single linkage method resulted in 0.7093 using the Euclidean index and 0.4648 for the dissimilarity index. Ward's method resulted in a correlation of 0.7437. This means that again, the UPGMA hierarchical clustering with a Euclidean distance index gives the least inaccurate phenogram for

the non-scaled dataset. The UPGMA phenograms were then subjected to bootstrap analysis using 100 resamples (Figures 4.9 and 4.10).

The phenogram of the non-scaled dataset (Figure 4.12) has much stronger bootstrapping probabilities than those of the scaled dataset (Figure 4.14). When compared with the accepted phylogenetic relationships presented in the dendrogram, the non-scaled phenogram (Figure 4.13) correctly grouped *M. nigra* one and two with high probability (100%) but separated *G. moholi* one and two although with only medium probability (46%), The two *L. tardigradus* specimens were significantly separated. *D. madagascariensis* remains a significant outlier (100%), although the Cynocephalidae cluster together, they are also clustered with *Hapalemur* and one *Otolemur* individual. Once scaled (Figure 4.15), the Cynocephalidae and *D. madagascariensis* cluster together although with fairly low probability. Overall in both the scaled and non-scaled phenograms, taxa within the families cluster quite well, although more obviously in the scaled data and with stronger bootstrap probabilities in the non-scaled data, but the hierarchical clustering between the families are significantly different in both phenograms when compared to the dendrogram.

Figure 4.12 – Results of the bootstrap analysis of the non-scaled dissimilarity matrix using 100 resample.

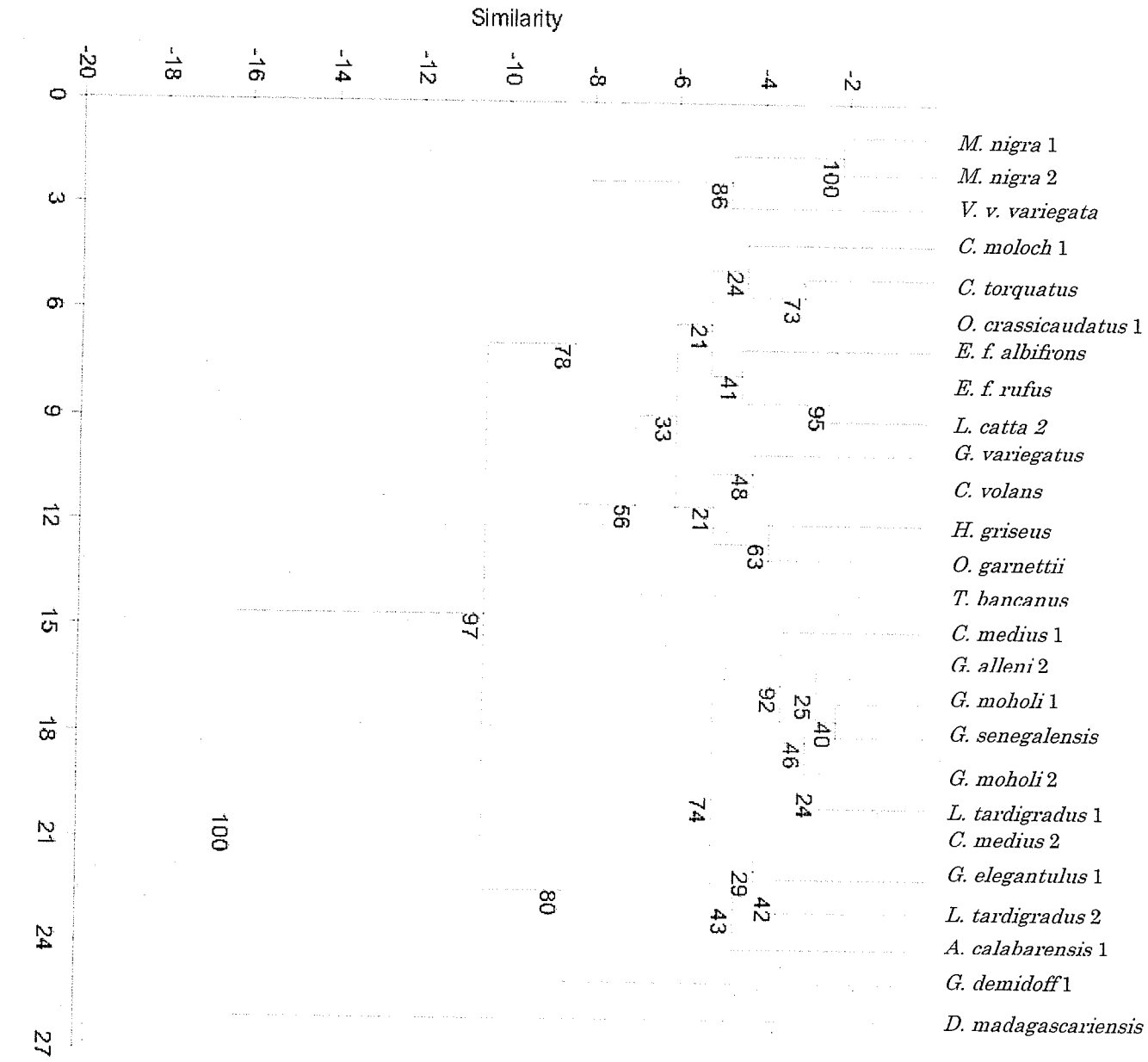

Figure 4.13 – Results of the bootstrap analysis of the non-scaled dissimilarity matrix compared to the dendrogram of species relationships After Purvis (1995).

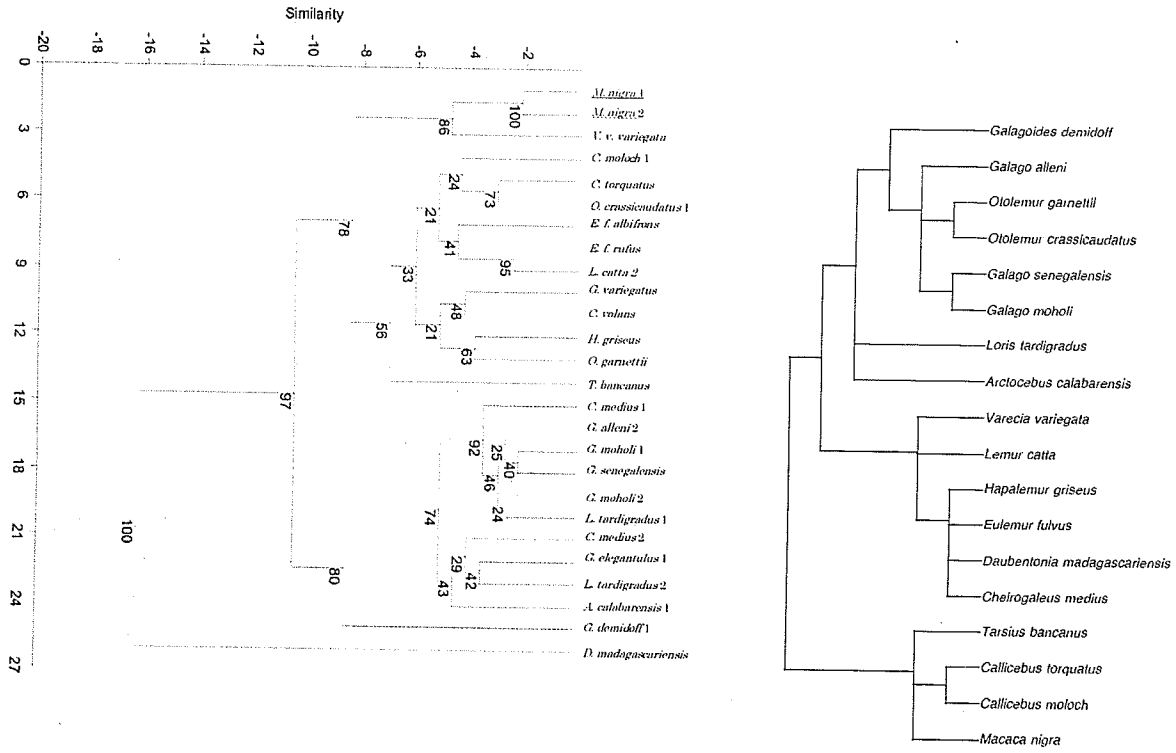

Figure 4.14 – Results of the bootstrap analysis of the scaled dissimilarity matrix using 100 resamples.

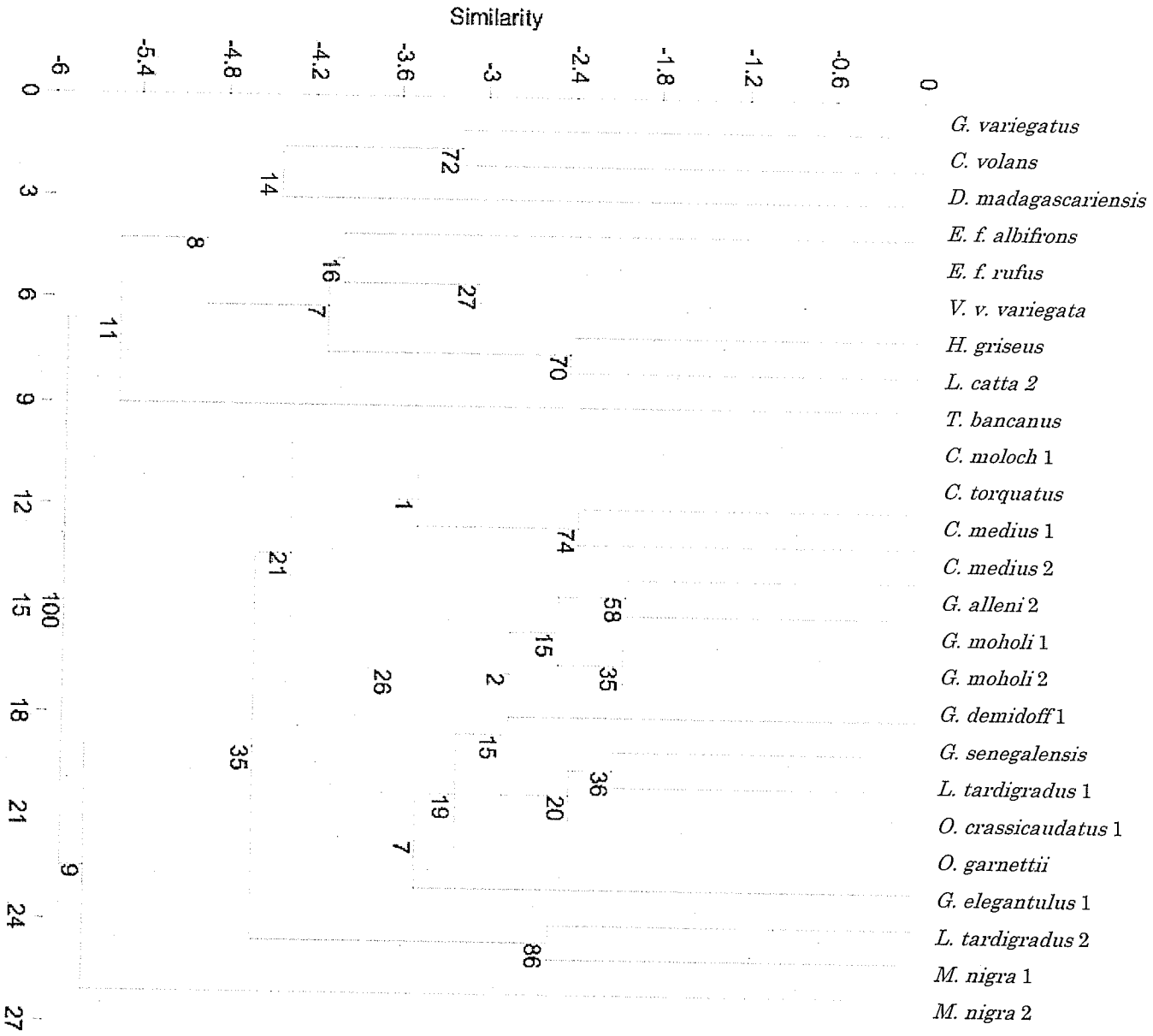

Figure 4.15 – Results of the bootstrap analysis of the scaled dissimilarity matrix compared to the dendrogram of species relationships After Purvis (1995).

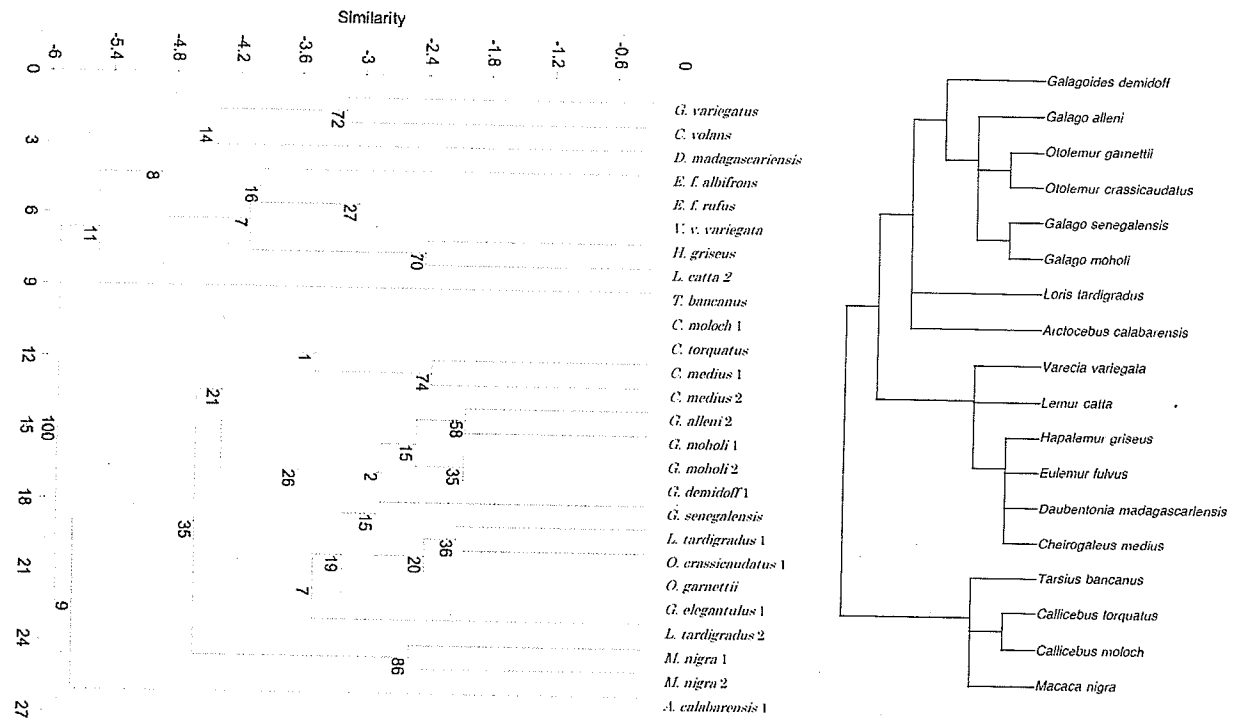
Similarity
0
-0.6
-1.2
-1.8
-2.4
-3
-3.6
-4.2
-4.8
-5.4
-6
G. variegatus
C. volans
D. madagascariensis
E. f. albifrons
E. f. rufus
V. v. variegata
H. griseus
L. catta 2
T. bancanus
C. moloch 1
C. torquatus
C. medius 1
C. medius 2
G. alleni 2
G. moholi 1
G. moholi 2
G. demidoff 1
G. senegalensis
L. tardigradus 1
O. crassicaudatus 1
O. garnettii
G. elegantulus 1
L. tardigradus 2
M. nigra 1
M. nigra 2
A. calabarensis 1
Galagoides demidoff
Galago alleni
Otolemur garnettii
Otolemur crassicaudatus
Galago senegalensis
Galago moholi
Loris tardigradus
Arctocebus calabarensis
Varecia variegata
Lemur catta
Hapalemur griseus
Eulemur fulvus
Daubentonia madagascariensis
Cheirogaleus medius
Tarsius bancanus
Callicebus torquatus
Callicebus moloch
Macaca nigra

CHAPTER V – DISCUSSION

Intra-observer Error Study

The auditory ossicles are the smallest bones in the primate body and the landmarks delineating them are also necessarily defining and measuring exceptionally small distances and biologically meaningful points. The results of the error trial suggest that the majority of the landmarks are repeatable based upon tests of mean differences for distances between repeated landmarks across three species. Three landmarks: the lateral process of the malleus (LAT), the medial (MFP) and superior (SFP) footplate of the stapes, did demonstrate mean differences that were significantly different than zero, suggesting errors in reproducibility of placing these landmarks in 3D space. The overall magnitude of distance between repeated landmarking is relatively small, even for those that are statistically significant, such as the LAT of the *Callicebus moloch* 1 with an ILD of 0.04mm, often within the reconstruction error of the rendered 3D models.

Interestingly, identification of the LAT as error-prone, is in contrast to the earlier error study of Schmidt and colleagues (2009). The LAT landmark is used in defining the axis of rotation for determining the functional length of the malleolar lever arm. The landmark coordinates MFP and SFP are used to determine the extent of the oval window and along with the lateral and superior coordinates are used to provide an estimate of the stapedial footplate dimensions, used in functional analyses. These landmarks may be difficult to locate depending on the resolution of the CT scan, an issue that may be reflected in the results of this study.

The causes of the errors in repeatability in the landmarks are open for interpretation. All three of the most error-prone landmarks represent very small points to define and were taken on the 3D

reconstructed model. The position of the 3D model and lighting within the virtual environment may change the visual appearance of the area affecting where the operator thinks the landmark is being placed. Other than being utilised to define the shape of the auditory chain, these measurements are also used for functional analysis. As such any future studies, however, of functional analysis or hearing estimation based on the footplate dimensions defined by these landmarks will need to take these issues into account.

The results of this small repeatability study seem to suggest that unlike previous multiple observer trials (Schmidt *et al.*, 2009) the replicability of the landmarks is greatly increased when conducted by a single observer. The results of the measurement error study demonstrate that generally, the sixteen landmarks used in the study, can be repeatedly located, although three landmarks (LAT, MFP and SFP) performed less well.

Morphometric Analysis

Overall, exclusive of a few limiting factors, the study provided useful data for discussion. Two trials were completed: one for form differences and one scaled to the geometric mean in order to evaluate shape differences. The twenty-six specimens grouped well according to family and clade, strongly reflecting the current accepted phylogeny, although little clustering was seen when comparing activity patterns and diet. The localisation of differences between the specimens suggested future applications in the study of auditory function suggested. The EDMA technique provided surprising opportunities for study beyond the traditional basic measures to examine primate auditory structural morphology in three dimensions. The outliers of both the non-scaled and scaled datasets revealed several interesting patterns and these inform debates of phylogeny as well as adaptation.

Study Limitations

There are a number of factors that limit any morphometric analysis. First is the type of data chosen for analysis and how accurately this is a representation of a biological group. Second, is the choice of analytical technique. With the use of landmark coordinate data comes the inherent limitation that no set of landmarks no matter how complete can ever fully describe a biological form. However, as long as these limitations are acknowledged morphometric analyses based on landmark data can be of great use in investigations (Richtsmeier *et al.*, 2002).

The first restriction on a morphometric study is sample size. It is not always possible, particularly in biological anthropology, to obtain a large enough number of specimens pertaining to the problem under study. The reasons for small sample size are diverse, from the condition of fossil specimens to the relative rarity of pathologies (Lele and Richtsmeier, 2001). In the current study, the number of specimens was restricted to twenty-six for two main reasons. First was the rarity of the dataset, the current study uses UhrCT scans of auditory ossicles *in-situ* within the skull, only a limited number of scans on a limited number of species have ever been undertaken. The second issue is one of condition, of the limited number of scans available, only those with all three ossicles complete and in correct anatomical alignment were used.

Even with a large sample set there are restrictions on what can be known about the population variability based on these specimens. As with all statistical studies, the true population parameters can never be known, they can only be estimated using a sample (Richtsmeier *et al.*, 2002). In studies with a large number of specimens representing each species, a mean form can be calculated to act as a model, or species representative. In the current study, the majority of species, twenty-two out of the twenty-six were represented by one sample so a mean was not

possible to calculate. Representing a species with one sample has some inherent problems. Variability is inescapable in nature and when comparing biological forms, within-population variability cannot be ignored, no two organisms, regardless of how closely genetically related they are, are ever identical. So the question becomes, if a larger sample set is not possible, is it still useful to conduct an analysis with a single specimen representing a species? Within the sample set there are two representatives of each of the species: *M. nigra, C. medius, G. moholi* and *L. tardigradus.* In the non-scaled trial the two *M. nigra* specimens cluster together, whilst the others remain close in the cluster analyses but appear to have forms more related to other species than each other. In the scaled trial the *C. medius* and *G. moholi* specimens cluster with their respective species, suggesting the lack of clustering in the non-scaled analysis may be due to individualistic changes in size rather than shape. However, the *L. tardigradus* and *M. nigra* specimens do not cluster together in the scaled trial. Overall, the inter-specific variation is greater than the intra-specific variation suggesting that the inclusion of one representative species does provide useful data on the morphology of the ossicles of that species.

Once a dataset has been decided on, there are then limitations based on the analytical method applied. Salient features of morphology are missed when landmark data are used exclusively. However, as explained in Chapter 3, the choice of methodology is based on a number of factors including the goals of the study, issues or repeatability and the nature of the objects under scrutiny, to name a few. With the adoption of landmark-based methods comes the knowledge that there are certain things that can be known about the forms under study and those that cannot. The problem is simply that landmarks reflect a single point; they do not contain information on the spaces, curves, surfaces or structures between them. So discussions of form and shape change are limited to specific areas and not the whole form-shape.

One option is to increase the number of landmarks, as this study has done compared to earlier works (e.g. Hyrtl, 1845; Arione, 1923; Werner, 1956; Parizek and Varacka, 1967; Masali, 1968; Masali, 1971; Siori and Masali, 1983; Masali 1992; Masali *et al.*, 1992) that looked at simple length measurements or a handful of landmarks. The main problem here is that by very definition the landmarks chosen have to represent biologically meaningful loci as well as being able to located repeatedly. Schmidt and colleagues (2009) determined that, by this definition, only sixteen landmarks were available for study on the auditory ossicles. Another issue with the addition of more landmarks is the amount of information collected. With fifteen landmarks this study generated 105 EDMA pair-wise distances. If this were increased to 30 landmarks there would be 435 pair-wise distances, a large amount of data to sort for what may be little additional valuable information.

Landmarks are chosen to reflect a position representative of underlying processes and simply adding more does not necessarily provide more useful information on these processes, particularly because specific areas of the form may hold a larger number of biologically relevant loci. This means there may be situations in which one area of the form under study contains more closely spaced landmarks than another area, resulting in unequal representation of aspects of a single form (Lele and Richtsmeier, 2001). This is evident in the landmarks used in the current study; there are five landmarks on the malleus, the largest ear bone, six on the incus and five on the smallest, the stapes, of which four of these are specifically on the footplate.

Options other than increasing the number of landmarks are limited by practical considerations such as time, efficiency and measurement error. Bookstein (2005) argues that the 'toolkit' of landmark-based morphometrics has peaked and that the time is at hand for the introduction of new methods. One such technique being developed by Hallgrimsson *et al.* (2008) uses full 3D

volumetric datasets, which are superimposed on each other to a common orientation by rigid image registration with an isotropic scaling factor. Shape differences can then be visualised using the surface-to-surface distance measures between the superimposed images. Although these new methods would provide more information on the ossicular shape they still are subject to some of the limitations inherent to superimposition techniques. Regardless, these methods are still in the early stages of development and until such techniques are proved and become more efficient, the choice of a landmark-based approach was the most productive for the goals of the current study. It is important to remember that no matter how extensive, morphometric analyses can only describe and define differences in form and shape; they cannot explain the causes of these differences. To determine the relevance and effect of the changes in ossicular morphology uncovered in this study, previous studies of function must be used to interpolate differences in operation resulting from form and shape changes.

Scaling Factor

The greatest variable between the auditory ossicles in this study is size. Obviously the smaller the animals' general body dimensions, the smaller the ear ossicles, although the relationship is not linear and a strict correlation with body mass is undefined (Masali, 1971). Morphometrics commonly aims to compare differences in form – a combination of size and shape, or shape only. Shape, however, is not an individual measure that can be determined based on a single unit, it is arrived at by the removal of size from the form equation.

The term 'size' suggests magnitude and is generally represented by a single measurement such as length or weight, a linear combination of metrics such as arithmetic mean, or a more complex combination such as area volume or geometric mean (Richtsmeier *et al.*, 2002). Shape results change based on the choice of the surrogate for size, when choosing this surrogate, or scaling

factor, for analysis, none of these measures is intrinsically more suitable than any other. All size associations other than the one chosen as a scaling factor still exist in the "shape" analysis and the nature and importance of these associations will vary depending on the size variable and the aims of the study (Richtsmeier *et al.*, 2002). This is not to say that morphometric studies of shape have no value or even that form is better, it is simply important to remember that the scaled form is included as a representative for shape with many factors including aspects of size still influencing the study.

Size was a significant factor in the choice to include both form and shape differences in this study, as it was in the choice to use EDMA rather than more traditional morphometric techniques such as Procrustes. Some morphometric studies benefit from the attempt to reduce the influence of size especially those comparing taxa of significantly different general body dimensions which may overwhelm and obscure differences in shape (Lele and Richtsmeier, 2001). The choice of geometric mean as a scaling factor was based on an examination of the dataset and the biological information it provided. As the auditory ossicles are of a similar general shape, a geometric mean was the most logical choice.

In an EDMA analysis, the first assumption to test is that the mean form of one group is a scaled version of a comparable group. If this is proved then this indicates the populations tested are of a similar shape and differ only in size. Although size is the main factor affecting the position of the specimens along the first principal axis in the non-scaled dataset and heavily influences comparisons of the auditory ossicles, other factors are seen to cause significant variation after the dataset has been scaled showing that the ossicular chains in this data set vary in form.

The differences in general ossicle dimensions can be seen when looking at either the principal coordinate scores of the non-scaled data or at the centroid-size analysis. In terms of overall dimensions the auditory ossicles of the strepsirrhine primates are generally smaller than their haplorrhine counterparts, agreeing with the work of Masali (1971). The Cynocephalidae sit comfortably in the middle of the range in overall size. *D. madagascariensis*, however, is an outlier, significantly larger in terms of ossicle scale in both principal coordinate scores and calculated centroid size. The size of the middle ear chain sets constraints for the frequencies transmitted. It has been shown that the limits for high-frequency hearing can be predicted on the basis of ossicular mass. Hemillä and colleagues (1995) found that the high-frequency limits of a given auditory system are inversely proportional to the overall size of the ossicular chain. This suggests that *Daubentonia* have a lower high-frequency cutoff than that of the other primates in the study.

However, in general the larger the ossicular area, the better the low-frequency sensitivity and the smaller the area the better the high-frequency sensitivity. This rule suggests that *Daubentonia* have better low-frequency hearing compared to the Galagidae or the Lorisidae, which would have better high-frequency sensitivity. Although overall differences in ossicle size can be informative, especially in clustering and functional analyses, specific loci or landmark size differences and similarities can be just as informative if not more so. Ossicles restricted in specific loci or dimensions may suggest common adaptations or genetic relationships and these will be discussed in detail later as part of the shape analysis.

It should be noted that although correction for size allows for discussion of shape and its taxonomic significance, size differences could occur for many reasons such as individual variability, sexual dimorphism and pathology, so comparisons of auditory ossicles based solely

on shape are lacking vital information making the choice to include a form-based analysis such as EDMA an excellent choice.

Cluster Analyses

One of the chief objectives in this study was to determine what, if any, differences exist between the morphology of the primate auditory ossicles represented in this analysis. To do this, PCoA and cluster analyses were used to find groups in the EDMA data, such that the auditory ossicles of the members of a group are morphologically more similar to other members of the group than they are members of alternate groups. Cluster analysis is inherently subjective because the results of a grouping procedure can depend more on the method used than on an actual signal in the data (Lele and Richtsmeier, 2001).

Cluster analysis was used in the current study to find groups in the data resulting from the PCoA scores. These groups were not defined *a priori* and aimed to describe the natural 'falling-out' of primate auditory ossicle morphology. The results of the non-scaled cluster analyses, grouped the species along the first principal coordinate axis according to the general dimensions, with the galagos grouped at the low end and the lemuriforms, macaques and *D. madagascariensis* at the high end. It should be noted that these groups do not take the overall adult body dimensions of the species into account and so do not provide complete information for comparing ossicle morphology. Once scaled to a geometric mean to focus on shape, the groups tend to fall out into a low, middle and high range variation. The low variability groups once again include the galagos as well as the lorisforms. The mid-range group included *Macaca,* both the cynocephalids and *Hapalemur griseus*. The high-range included *D. madagascariensis, V.v. variegata* and the unexpected outlier *Tarsius bancanus.*

The related but distinct classification procedure, aims to classify the specimens into predefined groups to determine how well they follow cluster patterns. The groups compared in the classification analyses included behavioural and ecological groups such as activity cycle, diet and habitat as well as taxonomic groupings of clades and families. Comparisons of ecological behavioural patterns were restricted by a lack of representation. The majority of species in the study were arboreal with only the two specimens of *M. nigra* completely terrestrial and *L. catta* the only arboreal-terrestrial combination. Comparisons of activity cycles were more useful and yielded surprising results. Fourteen of the specimens represented nocturnal species, while six were diurnal, three were both crepuscular and nocturnal and three were crepuscular and diurnal. It would seem obvious that such differing activity cycles would have different sense requirements; sight changes are well reflected in the varying eye morphology of the nocturnal primates. Any hearing-based differences, however, are not immediately visible in the form or shape scores of the primates in this study.

Comparisons of the primate's main dietary sources were included for two reasons. Firstly, the food gathered for consumption may have differing hearing requirements, for example, insectivores 'hunting' a live diet may use their hearing more or in a different frequency range than herbivores, a group which includes gummivores, foliovores and frugivores. This study included five insectivores, seven omnivores and fourteen herbivores. The classification of the principal coordinate axis scores into the diet-type groups were not strong, although the non-scaled insectivores did all fall in the lower range of the first principal coordinate axis (size) and the omnivores fell closely in the middle range, excluding the outlier *D. madagascariensis*. This correlates with Kay's threshold, which finds that insectivorious primates are usually smaller with a limit of 500g, while folivorous primates are usually larger with a lower limit of 500g (Gingerich, 1980).

The results of the PCoA cluster and classification analyses indicate that although diet and activity patterns may be relevant when discussing the auditory ossicle morphology of a specific species, the clustering is not strong enough to suggest that these patterns are an important factor in morphology. Future studies may benefit from the inclusion of more species as well as more detailed analyses of communication habits and ecology, which may be stronger factors in ossicle morphology adaptation.

In order to examine the usefulness of auditory ossicle morphology in determining phylogenetic relationships, taxonomic cluster analyses were undertaken on the PCoA scores. To examine the larger scale trend first, the PCoA plots were clustered into two *a priori* categories. The living primates can be divided into two groups or clades, the Strepsirrhini and the Haplorrhini. When the PCoA scores are clustered into these categories, the non-scaled data demonstrate strong grouping of the Haplorrhini along the first and second principal coordinate axes, excluding the outlier *T. bancanus.* The strepsirrhines do not cluster well on the first axis but do so better on the second. The scaled scores of the haplorrhines are spread out with no evident grouping although the strepsirrhines show similar groupings to the non-scaled data.

The family groups were also subjected to cluster analysis. This technique would be enhanced if a larger number of representatives from each family were available. Nevertheless, the non-scaled PCoA plot demonstrated excellent grouping of the Lorisidae along the first principal coordinate axis and strong groupings of the Galagidae, Cynocephalidae and Lemuridae along the second axis. The lack of grouping along the first axis is caused by the difference in general ossicle dimensions. This improves significantly with scaling where all the families cluster well, except for the Pitheciidae. Because of the success in finding family clusters within the groupings this

suggests that these family clusters show promise for larger future studies including more primate families, where it is expected these trends will be more obvious. The results of these taxonomic analyses were subjected to hierarchical clustering with bootstrapping to test the strength of the clustering.

Hierarchical Analyses

When comparing morphometric classifications with a genealogical hypothesis, the comparison is one of the patterns of hierarchical relationships. The cladogram used in this study is based on Purvis (1995). The goal of the unweighted pair-group average (UPGMA) and hierarchical clustering analyses was to determine whether or not there was a hierarchical structure within the data. If such a structure to the clustering was identified, this was then compared to the patterns of the hierarchical relationships within the cladogram.

A hierarchical structure was evident in the non-scaled data to quite a high probability. However, the probabilities on the scaled data were substantially lower. Clustering into biological families was strong and the scaled data reflected the accepted taxonomy well. The hierarchy of the clustering within families tended to be out of order compared to the cladogram. The specimens do not strongly cluster at a species level, in either the non-scaled or scaled analyses, well when compared to the genealogical hypothesis. This may be related, however, to a small sample size rather than a true lack of taxonomic-based morphological signals. The phenograms of the scaled and non-scaled datasets show concordance with the currently accepted phylogeny, those groups which do not, including the percussive foragers and statistical outliers *A. calabrensis* and *T. bancanus* do not represent alternative phylogenetic hypotheses but instead demonstrate specific species in which adaptive traits have lead to ossicular morphology which is significantly different to their closest relations.

The haplorrhine–strepsirrhine split is reflected well in ossicle morphology and the taxonomic divisions are highly reflected in the scaled data although not with high bootstrap results. This would suggest that descendant taxa inherit aspects of their ossicular form from their ancestors. Hypotheses regarding the origins of these derived traits should focus on communication and sound windows within specific environments rather than diet, activity pattern or arboreality as there is little evidence in the cluster analyses for these being adaptation factors.

Localisation of Differences

Typically the first question posed in a morphometric analysis is, are the groups different? Data exploration and clustering methods are ideal for answering this, the question of how much and where they differ is one, which relies on the localisation of differences. Although the cluster analyses provide important information about form-shape dissimilarities between groups, characterising the relative locations of these differences can provide information on biological processes such as evolution and development. The locations of components that are most or least different between specimens are vital to the investigation of the mechanisms of change such as genetic, physiological, pathological and environmental (Lele and Richtsmeier, 2001).

The localisation of differences can be conducted in two ways. First is to look at the EDMA pair-wise landmark distances and compare these. Two issues with this are that analysis is restricted to the form differences only and secondly that one hundred and five inter-landmark distances are produced for each ossicular chain, requiring decisions to be made by the investigator regarding relevant distances, usually anatomical lengths.

When examining the anatomical lengths of the current dataset three lengths were chosen as most relevant, as these are functional lengths used in the mathematical modelling of auditory mechanics e.g. ossicular lever hypothesis. MAN-HEA which defines the maximum length of the malleus, LCR-MAH which provides the maximum length of the incus and LAT-SCR which gives the width of the ossicular chain bodies from the apex of the lateral crus of the malleus to the apex of the short crus of the incus. The two longest mallei occur in *D. madagascariensis* at 7.2587 and *M. nigra* 2 at 5.1435. The shortest mallei belong to *A. calabarensis* at 2.414 and *G. demidoff* at 2.4218. *D. madagascariensis* and *V.v. variegata* have the longest incudal bodies at 3.9292 and 3.3921 respectively, while *G. demidoff* and *L. tardigradus* 1 have the shortest with 1.5305 and 1.6043 respectively. The widest ossicular chain belongs to *D. madagascariensis* (4.4962) followed by *M. nigra* 1 (4.0227). The shortest are *C. volans* with 2.2895 and *G. demidoff* with 2.4218. Although interspecific comparisons of non-scaled lengths do not provide relevant information, these data may be useful in future studies comparing ossicular size with general body dimensions as well as intra-specific studies. The restriction with only using the form data for this type of localisation analysis can be seen by the fact that the primates with the lower and higher body dimensions dominate both the lowest and highest scores.

The second technique for examining the localisation of difference returns to the form-shape correlation matrices, looking for landmarks whose relative ranking is high in terms of their contribution to the form-shape differences. These landmarks are then referred to as influential landmark distances. The closer a score in the correlation matrix is to one then this landmark distance is positively correlated with position on the principal coordinate axis, a negative correlation score means the landmark distance is negatively correlated to axis score.

In the non-scaled trial's correlation matrix there are two negative values, IAR-IAI and SAR-MAH. There are ten values over 0.95; these are: LCR-MAH, MAH-ARI, SAR-MFP, MAH-MFP, IAI-MFP, IAR-LFP, SAR-LFP, MAH-FP, MAH-SFP and MAH-IFP. The issues in landmark placement discussed in the error study can in part explain the high values for the stapedial footplate landmarks. This means that in the non-scaled dataset the most influential landmark distances are: the maximum length of the incus, the distance between the most inferior point of the incus in its articulation with the malleus and the interior arch of the incus, the distance between the superior surface of the incus and the superior surface of the malleus and the distance between the superior surface of the incus to the incudostapedial joint. These landmark distances represent the distances of greatest change in the primate non-scaled dataset. It is important to remember when discussing localisation of differences that a specific landmark or distance may reflect differences local to a larger region and not just that one landmark. For example the SAR-MAH distance may represent a change in the incus articulation angle rather than a specific structure change. Many of these measures define the morphology of the incus and can be used in functional analyses such as the ossicular lever hypothesis. The distance between superior surfaces represents an increase in ossicular body size without an accompanying increase in process size, which would be seen if the changes were occurring between landmarks which define the ossicular chain width.

When looking at the scaled trial's correlation matrix the differences are less pronounced with far more negative values including four over –0.70, LAT-SCR, HEA-MAH, SAR-MAH and IAR-IAI. There are three positive values over 0.70, MAN-HEA, LCR-MAH and MAH-ARI. Therefore in the scaled dataset the most influential landmark distances are: the maximum width of the ossicular chain bodies, the maximum length of the malleus and the maximum length of the incus. These three measures are used in the ossicular lever hypothesis to determine the axis of

rotation as well as the ratio of the lever arms. Other influential landmarks included the inferior incudomalleal joint to the interior arch of the incus and the superior surface of the incus to three points, the superior surface of the malleus, the superior incudomalleal articulation and the incudostapedial joint, representing changes in the morphology of the incus. The results of the scaled dataset concur with the groups suggested in the first option. The four EDMA distances, which cause the most difference in both form and shape, are: IAR-IAI, MAH-SAR, MAH-LCR and MAH-ARI.

These specimen specific landmarks and pair-wise distances can also be very important for functional analyses. Analyses of the transmission of sound through the ear rely heavily on soft tissue, on which the present study is unable to provide additional information. Functional analyses that require bone measures, however, can use the 3D landmark data as well as some of the EDMA distances collected.

The ossicular lever hypothesis, commonly adopted by auditive scientist to study primate hearing, describes the middle ear as a mechanical and hydraulic system which gains signal strength due to the uneven lengths of the manubrium of the malleus, considered the effort arm and the long crus of the incus, the resistance arm, transforming small forces of low magnitude and high displacement at the tympanic membrane into small displacements with high force at the incudostapedial joint (Wever and Lawrence, 1954; Békésy, 1960; Dallos, 1973). The effective lever arms are determined by measuring the perpendicular distance fro the axis of rotation, the apex of the lateral crus of the malleus to the apex of the short crus of the incus, to the point of operation. For the malleal (effort) arm this would extend to the apex of the manubrium and for the incudal lever (resistance) arm this would extend to the apex of the long crus.

Aside from the issues previously discussed with the validity of such a simplified functional hypothesis, the landmarks taken as part of this study can be used in the future for determining these functional lengths. The axis of rotation is defined by the distance between the LAT and SCR landmarks, the lever arms can then be determined by separately calculating the perpendicular lengths from this distance to MAN and LCR. Once estimates of the mechanical lever advantage provided by the various auditory structures have been determined, it is then possible to calculate an overall ratio of the transformed sound pressures. Both models proposed to do this require the stapedial footplate area. This can be determined by calculating two perpendicular axes from MFP to LFP and SFP to IFP. This is not ideal as it assumes the footplate is a perfect oval, which it is not, however, it is the technique commonly used, generally because of the difficulty in measuring the footplate directly on specimens. If a higher degree of accuracy was required it may be possible for future studies to do a direct perimeter tracing on the 3D model.

The data provided by this study do suggest some differences in the function of the auditory systems of the included primates. Actual measurements of middle ear function in extant primate ears indicate that mass, stiffness and damping play a large role in determining overall auditory function (Rosowski and Graybeal, 1991). Species with the greatest low-frequency hearing have large ossicular lever ratios as represented by longer MAN-HEA measures to LCR-MAH measures, whilst smaller ratios suggest better high-frequency hearing. The longest malleus to incus ratios occur in *Daubentonia, L. catta, M. nigra* and both *Otolemur* whilst the shortest occur in *A. calabarensis* and *G. demidoff.*

According to the ossicular lever hypothesis, hearing models place the pivot of the rotational axis in the mass centre of the malleus and incus (Cancura, 1980). In the species with unusual

ossicular body sizes such as the constricted *T. bancanus*, the centre around which the ossicles rotate will be different. Joint size and the surface area of the connections between ossicles can also affect auditory function. Reduction in ossicular mobility as might result from flexing of relatively larger joints as seen in the longer measures between the landmarks IAR and SAR, produce reductions in stapedial velocity resulting in a broadband reduction in hearing sensitivity (Nakajima *et al.,* 2005). As previously mentioned rigidity is an important factor in the impedance functions of the middle ear; ossicular bending in a potential source of non-rigid behaviour in the chain. The *Daubentonia* malleal manubrium, being longer and more gracile than the other primates in the sample would be subject to greater bending forces and would contribute to flexibility of the ossicular chain. Decraemer and colleagues (1991) found that gracile manubrium's in cats tended to bend more to sounds of middle and high frequencies. Ossicular bending effects the results of functional modelling based on the ossicular lever ratio, as this assumes a rigid chain for calculating the rotational axis. The relative sizes of the stapedial footplates in the scaled datasets demonstrate changes in auditory function. An increase in relative stapedial footplate size is correlated with heightened low-frequency sensitivity suggesting the Lemuridae and Tarsier are more sensitive to lower frequencies whilst the Galagidae and Lorisidae may be less sensitive.

Dermoptera

One of the aims for the current study was to include the Dermoptera as an outgroup to the primates in order to provide a non-primate comparison for the morphometric and taxonomic analyses. Before scaling for size, the two representative species of Dermoptera, *Cynocephalus volans* and *Galeopterus variegatus,* were fairly close to each other in the PCoA analysis and sat in the middle of the primate range for size, both in the first principal coordinate axis scores and in the centroid size analysis. Once the specimens were scaled, the two Cynocephalidae stood out

more and clustered closely on the first few principal coordinate axes and separate to the other species.

As previously discussed, the relationship of the Dermoptera with primates is uncertain, with some studies suggesting no relationship while others based on morphology, mtDNA, and amino-acid sequencing, group the Dermoptera and primates on a common branch as sister to the Anthropoidea to the exclusion of the prosimians (Arnason, 2002; Janeka, 2007; and Murphy, 2001). In the non-scaled hierarchical clustering analysis, the two species were grouped together with a bootstrap probability of only 48% over one hundred resamplings. The Cynocephalidae were clustered with *H. griseus* and *O. garnetti* with a low probability of 21%. The bootstrapping was stronger in the separation from the galagos, *C. medius*, *L. tardigradus* and *A. calabarensis* at 97%. After scaling, the Cynocephalidae clustered together with much higher probability of 72%. The Cynocephalidae were grouped with *D. madagascariensis* at a low probability of 14%, probably reflecting the common outlying statistical characteristics rather than a taxonomic relationship. The split from the galagos, *C. medius, C. moloch* etc. was again strong, with a bootstrap probability of 100%. The inclusion of the Dermoptera as an outgroup demonstrates a problem with examining morphometric cluster analyses for phylogenetic signals. Both representatives of the Cynocephalidae fall within the primate groupings in the principal component analyses, more strongly so before scaling. This demonstrates a lack of concordance with the most phylogenetic hypotheses. Whether this is due to a closer relationship to the primates as proposed by Arnason, 2002; Janeka *et al.*, 2007; and Murphy, 2001 or whether it is due to morphological similarities as adaptive traits which, cross the primate non-primate barrier, are beyond the scope of the current study. This 'falling-out' of non-primate specimens within the primate cluster groupings illustrates an issue with the use of cluster analyses in taxonomic studies, as they compare morphological similarities rather than direct relationships and therefore,

implied phylogenetic signals in morphological cluster analyses may in fact be groupings of other factors affecting the morphology.

When looking specifically at shape difference both the Cynocephalidae had relatively long distances in the MAN-HEA, LCR-MAH and MAH-IAI landmarks compared to the other species, but had relatively short HEA-MAH, LAT-SCR, and IAR-IAI distances, resulting from a long malleal manubrium and smaller bulbous incus, the stapes is fairly standard. Hunt and Korth (1980) stated that the *C. volans* auditory ossicles were neither developed unusually in mass or size and had no evident morphological specifications to suggest atypical mass distribution, excessive stiffness or strong frictional resistance.

The lack in landmark-based techniques ability to capture the whole shape of an object is particularly obvious in the case of the Dermoptera specimens. In the 3D models, the manubrium of the malleus is of a significantly different shape compared to the other specimens in the study, a factor not obvious in the landmark dissimilarity results. The shape is more reminiscent of a 'bat-wing' than the straight 'handle' shape of the primate mallei. Figure 5.1 shows the difference in shape between the malleus of *G. variegatus* and a more traditionally shaped primate malleus, this 'bat-wing' shape is also present in *C. volans.*

Figure 5.1 – Comparison of malleal manubrium shape of *G. variegatus* left and right, a typical primate (*L. tardigardus* pictured). N/B not to scale.

This shape difference in the Dermoptera may be a taxonomic difference between primates and non-primates or may represent an adaptive trait specific to the Cynocephalidae. It is unlikely to be an ecological adaptation as the Cynocephalidae are nocturnal, arboreal, omnivores similar to many of the other species represented in this study. The flattening and extension of the manubrium correlates with the attachment for the tensor tympani muscle and may represent hyper-development of this tissue. Further research into non-primate malleal shape is necessary before any conclusions can be drawn on the development and functional difference caused by this shape change.

Percussive Foragers

The other unusual species relevant to the aims of this study is *Daubentonia madagascariensis*, the percussive forager. The goal in including *Daubentonia* was two-fold, firstly, to see if and by how much the auditory ossicles of percussive foragers differ from other primates. Secondly, to examine the morphological evidence for *Daubentonia*'s phylogenetic relationship to the other primates.

In both the first principal coordinate axis scores and centroid size analysis, the *Daubentonia* specimen was the largest, with a significant centroid size of 9.4346. The dissimilarity matrix once scaled for size shows long MAN-HEA, LCR-MAH and MAH-IAI distances but with relatively short HEA-MAH, LAT-SCR and IAR-IAI distances. These represent a very long malleus, seen in the 3D model to be relatively thin with a prominent flattened tip for attachment to the tympanic membrane, and a laterally constricted incudal body. The short crus of the incus has a constricted neck with a thick tubular shape topped by a rounded end.

The overall dimensions of the auditory ossicles are unusual. Although *D. madagascariensis* is the largest of the nocturnal primates, they have a mean body mass of only 2.5kg (Quinn and Wilson, 1994) and certainly do not have the largest body dimensions of the species in this study. As previously mentioned there is a correlation between general body size and ossicle size, however, this would not be enough to explain the obvious differences in the *Daubentonia* ossicles. Again, these shape differences are unlikely to be related to their habitat, as nocturnal and both terrestrial and arboreal primates, they occupy a wide variety of habitats and adaptations to these factors should have been seen in primates who share similar environments and behaviours. It is interesting to note that *Daubentonia* and galagos have the largest relative pinnae. Further, galagos in both the PCoA and centroid size studies have relatively large auditory ossicles for their size, indicating that relative outer ear size may correlate to relatively larger auditory ossicles.

The family Daubentoniidae are classified as strepsirrhines primates, chromosomal and DNA investigations (Dene *et al.*, 1980; Rumpler *et al.*, 1988; Del Pero *et al.*, 1995; Porter *et al.*, 1995) indicate that *Daubentonia* is a sister group to the lemuriformes. Alternative morphological studies (Groves, 1989; Jablonski, 1986) as well as mitochondrial DNA analyses (Adkins and

Honeycutt, 1994) suggest that *Daubentonia* may be a sister group to both lemuriformes and lorisformes. The dendrogram based on Purvis (1995) used throughout this study, groups *Daubentonia* with *H. griseus,* both *Eulemur* and the *C. medius* specimens, as a sister group to the lemuriformes. Once scaled, the *Daubentonia* specimen is somewhat different to the majority of other species in the first principal coordinate axis but clusters in the mid-range in subsequent axes. In the hierarchical cluster *Daubentonia* is grouped with the Cynocephalidae, as previous mentioned, then sister to both *Eulemur, V. v. variegata, H. griseus* and *L. catta*, strongly mirroring the accepted taxonomy with only a few order changes. Only missing in this group is *C. medius*, which has been grouped with the Pitheciidae, although with very low repeatability of 1%.

Daubentonia's unique method of 'hunting' would seem a likely cause of the outstanding shape differences, although this remains impossible to prove with only one specimen representing percussive foragers. A future study comparing the ossicles of *Daubentonia* with non-primate percussive foragers would provide an excellent base for morphological discussions of hearing specialisation. What this study has shown is that although the auditory ossicles of *D. madagascariensis* are unique in form, morphometrics of the scaled shape fit well with the inclusion of *Daubentonia* as a sister group to the Lemuriformes.

Statistical Outliers

The outliers in the non-scaled data PCoA plot are a representation of the extremes in ossicular chain size. As mentioned, at the highest end of the scale is *D. madagascariensis* with a centroid size of 9.4346, whilst at the low end is *G. demidoff*, which has a centroid size of 3.84135. The low score of *G. demidoff* is unsurprising considering it has one of the smallest general body dimensions of any primate (Wilson and Reeder, 2005). When examining the

outliers in the shape plot, *G. demidoff* does not stand out and instead clusters with the rest of the Galagidae. In the scaled data the three most outlying species are *A. calabarensis* at the low end and *T. bancanus* and *V.v. variegata* at the high end.

A. calabarensis is at the low end of the PCoA plot with short distances in the superior-inferior landmarks. These shape differences represent a bulbous ossicular chain, with a shortened malleal manubrium, which is about equal to the long crus of the incus (Figure 5.2). The majority of other primates have a manubrium almost twice the length of the incudal crus. The *A. calabarensis* malleus is much thicker than its fellow Lorisidae. The mass and stiffness of the ossicular chain affect the impedance matching function of the middle ear (Wilson, 1987). Species with the greatest low-frequency hearing have large ossicular lever ratios. *A. calabarensis* provides an interesting case for functional analysis, as the ossicular lever advantage would be close to nil, as the maximum incudal length is approximately equal to the maximum malleal length negating the mechanical advantage supposedly provided according to the ossicular lever hypothesis.

Reduction in ossicular mobility as might result from flexing of thicker bone such as that seen in *A. calabarensis*, produces reductions in sound-induced stapedial velocity. This reduction in acoustic transmission is reduced at all frequencies resulting in a broadband reduction in hearing sensitivity (Nakajima *et al.*, 2005).

Figure 5.2 – Comparison of ossicular shape and malleal shortening of *A. calabarensis* left and right, a typical primate (*L. tardigardus* pictured). N/B not to scale.

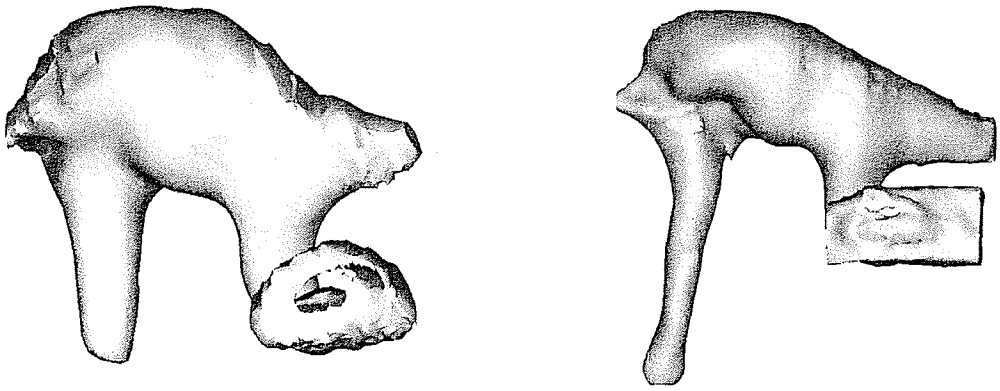

Although the overall size of the *T. bancanus* ossicular chain does not stand out, it has an unusual shape. *T. bancanus* has the longest distances of all the species between MAN-HEA, LCR-MAH and MAH-IAI as well as the shortest HEA-MAH, LAT-SCR and SAH-MAH. These dimensions represent an ossicular chain, which appears mediolaterally compressed (Figure 5.3). The malleus is flattened with a wide manubrium and a shape similar to, although not as pronounced as, the Cynocephalidae 'bat-wing'. The incus is long with thick crus as well as extended stapedial crus and a relatively large footplate.

Figure 5.3 – Comparison of ossicular shape and mediolateral compression of *T. bancanus* left and right, a typical primate (*L. tardigardus* pictured). N/B not to scale.

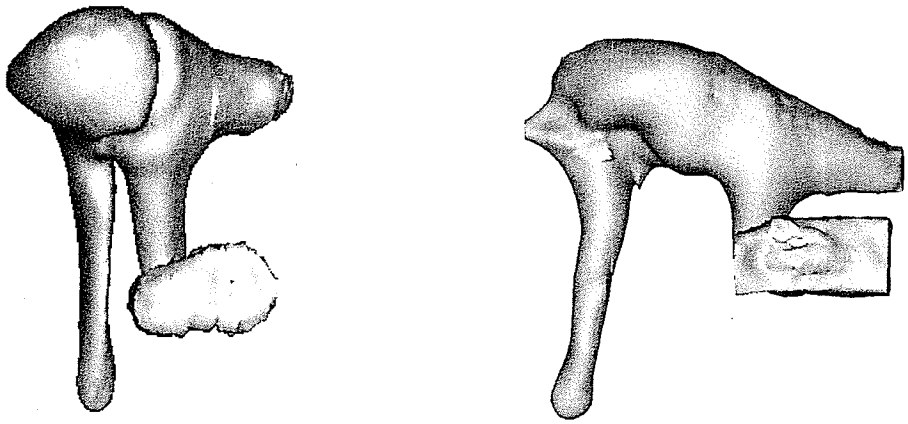

The causes of this unusual ossicular morphology are unknown; speculation and future studies may tend towards their unusual diet. *T. bancanus* represents the only carnivore in the study, consuming not only insects but small bats and snakes, the predation of which appears to rely on sound location (Wilson and Reeder, 2005). Before too many suggestions are made it would be useful to acquire scans of at least a second representative of the species to ensure the difference is not individualistic.

The *V.v. variegata* ossicular morphology is an interesting case and demonstrates a benefit in the application of the EDMA technique. *V.v. variegata* appears as an outlier in the shape dissimilarity matrix. An examination, however, of the individual landmark distances shows that although *V.v. variegata* has a slightly longer incudal long crus than the other primates (LCR-MAH), the majority of the shape differences occur between landmarks which do not measure functional or bone lengths but instead are a biproduct of the large number of inter-landmark distances produced by the EDMA process, for example the distance between the apex of the manubrium and the apex of the long crus. These distances represent not only the morphology of the individual bones but also how they articulate with each other. The majority of shape differences in the *V.v. variegata* scores represent the unusual articulation angle of the malleus and incus (Figure 5.4).

Figure 5.4 – Comparison of the malleus-incus articulation angle of *V.v. variegata* left and right, a typical primate (*L. tardigardus* pictured). N/B not to scale.

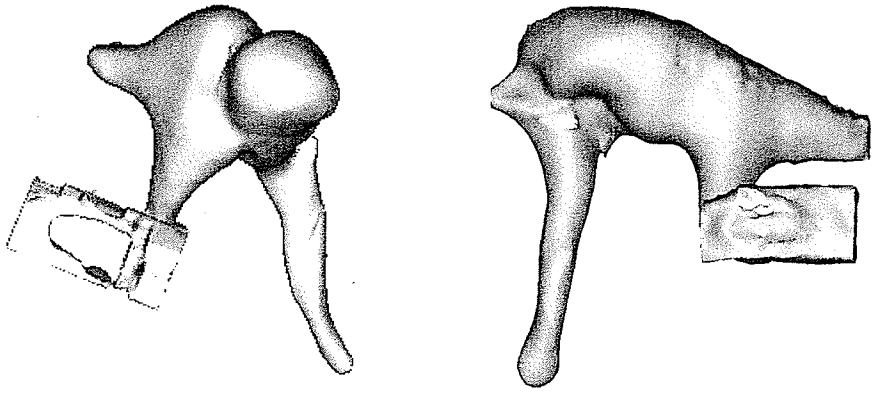

These angles are not something examined in other studies, which generally concentrate on measures of single bones but if we are to accept that these three bones act as a functional unit, then the angle of articulation must be as relevant in functional and morphological studies as the total length, width or other basic measures.

The 'bonus' of gaining these measures can only be put to full use when data exploration studies are conducted rather than trying to classify according to *a priori* groups. Opponents of the EDMA technique have focused on the 'excessive' data produced (Rohlf 2000) such as the 105 inter-landmark distances for each ossicular chain seen here. The discovery of the unique nature of the articulation shape of *V.v. variegata*, however, would not have been visualised without the 'extra' data gathered. The differences these angles of articulation have on function are unknown, but they are a useful component for future studies to consider. The angle of articulation may impact the axis of rotation vital to the transmission of sound during hearing. The spring-like arrangement of the *V.v. varecia* malleoincudal complex has a lower stiffness meaning resonance occurs at lower frequencies (Hüttenbrink, 1992).

CONCLUSIONS

The aims of the current study were to evaluate and validate the methodological frameworks specifically used for the measurement of primate auditory ossicles, and then use these to determine if there are any measurable differences in auditory ossicle morphology between primates at the suborder, family and species level as well as between percussive and non-percussive foragers. The findings of this study strongly indicate that the use of landmark methodologies on UhrCT scans provide a great deal of information on the auditory ossicles which has not been available until now. The EDMA technique achieved the goals of this study allowing data exploration of the samples clustering patterns, as well as providing additional

information on specific difference and articulation angle. Although caution must be applied when using the clustering techniques and the limitations acknowledged, the results were strong with high probability clustering at the suborder and family level although examination of shared traits such as activity cycles and diets did not cluster well suggesting alternative causes of adaptation.

1. **The evaluation and validation of the methodological frameworks specifically used for the measurement of primate auditory ossicles set out by Schmidt *et al.* (2009).**

- Overall, exclusive of a few limiting factors, the landmark technique set out by Schmidt and Colleagues (2009) provided useful data for statistical analysis and discussion of auditory ossicle morphology.
- The EDMA method provided unanticipated information, about the articulation angles of the ossicular chains, particularly that of *V.v. variegata*. These findings disagree with opponents of the EDMA technique, who have called the data produced 'excessive' (e.g. Rohlf, 2000).

2. **Determine if there are any measurable differences in auditory ossicle morphology between primates at the suborder, family and species level.**

- The greatest auditory ossicle variable between in this study was size, which was therefore a significant factor in the choice to include both form and shape differences in this study, as it was in the choice to use EDMA rather than more traditional morphometric techniques such as Procrustes.
- The longest malleus occurs in *D. madagascariensis* at 7.2587. The shortest malleus belongs to *A. calabarensis* at 2.414. *D. madagascariensis* has the longest incudal

bodies at 3.9292, while *G. demidoff* has the shortest with 1.5305. The widest ossicular chain belongs to *D. madagascariensis* (4.4962), the shortest is *C. volans* with 2.2895.

- The haplorrhine–strepsirrhine split is well reflected in ossicle morphology.
- Clustering into biological families was strong and the scaled data reflected the accepted taxonomy well.
- The hierarchy of the clustering within families tended to be out of order compared to the cladogram.
- The results of the non-scaled cluster analyses, grouped the species along the first principal coordinate axis according to magnitude, with the galagos grouped at the low end and the Lemuriformes, Macaques and *D. madagascariensis* at the high end.
- Once scaled to a geometric mean in order to focus on shape, the groups tend to fall out into a low, middle and high range variation. The low variability groups included the galagos as well as the Lorisformes. The mid-range group included the *Macaca,* both the Cynocephalidae and *H. griseus*. The high-range included *D. madagascariensis, V.v. variegata* and the unexpected outlier *Tarsius bancanus.*
- The results of the PCoA cluster and classification analyses indicate that although diet and activity patterns may be relevant when discussing the auditory ossicle morphology of a specific species, the clustering is not strong enough to suggest that these patterns are an important factor in determining differences in morphology between clades.
- Localisation of difference of the non-scaled dataset found the most influential landmark distances are: the maximum length of the incus, the distance between the most inferior point of the incus in its articulation with the malleus and the interior arch of the incus, the distance between the superior surface of the incus and the

superior surface of the malleus and the distance between the superior surface of the incus to the incudostapedial joint. Many of these measures define the morphology of the incus and can be used in functional analyses. The distance between superior surfaces represents an increase in ossicular body size without an accompanying increase in process size which would be seen in changes in the ossicular chain width.

- In the scaled dataset the most influential landmark distances are: the maximum width of the ossicular chain bodies, the maximum length of the malleus and the maximum length of the incus. These three measures are used in the ossicular lever hypothesis to determine the axis of rotation as well as the ratio of the lever arms. Other influential landmarks included the inferior incudomalleal joint to the interior arch of the incus and the superior surface of the incus to three points, the superior surface of the malleus, the superior incudomalleal articulation and the incudostapedial joint, representing changes in the morphology of the incus.
- Unexpected morphometric statistical outliers included: *A. calabarensis,* with a bulbous ossicular chain and shortened manubrium, *T. bancanus,* with mediolaterally constricted bodies and *V.v. variegata* with unusual articulation angles between the malleus and incus.
- The xyz coordinate data collected along with some of the EDMA distances calculated can be used for future functional analyses including determining the lever arm lengths and stapedial footplate area.

3. **Examine included species, specifically *Daubentonia madagascariensis* to answer the question, what, if any, variation exists between percussive and non-percussive foragers?**

- The auditory ossicles of *D. madagascariensis* are unique in form. In both the principal coordinate axis scores and centroid size analysis, the *Daubentonia* specimen was the largest, with a significant centroid size of 9.4346.
- The shape of the ossicular chain is unusual, including a very long thin malleus, with a prominent flattened tip for attachment to the tympanic membrane, and a laterally constricted incudal body.
- *Daubentonia*'s unique method of 'hunting' would seem a likely cause of the outstanding shape differences, although this remains impossible to prove without further study.
- Morphometrics of the shape fit well with the inclusion of *Daubentonia* as a sister group to the Lemuriformes.

4. **To include the Dermoptera as an outgroup to the primates in order to provide a non-primate comparison for the morphometric and taxonomic analyses.**

- The Dermoptera have a unique ossicular morphology within the context of this study, specifically a 'bat-wing' rather than a straight 'handle' shape to the manubrium, whether this is due to a non-primate taxonomic difference or an adaptive trait is unknown.
- The two representative species of Dermoptera, *Cynocephalus volans* and *Galeopterus variegatus,* were in the middle of the primate range for size, both in the PCoA and centroid size analyses. Once the specimens were scaled, the two Cynocephalidae stood out more and clustered closely on the first few principal coordinate axes and separate to the other species. This 'falling-out' of non-primate specimens within the primate cluster groupings demonstrates a serious lack of concordance with the

majority of phylogenetic hypotheses. This illustrates the issue with cluster analyses in taxonomic studies as they compare morphological similarities rather than direct relationships.

Future Directions

The results of the current study raise many questions for further study. One of the greatest issues with the use of landmarks is the loss of information on morphology between the points placed, although adding more landmarks is not practical, future studies of the auditory ossicles may benefit from adapted superimposition volumetric or surface-render studies such as that being developed by Hallgrimsson and colleagues (2008) if the techniques can overcome the inherent limitations of superimposition methods, which they currently do not. The greatest variable between the auditory ossicles in this study is size and a larger scale study will need to be conducted in the future, which compares the primate's general body dimensions with auditory ossicle size. The use of the EDMA technique provided valuable results, it would be useful however to run the same data through a more tradition statistical analysis registration-based method to compare results.

The morphometric analysis resulted in some unusual findings, which warrant future study. The unusual morphology of the Dermoptera 'bat-wing' malleal manubrium is unlikely to be an ecological adaptation as the Cynocephalidae are nocturnal, arboreal, omnivores similar to many of the other species represented in this study. Further research into non-primate malleal shape is necessary before any conclusions can be drawn on the development and functional difference caused by this morphological anomaly. In the course of the study it was noted that *Daubentonia* and galagos have the largest relative pinnae. *Daubentonia* andgalagos in both the PCoA and centroid size studies have relatively large auditory ossicles for their size, indicating that relative

outer ear size may correlate to relatively larger auditory ossicles, an interesting concept which deserves future attention.

The cluster analyses of the PCoA plots provided useful and informative groupings but as with any study, would have been improved by the inclusion of both a larger sample set and a larger number of representatives of each group, family, suborder etc. Future studies may benefit from the inclusion more variables of primate lifestyle with a focus on communication habits and ecology, which may be stronger factors in ossicle morphology adaptation. Comparisons of ecological behavioural patterns were restricted by a lack of representation. The majority of species in the study were arboreal with only the two terrestrial specimens, the inclusion of more terrestrial species would be useful.

Both the data collected and the results of the EDMA analysis have possible uses in future functional analyses. The landmark coordinates along with the pair-wise interlandmark distances generated by the EDMA process provide measures for ossicular lever hypotheses. Stapes footplate area measures used to calculate overall ratio of the transformed sound pressures can be determined by calculating two perpendicular axes from specific landmarks, although not ideal it may be possible for future studies to do a direct perimeter tracing on the 3D model.

Auditory sensitivity and function is affected, to some degree, by ossicular morphology and this is of particular interest in the specimens, which have substantially different ossicles. Examples of this that should be included in future studies are *A. calabarensis* with its bulbous ossicular chain and shortened malleal manubrium or the *T. bancanus* ossicular chain, which appears mediolaterally compressed with a wide manubrium and a shape similar to, although not as pronounced as, the Cynocephalidae 'bat-wing'. The effect of ossicular morphology on hearing

sensitivity is particularly of interest with percussive foragers. The overall dimensions of the *D. madagascariensis* auditory ossicles are large and they have a unique morphology. These shape differences are unlikely to be related to their unique method of 'hunting', however, this remains impossible to prove with only one specimen representing percussive foragers. A future study comparing the ossicles of *Daubentonia* with non-primate percussive foragers would provide an excellent base for morphological discussions of hearing specialisation.

The difference in ossicles articulation angle first noted in the stand-out results of the *V.v. variegata* specimen is an interesting case and would benefit from future study. Many functional analyses rely on the ossicular chain functioning as a mechanical lever unit, however, changes in the angles between these bones have not been considered and until such studies are conducted, the movements of the ossicular chain under sound pressure cannot be accurately modelled.

Overall, although the technique of using UhrCT scans to produce a 3D model which is then landmarked, do provide opportunity for functional analyses, EDMA is more useful for exploration of form-shape difference in the data. It is in this area that the current study, with its focus on morphology, has a great deal to add to future function studies. Many of the acoustic hypotheses are limited by their assumption of perfect conditions or ideal movements. A study such as this one allows visualisation of the angles between bones, size of articulations and may answer questions regarding ossicle flexibility and relative motions.

Now that the technology has caught up with the need for greater understanding of auditory anatomy, this may be a suitable time to step back from the testing of multiple impedance matching and power theories to examine the variables that occur within and between species ossicle morphology and compare this to the currently accepted audiograms. In short, the

morphometric analyses of primate auditory ossicles have much to add to the examination of auditory mechanics and primate hearing.

REFERENCES

Adkins, R.M and R.L. Honeycutt (1994) Evolution of the primate cytochrome *c* oxidase subunit II gene. *Journal of Molecular Evolution* 38: 215-231.

Allin, E.F. Evolution of the mammalian middle ear. *Journal of Morphology* 147(4): 403-437.

Amin, S. and A.S. Tucker (2006) Joint formation in the middle ear: lessons from the mouse and the guinea pig. *Developmental Dynamics* 235: 1326-1333.

Ancrenaz, M., Lackman-Ancrenaz, I. And N. Mundy (1994) Field observations of aye-ayes (*Daubentonia madagascariensis*) in Madagascar. *Folio Primatologica* 62: 22-36.

Anderson, S.D. and D.T. Kemp (1979) The evoked cochlear mechanical response in laboratory primates: a preliminary report. *Archives of Otorhinolaryngology* 224: 47-54.

Anson, B.J. and T.H. Bast (1959) I: Development of the incus of the human ear. *Quarterly Bulletin of the Northwestern University Medical School Chicago, IL.* 110-119.

Arensburg, B., Belkin, V. and M. Wolf (2005) Middle ear pathology in ancient and modern populations: incudal osteoma. *Acta Oto-Laryngologica* 125(11): 1164-1167.

Arensburg, B., Harell, M., and H. Nathan (1981) The human middle ear ossicles: morphometry and taxonomic implications. *Journal of Human Evolution* 10: 199-205.

Arensburg, B., Schepartz, L.A., Tillier, A.M., Vandermeersch, B. and Y. Rak (1990) A reappraisal of the Anatomical basis for speech in Middle Palaeolithic Hominds. *American Journal of Physical Anthropology* 83: 137-146.

Arensburg, B. and A.M. Tillier (1991) Speech and the Neanderthals. *Endeavour* 15(1): 26-28.

Arione, L. (1923) Variazoni della grandezza degli ossicini dell'udito nel periodo di accrescimento e nell'adulto. *Monitore Zoologico Italiano* 34: 45-48.

Arnason, U., Adegoke, J.A., Bodin, K., Born, E.W., Esa, Y.B., Gullberg, A., Nilsson, M., Short, R.V., Xu, X. and A. Janke (2002) Mammalian mitogenomic relationships and the root of the eutherian tree. *Proceedings of the National Academy of Sciences* 99(12): 8151:8156.

Bass, R.W. (1995) *Human osteology: a laboratory and field manual.* Special Publications Missouri Archaeological Society, No. 2.

Beecher, M.D. (1974a) Pure-tone thresholds of the squirrel monkey (*Saimiri sciureus*). *Journal of the Acoustical Society of America* 55(1): 196-198.

Beecher, M.D. (1974b) Hearing in the owl monkey (*Aotus trivirgatus*). *Journal of Comparative and Physiological Psychology* 86(5): 898-901.

Beer, H.J., Bornitz, M., Hardtke, H.J.,Schmidt, R., Hofmann, G., Vogel, U., Zahnert, T. and K.B. Hüttenbrink (1999) Modelling of components of the human middle ear and simulation of their dynamic behaviour. *Audiology and Neuro-Otology* 4: 156-162.

Békésy, G. von (1941) On the measurement of the amplitude of vibration of the ossicles with a capacitive probe. *Akustische Zeitschrift* 6: 1-16.

Békésy, G. von (1960) *Experiments in hearing*. New York: McGraw-Hill.

Birkby, W.H and J.B. Gregg, J.B. (1975) Otosclerotic stapedial footplate fixation in an 18th Centurial burial. *American Journal of Physical Anthropology* 42: 81-84.

Bloch, J.I. and M.T. Silcox (2006) Cranial anatomy of the Paleocene plesiadapiform *Carpolestes simpsoni* (Mammalia, Primates) using ultra high-resolution X-ray computer tomography, and the relationships of pleasiadapiforms to Euprimates. *Journal of Human Evolution* 50: 1-35.

Bookstein, F. (1991) *Morphometric tools for landmark data.* Cambridge: University Press.

Bouchet, A. and M. Giraud (1968) Contribution a l'etude morphologique et radiologique des osselets de l'ouie. *Comptes Rendu de l'Association des Anatomists 53 Congress.* 140: 588-600.

Brosch, S. and W. Pirsig (2003a) Gehörlosigkeit im kulturgeschichtlichen Kontext: teil 1. *HNO* 51: 25-29.

Brosch, S. and W. Pirsig (2003b) Gehörlosigkeit im kulturgeschichtlichen Kontext: teil 2. *HNO* 51: 113-117.

Brown, C.H. and P.M. Waser (1984) Hearing and communication in blue monkeys (*Cercopithecus mitis*). *Animal Behavior* 32: 66-75.

Bruintjes, T.D. (1990) The auditory ossicles in human skeletal remains from a leper cemetery in Chichester, England. *Journal of Archaeological Science* 17: 627-633.

Burkert, S., Haberland, E.J., Raum, K., Klemenz, A., Brandt, J. and A. Berghaus (2002) Tissue characterization of human auditory ossicles by scanning acoustic microscopy. *IEEE Ultrasonics Symposium 1305:* 1273-1276.

Cancura, W. (1980) On the statics of the malleus and incus and on the function of the malleus-incus joint. *Acta Otolaryngologica* 89: 342-344.

Cartmill, M. (1975) Strepsirrhine basicranial structures and affinities of the Cheirogaleidae. In Luckett, W.P. and F.S. Szalay (eds) *Phylogeny of the Primates*. New York: Raven Press, pp. 313-354.

Chakeres, D.W. (1983) Clinical significance of partial volume averaging the temporal bone. *American Journal of Neuroradiology* 5(3): 297-302.

Chakeres, D.W. and P.K. Spiegel(1983) A systematic technique for comprehensive evaluation of the temporal bone by computed tomography. *Head and Neck Radiology* 146: 97-106.

Clack, J.A. (1997) The evolution of Tetrapod ears and the fossil record. *Brain Behavior and Evolution* 50(4): 198-212.

Cockerell, T.D.A., Miller, L.I. and M. Printz (1913) The auditory ossicles of American rodents. *Bulletin of the American Museum of Natural History* 33: 347-364.

Cole, T.M. (2002) *WinEDMA:* Software for Euclidean distance matrix analysis. Version 1.0.1 beta. Kansas City: University of Missouri – Kansas City School of Medicine.

Coleman, M.N. (2007) *The functional morphology and evolution of the primate auditory system.* Thesis (PhD): Stony Brook University. 506 leaves pp.

Coleman, M.N. and M.W. Colbert (2007) Technical note: CT thresholding protocols for taking measurements on three-dimensional models. *American Journal of Anthropology* 133: 723-725.

Coleman, M.N., Di Fiore, A. and E. Fernandez- Duque (2009) Histomorphological variation in human auditory ossicles. American Association of Physical Anthropologists Annual Meeting. Chicago, Illinois: *American Journal of Physical Anthropology Supplement* 45: 157.

Coleman, M.N. and C.F. Ross (2004) Primate auditory diversity and its influence on hearing performance. *The Anatomical Record* 281A: 1123-1137.

Dalby, G., Manchester, K., and C.A. Roberts (1993) Otosclerosis and stapedial footplate fixation in archaeological material. *International Journal of Osteoarchaeology* 3: 207-212.

Dallos, P. (1973) *The Auditory Periphery: Biophysics and Physiology.* New York: Academic Press.

Décory, L. (1989) Origine des differences interspecifiques de susceptibilité an bruit. *Thése de Doctorat de l'Université de Bordeux, France.*

Decraemer, W.F. and S.M. Khanna (1995) Malleus vibration modelled as rigid body motion. *Acta Oto-rhino-laryngologica Belgium* 49: 139-145.

Decraemer, W.F. and S.M. Khanna (2004) Measurement, visualization, and quantitative analysis of complete three-dimensional kinematical data sets of human and cat middle ear. In: Gyo, K., Wada, H., Hato, N. and T. Koike (eds), *Middle Ear Mechanics in Research and Otology.* World Scientific, Singapore. pp3-10.

Decraemer, W.F., Khanna, S.M. and W.R.J. Funnell (1991) Malleus vibration mode changes with frequency. *Hearing Research* 54: 305-318.

Del Pero, M., Crovella, S., Cervella, P., Arditor, G. and Y. Rumpler (1995) Phylogenetic relationships among Malagasy lemurs as revealed by mitochrondrial DNA sequence analysis. *Primates* 36: 431-440.

Delson, E. and P. Andrews (1975) Evolution and interrelationships of the catarrhine primates. In Luckett, W.P. and F.S. Szalay (eds) *Phylogeny of the Primates*. New York: Raven Press, pp. 405-446.

Dene, H., Goodman, M. and W. Prychodko (1980) Immunodiffusion systematics of the primates. *Mamalia* 44: 27-31.

De Ruiter, D., Moggi-Cecchi, J. and M. Masali (2002) Auditory ossicles of *Paranthropus robustus* from Swartkrans, South Africa. *American Journal of Physical Anthropology Supplement* 34: 60.

Doran, A.H.G. (1878) Morphology of the mammalian ossicula auditus. *Transactions of the Linnaean Society, Series 2, Zoology* 1: 371-497.

Duff, A. and A. Lawson (2004) *Mammals of the World: a checklist*. New Haven: Yale University Press.

Erickson, C.J. (1991) Percussive foraging in aye-ayes, *Daubentonia madagascariensis. Animal Behaviour* 41: 793-801.

Erickson, C.J. (1994) Tap-scanning and extractive foraging in aye-ayes, *Daubentonia madagascariensis. Folio Primatologica* 62: 125-135.

Erickson, C.J. (1995) Perspectives on percussive foraging in the aye-aye (*Daubentonia madagascariensis).* In: Alterman, L., Doyle, G.A. and M.K. Izard (eds) *Creatures of the Dark: the nocturnal prosimians.* New York: Plenum Press. 251-159pp.

Erickson, C.J. (1998) Cues for prey location by aye-ayes (*Daubentonia madagascariensis). Folio Primatologica* 69 (suppl 1): 35-40.

Erickson, C.J., Nowicki, S., Dollar, L. and N. Goehring (1998) Percussive foraging: stimuli for prey location by aye-ayes (*Daubentonia madagascariensis*). *International Journal of Primatology* 19(1): 111-122.

Falk, D. (1975) Comparative anatomy of the larynx in Man and the chimpanzee: Implications for language in Neanderthal. *American Journal of Physical Anthropology* 43: 123-132.

Falk, D. (2000) *Primate Diversity.* New York: W.W. Norton & Company.

Feistner, A.T.C. and E.J. Sterling (1995) Body mass and sexual dimorphism in the aye-aye *Daubentonia madagascariensis.* Dodo Journal of the Jersey Wildlife Preservation Trust 31: 73-76.

Finneran, J.J. and M.C. Hastings (2000) A mathematical analysis of the peripheral auditory system mechanics in the goldfish (*Carassius auratus*). *Journal of the Acoustical Society of America* 108(3): 1308-1314.

Fleischer, G. (1973) Studien am skelett des gehörorganes der säugetiere, einschlißich des menschen. *Säugetierkundliche Mitteilungen.* 21: 131-239.

Fleischer, G. (1978) Evolutionary principles of the mammalian middle ear. *Advances in Anatomy, Embryology and Cell Biology.* 55(5): 1-70.

Flohr, S. and M. Schultz (2005) Diseases of the middle ear region in early medieval German populations – new standards in paleopathological research. *Gesellschaft Für Anthropology E.V. (Veranst.): 6 Kongress Der GFA, Abstracts (Facetten der Modernen Anthropologie München 13.-16.09.2005).*

Flohr, S., Strympe, K., Thielsch, A., Volmer, R. und N.J. Rehbach (2006) Möglichkeiten der Geschlectsbestimmung anhand von Gehörknöchelchen beim Menschen. *Beiträge zur Archäozoologie und Prähistorischen Anthropologie* 5:166-175.

Garland, T. Dickerman, A.W., Janis, C.M. and J.A. Jones (1993) Phylogenetic analysis of covariance by computer simulation. *Systematic Biology* 42(3): 265-292.

Ghorayeb, B.Y. and M.D Graham (1978) Human incus long process depressions in the surface of the normal ossicle. *The Laryngoscope* 88: 1184-1189.

Gillette, R.G., Brown, R., Herman, P., Vernon, S. and J. Vernon (1973) The auditory sensitivity of the lemur. *American Journal of Physical Anthropology* 38: 365-370.

Gingerich, P.D (1980) Evolutionary Patterns in Early Cenozoic Mammals. *Annual Review of Earth and Planetary Sciences* 8: 407 – 424.

Glander, K.E. (1994) Morphometrics and growth in captive aye-ayes (*Daubentonia madagascariensis). Folio Primatologica* 62: 108-114.

Graham, M.D., Reams, D. and R. Perkins (1978) Human tympanic membrane-malleus attachment. *Annals of Otology, Rhinology and Laryngology* 87: 426-431.

Gregg, J.B., J.P. Steele and A. Holzhueter, (1965) Roentgenographic evaluation of temporal bones from South Dakota Indian burials. *American Journal of Physical Anthropology* 23: 51-62.

Greiner, T.M. and R.A. Walker (1999) Morphometric variation of the human auditory ossicles. *American Journal of Physical Anthropology Supplement 18: 140.*

Groves, C. (1989) *A theory of human and primate evolution.* Oxford: Clerendon Press.

Guild, S.R. (1944) Histologic Otosclerosis. *Annals of Otology, Rhinology and Laryngology* 53: 246.

Hallgrimsson, B. Zelditch, M.L Parsons, T.E. Kristensen, E., Young, N.M. and S.K. Boyd (2008) Morphometrics and biological anthropology in the postgenomic age. In: Katzenburg, M.A. and S.R. Saunders (eds) *Biological Anthropology of the Human Skeleton (Second Edition)*. New York: John Wiley and Sons.

Hammer, Ø. and D.A.T Harper (2005) *Paleontological Data Analysis*. Malden, Massachusetts: Blackwell.

Heffner, H. and B. Masterton (1970) Hearing in primative primates: slow loris (*Nycticebus coucang*) and potto (*Perodicticus potto). Journal of Comparative and Physiological Psychology* 71(2): 175-182.

Heffner, R.S. (2004) Primate hearing from a mammalian perspective. *The Anatomical Record* 281A: 1111-1122.

Heffner, R.S. and H.E. Heffner (1985) Hearing range of the domestic cat. *Hearing Research* 19: 85-88.

Helmholtz, H.L.F. (1954) *On the Sensations of Tone (2nd English Edition).* New York: Dover.

Hemilä, S., Nummela, S. and T. Reuter (1995) What middle ear parameters tell about impedance matching and high frequency hearing. *Hearing Research* 85: 31-44.

Henson, O.W. (1974) Comparative anatomy of the middle ear. In Keidel, W.D. and Neff, W.D. (eds) *Handbook of Sensory Physiology Volume 1.* Berlin: Springer-Verlag.

Heron, I.C. (1923) Measurements and observations upon the human auditory ossicles. *American Journal of Physical Anthropology* 6: 11-26.

Hershkovitz, P. (1974) The ectotympanic bone and the origin of higher primates. *Folio Primatologica.* 22: 237-242.

Hershkovitz, P. (1977) *Living New World Monkeys (Platyrrhine) Volume 1.* Chicago: University of Chicago Press.

Hill, C.A. and J.T. Richtsmeier (2008) A quantitative method for the evaluation of three-dimensional structure of temporal bone pneumatization. *Journal of Human Evolution* 55: 682-690.

Hinchcliffe, R. and A. Pye (1969) Variations of the middle ear of the Mammalia. *Journal of Zoology.* 157: 277-288.

Holzhueter, A.M., Gregg, J.B. and S. Clifford (1965) A search for stapes footplate fixation in an Indian population, prehistoric and historic. *American Journal of Physical Anthropology* 23: 35-40.

Hunt, R.M and W.W. Korth (1980) The auditory region of Dermoptera: morphology and function relative to other living mammals. *Journal of Morphology* 164: 167-211.

Hyrtl, J. (1845) *Vergleichend-anatomische Untersuchungen über das innere Gehörorgan des Menschen und der Säugerthiere.* Prague: Verlag von Fredrich Ehrlich.

Hüttenbrink, K.B. (1988) The mechanics of the middle ear at static pressures. *Acta Laryngologica Supplement.* 451: 1-35.

Hüttenbrink, K.B. (1992) Die mechanik und function des mittelohres. Teil 1: die ossikelkette und die mittelohrmuskeln. *Laryngo-Rhino-Otol.* 71: 545-551.

Jablonski, N.G. (1986) A history of form and function in the primate masticatory apparatus from the ancestral primate through the strepsirrhines. In: Swindler, D.R. and J. Erwin (eds) *Comparative Primate Biology: systematics, evolution and anatomy.* New York: Alan R. Liss, Inc. 537-558.

Janecka, J.E., Helgen, K.M., Lim, T.L., Baba, M., Izawa, M., Boeadi., and W.J. Murphy (2008) Evidence for multiple species of Sunda colugo. *Current Biology* 18(21): 1001-1002.

Janecka, J.E., Miller, W., Pringle, T.H., Wiens, F., Zitzmann, A., Helgen, K.M., Springer, M.S. and W.J. Murphy (2007) Molecular and genomic data identify the closest living relative of primates. *Science* 318: 792-794.

Kaufman, J.A., Ahrens, E.T., Laidlaw, D.H., Zhang, S. and J.M. Allman (2005) Anatomical analysis of an aye-aye brain (*Daubentonia madagascariensis,* Primates: Prosimii) combining histology, structural magnetic resonance imaging, and diffusion-tensor imaging. *The Anatomical Record Part A* 287A: 1026-1037.

Kelly, D.J. and P.J. Prendergast (2001) An investigation of middle-ear biomechanics using finite element modelling. *2001 proceedings of the Bioengineering Conference: Summer Bioengineering Conference.* New York: ASME Books. pp 369-370.

Khanna, S.M. and J. Tonndorf (1972) Tympanic membrane vibrations in cats studied by time-average holography. *Journal of the Acoustic Society of America* 51: 1904-1920.

Knight, R.D. and D.T. Kemp (2001) Wave and place fixed DPOAE maps of the human ear. *Journal of the Acoustical Society of America* 109(4): 1513-1525.

Kojima, S. (1990) Comparison of auditory functions in the chimpanzee and human. *Folio Primatologica* 55: 62-72.

Lannigan, F.J., O'Higgins, P. and P. McPhie (1993) Remodelling of the normal incus. *Clinical otolaryngology* 18: 155-160.

Lannigan, F.J., O'Higgins, P., Oxnard, C.E. and P. McPhie (1995) Age-related bone resorption in the normal incus: a case of maladaptive remodelling? *Journal of Anatomy* 186: 651-655.

Lasky, R.E., Soto, A.A., Luck, M.L. and N.K. Laughlin (1999) Otoacoustic emission, evoked potential, and behavioural auditory thresholds in the resus monkey (*Macaca mulatta*). *Hearing Research* 136: 35-43.

Lay, D.M. (1972) The anatomy, physiology, functional significance and evolution of specialised hearing organs or gerbilline rodents. *Journal of Morphology* 138: 41-120.

Lele, S.H. and J.T. Richtsmeier (1991) Euclidean distance matrix analysis: a coordinate free approach to comparing biological shapes using landmark data. *American Journal of Physical Anthropology* 98: 73-86.

Lele, S.H. and J.T. Richtsmeier (2001) *An Invariant Approach to Statistical Analysis of Shapes*. Boca Raton: Chapman & Hall.

Lewis, R.F., Haburcakova, C. and D.M. Merfeld (2005) Tilt psychophysics measured in nonhuman primates. *Annals of the New York Academy of Science* 1039: 294-305.

Lindsay, J.R. (1971) Inner ear pathology in congenital deafness. *Otolaryngologic Clinics of North America* 4(2): 249-318.

Lloyd, G.A.S, du Boulay, G.H., Phelps, P.D. and P. Pullicino (1979) The demonstration of the auditory ossicles by high resolution CT. *Neuroradiology* 18: 243-248.

Lombard, R.E. and T. Hetherington (1993) Structural basis of hearing and sound transmission. In: Hanken, J. and B.K. Hall (eds) *The Skull Volume 3: Functional and Evolutionary Mechanics.* Chicago: University of Chicago Press.

Lynch, T.J. III, Nedzelbitsky, V. and W.T Peake (1982) Input impedance of the cochlea in the cat. *Journal of the Acoustic Society of America* 72: 108-130.

MacPhee, R.D.E. (1981) Auditory regions of primates and eutherian insectivores. In: Szalay, F.S. (ed) *Contributions to Primatology Volume 8*. Basel: S. Karger.

Majdalawieh, O.F., Alian, W.A., Katlai, B., Van Wijhe, R.G. and M.L. Bance (2008) Linearity and lever ration of the normal and reconstructed cadaveric human middle ear. *Otology and Neurotology* 29: 796-802.

Marten, K., Quine, D. and P. Marler (1977) Sound transmission and its significance for animal communication: tropical forest habitats. *Behavioural Ecology and Sociobiology* 2: 271-290.

Martin, R.D. (1990) *Primate Origins and Evolution: A Phylogenetic Reconstruction*. London: Chapman and Hill.

Martin, R.D. (2008) Colugos: obscure mammals glide into the evolutionary limelight. *Journal of Biology* 7:13.

Martinez, I and J.L Arsuaga (1997) The temporal bones from Sima de los Huesos Middle Pleistocene site (Sierra de Atapuerca, Spain). A phylogenetic approach. *Journal of Human Evolution* 33: 283-318.

Martinez, I., Rosa, M., Arsuaga, J.L., Jarabo, P., Quam, R., Lornenzo, C., Grada, A., Carretero, J.M., Bermúdez de Castro, J.M. and E. Carbonell (2004) Auditory capacities in Middle

Pleistocene humans from the Sierra de Atapuerca in Spain. *Proceedings of the National Academy of Sciences* 101(27): 9976-9981.

Masali, M. (1968) The ear bones and the vertebral column as indications of taxonomic and postural distinction among Old World primates. In: Chiarelli, B. (ed) *Taxonomy and Phylogeny of Old World Primates with References to the Origin of Man.* Rosenburg and Sellier, Turin, pp 69-94.

Masali, M. (1971) Morphometry of ear bones of some New World Primates. In: *Proceedings of the 3rd International Congress of Primatology, Zurich 1970*, vol. 1. Karger, Basel, pp 226-232.

Masali, M. (1992) The ear ossicles and the evolution of the primate ear: biomechanical approach. *Human Evolution* 7(4): 1-5.

Masali, M., Borgognini Tarli, S. and M. Maffei (1992) Auditory ossicles and the evolution of the primate ear: biomechanical approach. In: Wind, J. (ed) *Language Origin: a multidisciplinary approach.* Netherlands: Kluwer, pp 67-86.

Masali, M. and B. Chiarelli (1967) The ear bones of the Old World primates. In: Starck, D., Schneider, R., and H.J Kuhn (eds) *Neue Ergebnisse der Primatologie* (Progress in Primatology). Stuttgart: Fischer, pp 145-149.

Masali, M. and M.M. Cremasco (2006) Hoc alterum auditus organi ossiculum est: ear ossicles in physical anthropology. *Human Evolution* 21: 1-17.

Masali, M., Maffei, M. and S. Borgognini Tarli (1991) Application of a morphometric model for the reconstruction of some functional characteristics of the external and middle ear in Circeo 1. In: Piperno, M. and G. Scichilone (eds) *The Circeo 1 Neanderthal Skull: Studies and Documentation.* Rome: Instituto Poligrafico and Zecca Dello Stato, pp 321-338.

Masali, M. and M.S. Siori (1979) Gli ossicini dell'udito nell'evoluzione dei Primati. *Antropologia Contemporanea* 2: 77-85.

Masterton, B., Heffner, H. and R. Ravizza (1969) The evolution of human hearing. *Journal of the Acoustical Society of America* 45(4): 966-985.

Matshes, E., Burbridge, B., Sher, B., Mohamed, A. and B Juurlink (2004) *Human osteology and skeletal radiology: an atlas and guide*. Boca Raton: CRC Press.

Merker, H.J., Herger, W., Sames, K., Stürje, H. and D. Neubert (1988) Embryotoxic effects of thalidomide-derivatives in the non-human primate *Callithrix jacchus. Archives of Toxicology* 61: 165-179.

Moggi-Cecchi, J. and M. Collard (2002) A fossil stapes from Sterkfontein, South Africa, and the hearing capabilities of early hominids. *Journal of Human Evolution* 42: 259-265.

Morton, E. (1975) Ecological sources of selection on avian sounds. *American Nature* 109: 17-34.

Murphy, W.J., Eizirik, E., Johnson, W.E., Zhang, Y.P., Ryder, A.O. and S.J. O'Brien (2001) Molecular phylogenetics and the origins of placental mammals. *Nature* 409: 614-618.

Mutaw, R.J. (1986) *Human auditory ossicles variation and function*. Thesis (PhD): University of Colorado, 1986. xi, 127 leaves p.

Mutaw, R.J. (1988) Pathologies and anomalies in human auditory ossicles from two skeletal collections. American Association of Physical Anthropologists Annual Meeting. Kansas City, Missouri: *American Journal of Physical Anthropology Supplement* 2: 252.

Nager, G.T and M. Nager (1953) The arteries of the human middle ear, with particular regard to the blood supply of the auditory ossicles. *Annals of Otology, Rhinology and Laryngology* 62(4): 923-949.

Nakajima, H.H., Ravicz, M.E., Merchant, S.N., Peake, W.T. and J.J. Rosowski (2005) Experimental ossicular fixations and the middle ear's response to sound: Evidence for a flexible ossicular chain. *Hearing Research* 204: 60-77.

Newman, L.M. and A.G. Hendrickx (1981) Fetal ear malformations induced by maternal ingestion of thalidomide in the bonnet monkey (*Macaca radiata*). *Teratology* 23(3): 351-364.

Nie, W., Beiyuan, F., O'Brien, P.C.M., Wang, J., Su, W., Tanomtong, A., Volobouev, V., Ferguson-Smith, M.A., and F. Yang (2008) Flying lemurs – the 'flying tree shrews'?

Molecular cytogenetic evidence for a Scandentia-Dermoptera sister clade. *BMC Biology* 6: 18.

Nummela, S. (1995) Scaling of the mammalian middle ear. *Hearing Research* 85: 18-30.

Nummela, S. and M.R. Sánchez-Villagra (2006) Scaling of the marsupial middle ear and its functional significance. *Journal of Zoology:* 256-257.

Olson, E.S. (1998) Observing middle and inner ear mechanics with novel intracochlear pressure sensors. *Journal of the Acoustical Society of America* 103(6): 3445-3463.

Olszewski, J. (1990) Zur morphometrie der gehörknöchelchen beim menschen im rahmen der entwicklung. *Anatomischer Anzeiger.* 171: 187-191.

O'Malley, C.D. and E. Clarke (1961) The discovery of the auditory ossicles. *Bulletin of the History of Medicine.* 35: 419- 441.

O'Rahilly, R. (1983) The timing and sequence of events in the development of the human eye and ear during the embryonic period proper. *Anatomy and Embryology* 168: 87-99.

Owren, M.J., Hopp, S.L. Sinnott, J.M. and M.R. Petersen (1988) Absolute auditory thresholds in three old world monkey species (*Cercopithecus aethiops, C. neglectus, Macaca fuscata*) and humans (*Homo sapiens*). *Journal of Comparative Psychology* 102(2): 99-107.

Oxnard, C.E. (1981) The uniqueness of *Daubentonia. American Journal of Physical Anthropology* 54: 1-21.

Parizek, J. and M. Varacka (1967) Gehorknöchelchen bei Makaken. *Zeitschaft für Morphologie und Anthropologie* 58: 190-198.

Parker, W.K. (1886) On the structure and development of the skull in mammalia: Pat 1 Edentata, Part 2, Insectivora. *Philosophical Transactions of the Royal Society of London* 176: 1-275.

Pohlman, A.G. (1933) A reconsideration of the mechanics of the auditory apparatus. *The Journal of Laryngology and Otology* 48: 156-195.

Pollock, J.I., Constable, I.D., Mittermeier, R.A., Ratsirarson, J. and H. Simons (1985) A note on the diet and feeding behavior of the aye-aye *Daubentonia madagascariensis. International Journal of Primatology* 6(4): 435-447.

Porter, C.A., Sampaio, I., Schneider, H., Schneider, M.P.C., Czelusniak, J. and M. Goodman (1995) Evidence on primate phylogeny from ε-globin gene sequences and flanking regions. *Journal of Molecular Evolution* 40: 30-55.

Prendergast, P.J. (2002) Mechanics applied to skeletal ontogeny and phylogeny. *Meccanica* 37: 317-334.

Purvis, A. (1995) A composite estimate of primate phylogeny. *Philosophical Transactions of the Royal Society of London B.* 348, pp 405-421.

Quam, R., Martinez, I. and J. Arsuaga (2006) Middle Pleistocene auditory ossicles from the Sierra de Atapuerca (Spain). *American Journal of Physical Anthropology Supplement* 42: 149-149.

Quam, R. and Y. Rak (2008) Auditory ossicles from southwest Asian Mousterian sites. *Journal of Human Evolution* 54: 414-433.

Quinn, A. and D.E. Wilson (2004) *Daubentonia madagascariensis. Mammalian Species* 740: 1-6.

Qvist, M. and A.M. Grøntved (2000) Auditory ossicles in archaeological skeletal material from medieval Denmark. *Acta Oto-laryngologica Supplement* 543: 82-85

Rak, Y. and R.J. Clarke (1979a) Ear ossicle of *Australopithicus robustus. Nature* 279: 62-63.

Rak, Y. and R.J. Clarke (1979b) Aspects of the middle and external ear of early South African Hominids. *American Journal of Physical Anthropology* 51: 471-474.

Ramoutsaki, I.A., Papadakis, C.E., Ramoutsaki, I.A., and E.S. Helidonis (2002) Therapeutic methods used for otolaryngological problems during the Byzantine period. *Annals of Otology, Rhinology and Laryngology* 111: 553-557.

Rasband, W. S. (1997) ImageJ, U.S. National Institutes of Health, Bethesda, Maryland, USA, *http://rsb.info.nih.gov/ij/,* 1997 – 2009.

Raveh, E., Hu, W., Papsin, B.C. and V. Forte (2002) Congenital conductive hearing loss. *The Journal of Laryngology and Otology* 116: 92-96.

Richardson, M.P., Reid, A., Tarlow, M.J. and P.T. Rudd (1997) Hearing loss during bacterial meningitis. *Archives of Disease in Childhood* 76: 134-138.

Richtsmeier, J.T., Cole, T.M. and S.R. Lele (2005) An invariant approach to the study of fluctuating asymmetry: developmental instability in a mouse model for Down Syndrome. In: Slice, D.E. (ed) *Modern Morphometrics in Physical Anthropology.* New York: Kluwer, pp 187-212.

Richtsmeier, J.T., Deleon, V.B. and S.R. Lele (2002) The promise of geometric morphometrics. *Yearbook of Physical Anthropology* 45: 63-91.

Richtsmeier, J.T., Paik, C.H., Elfert, P.C. Cole, T.M. and H.R. Dahlman (1995) Precision, repeatability and validation of the localization of cranial landmarks using computed tomography scans. *Cleft Palate- Craniofacial Journal* 32(3): 217-227.

Rohlf, F.J. (2000) Statistical power comparisons among alternative morphometric methods. *American Journal of Physical Anthropology* 111: 463-478.

Rowe, T. (1996) Coevolution of the mammalian middle ear and neocortex. *Science* 273: 651-654.

Rosowski, J.J. (1992) Hearing in transitional mammals: predictions from the middle ear anatomy and hearing capabilities of extant mammals. In: Webster, D.B., Fay, R.R. and A.N. Popper (eds) *The Evolutionary Biology of Hearing.* New York: Springer-Verlag, pp 615-632.

Rosowski, J.J. (1994) Outer and Middle Ears. In Fay, R.R. and A.N. Popper (eds) *Comparative Hearing: Mammals*. New York: Springer-Verlag, pp 172-247.

Rosowski, J.J. and A. Graybeal (1991) What did morganucodon hear? *Zoological Journal of the Linnean Society* 101: 131-168.

Ross, A.H. and S. Williams (2002) Testing repeatability and error of coordinate landmark data acquired from crania. *Journal of Forensic Science* 53(4): 782-785.

Ruggero, M.A. and A.N. Temchin (2002) The roles of the external, middle and inner ears in determining the bandwidth of hearing. *Proceedings of the National Academy of Sciences* 99(20): 13206-13210.

Rumpler, Y., Warter, S., Petter, J.J., Albignac, R. and B. Dutrillaux (1988) Chromosomal evolution of the Malagasy lemurs. *Folio Primatologica* 50: 124-129.

Sakaliskas, V., Jankauskas, R. and A. Laurinavicius (1995) Sex estimation from auditory ossicles. In: *Forensic Odontology and Anthropology.* Berlin: Koster.

Sánchez-Villagra, M.R., Gemballa, S., Nummela, S., Smith, K.K. and W. Maier (2002) Ontogenetic and phylogenetic transformations of the ear ossicles in marsupial mammals. *Journal of Morphology* 251: 219-238.

Sarrat, R., Guzman, A.G. and A. Torres (1988) Morphological variation of human ossicula tympani. *Acta Anatomica* 131: 146-149.

Sarrat, R., Torres, A., Guzman, A.G., Lostalé, F. and J. Whyte (1992) Functional structure of human auditory ossicles. *Acta Anatomica* 144: 189-195.

Schmidt, J.L., Silcox, M.T. and T.M. Cole (2009) A landmark based approach to the study of the ear ossicles using X-ray computer tomography data. American Association of Physical Anthropologists Annual Meeting. Chicago, Illinois.

Schmitz, J., Ohme, M., Suryobroto, B. and H. Zischler (2002) The Colugo (*Cynocephalus variegatus,* Dermoptera): the primate's gliding sister? *Molecular Biology and Evolution* 19(12): 2308-2312.

Schmitz, J. and H. Zischler (2003) A novel family of tRNA-derived SINEs in the colugo and two new retrotransportable markers separating dermopterans from Primates. *Molecular Phylogenetics and Evolution* 28: 341-349.

Schultz, A.H. (1969) *The Life of Primates*. New York: Universe Books.

Schultz, A.H. (1973) The skeleton of the hylobatidae and other observations on their morphology. In: Rumbaugh, D.M. (ed) *Gibbon and Siamang Volume 2: Anatomy, Dentition, Taxonomy, Molecular Evidence and Behavior.* Basel: S. Kager.

Shaw, E.A.G. (1974) The external ear. In Keidel, W.D. and Neff, W.D. (eds) *Handbook of Sensory Physiology Volume 1.* Berlin: Springer-Verlag.

Shera, C.A. and J.J. Guinan (1998) Evoked otoacoustic emissions arise by two fundamentally different mechanisms: a taxonomy for mammalian OAE's. *Journal of the Acoustical Society of America* 105(2): 782-798.

Silcox, M.T. (2002) Primate origins and adaptations: a multidisciplinary perspective. *Evolutionary Anthropology* 11(5): 171-172.

Silcox, M.T. (2007) Primate taxonomy, plesiadapiforms, and approaches to primate origins. In: Ravosa, M.J. and M. Dagosto (eds) *Primate Origins: Adaptation and Evolution.* New York: Springer, pp. 143-178.

Silcox, M.T. and J.I. Bloch (2004) Reconstruction of ear ossicles from the most primitive primate cranium known using ultra high resolution computer tomography. American Association of Physical Anthropologists Annual Meeting. Tampa, Florida: *American Journal of Physical Anthropology Supplement* 38: 182.

Silcox, M.T., Bloch, J.I., Sargis, E.J. and D.M. Boyer (2005) Euarchonta (Dermoptera, Scandentia, Primates). In: Rose, K.D. and J.D. Archibald (eds) *The Rise of the Placental Mammals*. Baltimore: Johns Hopkins University Press, pp 127-144.

Silcox, M.T., Boyer, D.M., Bloch, J.I. and E.J. Sargis (2007) Revisiting the adaptive origins of primates (again). *Journal of Human Evolution* 53: 321-324.

Siori, M.S. and M. Masali (1983) Multivariate analysis of the ear bones of primates in taxonomic and evolutionary surveys. *Journal of Human Evolution* 12: 563.

Siori, M.S., Monchietto, M.J. and M. Masali (1995) Morphometrics of human auditory ossicles from Antinoe Necropolis (Egypt). *International Journal of Anthropology* 10(1): 29-36.

Slice, D.E. (2005) Modern morphometrics In: Slice, D.E. (ed) *Modern Morphometrics in Physical Anthropology.* New York: Kluwer, pp 1-45.

Spoor, F., Jeffery, N. and F. Zonneveld (2000) Imaging skeletal growth and evolution. In: O'Higgins, P. and M. Cohn (eds) *Development, Growth and Evolution: Implications for the Study of the Hominid Skeleton.* London: Academic Press, pp 123-162.

Spoor, F., Stringer, C. and F. Zonneveld (1998) Rare temporal bone pathology of the singa calvaria from Sudan. *American Journal of Physical Anthropology* 107: 41-50.

Stafford, B.J. (2005) Order Dermoptera. In: Wilson J.E. and D.M. Reeder (eds) *Mammal Species of the world: A taxonomic and Geographic Reference (third edition)*. Baltimore: Johns Hopkins University Press, pp 110.

Stafford, B.J. and F.S. Szalay (2000) Craniodental function morphology and taxonomy of Dermopterans. *Journal of Mammology* 81(2): 360-385.

Stanford, C., Allen, J.S., Anton, S.C. and N.C. Lovell (2009) *Biological Anthropology.* Toronto: Pearson, Prentice Hall.

Stanger, K.F. and J.M. Macedonia (1994) Vocalisations of aye-ayes (*Daubentonia madagascariensis*) in captivity. *Folio Primatologica* 62: 160-169.

Stebbins, W.C. (1973) Hearing of old world monkeys (Cercopithecinae). *American Journal of Physical Anthropology* 38: 357-364.

Stebbins, W.C. (1975) Hearing of the anthropoid primates: a behavioural analysis. In: Tower, D.B. (ed) *The Nervous System, Volume 3: Human Communication and its Disorders.* New York: Raven Press, pp 113-124.

Stebbins, W.C. and D.B Moody (1994) How monkeys hear the world: auditory perception in nonhuman primates. In Fay, R.R. and A.N. Popper (eds) *Comparative Hearing: Mammals*. New York: Springer-Verlag, pp 97-133.

Steele, D. and C. Bramblett (1988) *The anatomy and biology of the human skeleton.* Texas: University Press.

Sterling, E.J. (1994) Taxonomy and distribution of *Daubentonia madagascariensis*: a historical perspective. *Folio Primatologica* 62: 8-13.

Subotic, R., Mladina, R. and R. Risavi (1998) Congenital bony fixation of the malleus. *Acta Oto-Laryngologica* 118(6): 833-836.

Swartz, J.D., Mandell, D.M., Faerber, E.N., Popky, G.L., Ardito, J.M., Steinberg, S.B., and C.L. Rojer (1985) Labyrinthine ossification: etiologies and CT findings. *Radiology* 157: 395-398.

Szalay, F.S (1975) Phylogeny of primate higher taxa. In Luckett, W.P. and F.S. Szalay (eds) *Phylogeny of the Primates*. New York: Raven Press, pp. 91-125.

Tonndorf, J. and S.M. Khanna (1970) The role of the tympanic membrane in middle ear transmission. *Annals of Otolaryngology* 79: 743-753.

Tonndorf, J. and S.M. Khanna (1972) Tympanic-membrane vibrations in human cadaver ears studied by time-averaged holography. *Journal of the Acoustical Society of America* 52(4): 1221-1233.

Unur, E., Ülger, H. and N. Ekinci (2002) Morphometrical and morphological variations of middle ear ossicles in the newborn. *Erciyes Tip Dergisi (Erciyes Medical Journal)* 24(2): 57-63.

Valeri, C.J., Cole, T.M., Lele, S. and J.T. Richtsmeier (1998) Capturing data from three-dimensional surfaces using fuzzy landmarks. *American Journal of Physical Anthropology* 107: 113-124.

van Kampen, P.N. (1905) Die tympanalgegend des Säugetierschädels. *Gegenbaurs Morphologisches Jarhrbuch* 34: 321-722.

Walker, A., Ryan, T.M., Silcox, M.T., Simons, E.L. and F. Spoor (2008) The semicircular canal system and locomotion: the case of extinct Lemuroids and Lorisoids. *Evolutionary Anthropology* 17: 135-145.

Walker, R.A., Greiner, T.M. and R. Cordes (2006) Histomorphological variation in human auditory ossicles. American Association of Physical Anthropologists Annual Meeting. Fairbanks, Alaska: *American Journal of Physical Anthropology Supplement* 42: 183-184.

Waser, P.M. and C.H. Brown (1984) Is there a "sound window" for primate communications? *Behavioural Ecology and Sociobiology* 15: 73-76.

Waser, P.M. and C.H. Brown (1986) Habitat acoustics and primate communication. *American Journal of Primatology* 10: 135-154.

Waser, P.M. and M.S. Waser (1977) Experimental studies of primate vocalisation: specialisations for long-distance propagation. *Zeitschrift fur Teirpsychologie* 43: 239-263.

Watson, D.M.S. (1953) The evolution of the mammalian ear. *Evolution* 7(2): 159-177.

Werner, F. (1956) Mittel- und innenohr. *Primatologia* 5: 1-38.

Wever, E.G. and M. Lawrence (1954) *Physiological Acoustics.* Princeton: Princton University Press.

Whyte, J., Cisneros, A., Urieta, J., Yus, C., Gañet, J., Torres, A., and R. Serrat (2002) Fetal development of the human tympanic ossicular chain articulations. *Cells Tissues Organs* 171: 241-249.

Whyte, J., Cisneros, A., Yus, C., Obón, J., Whyte, A., Serrano, P., Pérez-Castejón, C. and A. Vera (2008) Development of the dynamic structure (force lines) of the middle ear ossicles in human foetuses. *Histology and Histopathology* 23(9): 1049-1060.

Wible, J.R. and H.H. Covert (1987) Primates: cladistic diagnosis and relationships. *Journal of Human Evolution* 16: 1-22.

Willi, U.B., Ferrazzini, M.A. and A.M. Huber (2002) The incudo-malleolar joint and sound transmission losses. *Hearing Research* 174: 32-44.

Wilson, D.B., Sawyer, R.H. and A.G. Hendrickx (1975) Proliferation gradients in the inner ear of the monkey (*Macaca mulatta*) embryo. *The Journal of Comparative Neurology* 164(1): 23-29.

Wilson, E. and D.M. Reeder (2005) *Mammal species of the world: a taxonomic and geographic reference*. Baltimore: Johns Hopkins University Press.

Wilson, J.P. (1987) Mechanics of middle and inner ear. *British Medical Bulletin* 43(4): 821-837.

Wysocki, J. (2001) Dimensions of the vestibular and tympanic scalae of the cochlea in selected mammals. *Hearing Research* 161: 1-9.

Zollikofer, C.P.E. and M.S. Ponce de León (2005) *Virtual Reconstruction: a primer in computer-assisted paleontology and biomedicine.* New York: John Wiley and Sons. pp.330.

Zwislocki, J. (1975) The role of the external and middle ear in sound transmission. In: Tower, D.B. (ed) *The Nervous System, Volume 3: Human Communication and its Disorders.* New York: Raven Press, pp 45-55.

APPENDICES

Appendix 1 – List of specimens with sixteen identifiable landmarks versus fifteen:

Sixteen Landmarks Visible	Fifteen Landmarks Visible
Callicebus moloch 1	*Arctocebus calabarensis 1*
Callicebus torquatus	*Cheirogaleus medius* 1
Loris tardigradus 1	*Cheirogaleus medius* 2
Macaca nigra 2	*Galeopterus variegatus*
Tarsius bancanus	*Cynocephalus volans*
Varecia variegata variegata	*Daubentonia madagascariensis*
	Eulemur fulvus albifrons
	Eulemur fulvus rufus
	Galago alleni 2
	Galago elegantulus 1
	Galago moholi 1
	Galago moholi 2
	Galago senegalensis
	Galagoides demidoff 1
	Hapalemur griseus
	Lemur catta 2
	Loris tardigradus 2
	Macaca nigra 1
	Otolemur crassicaudatus 1

APPENDIX 2 – Euclidean pair-wise landmark distances resulting from EDMA analysis on non-scaled dataset:

	MAN – LAT	MAN – HEA	MAN – IAM	MAN – LCR	MAN – SCR	MAN – IAR	MAN – SAR	MAN – MAH	MAN – IAI	MAN – ARI	MAN – MFP	MAN – LFP	MAN – SFP	MAN – IFP	LAT – HEA	LAT – IAM	LAT – LCR	LAT – SCR	LAT – IAR	LAT – SAR	LAT – MAH	LAT – IAI	LAT – ARI	LAT – MFP	LAT – LFP
Acalaba1	1.718	2.414	1.1299	1.5902	2.7379	1.221	2.3843	2.3699	1.3233	1.5384	2.6671	2.1888	2.4138	2.4288	1.3589	1.0623	2.787	3.155	1.1577	1.5821	2.2101	1.9254	2.7199	3.4497	2.8985
Cmoloch1	3.0076	4.029	2.8669	2.2605	4.1068	3.5957	3.9988	4.1244	3.0421	2.4072	3.3095	2.9125	3.1944	3.0067	1.3491	1.5993	3.0168	3.6212	1.9557	1.7726	2.7999	1.9792	3.0105	3.648	3.1297
Ctorquat	2.8086	3.9574	2.6142	1.5249	3.9218	2.4595	3.6341	3.9496	2.4198	1.671	2.9424	2.3497	2.6397	2.6272	1.6763	1.0952	2.9459	3.8371	1.5785	1.5675	2.4579	1.913	2.9948	4.0193	3.454
Cmedius1	2.9154	3.888	2.3197	1.9913	3.5086	2.6807	3.6896	3.7687	2.6235	1.9681	2.6816	2.4286	2.559	2.436	1.2022	1.0017	2.1604	2.6502	1.1743	1.246	1.8749	1.3021	2.0682	2.7354	2.3416
Cmedius2	2.0847	3.0776	1.8435	1.643	3.0036	1.9977	2.9102	3.0983	2.0053	1.6639	2.4031	1.9949	2.2388	2.1764	1.2744	0.79612	1.7899	2.4771	1.0137	1.2077	1.8807	1.2265	1.7404	2.6048	2.0697
Gvariega	3.4982	4.4121	3.3416	2.7502	4.6619	3.5315	4.4374	4.9798	3.313	3.075	3.6797	2.8857	3.6044	3.103	1.12	1.3693	2.2494	2.8775	1.4517	1.5273	2.1822	1.6415	2.3049	3.4052	2.5888
Cvolans	2.9592	3.9055	2.8192	2.282	4.1513	2.9899	4.032	4.5698	2.8434	2.5535	3.1287	2.7796	3.1396	2.8642	1.0819	1.2363	2.0026	2.2895	1.3583	1.2484	1.9242	1.5115	2.057	2.8094	2.5137
Dmadagas	4.5958	7.2587	5.0295	4.8111	7.1776	5.2346	7.2725	7.5966	4.9867	4.6834	5.7477	4.5846	5.2626	5.0337	3.056	1.9511	3.3946	4.4962	2.0772	3.1802	3.5205	2.4685	3.5664	5.1702	4.23
Efalbifo	3.7737	4.7031	4.0354	3.1699	5.0736	3.3673	4.6768	4.8868	3.361	3.1038	4.2955	3.3732	3.8934	3.6401	1.2572	2.6109	3.2525	3.5845	1.6208	1.597	1.86	2.0332	3.1222	4.2888	3.6971
Efrufus	3.6106	4.7599	3.3758	2.963	4.9632	3.5147	4.7029	4.9095	3.5946	2.9924	4.1482	3.2544	3.7601	3.5363	1.3216	1.2418	2.8416	3.3048	1.3878	1.5297	1.7365	1.5368	2.7566	3.9283	3.3137
Galleni2	2.6091	3.4562	2.2819	2.007	3.481	2.5718	3.4592	3.5269	2.4642	2.1073	2.8552	2.5047	2.7499	2.6277	1.0557	0.96421	2.2691	2.716	1.1234	1.2491	1.7894	1.5324	2.3704	3.0748	2.7535
Gelegan1	2.4339	3.1203	1.998	2.0207	3.2125	2.1921	2.9743	2.9409	2.2739	2.0151	2.8026	2.2522	2.6206	2.4875	1.0397	0.79221	2.279	2.5868	0.84309	1.0436	1.4483	1.4059	2.2115	2.9933	2.4916
Gmoholi1	2.6572	3.0955	2.1453	1.7189	3.1305	2.349	3.1094	3.246	2.2351	1.6878	2.7381	2.213	2.6084	2.5175	0.74223	0.95053	2.2812	2.8353	1.1078	0.91187	1.7682	1.4624	2.3268	3.1731	2.6215
Gmoholi2	2.6976	3.2546	2.2693	1.7656	3.3417	2.4417	3.2915	3.3317	2.3238	1.8781	2.9601	2.4725	2.7018	2.6433	0.751	0.89677	2.2619	2.9711	0.95021	1.2264	1.7466	1.5159	2.248	3.0006	2.5268
Gsenegal	2.7618	3.2774	2.3329	2.0459	3.5098	2.5053	3.1634	3.4678	2.5718	2.1536	3.1335	2.7619	3.0035	2.8463	0.90449	1.0588	2.3841	3.0041	1.2092	0.94472	1.9059	1.5826	2.4147	3.2822	2.8376
Gdemido1	2.1935	2.4218	1.7012	1.599	2.7785	1.8898	2.4659	2.6396	1.9385	1.613	2.1754	1.9782	2.1842	2.1085	0.62594	0.76968	1.9574	2.2403	0.81939	0.68884	1.2553	1.0999	1.8768	2.2651	2.0694
Hgriseus	2.9607	4.3721	2.7973	2.6061	4.2924	2.9659	4.1591	4.4338	2.9184	2.5961	3.5113	2.7437	3.1945	3.2041	1.6594	1.1097	2.5012	3.1842	1.2274	1.5805	2.0164	1.5016	2.4413	3.4114	2.7616
Lcatta2	3.8644	4.7053	3.3013	3.1686	5.0978	3.6021	4.6352	4.9095	3.5285	3.1661	4.2088	3.3876	3.8073	3.6491	1.1374	1.4076	3.0021	3.3859	1.5503	1.3329	1.6228	1.8072	2.9026	3.8211	3.2589
Ltardig1	2.4443	3.2208	2.2069	1.9274	3.4623	2.2872	3.1446	3.1595	2.372	2.0147	3.1042	2.5253	2.8417	2.7312	1.37	0.96462	2.3565	3.1558	1.2932	1.6572	2.0282	1.5813	2.3723	3.284	2.6744
Ltardig2	2.3398	2.9501	2.0514	1.8361	3.1966	2.1017	2.9853	3.0261	2.0935	1.8172	2.6111	2.3021	2.5894	2.4798	0.87875	1.0597	2.3635	2.9223	1.1708	1.4824	1.8851	1.6329	2.3093	3.0101	2.6279
Mnigra1	4.1478	5.0279	2.9571	1.6107	4.3354	3.1395	4.6197	4.7058	3.074	1.6827	3.0647	2.2976	2.7034	2.5271	1.1572	1.7984	3.4567	4.0227	1.7521	1.9095	2.4573	2.0514	3.6108	4.8103	4.2752
Mnigra2	3.8328	5.1435	3.1392	1.7835	4.4978	3.3775	4.801	4.9606	3.197	1.7851	3.2575	2.5409	2.8795	2.863	1.6151	1.2807	2.9887	3.7578	1.4662	1.7345	2.4369	1.8324	3.0036	4.3112	3.9095
Ocrassi1	3.1757	4.1992	2.8938	2.5556	4.3329	3.1199	4.0302	4.3125	3.1752	2.7286	4.0133	3.3637	3.8158	3.584	1.3824	0.94372	2.7453	3.498	1.3358	1.4665	2.1092	1.7905	2.7761	4.4531	3.8405
Ogarnett	3.3736	4.0428	2.9508	2.6362	4.1923	3.0787	4.1324	4.1879	3.0975	2.8202	3.7203	3.193	3.4691	3.3401	1.1961	0.93429	2.8766	3.3632	1.4901	1.6783	2.0404	2.0557	2.8946	3.7518	3.2917
Tbancanu	3.1592	3.9602	2.4221	1.2019	3.2674	2.4457	3.7816	3.8078	2.3619	1.3655	3.0779	2.8828	2.9703	2.9145	1.3955	1.153	2.4598	2.5504	1.1492	1.4128	1.437	1.2708	2.3851	3.1083	2.6619
V.v.vari	3.8909	4.8949	3.0329	3.1485	5.412	3.4473	4.8606	5.1662	3.4162	3.3402	5.0193	4.265	4.5073	4.3705	1.2631	1.6349	3.3782	3.5803	1.8104	1.5513	1.8555	1.8866	3.2615	4.2569	3.7356

	LAT – SFP	LAT – IFP	HEA – IAM	HEA – LCR	HEA – SCR	HEA – IAR	HEA – SAR	HEA – MAH	HEA – IAI	HEA – ARI	HEA – MFP	HEA – LFP	HEA – SFP	HEA – IFP	IAM – LCR	IAM – SCR	IAM – IAR	IAM – SAR	IAM – MAH	IAM – IAI	IAM – ARI	IAM – MFP	IAM – LFP	IAM – SFP	IAM – IFP	LCR – SCR
Acalaba1	3.0545	3.287	1.2976	2.7117	2.3788	1.2352	0.36083	1.2884	1.754	2.6402	2.9219	2.5932	2.5625	2.9069	1.7473	2.1905	0.14177	1.2644	1.4456	0.86741	1.6773	2.4926	2.0805	2.1719	2.3692	1.5273
Cmoloch1	3.3445	3.413	1.5382	3.2505	3.1373	1.2923	0.73417	2.0816	1.7495	3.1733	3.5695	3.2121	3.3039	3.4684	1.7137	2.1261	0.74659	1.2131	1.5308	0.39038	1.6565	2.366	2.0976	2.1974	2.2859	2.0292
Ctorquat	3.6247	3.7879	1.358	3.4551	3.2145	1.6606	0.46883	1.2551	1.9409	3.4104	4.0132	3.7438	3.7578	3.944	2.2655	2.9304	0.58617	1.0995	1.6928	0.98656	2.2409	3.0611	2.6407	2.7369	2.9016	2.4598
Cmedius1	2.4413	2.5818	1.6361	2.5771	2.3328	1.4223	0.46626	1.2319	1.5288	2.4951	2.8847	2.6748	2.6746	2.8727	1.1698	1.9014	0.44956	1.3813	1.5668	0.50448	1.0959	2.1174	1.9028	1.936	2.0331	1.5176
Cmedius2	2.2538	2.4597	1.2657	2.0872	2.0199	1.2082	0.38601	1.0624	1.3379	2.0134	2.5134	2.1896	2.2005	2.4951	1.0302	1.7651	0.2642	1.07	1.3845	0.45277	0.97144	1.9055	1.5046	1.6043	1.8098	1.3652
Gvariega	3.0389	3.1494	1.8727	2.8278	2.799	1.7503	0.67676	1.3167	2.0283	2.7338	3.5032	2.7915	3.0519	3.3601	1.0849	1.7072	0.32772	1.8272	2.1151	0.3821	1.0578	2.3582	2.0315	2.187	2.2805	1.922
Cvolans	2.6567	2.785	2.0017	2.8056	2.507	1.986	0.36742	1.4651	2.1743	2.7279	3.1526	2.8757	2.9292	3.198	1.0036	1.423	0.28723	1.9474	1.939	0.39408	1.0679	2.1248	2.051	2.1125	2.1372	1.9582
Dmadagas	4.4748	4.6439	2.6452	3.9561	3.2467	2.3852	0.28758	0.61814	2.8872	4.0845	5.0568	4.8223	4.5684	4.929	1.6773	2.6355	0.37974	2.5937	2.7899	0.70795	2.0245	3.9956	3.5719	3.5058	3.6402	2.4186
Efalbifo	3.7608	3.9125	2.1783	3.2579	2.8491	1.6595	0.53749	0.75372	1.9842	3.1419	4.0581	3.7999	3.6468	3.8696	1.3274	1.1466	1.093	1.7069	1.6886	0.79145	1.2768	2.5207	2.689	2.4186	2.4117	2.0324
Efrufus	3.4582	3.6427	1.6066	3.2015	2.7879	1.6008	0.53759	0.69814	1.658	3.0927	3.9355	3.6465	3.5765	3.8622	1.6858	2.2093	0.20445	1.3762	1.5708	0.3618	1.6104	2.9535	2.5651	2.5986	2.7393	2.0865
Galleni2	2.8176	3.0096	1.3457	2.6247	2.5277	1.251	0.40866	1.2713	1.6551	2.6624	3.0305	2.7981	2.7624	3.0428	1.3552	1.8749	0.33	1.2333	1.3058	0.59068	1.4341	2.2178	2.0288	2.0429	2.2022	1.5051
Gelegan1	2.6391	2.8913	1.1421	2.2435	2.0295	0.97514	0.23601	0.73973	1.2223	2.152	2.6803	2.3973	2.3662	2.7197	1.633	2.0989	0.22091	1.0269	1.1543	0.83367	1.5298	2.2291	1.7164	1.8797	2.1067	1.25
Gmoholi1	2.8113	3.0813	1.0595	2.343	2.5587	1.0656	0.33853	1.3195	1.3692	2.3729	2.935	2.496	2.5661	2.9008	1.3512	1.9853	0.30496	0.98245	1.2715	0.54443	1.3981	2.3324	1.9087	2.0334	2.2949	1.4129
Gmoholi2	2.5422	2.7701	1.0869	2.4312	2.7496	1.0092	0.67209	1.3132	1.5243	2.3717	2.8465	2.4988	2.4259	2.6997	1.3982	2.1546	0.20125	1.0294	1.2395	0.63537	1.3748	2.2341	1.862	1.8487	2.0573	1.5999
Gsenegal	2.9877	3.1175	1.0167	2.2622	2.4198	0.97314	0.20785	1.1319	1.2349	2.2552	2.995	2.6885	2.7247	2.9265	1.3515	2.0382	0.24718	0.87321	1.2647	0.57671	1.3808	2.4163	2.0946	2.1721	2.2888	1.4676
Gdemido1	2.1564	2.3803	0.79082	1.9073	2.0086	0.7486	0.4859	0.95258	1.0068	1.7821	1.9331	1.7231	1.7667	2.0351	1.2298	1.7293	0.24536	0.77878	1.0407	0.51633	1.1295	1.5483	1.4107	1.4945	1.6851	1.2148
Hgriseus	3.0472	3.3003	1.7438	3.015	2.8251	1.682	0.5143	0.78956	1.881	2.9278	3.3658	3.0596	3.1094	3.409	1.4614	2.1737	0.20833	1.4093	1.6514	0.39862	1.3932	2.4508	1.9708	2.1846	2.4084	1.7171
Lcatta2	3.3301	3.6011	1.7495	3.1103	2.8791	1.6459	0.62881	0.74893	1.8704	2.9769	3.5137	3.2078	3.1153	3.4658	1.6333	2.3434	0.35861	1.43	1.6824	0.50577	1.5804	2.935	2.5454	2.5565	2.724	2.0126
Ltardig1	2.8885	3.0317	1.0275	2.1737	2.2587	1.0187	0.46282	0.95237	1.1184	2.1277	2.7003	2.4151	2.4103	2.6484	1.4628	2.2172	0.34147	1.0283	1.2239	0.63577	1.4692	2.4831	2.0461	2.1639	2.3069	1.548
Ltardig2	2.8105	2.9235	1.0856	2.3984	2.5199	1.1145	0.83319	1.2931	1.5196	2.3388	2.8601	2.5594	2.6374	2.8171	1.3719	1.9031	0.14457	0.94159	1.1126	0.58881	1.33	2.1549	1.89	1.9905	2.1073	1.3886
Mnigra1	4.2537	4.707	2.2615	4.0473	3.8378	2.1063	1.3325	1.9049	2.3504	4.165	5.1082	4.8595	4.6494	5.184	1.8074	2.5254	0.36565	1.6879	1.8593	0.38484	1.953	3.3342	3.1822	2.9547	3.3784	2.7414
Mnigra2	3.7998	4.2398	2.1701	3.9117	3.7251	1.985	1.1726	1.8337	2.3847	3.9037	4.6416	4.5624	4.2686	4.7566	1.8853	2.6407	0.4668	1.6648	1.9682	0.60548	1.9272	3.3932	3.2469	3.0501	3.4557	2.8035
Ocrassi1	4.1158	4.1369	1.4199	2.9518	3.0673	1.3706	0.76538	1.2845	1.695	2.8644	4.1678	3.7112	3.8327	3.9622	1.8429	2.6125	0.45673	1.1432	1.564	0.87441	1.8638	3.6395	3.1524	3.3673	3.3698	1.818
Ogarnett	3.3515	3.6551	1.0995	2.7024	2.6591	1.2313	0.59716	1.0463	1.672	2.6191	3.2078	2.9517	2.8617	3.2577	1.9726	2.551	0.62081	1.2773	1.501	1.1583	1.9696	2.8796	2.4955	2.5072	2.7988	1.58
Tbancanu	2.6678	3.0074	1.649	2.9438	2.2516	1.5586	0.4293	0.48374	1.6154	2.7961	2.6952	2.4959	2.3473	2.7436	1.4781	1.6213	0.18815	1.4116	1.4264	0.35454	1.4273	2.4425	2.2553	2.1593	2.4338	2.173
V.v.vari	3.6156	4.0905	2.1254	3.5572	2.9535	1.9946	0.63482	0.89398	2.0751	3.3434	3.859	3.6227	3.3462	3.9482	1.7988	2.6953	0.48425	1.9016	2.1742	0.4986	1.8012	3.4071	3.0754	2.9402	3.2431	2.6037

	LCR – IAR	LCR – SAR	LCR – MAH	LCR – IAI	LCR – ARI	LCR – MFP	LCR – LFP	LCR – SFP	LCR – IFP	SCR – IAR	SCR – SAR	SCR – MAH	SCR – IAI	SCR – ARI	SCR -MFP	SCR – LFP	SCR – SFP	SCR -IFP	IAR – SAR	IAR – MAH	IAR – IAI	IAR – ARI	IAR – MFP	IAR – LFP	IAR – SFP	IAR – IFP
Acalaba1	1.6913	2.4727	1.8637	0.96912	0.10863	1.6411	1.7771	1.7137	1.6291	2.0585	2.0271	1.1173	1.4507	1.5174	1.5825	2.1008	1.7382	1.8884	1.1683	1.3052	0.77492	1.621	2.4048	2.0298	2.0938	2.302
Cmoloch1	2.1896	2.8377	2.3822	1.5663	0.2953	1.6907	1.7536	1.8084	1.7009	2.0035	2.4306	1.149	1.7576	2.0224	2.7234	3.0457	2.9136	2.9897	0.75452	1.1767	0.66498	2.0728	2.4682	2.3001	2.3105	2.476
Ctorquat	1.8028	3.0528	2.9902	1.5351	0.24352	2.1122	1.9906	2.0867	2.0361	2.3955	2.8311	2.0301	2.0504	2.3614	3.0247	3.4656	3.3012	3.2941	1.2919	1.53	0.4046	1.7624	2.7051	2.4188	2.4762	2.6072
Cmedius1	1.1875	2.2242	1.9883	1.0549	0.16763	1.6525	1.7709	1.699	1.6948	1.5209	1.9033	1.2025	1.4208	1.5532	2.1352	2.4991	2.3053	2.4001	1.0799	1.1291	0.16733	1.1287	2.0746	1.9737	1.9494	2.0723
Cmedius2	0.92704	1.8344	1.6476	0.75776	0.10817	1.3645	1.3169	1.2706	1.3516	1.5062	1.7449	1.0098	1.3203	1.3583	1.7652	2.0761	1.8018	1.9782	0.97329	1.1498	0.21726	0.86458	1.7862	1.4786	1.5132	1.7347
Gvariega	1.1847	2.6508	2.874	0.86977	0.38013	1.7313	1.6425	1.77	1.6033	1.5126	2.4502	2.1361	1.5235	1.5969	2.0743	2.6504	2.1517	2.4858	1.6043	1.8279	0.31906	1.0544	2.1954	1.9119	1.988	2.1614
Cvolans	1.0222	2.7407	2.749	0.78651	0.399	1.583	1.5679	1.6864	1.5093	1.2225	2.2739	1.4701	1.3286	1.8015	2.4351	2.6415	2.4756	2.6103	1.8807	1.7732	0.2486	0.97775	1.941	1.9116	1.9274	1.9873
Dmadagas	1.7308	3.8123	3.9292	1.1618	0.73743	3.0921	3.0587	2.8728	2.8189	2.4857	3.0141	2.8488	2.3871	2.747	4.079	4.5988	4.0562	4.1962	2.311	2.5169	0.61205	1.9816	3.7823	3.4084	3.2898	3.4637
Efalbifo	1.6813	2.8791	2.9274	1.2919	0.22204	2.2235	2.2707	2.2078	1.9274	2.2052	2.3149	2.1572	1.9321	2.0628	2.8017	3.3912	2.9544	2.9508	1.416	1.5681	0.41304	1.5647	3.0019	2.6938	2.6454	2.6751
Efrufus	1.6438	2.8458	2.986	1.5803	0.27893	2.0946	1.9864	1.9864	1.8691	2.0156	2.2601	2.226	1.8584	2.085	2.7603	3.2446	2.8755	3.0091	1.3064	1.4786	0.16155	1.5794	2.9265	2.6186	2.6092	2.7526
Galleni2	1.3876	2.3953	1.9988	0.99298	0.20224	1.6326	1.7576	1.7347	1.6812	1.6202	2.1491	1.3264	1.3225	1.4504	2.0428	2.4443	2.2161	2.3088	1.0497	0.98158	0.45144	1.4457	2.1892	2.0841	2.0438	2.2254
Gelegan1	1.6585	2.0146	1.6394	1.0257	0.19105	1.5393	1.5744	1.5695	1.5675	1.9972	1.821	1.2979	1.2735	1.2392	1.753	2.1128	1.8473	2.0401	0.86058	0.98372	0.77084	1.5433	2.154	1.6772	1.7976	2.0623
Gmoholi1	1.3225	2.1884	1.8431	0.99825	0.18628	1.6125	1.5559	1.574	1.6747	1.7429	2.2756	1.3858	1.4596	1.475	1.8017	2.2478	1.8953	2.1439	0.89409	0.98417	0.39573	1.3883	2.2904	1.9814	2.0224	2.3118
Gmoholi2	1.4462	2.1226	1.8867	0.96198	0.20224	1.5963	1.4764	1.497	1.5161	2.0367	2.1317	1.5203	1.5388	1.5513	1.8266	2.2635	2.0358	2.1337	0.8565	1.0439	0.57567	1.4151	2.2241	1.912	1.864	2.0869
Gsenegal	1.3016	2.0881	1.8019	1.0516	0.32265	1.8062	1.7724	1.7391	1.7297	1.8242	2.2562	1.3742	1.465	1.4397	2.0303	2.327	2.0557	2.2074	0.80287	1.0377	0.38066	1.3303	2.3661	2.1059	2.1379	2.275
Gdemido1	1.1914	1.7304	1.5305	0.9639	0.18841	1.0136	1.354	1.3305	1.353	1.5241	1.6759	1.1421	1.2217	1.2077	1.3388	1.8951	1.7004	1.8579	0.61879	0.80062	0.32062	1.092	1.4874	1.439	1.4749	1.6895
Hgriseus	1.4404	2.6	2.6271	1.1673	0.17117	1.7705	1.6364	1.7605	1.7925	1.996	2.3523	2.0999	1.7979	1.7416	2.3098	2.6968	2.5287	2.6053	1.3017	1.51	0.30083	1.3809	2.4449	2.0434	2.2167	2.4384
Lcatta2	1.581	2.7106	2.8404	1.3069	0.26907	2.1079	2.0679	2.0026	1.9286	2.0119	2.319	2.2238	1.8707	2.0336	2.7603	3.2279	2.8661	2.9971	1.2359	1.4477	0.28178	1.5227	2.8052	2.5373	2.4755	2.6644
Ltardig1	1.2296	1.8539	1.6043	1.0592	0.18974	1.7151	1.6459	1.6371	1.628	1.8971	1.8203	1.3073	1.6367	1.504	1.9351	2.4147	2.1067	2.226	0.86643	0.95964	0.29496	1.2137	2.1947	1.8498	1.9111	2.0629
Ltardig2	1.2985	1.9233	1.6866	0.88848	0.16279	1.3728	1.3753	1.383	1.3721	1.7847	1.7268	1.2745	1.398	1.4214	1.7551	1.9985	1.743	1.8839	0.8847	1.0017	0.47053	1.2495	2.034	1.7833	1.8674	1.9927
Mnigra1	1.9566	3.3175	3.2777	1.7664	0.26646	2.2424	2.2208	2.0439	2.1809	2.5166	2.5404	2.0347	2.2066	2.7275	3.3128	4.26	3.541	3.9381	1.4908	1.688	0.351	2.0618	3.2289	3.098	2.8298	3.3001
Mnigra2	1.9593	3.3937	3.3738	1.6653	0.18028	2.2386	2.1497	2.0654	2.2487	2.445	2.705	2.0475	2.1089	2.8845	3.6291	4.3527	3.9041	4.1712	1.4927	1.705	0.44822	1.9757	3.1664	3.1444	2.8695	3.2992
Ocrassi1	1.6364	2.5068	2.3893	1.3045	0.28705	2.3158	2.1764	2.2809	2.1388	2.2041	2.4477	1.8929	1.7698	1.7328	2.817	3.1724	2.9508	2.9618	0.9734	1.2184	0.46065	1.6096	3.3328	2.9395	3.0885	3.1118
Ogarnett	1.5127	2.4034	2.1935	1.0481	0.28018	1.9056	1.9777	1.8196	1.8725	1.9324	2.1107	1.6817	1.4509	1.4406	2.2188	2.6991	2.2884	2.5154	1.0953	1.1249	0.56754	1.4837	2.5199	2.3142	2.2156	2.5149
Tbancanu	1.4714	2.7255	2.7504	1.3572	0.26476	2.1487	2.1094	2.0682	2.0962	1.6707	1.8355	1.8024	1.7105	2.1726	2.736	3.0577	2.7682	2.9793	1.3468	1.3706	0.19105	1.3875	2.2828	2.0789	1.9833	2.2673
V.v.vari	1.6976	3.1908	3.3921	1.6229	0.50398	2.6213	2.6554	2.5307	2.5035	2.2177	2.3381	2.2188	2.201	2.5561	3.2842	3.8906	3.4329	3.8037	1.6494	1.8834	0.083066	1.6654	3.1844	3.0196	2.8034	3.1478

	SAR – MAH	SAR – IAI	SAR – ARI	SAR – MFP	SAR – LFP	SAR – SFP	SAR – IFP	MAH – IAI	MAH – ARI	MAH – MFP	MAH – LFP	MAH – SFP	MAH – IFP	IAI – ARI	IAI – MFP	IAI – LFP	IAI – SFP	IAI – IFP	ARI – MFP	ARI – LFP	ARI – SFP	ARI – IFP
Acalaba1	0.93429	1.5395	2.405	2.664	2.4299	2.3464	2.6899	1.1351	1.8174	2.1185	2.1902	1.9716	2.2604	0.90366	1.8559	1.7264	1.6883	1.824	1.5771	1.6788	1.6251	1.5503
Cmoloch1	1.3553	1.273	2.7597	3.2131	2.995	3.0282	3.1976	1.2485	2.3422	2.9756	3.0611	2.9919	3.129	1.492	2.199	2.0528	2.0951	2.1939	1.4072	1.49	1.524	1.4309
Ctorquat	0.98529	1.5309	3.0178	3.7667	3.5294	3.5447	3.7114	1.5446	2.9127	3.5175	3.5332	3.4561	3.5901	1.4911	2.5741	2.3985	2.4292	2.5269	1.884	1.8125	1.8815	1.8301
Cmedius1	0.79912	1.1826	2.1607	2.6969	2.5712	2.5395	2.7252	1.1581	1.9667	2.5748	2.6565	2.5476	2.7132	0.99015	1.9264	1.8587	1.8205	1.9386	1.5259	1.612	1.5478	1.5499
Cmedius2	0.84178	1.0847	1.7733	2.4279	2.159	2.145	2.4289	1.0951	1.5939	2.0481	2.0519	1.8863	2.1624	0.69592	1.6478	1.4224	1.4115	1.6251	1.2977	1.2252	1.1822	1.278
Gvariega	0.76655	1.8549	2.4825	3.0077	2.3919	2.5307	2.9176	2.0711	2.6206	2.9364	2.6444	2.5169	3.0141	0.74498	1.9773	1.7391	1.8198	1.9263	1.4734	1.5526	1.5152	1.4586
Cvolans	1.1519	2.0698	2.6174	2.9699	2.7417	2.749	3.0462	1.9772	2.5645	2.9259	2.9219	2.7907	3.093	0.73253	1.7593	1.7456	1.7719	1.7909	1.2323	1.282	1.3383	1.2067
Dmadagas	0.43612	2.7764	3.9283	4.8592	4.6967	4.4016	4.7628	2.9604	4.0844	5.0325	4.979	4.6308	4.9851	1.3718	3.3156	3.0178	2.8762	2.9942	2.3876	2.3581	2.1593	2.083
Efalbifo	0.29967	1.6596	2.774	3.6793	3.5529	3.3372	3.5406	1.7622	2.8393	3.7473	3.7119	3.4564	3.6512	1.1838	2.7212	2.5239	2.4394	2.418	2.0981	2.0806	2.0289	1.7705
Efrufus	0.29189	1.3168	2.7534	3.6455	3.4763	3.3509	3.6199	1.4687	2.9125	3.8318	3.7177	3.5697	3.8338	1.5248	2.8778	2.6324	2.5921	2.7327	1.8753	1.7337	1.7273	1.6367
Galleni2	0.87658	1.4036	2.4171	2.7701	2.6204	2.5425	2.8236	1.1022	1.9992	2.4584	2.5351	2.3727	2.6122	1.0234	1.8263	1.8163	1.7493	1.8924	1.4434	1.6155	1.5718	1.5109
Gelegan1	0.53488	0.9983	1.9277	2.5155	2.2585	2.2219	2.5621	0.71183	1.5507	2.11	1.9977	1.8861	2.22	0.93515	1.8055	1.6046	1.5972	1.8293	1.3867	1.3936	1.3884	1.4058
Gmoholi1	0.99649	1.1943	2.2341	2.8257	2.4827	2.4928	2.8412	1.0236	1.9123	2.409	2.4013	2.2135	2.5795	1.0462	1.9163	1.6811	1.6805	1.9621	1.4603	1.3834	1.4174	1.4995
Gmoholi2	0.64938	1.1682	2.0494	2.459	2.2839	2.1385	2.4177	1.0175	1.8131	2.1979	2.2196	2.0177	2.2741	0.9181	1.8144	1.6399	1.5608	1.7487	1.4044	1.2915	1.2981	1.3251
Gsenegal	1.0153	1.0626	2.0971	2.9115	2.6292	2.6538	2.8477	0.89811	1.7533	2.3724	2.3216	2.1943	2.4307	1.0516	2.0876	1.9174	1.8924	2.0356	1.4904	1.4605	1.4165	1.4141
Gdemidol	0.58796	0.76688	1.6371	1.9072	1.869	1.8629	2.1293	0.70753	1.4426	1.618	1.7759	1.6818	1.953	0.88045	1.3341	1.4353	1.4225	1.6259	0.86308	1.1748	1.152	1.1917
Hgriseus	0.46594	1.4843	2.5282	3.109	2.8601	2.901	3.1809	1.6175	2.5556	2.991	2.8867	2.851	3.1207	1.1001	2.1847	1.8389	1.9903	2.1942	1.6391	1.4747	1.6029	1.6492
Lcatta2	0.31	1.4522	2.6124	3.3553	3.1674	3.0255	3.3409	1.6333	2.7405	3.3768	3.2743	3.0878	3.4157	1.2492	2.5997	2.3778	2.3014	2.4628	1.8828	1.8119	1.7441	1.6901
Ltardig1	0.52249	0.84172	1.7908	2.3123	2.1418	2.0733	2.3133	0.80455	1.5468	2.131	2.1455	1.996	2.216	1.0161	1.9453	1.6961	1.7009	1.8578	1.532	1.4767	1.4504	1.4493
Ltardig2	0.50725	1.0724	1.8861	2.4198	2.2589	2.2282	2.4276	0.95184	1.6469	2.052	1.9809	1.8785	2.0908	0.83779	1.6564	1.4928	1.5217	1.6394	1.2492	1.2202	1.2446	1.2369
Mnigra1	0.59042	1.5685	3.3969	4.2213	4.3622	3.9372	4.4903	1.6451	3.3361	4.0746	4.4329	3.9047	4.4537	1.871	3.098	3.1102	2.7773	3.2325	1.9807	2.0507	1.8177	1.9468
Mnigra2	0.81449	1.7311	3.4303	4.4242	4.5369	4.1982	4.6541	1.7737	3.4177	4.2527	4.5984	4.1826	4.6113	1.7069	3.0223	3.0992	2.812	3.2055	2.0868	1.9715	1.8883	2.0754
Ocrassi1	0.686	1.2042	2.452	3.9818	3.6631	3.7361	3.8265	1.1847	2.2987	3.6886	3.5453	3.5157	3.6219	1.2545	3.0078	2.735	2.8232	2.8366	2.0889	1.962	2.0375	1.9219
Ogarnett	0.45541	1.3612	2.2898	2.8759	2.7773	2.593	3.0001	1.2013	2.0653	2.6945	2.7296	2.4749	2.8729	0.97488	2.118	2.0719	1.8899	2.1623	1.6568	1.7819	1.5795	1.6628
Tbancanu	0.076811	1.4219	2.6001	2.649	2.5493	2.3611	2.7404	1.4524	2.6307	2.7029	2.6162	2.4238	2.8008	1.2476	2.1055	1.9021	1.8074	2.0828	1.902	1.8459	1.805	1.838
V.v.vari	0.38445	1.7219	3.0118	3.6635	3.5943	3.262	3.8411	1.9493	3.234	3.8648	3.8901	3.5271	4.1104	1.6045	3.1682	3.0155	2.801	3.1308	2.1482	2.1769	2.029	2.0363

	MFP - LFP	MFP - SFP	MFP - IFP	LFP - SFP	LFP - IFP	SFP - IFP
Acalaba1	0.9089	0.53245	0.44317	0.46454	0.54964	0.41316
Cmoloch1	0.7431	0.46368	0.4653	0.34728	0.33985	0.28513
Ctorquat	0.93499	0.62386	0.48229	0.36359	0.47265	0.25259
Cmedius1	0.69613	0.43451	0.41304	0.27964	0.34205	0.22672
Cmedius2	0.74873	0.41049	0.33481	0.3923	0.47508	0.30757
Gvariega	1.3432	0.61919	0.68717	0.89493	0.78339	0.61725
Cvolans	0.57567	0.33526	0.30083	0.39522	0.43646	0.44418
Dmadagas	1.4932	0.81031	0.74572	0.82347	0.82183	0.47529
Efalbifo	1.2258	0.72284	0.67097	0.64661	0.67276	0.51352
Efrufus	1.148	0.62825	0.65521	0.60008	0.57645	0.43428
Galleni2	0.70449	0.45891	0.36524	0.34132	0.41146	0.35525
Gelegan1	0.8175	0.47592	0.43909	0.44967	0.49183	0.42907
Gmoholi1	0.90956	0.4654	0.45398	0.55615	0.55498	0.40509
Gmoholi2	0.78147	0.5648	0.48888	0.32879	0.31765	0.30067
Gsenegal	0.67454	0.34307	0.36401	0.39812	0.39051	0.31623
Gdemido1	0.69203	0.48713	0.52972	0.29086	0.3662	0.31417
Hgriseus	0.95776	0.53861	0.42154	0.47896	0.63056	0.31969
Lcatta2	1.0549	0.61758	0.59211	0.51875	0.56223	0.42732
Ltardig1	0.92109	0.5001	0.50754	0.46314	0.46861	0.3015
Ltardig2	0.52811	0.26287	0.19235	0.38393	0.36455	0.26249
Mnigra1	1.6219	0.82152	0.91433	0.91924	0.81062	0.61717
Mnigra2	1.3198	0.83528	0.78422	0.62233	0.60481	0.49285
Ocrassi1	1.0443	0.56868	0.53544	0.56886	0.54083	0.35567
Ogarnett	0.88102	0.47276	0.49	0.5001	0.53824	0.45453
Tbancanu	0.88482	0.57184	0.44788	0.40012	0.51078	0.402
V.v.vari	1.2297	0.86	0.91263	0.54378	0.549	0.68476

APPENDIX 3 – Complete principal axis scores sorted by first axis:

3.1 - 15-landmark non-scaled trial principal axis scores sorted by first axis:

Gdemido1	-3.905	-0.363	-0.370	-0.259	-0.636	0.465	0.229	-0.003	0.433	0.062	0.116	0.308	0.231	-0.102	-0.006	0.116	0.308	0.202	0.126	0.019	0.021	0.004	-0.015	-0.003	-0.000	-0.000
Cmedius	-2.874	-0.469	0.540	-0.515	0.248	-0.112	0.128	-0.526	-0.569	0.348	0.104	0.020	-0.189	0.039	-0.042	0.048	-0.007	-0.138	0.177	0.024	-0.040	0.104	0.095	-0.037	0.020	-0.000
Ltardig2	-2.423	0.175	-0.082	-0.076	0.357	-0.071	-0.872	0.816	-0.448	-0.343	-0.188	-0.299	-0.106	-0.159	-0.019	0.152	0.010	0.038	0.010	0.082	0.047	0.047	-0.048	0.025	0.059	-0.000
Gelegan1	-2.196	0.131	-0.581	1.030	0.258	0.207	0.246	-0.083	0.371	0.314	-0.124	0.070	0.083	0.240	-0.260	0.170	-0.006	-0.179	-0.179	0.127	0.002	0.019	-0.005	0.029	0.014	-0.000
Gmoholi2	-1.793	0.334	-0.183	-0.001	-0.002	0.284	-0.257	0.458	0.159	-0.078	0.062	0.384	0.381	-0.062	0.434	0.060	-0.212	-0.140	-0.024	-0.063	-0.004	0.041	0.046	0.006	-0.044	-0.000
Acalaba1	-1.678	1.082	-0.473	0.263	1.599	-0.023	0.318	-0.416	-0.086	-0.465	0.330	-0.352	0.281	0.054	0.035	-0.089	0.082	0.053	0.011	-0.042	-0.073	-0.023	-0.010	0.002	-0.010	-0.000
Ltardig1	-1.591	-0.057	-0.505	0.266	-0.391	0.083	0.101	-0.154	-0.481	0.012	0.508	0.064	-0.466	-0.002	0.108	0.115	0.033	-0.085	-0.049	-0.094	0.081	-0.157	-0.020	0.027	-0.008	-0.000
Gmoholi1	-1.573	0.399	0.083	-0.017	-0.028	0.280	0.587	-0.054	0.256	0.169	-0.263	-0.184	-0.190	-0.128	-0.040	-0.203	-0.238	0.056	0.117	-0.032	0.060	0.020	-0.021	0.137	0.004	-0.000
Gsenegal	-1.460	0.233	0.238	0.638	-0.389	-0.496	0.613	0.398	0.353	0.076	-0.175	-0.400	-0.285	-0.106	0.178	0.010	-0.060	-0.017	0.042	0.044	-0.068	-0.020	-0.055	-0.125	-0.020	-0.000
Cmedius1	-1.214	-0.312	0.529	-0.624	-0.583	-0.627	-0.060	-0.469	-0.345	0.140	0.014	0.017	0.126	0.266	0.148	0.062	-0.140	0.216	-0.147	0.064	-0.093	0.003	-0.054	0.043	-0.008	-0.000
Galleni2	-1.152	0.330	0.334	0.111	-0.038	-0.208	-0.072	-0.077	0.156	-0.023	-0.188	-0.033	0.150	0.248	-0.050	-0.083	-0.105	0.129	-0.062	-0.114	0.157	-0.034	0.079	-0.087	0.073	-0.000
Cvolans	-0.396	-0.736	1.997	-0.366	0.355	-0.418	-0.056	0.072	0.293	-0.351	-0.392	0.014	0.001	0.055	-0.092	0.108	0.145	-0.105	0.006	-0.063	0.003	-0.076	0.017	0.045	-0.055	-0.000
Tbancanu	-0.086	-1.985	-1.471	-0.415	0.487	-0.525	-0.576	-0.174	0.535	-0.146	-0.061	0.172	-0.335	0.115	0.067	-0.200	0.013	-0.020	0.007	0.002	-0.015	0.015	-0.008	-0.003	-0.002	-0.000
Ogarnett	0.204	0.398	-0.213	0.972	-0.472	0.368	-0.303	-0.119	-0.301	-0.477	-0.177	0.405	-0.149	0.065	-0.332	0.000	-0.141	0.080	0.065	-0.087	-0.071	0.038	-0.023	-0.039	-0.056	-0.000
Hgriseus	0.251	-0.580	0.059	-0.088	0.497	-0.163	-0.182	0.216	-0.371	0.521	0.136	-0.018	0.278	-0.172	-0.172	-0.169	-0.027	0.038	-0.019	0.081	0.117	-0.023	-0.033	-0.043	-0.100	-0.000
Cmoloch1	0.438	1.416	0.681	-0.200	-0.824	-0.197	-0.699	0.217	0.483	0.078	0.708	-0.220	-0.035	0.116	-0.139	-0.171	0.052	-0.077	0.016	0.005	-0.030	0.035	0.006	0.018	-0.000	-0.000
Gvariega	0.531	-0.778	1.309	-0.141	0.391	1.147	0.178	0.053	-0.035	-0.061	0.153	0.285	-0.177	-0.142	0.056	-0.208	0.026	-0.001	-0.162	0.028	-0.043	0.016	-0.044	-0.036	0.053	-0.000
Ctorquat	1.195	1.273	-0.242	-0.189	-0.054	-0.934	0.089	-0.463	0.073	-0.033	-0.104	0.400	-0.026	-0.571	-0.074	0.015	0.039	-0.015	-0.115	0.003	-0.008	0.011	0.027	0.004	0.029	-0.000
Lcatta2	1.376	-0.689	-0.307	0.169	-0.324	0.181	-0.154	0.225	-0.096	0.030	-0.062	-0.061	0.294	-0.101	-0.088	-0.062	-0.104	-0.009	0.101	0.103	-0.119	-0.179	0.081	0.012	0.047	-0.000
ocrassi1	1.395	0.877	-0.403	0.403	-0.491	-0.019	0.223	0.311	-0.511	-0.031	-0.449	0.042	-0.069	0.213	0.193	-0.252	0.298	-0.022	-0.040	0.053	0.006	0.026	0.055	0.031	-0.020	-0.000

Efrufus	1.562	-1.018	-0.558	-0.224	-0.140	-0.110	0.316	0.608	-0.168	0.372	0.017	-0.279	0.173	-0.058	-0.144	0.058	0.072	-0.010	-0.082	-0.249	-0.081	0.058	-0.009	0.016	0.019	-0.000
Efalbifo	2.066	-0.357	-0.047	0.498	-0.485	0.664	-0.652	-1.048	0.098	0.082	-0.269	-0.575	0.124	-0.167	0.153	0.075	0.054	-0.040	-0.013	-0.028	0.029	0.022	-0.012	-0.008	-0.013	-0.000
Mnigra2	2.757	1.196	-0.241	-1.012	0.263	0.096	-0.031	-0.109	-0.037	0.249	-0.259	0.285	0.135	0.209	0.018	0.044	0.007	-0.129	0.143	-0.024	0.010	-0.044	-0.133	-0.029	0.038	-0.000
Mnigra1	2.916	0.877	-0.474	-1.320	0.412	0.631	0.110	0.221	0.230	0.042	-0.022	-0.155	-0.358	0.049	-0.035	0.209	-0.050	0.132	-0.060	0.052	-0.007	-0.003	0.087	-0.016	-0.048	-0.000
V.v.vari	2.931	-1.007	-0.233	-0.422	-0.670	-0.153	0.785	-0.033	-0.094	-0.737	0.298	-0.118	0.218	0.033	-0.053	0.045	-0.064	-0.092	0.019	0.089	0.093	0.062	-0.013	-0.003	0.007	-0.000
Dmadagas	4.720	-0.368	0.611	1.517	0.660	-0.348	-0.012	0.133	0.103	0.249	0.286	0.226	-0.089	0.067	0.156	0.151	0.017	0.134	0.112	0.019	0.025	0.037	0.009	0.034	0.021	-0.000

3.2 - 15-landmark scaled trial principal axis scores sorted by first axis:

Gdemido1	-1.624	0.485	-0.304	-1.557	0.102	-0.027	0.517	-0.257	-0.314	-0.086	0.431	0.035	0.333	0.129	-0.021	0.134	0.033	-0.039	0.006	-0.017	-0.076	0.005	0.005	-0.010	0.003	-0.000
Cmedius	-1.111	-0.504	0.631	0.920	0.351	0.549	-0.523	0.360	-0.308	-0.653	0.315	0.167	0.020	0.120	0.141	0.184	0.034	0.088	0.011	0.031	-0.009	-0.030	0.013	0.001	-0.007	-0.000
Ltardig2	-0.901	0.049	-0.056	-0.405	0.010	0.142	-1.208	-0.504	0.014	0.340	0.300	0.083	-0.020	-0.163	0.018	-0.143	-0.097	-0.061	0.020	0.047	0.052	-0.045	0.045	0.057	0.021	-0.000
Gelegan1	-0.896	0.462	-1.155	-0.214	-0.179	-0.039	0.235	0.427	0.013	-0.054	-0.130	-0.258	-0.158	0.202	0.260	-0.168	-0.126	0.148	-0.172	0.119	0.020	-0.007	0.030	0.014	0.001	-0.000
Gmoholi2	-0.877	0.168	-0.075	-0.039	-0.351	-0.038	-0.539	0.045	-0.240	-0.108	-0.386	-0.227	0.235	-0.019	-0.433	-0.141	0.162	0.167	-0.036	-0.020	0.019	-0.023	-0.016	-0.040	-0.031	-0.000
Acalaba1	-0.850	-0.078	0.009	0.006	-0.339	-0.342	0.391	0.392	0.095	0.190	0.130	-0.055	-0.267	-0.206	0.016	0.075	0.255	-0.021	0.110	-0.021	0.069	0.003	0.132	0.009	-0.029	-0.000
Ltardig1	-0.754	0.284	-0.031	0.490	-0.685	-0.335	0.074	0.180	-0.409	-0.237	-0.324	-0.237	0.113	-0.071	0.018	0.023	-0.283	-0.241	0.141	-0.032	0.004	-0.016	0.000	0.001	-0.014	-0.000
Gmoholi1	-0.743	-0.289	-0.603	0.425	0.375	-0.722	0.006	0.522	0.040	0.185	0.372	0.076	-0.229	-0.156	-0.191	-0.052	-0.019	0.004	0.047	0.019	-0.090	-0.025	-0.085	-0.030	0.063	-0.000
Gsenegal	-0.699	0.409	0.516	0.170	1.075	0.115	0.450	0.071	-0.008	0.098	-0.392	0.143	0.235	-0.524	0.073	0.006	-0.029	0.011	-0.115	0.017	0.004	-0.002	-0.010	0.031	-0.011	-0.000
Cmedius1	-0.671	-0.329	-0.057	0.057	0.218	0.037	0.015	0.058	-0.146	0.139	-0.012	-0.238	-0.089	0.220	0.046	0.034	0.142	-0.109	-0.067	-0.129	0.134	0.068	-0.111	0.072	0.009	-0.000
Galleni2	-0.440	0.177	-0.863	0.563	-0.256	0.408	-0.050	-0.374	-0.098	0.354	-0.363	0.334	0.028	0.070	0.333	-0.043	0.185	-0.046	0.056	-0.053	-0.065	-0.060	-0.026	-0.058	0.011	-0.000
Cvolans	-0.421	0.448	-0.383	0.362	-0.161	-0.122	0.143	-0.483	0.169	-0.418	0.038	0.505	-0.194	-0.029	-0.110	-0.100	-0.109	0.067	-0.048	-0.136	0.013	0.147	0.037	-0.009	0.009	-0.000
Tbancanu	-0.421	0.477	-0.176	0.582	0.065	-0.162	-0.093	-0.108	0.576	0.503	-0.071	0.131	0.087	0.254	-0.179	0.365	-0.124	0.014	-0.039	0.070	0.035	0.003	0.002	-0.015	-0.034	-0.000
Ogarnett	-0.351	-0.588	0.327	-0.349	0.013	-0.087	0.442	-0.585	0.351	-0.247	-0.040	-0.031	-0.270	-0.019	0.034	-0.056	-0.046	0.136	0.175	0.049	0.008	-0.082	-0.084	0.027	-0.060	-0.000
Hgriseus	-0.119	0.479	1.313	-0.223	0.062	0.309	0.143	0.192	0.328	0.133	-0.335	-0.138	0.043	0.222	-0.012	-0.037	-0.040	0.123	0.143	-0.061	-0.036	-0.001	0.039	0.026	0.093	-0.000
Cmoloch1	0.049	-0.510	0.601	0.517	0.518	-0.094	0.268	-0.540	0.024	-0.133	-0.056	-0.279	-0.180	0.220	-0.154	-0.123	0.084	-0.217	-0.141	0.067	-0.088	-0.029	0.061	-0.008	0.003	-0.000
Gvariega	0.264	0.702	1.510	-0.433	-0.523	0.174	-0.027	0.511	0.193	0.106	0.186	0.382	-0.034	0.065	0.044	-0.199	0.020	-0.130	-0.058	0.068	0.017	0.031	-0.054	-0.043	-0.038	-0.000
Ctorquat	0.502	-2.026	0.389	-0.388	0.363	-0.144	-0.124	0.103	-0.378	0.465	-0.050	-0.033	0.011	0.068	0.101	-0.035	-0.157	0.089	0.005	-0.070	-0.021	0.073	0.032	-0.051	-0.036	-0.000
Lcatta2	0.586	-0.108	-0.039	-0.527	0.133	-0.037	-0.298	-0.218	0.439	-0.361	-0.029	-0.396	-0.009	-0.203	0.157	0.127	0.024	-0.048	-0.011	0.034	0.098	0.036	-0.016	-0.107	0.044	-0.000
ocrassi1	0.724	-1.368	0.068	-0.456	-1.160	0.063	0.088	0.021	0.013	-0.108	-0.237	0.259	-0.038	-0.157	-0.065	0.192	0.021	-0.002	-0.161	0.032	-0.042	-0.036	-0.012	0.048	0.041	-0.000

Efrufus	0.988	0.038	-0.362	0.580	-0.341	1.291	0.589	-0.044	-0.038	0.228	0.504	-0.299	0.046	-0.154	-0.151	-0.050	-0.088	0.028	-0.011	-0.040	0.024	-0.024	-0.003	-0.014	0.001	-0.000
Efalbifo	1.024	0.254	-0.254	0.307	-0.213	0.013	-0.277	-0.078	0.050	0.023	0.033	-0.265	0.137	-0.089	0.084	0.016	0.113	0.024	0.100	0.127	-0.129	0.177	-0.022	0.050	-0.019	-0.000
Mnigra2	1.463	0.507	0.042	0.073	-0.047	-0.579	-0.339	0.148	0.455	-0.118	0.247	-0.202	0.155	-0.018	0.155	-0.004	0.000	0.029	-0.096	-0.199	-0.082	-0.088	0.009	0.023	-0.037	-0.000
Mnigra1	1.489	-0.672	-1.254	-0.427	0.632	0.295	-0.006	0.456	0.350	-0.281	-0.162	0.321	0.223	0.142	-0.136	-0.109	0.019	-0.124	0.112	0.024	0.043	-0.019	0.027	0.023	-0.007	-0.000
V.v.vari	1.791	0.217	0.313	0.583	-0.094	-0.849	0.378	-0.331	-0.498	0.029	0.221	0.170	0.301	0.093	0.062	-0.059	0.042	0.095	0.020	0.081	0.115	-0.032	0.007	0.004	0.033	-0.000
Dmadagas	2.001	1.317	-0.107	-0.616	0.434	0.181	-0.253	0.037	-0.672	0.013	-0.192	0.049	-0.479	0.002	-0.088	0.163	-0.016	0.013	0.010	-0.007	-0.016	-0.024	-0.002	-0.001	-0.010	-0.000

3.3 - 16-landmark non-scaled trial principal axis scores sorted by first axis:

Ltardig1	-2.691	-0.801	0.510	0.674	0.433
Tbancanu	-1.970	2.034	-0.740	-0.517	-0.093
Cmoloch1	-0.012	-1.867	0.464	-0.987	-0.168
Ctorquat	0.673	-0.823	-0.701	0.634	-0.798
V.v.vari	1.722	1.680	1.212	0.165	-0.155
Mnigra2	2.278	-0.223	-0.745	0.032	0.783

3.4 - 16-landmark scaled trial principal axis scores sorted by first axis:

Tbancanu	-2.248	0.622	-0.790	0.395	0.049
V.v.vari	-1.471	-1.067	0.911	-0.032	0.220
Ltardig1	0.485	-0.670	-0.738	-0.798	-0.529
Mnigra2	0.489	0.894	0.822	0.137	-0.705
Ctorquat	0.896	0.725	0.106	-0.640	0.788
Cmoloch1	1.849	-0.504	-0.311	0.938	0.178

APPENDIX 4 – Complete correlation matrices:

4.1 - 15-landmark non-scaled trial correlations between distances and axis scores:

Axis 1:

	MAN	LAT	HEA	IAM	LCR	SCR	IAR	SAR	MAH	IAI	ARI	MFP	LFP	SFP	IFP
MAN															
LAT	0.92														
HEA	0.93	0.67													
IAM	0.86	0.73	0.86												
LCR	0.65	0.86	0.94	0.53											

SCR	0.89	0.84	0.83	0.48	0.89									
IAR	0.84	0.86	0.88	0.46	0.64	0.70								
SAR	0.91	0.75	0.41	0.79	0.94	0.84	0.76							
MAH	0.90	0.62	0.01	0.85	0.95	0.89	0.84	-0.26						
IAI	0.85	0.77	0.87	0.02	0.72	0.92	-0.09	0.75	0.83					
ARI	0.66	0.88	0.93	0.64	0.66	0.89	0.70	0.93	0.95	0.77				
MFP	0.83	0.93	0.94	0.89	0.93	0.95	0.93	0.95	0.98	0.95	0.91			
LFP	0.76	0.91	0.93	0.94	0.90	0.96	0.95	0.93	0.96	0.93	0.90	0.82		
SFP	0.78	0.91	0.92	0.91	0.92	0.94	0.93	0.92	0.96	0.94	0.90	0.82	0.69	
IFP	0.79	0.92	0.93	0.89	0.90	0.94	0.93	0.94	0.97	0.91	0.87	0.76	0.71	0.61

Axis 2:

	MAN	LAT	HEA	IAM	LCR	SCR	IAR	SAR	MAH	IAI	ARI	MFP	LFP	SFP	IFP
MAN															
LAT	-0.19														
HEA	-0.16	-0.01													
IAM	-0.20	-0.09	-0.21												
LCR	-0.28	0.22	0.13	0.50											
SCR	-0.20	0.38	0.41	0.46	0.04										
IAR	-0.16	0.12	-0.18	0.25	0.50	0.44									
SAR	-0.20	0.09	0.34	-0.30	0.04	0.31	-0.32								
MAH	-0.22	0.44	0.72	-0.15	-0.16	-0.26	-0.22	0.62							
IAI	-0.21	0.39	0.04	0.49	0.19	0.05	0.65	-0.14	-0.26						
ARI	-0.29	0.28	0.18	0.49	-0.27	0.04	0.51	0.10	-0.10	0.24					
MFP	-0.27	0.24	0.25	0.18	-0.08	0.02	0.17	0.20	0.02	0.07	-0.02				
LFP	-0.33	0.28	0.25	0.15	-0.08	0.05	0.17	0.21	0.10	0.13	-0.00	-0.01			
SFP	-0.31	0.30	0.28	0.19	-0.08	0.07	0.19	0.24	0.09	0.13	0.01	-0.02	-0.04		
IFP	-0.29	0.26	0.24	0.20	-0.03	0.04	0.21	0.20	0.05	0.13	0.06	-0.03	-0.13	-0.23	

Axis 3:

	MAN	LAT	HEA	IAM	LCR	SCR	IAR	SAR	MAH	IAI	ARI	MFP	LFP	SFP	IFP
MAN															
LAT	0.04														
HEA	0.13	0.06													
IAM	0.22	0.13	0.25												
LCR	0.28	-0.27	-0.03	-0.51											
SCR	0.20	-0.15	0.02	-0.31	-0.06										
IAR	0.29	0.20	0.24	0.12	-0.36	-0.44									
SAR	0.18	0.07	-0.15	0.36	0.07	0.24	0.32								
MAH	0.26	0.32	0.35	0.37	0.08	-0.07	0.29	0.60							
IAI	0.22	0.05	0.28	-0.24	-0.43	-0.20	-0.05	0.41	0.36						
ARI	0.33	-0.21	-0.01	-0.40	0.33	-0.11	-0.31	0.06	0.06	-0.37					
MFP	0.06	-0.15	0.04	-0.20	-0.16	-0.03	-0.19	0.03	0.03	-0.19	-0.29				
LFP	0.07	-0.19	-0.01	-0.16	-0.17	-0.08	-0.14	-0.05	0.01	-0.18	-0.25	-0.15			
SFP	0.13	-0.11	0.06	-0.12	-0.11	-0.06	-0.12	0.02	0.03	-0.13	-0.25	-0.27	0.06		
IFP	0.06	-0.18	0.02	-0.21	-0.21	-0.07	-0.19	-0.00	0.03	-0.22	-0.35	-0.20	-0.00	0.03	

Axis 4:

	MAN	LAT	HEA	IAM	LCR	SCR	IAR	SAR	MAH	IAI	ARI	MFP	LFP	SFP	IFP
MAN															
LAT	-0.00														
HEA	0.09	0.31													
IAM	0.25	0.03	-0.16												
LCR	0.53	0.08	-0.20	0.11											
SCR	0.25	0.15	-0.26	0.06	-0.36										
IAR	0.19	0.04	-0.20	0.10	-0.01	0.11									
SAR	0.16	0.25	-0.59	0.04	-0.10	0.05	0.01								
MAH	0.14	0.15	-0.50	0.02	-0.13	0.12	0.00	-0.17							
IAI	0.24	0.32	-0.07	0.60	-0.35	-0.10	0.54	0.13	0.03						
ARI	0.51	0.09	-0.18	0.16	0.35	-0.29	0.04	-0.09	-0.12	-0.31					
MFP	0.39	0.14	-0.06	0.14	0.18	-0.08	0.15	-0.01	-0.02	-0.01	0.10				
LFP	0.41	0.06	-0.08	0.04	0.21	-0.13	0.01	-0.07	-0.10	-0.10	0.11	-0.07			
SFP	0.42	0.13	-0.08	0.12	0.21	-0.14	0.10	-0.05	-0.08	-0.06	0.11	-0.15	0.02		
IFP	0.43	0.06	-0.11	0.03	0.11	-0.19	0.01	-0.09	-0.11	-0.15	-0.03	-0.18	0.07	-0.08	

Axis 5:

	MAN	LAT	HEA	IAM	LCR	SCR	IAR	SAR	MAH	IAI	ARI	MFP	LFP	SFP	IFP
MAN															
LAT	-0.15														
HEA	0.01	0.30													
IAM	-0.14	-0.05	0.20												
LCR	-0.11	-0.04	0.13	-0.02											
SCR	-0.08	-0.00	0.01	-0.03	0.06										
IAR	-0.19	-0.13	0.25	-0.52	-0.02	0.06									
SAR	-0.01	0.28	-0.05	0.26	0.18	0.07	0.38								
MAH	-0.02	0.22	-0.02	0.19	0.11	0.07	0.32	-0.01							
IAI	-0.19	0.09	0.33	-0.02	-0.22	0.00	0.31	0.40	0.25						
ARI	-0.15	-0.00	0.16	0.04	-0.04	0.09	0.03	0.20	0.13	-0.16					
MFP	-0.12	0.04	0.08	0.05	0.02	-0.03	0.01	0.06	0.01	-0.08	0.05				
LFP	-0.20	-0.02	0.07	0.01	-0.02	-0.01	-0.05	0.03	0.00	-0.10	0.01	0.17			
SFP	-0.14	0.02	0.06	0.02	-0.03	-0.06	-0.04	0.02	-0.03	-0.12	-0.00	0.05	0.27		
IFP	-0.12	0.05	0.10	0.06	0.01	-0.03	0.01	0.06	0.01	-0.09	0.04	-0.09	0.39	0.16	

Axis 6:

	MAN	LAT	HEA	IAM	LCR	SCR	IAR	SAR	MAH	IAI	ARI	MFP	LFP	SFP	IFP
MAN															
LAT	0.16														
HEA	-0.01	-0.33													
IAM	0.11	0.22	0.03												
LCR	0.10	0.05	-0.06	-0.18											
SCR	0.05	-0.00	0.10	-0.22	-0.08										
IAR	0.06	-0.04	-0.07	0.13	-0.01	0.02									
SAR	0.01	-0.07	0.38	0.05	-0.10	-0.08	-0.06								
MAH	0.01	-0.15	0.10	-0.02	-0.03	0.10	-0.02	-0.22							
IAI	0.07	0.08	-0.01	-0.02	-0.10	-0.08	0.14	-0.06	-0.01						
ARI	0.11	0.05	-0.06	-0.19	-0.10	-0.14	-0.05	-0.11	-0.06	-0.13					
MFP	0.04	0.07	0.05	-0.08	-0.14	-0.19	-0.01	-0.06	-0.05	-0.04	-0.10				

LFP	-0.07	0.04	-0.01	-0.04	-0.12	-0.06	-0.03	-0.08	-0.05	-0.02	-0.03	0.40		
SFP	0.04	0.06	0.00	-0.08	-0.16	-0.17	-0.05	-0.11	-0.10	-0.06	-0.11	0.24	0.55	
IFP	-0.03	0.09	0.04	-0.05	-0.18	-0.10	0.00	-0.05	-0.03	-0.02	-0.09	0.40	0.43	0.52

Axis 7:

	MAN	LAT	HEA	IAM	LCR	SCR	IAR	SAR	MAH	IAI	ARI	MFP	LFP	SFP	IFP
MAN															
LAT	-0.05														
HEA	-0.06	-0.08													
IAM	-0.16	-0.25	-0.09												
LCR	0.02	-0.05	-0.08	0.07											
SCR	0.00	-0.03	-0.07	0.32	-0.01										
IAR	-0.10	-0.12	-0.02	-0.30	-0.14	0.04									
SAR	-0.08	-0.23	-0.25	-0.03	-0.03	0.12	0.04								
MAH	-0.04	-0.09	-0.08	0.10	-0.01	0.04	0.06	0.16							
IAI	-0.04	-0.12	-0.11	0.00	0.02	0.02	-0.20	-0.03	-0.04						
ARI	0.03	-0.03	-0.07	0.10	0.16	-0.03	-0.07	-0.01	-0.01	0.07					
MFP	0.07	0.05	0.02	0.18	0.09	-0.05	0.10	0.08	0.03	0.14	0.05				
LFP	0.03	0.03	-0.01	0.07	0.09	0.00	0.07	0.04	0.03	0.14	0.06	0.20			
SFP	0.04	0.03	-0.01	0.13	0.09	-0.04	0.08	0.05	0.02	0.14	0.04	0.19	0.18		
IFP	0.04	0.07	0.04	0.17	0.14	0.02	0.13	0.10	0.06	0.19	0.11	0.30	0.16	0.29	

Axis 8:

	MAN	LAT	HEA	IAM	LCR	SCR	IAR	SAR	MAH	IAI	ARI	MFP	LFP	SFP	IFP
MAN															
LAT	0.10														
HEA	0.06	-0.13													
IAM	0.04	-0.23	-0.13												
LCR	0.10	-0.02	-0.00	0.05											
SCR	0.09	0.05	0.17	0.25	-0.02										
IAR	0.17	-0.00	-0.06	-0.53	0.04	0.02									
SAR	0.08	0.03	0.26	-0.11	-0.04	0.05	-0.10								
MAH	0.09	0.03	0.14	-0.07	-0.01	0.09	-0.05	-0.04							
IAI	0.17	-0.02	-0.02	-0.31	0.05	0.01	0.03	-0.09	-0.06						
ARI	0.13	0.01	0.01	0.09	0.21	-0.02	0.09	-0.02	-0.00	0.09					
MFP	0.09	0.03	0.07	0.13	-0.03	0.00	0.06	0.03	0.02	0.05	-0.13				
LFP	0.11	0.04	0.04	0.04	-0.10	-0.03	0.06	0.02	-0.01	0.02	-0.21	-0.08			
SFP	0.13	0.07	0.07	0.11	-0.07	-0.02	0.09	0.04	0.01	0.05	-0.20	-0.18	0.05		
IFP	0.11	0.05	0.06	0.11	-0.04	-0.00	0.09	0.03	0.02	0.07	-0.16	-0.07	-0.12	-0.07	

Axis 9:

	MAN	LAT	HEA	IAM	LCR	SCR	IAR	SAR	MAH	IAI	ARI	MFP	LFP	SFP	IFP
MAN															
LAT	0.08														
HEA	-0.02	-0.15													
IAM	0.02	0.19	0.06												
LCR	-0.15	0.05	0.09	-0.02											
SCR	-0.06	-0.10	0.03	-0.23	0.14										

IAR	0.04	0.03	-0.00	0.04	0.27	-0.03									
SAR	-0.00	-0.15	-0.14	0.05	0.18	0.13	0.03								
MAH	-0.00	-0.06	0.11	-0.02	0.11	-0.04	0.03	0.19							
IAI	-0.03	-0.03	0.05	-0.20	0.16	-0.01	0.22	0.12	0.04						
ARI	-0.14	0.08	0.10	0.01	0.21	0.14	0.26	0.19	0.11	0.17					
MFP	-0.10	-0.07	-0.03	-0.16	-0.02	0.07	-0.08	-0.01	-0.01	-0.08	-0.12				
LFP	-0.06	-0.02	-0.02	-0.07	0.05	0.08	-0.02	0.01	0.02	-0.02	-0.02	-0.03			
SFP	-0.07	-0.07	-0.04	-0.14	0.05	0.09	-0.08	-0.01	-0.00	-0.06	-0.04	0.07	-0.05		
IFP	-0.09	-0.04	-0.02	-0.11	0.05	0.10	-0.03	0.02	0.02	-0.03	-0.06	0.09	-0.07	0.16	

Axis 10:

	MAN	LAT	HEA	IAM	LCR	SCR	IAR	SAR	MAH	IAI	ARI	MFP	LFP	SFP	IFP
MAN															
LAT	0.06														
HEA	0.17	0.22													
IAM	0.17	-0.03	0.05												
LCR	0.06	-0.16	-0.01	-0.16											
SCR	0.06	0.03	0.04	-0.08	-0.08										
IAR	0.17	-0.15	-0.03	-0.06	0.02	0.08									
SAR	0.12	0.02	-0.08	-0.09	-0.03	0.13	-0.11								
MAH	0.11	0.08	-0.11	-0.05	-0.00	0.10	-0.04	-0.00							
IAI	0.16	-0.23	-0.07	-0.26	0.06	0.07	-0.02	-0.11	-0.03						
ARI	-0.00	-0.14	0.03	-0.14	-0.19	0.01	0.04	0.03	0.05	0.09					
MFP	-0.08	-0.01	0.10	-0.06	-0.05	0.06	0.03	0.14	0.11	0.05	0.01				
LFP	-0.19	-0.07	0.10	-0.10	-0.13	0.05	-0.04	0.12	0.10	-0.01	-0.12	0.14			
SFP	-0.10	-0.01	0.13	-0.08	-0.10	0.07	0.01	0.16	0.14	0.04	-0.06	0.03	0.10		
IFP	-0.10	-0.04	0.09	-0.08	-0.05	0.04	0.00	0.11	0.09	0.04	-0.01	-0.02	0.16	-0.29	

Axis 11:

	MAN	LAT	HEA	IAM	LCR	SCR	IAR	SAR	MAH	IAI	ARI	MFP	LFP	SFP	IFP
MAN															
LAT	-0.07														
HEA	0.04	0.27													
IAM	-0.03	0.11	0.02												
LCR	0.13	0.15	0.04	0.05											
SCR	0.08	0.19	-0.04	0.15	0.04										
IAR	0.09	0.29	-0.02	-0.02	0.20	0.10									
SAR	0.05	0.33	-0.06	0.08	0.05	-0.04	-0.04								
MAH	0.02	0.34	0.03	0.12	-0.01	-0.08	0.09	0.06							
IAI	0.03	0.15	-0.02	-0.24	0.11	0.17	0.09	-0.00	0.06						
ARI	0.12	0.13	0.03	0.03	0.15	0.07	0.17	0.03	0.00	0.10					
MFP	0.11	0.01	-0.07	-0.05	-0.00	-0.01	-0.04	-0.12	-0.07	-0.04	-0.07				
LFP	0.11	-0.07	-0.08	-0.12	0.05	0.02	-0.07	-0.12	-0.06	-0.08	-0.02	0.10			
SFP	0.09	-0.04	-0.09	-0.11	0.02	0.01	-0.08	-0.13	-0.07	-0.07	-0.06	0.14	-0.01		
IFP	0.11	-0.04	-0.08	-0.09	0.02	0.02	-0.05	-0.11	-0.06	-0.06	-0.06	0.18	-0.01	-0.04	

Axis 12:

	MAN	LAT	HEA	IAM	LCR	SCR	IAR	SAR	MAH	IAI	ARI	MFP	LFP	SFP	IFP

MAN														
LAT	0.06													
HEA	0.10	0.18												
IAM	0.04	-0.40	-0.07											
LCR	-0.08	-0.19	0.00	0.17										
SCR	0.01	-0.04	0.05	0.34	0.10									
IAR	0.08	-0.11	0.06	-0.14	-0.11	-0.02								
SAR	0.10	0.09	0.07	0.06	0.04	0.12	0.11							
MAH	0.10	0.08	-0.02	0.15	0.09	0.13	0.09	-0.05						
IAI	0.07	-0.10	0.08	0.22	-0.09	-0.00	0.03	0.10	0.11					
ARI	-0.03	-0.14	0.00	0.19	0.14	0.05	-0.08	0.03	0.07	-0.08				
MFP	-0.06	-0.08	-0.05	0.09	0.01	0.07	-0.10	-0.02	0.00	-0.08	-0.05			
LFP	-0.05	-0.09	-0.04	0.02	-0.02	0.08	-0.07	-0.02	0.01	-0.04	-0.03	0.05		
SFP	-0.05	-0.10	-0.05	0.05	-0.00	0.11	-0.10	-0.02	0.01	-0.07	-0.06	0.14	-0.05	
IFP	-0.04	-0.07	-0.03	0.11	0.10	0.12	-0.04	0.01	0.04	-0.01	0.08	0.08	-0.01	-0.07

Axis 13:

	MAN	LAT	HEA	IAM	LCR	SCR	IAR	SAR	MAH	IAI	ARI	MFP	LFP	SFP	IFP
MAN															
LAT	-0.04														
HEA	-0.02	-0.08													
IAM	-0.02	0.01	0.06												
LCR	0.18	0.06	0.06	0.05											
SCR	0.09	-0.04	0.02	0.03	-0.04										
IAR	0.00	-0.14	0.01	-0.00	0.15	0.08									
SAR	0.01	-0.15	-0.04	0.04	0.06	0.03	0.00								
MAH	0.01	-0.21	-0.11	0.02	0.06	0.09	0.03	-0.06							
IAI	0.01	-0.05	0.08	0.05	0.03	-0.01	0.12	0.07	0.04						
ARI	0.15	-0.02	0.01	-0.04	-0.12	-0.01	0.08	0.03	0.04	-0.02					
MFP	0.10	-0.08	-0.05	-0.07	-0.07	-0.06	0.02	-0.00	0.03	0.00	-0.03				
LFP	0.09	-0.05	-0.03	-0.07	-0.02	-0.05	0.02	0.02	0.03	0.03	-0.02	-0.09			
SFP	0.07	-0.10	-0.05	-0.08	0.00	-0.00	0.03	0.01	0.05	0.04	0.04	0.15	-0.27		
IFP	0.11	-0.08	-0.05	-0.09	-0.05	-0.04	0.01	0.00	0.03	0.01	-0.02	0.05	-0.19	-0.03	

Axis 14:

	MAN	LAT	HEA	IAM	LCR	SCR	IAR	SAR	MAH	IAI	ARI	MFP	LFP	SFP	IFP
MAN															
LAT	0.05														
HEA	0.07	0.05													
IAM	-0.06	-0.12	0.13												
LCR	0.01	-0.07	-0.01	-0.11											
SCR	-0.03	-0.15	-0.09	-0.05	-0.07										
IAR	0.08	-0.09	0.01	-0.09	0.06	-0.12									
SAR	0.07	0.06	0.08	0.15	-0.01	-0.21	-0.01								
MAH	0.01	-0.01	0.14	0.02	-0.09	-0.23	-0.08	0.02							
IAI	0.07	-0.08	0.02	-0.09	-0.02	-0.16	0.15	-0.00	-0.08						
ARI	0.01	-0.06	-0.00	-0.06	0.02	-0.03	0.09	0.01	-0.06	0.01					
MFP	0.01	-0.03	-0.02	0.06	0.05	0.05	0.05	0.01	0.00	0.02	0.04				
LFP	0.08	0.01	0.02	0.08	0.12	0.04	0.10	0.05	0.04	0.08	0.12	-0.02			

SFP	0.03	-0.04	-0.02	0.06	0.05	0.03	0.05	0.01	0.01	0.02	0.04	-0.00	-0.03		
IFP	0.02	-0.01	0.01	0.08	0.10	0.06	0.10	0.04	0.03	0.06	0.09	0.04	-0.08	0.12	

Axis 15:

	MAN	LAT	HEA	IAM	LCR	SCR	IAR	SAR	MAH	IAI	ARI	MFP	LFP	SFP	IFP
MAN															
LAT	0.02														
HEA	0.03	0.03													
IAM	0.06	0.13	0.05												
LCR	-0.00	-0.07	-0.05	-0.26											
SCR	0.01	0.06	0.05	-0.13	0.01										
IAR	0.00	-0.08	-0.04	-0.03	-0.14	0.07									
SAR	0.03	0.06	0.02	0.04	-0.04	0.07	0.01								
MAH	0.03	0.09	0.02	0.04	-0.03	0.04	0.04	-0.00							
IAI	0.00	-0.01	0.02	-0.06	-0.13	0.10	-0.03	0.04	0.05						
ARI	-0.01	-0.05	-0.03	-0.18	0.09	0.04	-0.08	-0.02	-0.01	-0.08					
MFP	0.05	0.05	0.05	0.05	0.14	0.03	0.11	0.04	0.03	0.06	0.14				
LFP	0.07	0.02	0.03	0.10	0.10	0.03	0.09	0.03	0.03	0.04	0.08	0.07			
SFP	0.06	0.02	0.02	0.06	0.12	0.03	0.09	0.03	0.02	0.04	0.10	0.12	0.02		
IFP	0.05	-0.02	-0.01	0.00	0.08	-0.00	0.03	-0.02	-0.01	-0.02	0.05	0.07	-0.08	-0.15	

Axis 16:

	MAN	LAT	HEA	IAM	LCR	SCR	IAR	SAR	MAH	IAI	ARI	MFP	LFP	SFP	IFP
MAN															
LAT	0.09														
HEA	0.10	0.05													
IAM	0.07	0.15	0.11												
LCR	0.07	0.08	0.05	-0.02											
SCR	0.10	0.09	-0.00	0.04	0.07										
IAR	0.01	0.02	0.09	-0.02	-0.04	0.17									
SAR	0.09	0.15	0.09	0.13	0.01	-0.12	0.14								
MAH	0.06	0.04	-0.06	0.05	0.03	-0.01	0.10	-0.18							
IAI	0.06	0.09	0.07	0.09	0.00	0.09	0.01	0.03	0.02						
ARI	0.03	0.09	0.07	0.04	0.10	0.13	0.03	0.04	0.05	0.07					
MFP	-0.02	0.04	0.09	0.01	0.00	0.08	0.01	0.04	0.06	0.05	-0.05				
LFP	-0.06	0.09	0.16	0.07	0.07	0.13	0.05	0.14	0.12	0.12	0.00	0.06			
SFP	-0.06	0.02	0.10	-0.02	-0.04	0.09	-0.02	0.06	0.07	0.03	-0.13	0.09	0.03		
IFP	-0.05	0.06	0.12	0.02	0.00	0.10	0.01	0.09	0.09	0.07	-0.09	0.15	-0.03	0.07	

Axis 17:

	MAN	LAT	HEA	IAM	LCR	SCR	IAR	SAR	MAH	IAI	ARI	MFP	LFP	SFP	IFP
MAN															
LAT	-0.11														
HEA	-0.04	0.12													
IAM	0.01	0.03	0.03												
LCR	0.03	-0.03	0.01	0.02											
SCR	0.02	-0.05	-0.05	-0.11	0.04										
IAR	-0.03	0.00	0.03	0.03	0.03	-0.03									

SAR	-0.04	0.02	0.03	0.01	0.02	-0.02	0.03							
MAH	-0.00	0.03	-0.02	0.03	0.05	0.00	0.08	0.02						
IAI	-0.01	-0.04	-0.00	0.02	0.05	-0.01	0.00	-0.00	0.03					
ARI	0.04	-0.04	-0.02	-0.01	0.07	0.01	-0.04	-0.01	0.02	-0.01				
MFP	0.01	0.04	0.03	0.03	-0.04	0.04	0.01	0.07	0.07	0.05	-0.05			
LFP	0.03	0.06	0.03	0.07	0.01	0.03	0.02	0.06	0.06	0.07	0.01	-0.00		
SFP	0.05	0.12	0.07	0.13	0.09	0.07	0.09	0.12	0.10	0.15	0.09	-0.00	0.01	
IFP	0.03	0.05	0.03	0.04	-0.03	0.03	0.00	0.06	0.06	0.05	-0.03	0.01	0.03	-0.04

Axis 18:

	MAN	LAT	HEA	IAM	LCR	SCR	IAR	SAR	MAH	IAI	ARI	MFP	LFP	SFP	IFP
MAN															
LAT	0.07														
HEA	0.07	0.08													
IAM	0.03	0.02	0.02												
LCR	0.09	0.05	0.03	-0.05											
SCR	0.03	0.05	0.01	0.01	-0.11										
IAR	0.05	0.04	0.03	-0.05	-0.09	-0.08									
SAR	0.08	0.12	0.00	0.06	0.03	0.01	0.04								
MAH	0.07	0.10	-0.03	0.05	0.00	0.04	-0.02	-0.07							
IAI	0.06	0.06	0.06	0.00	-0.06	-0.03	-0.08	0.07	0.05						
ARI	0.05	0.09	0.07	0.02	0.07	-0.06	-0.00	0.07	0.04	0.01					
MFP	-0.04	0.02	0.03	-0.01	-0.01	-0.04	-0.01	0.01	0.01	-0.04	-0.04				
LFP	-0.02	0.04	0.04	0.03	0.12	0.01	0.05	0.04	0.04	0.02	0.13	0.06			
SFP	-0.02	0.06	0.06	0.03	0.06	-0.02	0.05	0.04	0.04	0.00	0.06	-0.02	0.08		
IFP	-0.02	0.05	0.05	0.03	0.09	-0.02	0.04	0.04	0.04	0.01	0.08	0.03	0.13	-0.10	

Axis 19:

	MAN	LAT	HEA	IAM	LCR	SCR	IAR	SAR	MAH	IAI	ARI	MFP	LFP	SFP	IFP
MAN															
LAT	0.04														
HEA	0.06	0.11													
IAM	0.04	0.03	0.01												
LCR	0.08	0.04	-0.00	-0.06											
SCR	0.07	0.07	0.02	0.03	0.02										
IAR	0.07	0.07	0.00	-0.01	-0.07	0.02									
SAR	0.08	0.06	0.02	0.03	0.03	0.02	0.02								
MAH	0.08	0.09	-0.00	0.06	0.02	-0.02	0.04	0.02							
IAI	0.05	0.08	0.07	-0.05	-0.06	0.08	-0.03	0.09	0.09						
ARI	0.04	0.04	0.01	0.01	0.07	0.12	0.02	0.06	0.06	0.01					
MFP	0.07	0.03	-0.03	0.06	0.04	0.10	0.05	0.06	0.04	0.03	0.01				
LFP	0.10	0.06	0.01	0.08	0.08	0.09	0.10	0.11	0.09	0.06	0.00	-0.02			
SFP	0.06	0.01	-0.04	0.04	0.00	0.08	0.04	0.07	0.05	0.01	-0.06	0.04	-0.05		
IFP	0.12	0.06	-0.00	0.09	0.11	0.10	0.09	0.10	0.07	0.06	0.04	0.02	-0.00	-0.00	

Axis 20:

	MAN	LAT	HEA	IAM	LCR	SCR	IAR	SAR	MAH	IAI	ARI	MFP	LFP	SFP	IFP
MAN															

LAT	0.04													
HEA	0.03	0.01												
IAM	-0.05	0.05	0.11											
LCR	0.02	0.05	0.02	-0.02										
SCR	0.02	0.02	0.02	0.10	-0.00									
IAR	-0.00	0.02	0.06	-0.02	0.04	0.10								
SAR	-0.00	-0.05	0.09	0.02	-0.02	-0.01	-0.02							
MAH	0.01	0.00	-0.01	0.09	0.00	0.02	0.07	-0.04						
IAI	-0.01	0.00	0.05	-0.04	-0.01	0.08	0.04	-0.02	0.04					
ARI	0.01	0.02	0.01	-0.03	0.07	0.02	0.02	-0.03	-0.00	-0.01				
MFP	0.00	0.01	0.00	0.03	0.04	0.04	0.02	0.02	-0.02	0.03	0.02			
LFP	0.02	0.00	-0.01	-0.00	0.05	0.03	-0.01	0.01	-0.03	0.00	0.03	0.03		
SFP	0.01	0.01	0.00	0.03	0.06	0.03	0.01	0.02	-0.03	0.02	0.03	0.03	0.03	
IFP	0.02	0.03	0.02	0.04	0.10	0.05	0.04	0.03	-0.01	0.05	0.09	0.02	0.06	0.04

Axis 21:

	MAN	LAT	HEA	IAM	LCR	SCR	IAR	SAR	MAH	IAI	ARI	MFP	LFP	SFP	IFP
MAN															
LAT	-0.07														
HEA	-0.00	0.06													
IAM	-0.01	0.04	0.04												
LCR	0.00	-0.04	0.01	-0.07											
SCR	0.01	0.00	0.04	-0.03	0.00										
IAR	-0.03	-0.05	0.03	-0.00	-0.04	0.06									
SAR	0.01	0.06	-0.00	0.04	0.01	0.03	0.05								
MAH	-0.00	0.00	-0.03	-0.01	-0.00	0.03	-0.00	-0.05							
IAI	-0.04	-0.04	0.04	-0.06	-0.03	0.08	-0.03	0.05	0.02						
ARI	-0.00	-0.00	0.03	0.00	0.04	0.03	0.03	0.03	0.02	0.03					
MFP	0.03	0.01	0.00	-0.01	0.02	0.02	0.01	-0.01	-0.00	-0.01	-0.01				
LFP	0.02	0.03	0.02	0.01	0.02	0.03	0.01	0.01	0.01	-0.02	-0.01	-0.00			
SFP	0.03	0.02	0.01	0.01	0.06	0.05	0.02	0.00	0.01	-0.00	0.05	0.09	-0.02		
IFP	0.06	0.04	0.02	0.03	0.09	0.04	0.04	0.02	0.02	0.02	0.07	0.01	0.03	0.05	

Axis 22:

	MAN	LAT	HEA	IAM	LCR	SCR	IAR	SAR	MAH	IAI	ARI	MFP	LFP	SFP	IFP
MAN															
LAT	-0.02														
HEA	0.03	0.04													
IAM	0.03	0.03	-0.02												
LCR	0.02	0.02	0.02	0.02											
SCR	0.00	0.03	-0.01	-0.01	-0.02										
IAR	0.02	-0.00	-0.03	0.08	0.07	0.06									
SAR	0.03	0.07	-0.00	-0.01	0.03	-0.02	-0.02								
MAH	0.02	0.09	0.00	0.04	0.02	-0.01	0.04	-0.00							
IAI	0.01	-0.00	0.01	0.06	0.02	-0.00	0.08	0.02	0.02						
ARI	0.02	0.00	0.02	0.01	0.10	-0.01	0.06	0.02	0.02	0.02					
MFP	0.04	0.04	0.05	0.00	0.04	0.01	0.05	0.06	0.04	0.05	0.02				
LFP	0.06	0.02	0.03	-0.01	0.05	-0.00	0.02	0.04	0.03	0.03	0.02	0.02			
SFP	0.05	0.02	0.04	-0.02	0.03	-0.01	0.02	0.04	0.03	0.02	0.01	0.04	0.04		

IFP	0.05	0.02	0.04	-0.01	0.05	0.00	0.03	0.04	0.03	0.04	0.03	0.03	0.01	0.06	

Axis 23:

	MAN	LAT	HEA	IAM	LCR	SCR	IAR	SAR	MAH	IAI	ARI	MFP	LFP	SFP	IFP
MAN															
LAT	-0.02														
HEA	-0.01	-0.04													
IAM	-0.02	0.01	-0.01												
LCR	0.02	0.02	0.00	0.00											
SCR	0.01	0.02	0.00	0.04	-0.02										
IAR	-0.01	0.04	0.02	-0.04	-0.02	0.01									
SAR	-0.01	0.00	-0.03	-0.03	-0.02	0.00	-0.02								
MAH	-0.01	-0.03	-0.03	-0.04	-0.02	-0.01	-0.03	-0.01							
IAI	-0.01	0.04	0.01	-0.03	-0.03	0.01	-0.01	-0.01	-0.02						
ARI	0.03	0.06	0.02	0.05	0.03	-0.04	0.01	-0.01	-0.02	-0.00					
MFP	0.01	0.06	0.04	0.04	0.02	0.00	0.04	0.01	0.01	0.03	0.01				
LFP	0.00	0.05	0.02	0.00	0.01	-0.00	0.00	0.00	0.00	0.01	0.02	0.01			
SFP	0.00	0.05	0.03	0.01	0.01	-0.00	0.01	-0.01	-0.00	0.01	0.01	0.00	-0.01		
IFP	-0.00	0.04	0.02	-0.01	-0.03	-0.03	-0.01	-0.01	-0.01	-0.01	-0.05	-0.03	0.02	-0.02	

Axis 24:

	MAN	LAT	HEA	IAM	LCR	SCR	IAR	SAR	MAH	IAI	ARI	MFP	LFP	SFP	IFP
MAN															
LAT	-0.01														
HEA	0.01	0.03													
IAM	0.02	0.00	0.02												
LCR	0.05	-0.01	-0.01	0.01											
SCR	0.02	-0.01	-0.03	0.01	-0.03										
IAR	0.03	0.03	0.02	-0.00	0.03	-0.01									
SAR	0.03	0.05	-0.06	0.06	0.01	-0.01	0.05								
MAH	0.02	0.03	0.01	0.03	-0.01	-0.02	0.02	0.02							
IAI	0.01	-0.01	0.01	-0.00	-0.02	0.03	0.04	0.03	0.03						
ARI	0.02	-0.02	-0.01	0.02	0.04	0.03	0.03	0.01	0.02	0.00					
MFP	0.03	0.00	-0.00	0.05	0.02	0.02	0.04	0.01	0.04	0.01	0.01				
LFP	0.01	-0.03	-0.02	0.01	-0.00	-0.00	0.00	-0.00	0.03	-0.03	-0.05	-0.00			
SFP	0.04	-0.00	-0.01	0.04	0.03	0.01	0.04	0.01	0.04	0.00	0.01	-0.01	0.03		
IFP	0.04	-0.02	-0.02	0.02	0.01	-0.00	0.01	-0.00	0.03	-0.02	-0.02	-0.01	-0.00	-0.05	

Axis 25:

	MAN	LAT	HEA	IAM	LCR	SCR	IAR	SAR	MAH	IAI	ARI	MFP	LFP	SFP	IFP
MAN															
LAT	0.00														
HEA	0.02	0.03													
IAM	0.04	-0.00	-0.01												
LCR	0.05	-0.02	0.01	-0.01											
SCR	0.06	-0.00	-0.03	0.01	0.04										
IAR	0.06	0.03	-0.02	-0.04	0.02	-0.04									
SAR	0.03	0.01	-0.01	-0.01	0.03	0.01	-0.00								

MAH	0.03	0.01	-0.02	0.03	0.03	0.02	0.01	0.01						
IAI	0.04	-0.01	0.00	-0.04	0.00	-0.00	0.00	0.03	0.04					
ARI	0.04	-0.02	0.01	-0.00	0.04	0.06	0.02	0.04	0.04	0.02				
MFP	0.01	-0.01	0.01	0.02	0.02	0.05	-0.00	0.04	0.03	0.01	0.02			
LFP	0.01	-0.02	-0.00	0.02	0.05	0.04	0.02	0.01	0.01	0.02	0.06	0.03		
SFP	0.03	-0.01	-0.00	0.02	0.04	0.03	-0.00	0.02	0.01	0.02	0.04	0.05	0.04	
IFP	0.00	-0.03	-0.01	0.00	0.01	0.03	-0.01	0.01	0.01	-0.00	0.01	0.02	-0.03	0.03

Axis 26:

	MAN	LAT	HEA	IAM	LCR	SCR	IAR	SAR	MAH	IAI	ARI	MFP	LFP	SFP	IFP
MAN															
LAT	0.02														
HEA	0.08	0.13													
IAM	0.07	0.06	0.03												
LCR	0.11	0.01	0.02	-0.07											
SCR	0.10	0.06	-0.00	0.02	0.02										
IAR	0.08	0.05	0.02	-0.06	-0.06	0.00									
SAR	0.10	0.11	0.00	0.04	0.04	0.02	0.05								
MAH	0.09	0.09	-0.06	0.07	0.04	0.04	0.05	-0.04							
IAI	0.06	0.04	0.07	-0.06	-0.06	0.07	-0.03	0.10	0.10						
ARI	0.07	0.03	0.05	0.01	0.14	0.10	0.03	0.09	0.09	0.04					
MFP	0.04	0.04	0.04	0.05	0.06	0.09	0.04	0.08	0.07	0.03	0.02				
LFP	0.04	0.05	0.05	0.08	0.13	0.10	0.08	0.09	0.08	0.06	0.09	0.06			
SFP	0.05	0.04	0.03	0.06	0.08	0.08	0.05	0.08	0.07	0.04	0.04	0.10	0.04		
IFP	0.05	0.03	0.03	0.05	0.10	0.09	0.05	0.08	0.07	0.04	0.05	0.06	0.02	-0.01	

4.2 - 15-landmark trial correlations between SCALED distances and axis scores:

Axis 1:

	MAN	LAT	HEA	IAM	LCR	SCR	IAR	SAR	MAH	IAI	ARI	MFP	LFP	SFP	IFP
MAN															
LAT	0.56														
HEA	0.72	0.13													
IAM	0.56	0.32	0.60												
LCR	0.27	-0.45	0.01	-0.61											
SCR	0.52	-0.72	-0.67	-0.65	0.36										
IAR	0.43	-0.02	0.57	-0.06	-0.59	-0.65									
SAR	0.68	-0.00	-0.17	0.51	0.16	-0.63	0.52								
MAH	0.67	-0.63	-0.76	0.33	0.77	0.67	0.51	-0.73							
IAI	0.46	-0.69	0.12	-0.66	-0.06	0.00	-0.75	0.24	0.63						
ARI	0.30	-0.54	-0.05	-0.61	0.44	0.39	-0.60	0.09	0.76	-0.04					
MFP	0.42	-0.47	-0.20	-0.21	0.41	0.59	-0.20	-0.07	0.67	0.32	0.20				
LFP	0.32	-0.48	-0.00	0.11	0.22	0.57	0.02	0.09	0.52	0.25	0.02	0.25			
SFP	0.33	-0.62	-0.20	-0.22	0.18	0.46	-0.29	-0.10	0.49	0.16	-0.09	0.23	0.17		
IFP	0.29	-0.58	-0.19	-0.28	0.05	0.50	-0.38	-0.08	0.61	0.08	-0.17	0.25	0.15	0.20	

Axis 2:

	MAN	LAT	HEA	IAM	LCR	SCR	IAR	SAR	MAH	IAI	ARI	MFP	LFP	SFP	IFP
MAN															
LAT	-0.13														
HEA	-0.34	-0.04													
IAM	-0.43	-0.19	-0.44												
LCR	-0.47	0.55	0.15	0.61											
SCR	-0.53	0.31	-0.01	0.35	0.16										
IAR	-0.53	-0.37	-0.45	-0.11	0.50	0.57									
SAR	-0.46	-0.06	0.21	-0.61	-0.16	-0.37	-0.51								
MAH	-0.61	-0.39	-0.32	-0.74	-0.17	0.12	-0.53	-0.52							
IAI	-0.45	-0.04	-0.54	0.23	0.69	0.52	0.10	-0.64	-0.59						
ARI	-0.54	0.50	0.10	0.59	-0.47	0.30	0.53	-0.12	-0.12	0.69					
MFP	-0.17	0.52	-0.07	0.52	0.40	0.12	0.59	-0.07	-0.06	0.58	0.58				
LFP	-0.18	0.61	0.11	0.52	0.41	0.32	0.52	0.23	0.03	0.54	0.53	0.29			
SFP	-0.30	0.35	-0.11	0.37	0.27	0.23	0.41	-0.01	-0.04	0.43	0.47	0.48	-0.09		
IFP	-0.16	0.57	-0.01	0.59	0.49	0.24	0.66	0.05	-0.04	0.65	0.59	0.31	-0.02	-0.09	

Axis 3:

	MAN	LAT	HEA	IAM	LCR	SCR	IAR	SAR	MAH	IAI	ARI	MFP	LFP	SFP	IFP
MAN															
LAT	-0.02														
HEA	-0.06	-0.26													
IAM	-0.25	0.05	0.32												
LCR	-0.63	-0.21	0.61	-0.20											
SCR	-0.41	-0.19	0.45	-0.13	0.67										
IAR	-0.15	0.13	0.38	0.08	-0.05	-0.22									
SAR	-0.19	-0.20	0.60	0.02	0.32	-0.02	0.03								
MAH	-0.12	0.01	0.48	0.08	0.33	-0.24	0.08	0.20							
IAI	-0.30	-0.36	0.27	-0.50	0.37	0.16	-0.41	-0.06	0.11						
ARI	-0.60	-0.20	0.63	-0.22	-0.32	0.62	-0.06	0.37	0.38	0.42					
MFP	-0.70	-0.32	0.43	-0.29	-0.40	0.36	-0.34	0.29	0.31	0.08	-0.25				
LFP	-0.64	-0.11	0.47	-0.01	-0.45	0.52	0.10	0.45	0.52	0.34	-0.28	0.06			
SFP	-0.69	-0.26	0.46	-0.21	-0.49	0.49	-0.18	0.40	0.46	0.26	-0.28	0.14	-0.07		
IFP	-0.73	-0.19	0.56	-0.11	-0.30	0.56	-0.05	0.49	0.52	0.35	-0.11	0.17	-0.18	-0.09	

Axis 4:

	MAN	LAT	HEA	IAM	LCR	SCR	IAR	SAR	MAH	IAI	ARI	MFP	LFP	SFP	IFP
MAN															
LAT	0.37														
HEA	0.11	-0.36													
IAM	0.38	0.09	-0.34												
LCR	0.25	0.04	-0.42	0.01											
SCR	0.28	0.04	-0.03	0.02	-0.17										
IAR	0.46	0.31	-0.45	0.68	0.01	-0.08									
SAR	0.14	-0.38	0.02	-0.41	-0.50	-0.07	-0.56								
MAH	0.14	-0.22	-0.01	-0.35	-0.24	-0.09	-0.56	-0.01							
IAI	0.47	-0.12	-0.62	0.03	0.30	-0.02	-0.23	-0.58	-0.37						
ARI	0.28	0.01	-0.47	-0.02	0.17	-0.18	-0.01	-0.52	-0.26	0.28					

MFP	0.26	-0.06	-0.16	-0.08	-0.02	0.16	0.00	-0.07	0.10	0.26	-0.13			
LFP	0.32	0.11	-0.07	0.07	0.09	0.14	0.25	0.05	0.13	0.36	-0.04	-0.27		
SFP	0.26	0.02	-0.06	0.02	0.08	0.26	0.19	0.09	0.21	0.42	-0.06	-0.09	-0.37	
IFP	0.23	-0.10	-0.25	-0.13	0.00	0.16	0.00	-0.12	0.09	0.27	-0.12	0.15	-0.54	-0.29

Axis 5:

	MAN	LAT	HEA	IAM	LCR	SCR	IAR	SAR	MAH	IAI	ARI	MFP	LFP	SFP	IFP
MAN															
LAT	-0.37														
HEA	0.07	0.56													
IAM	-0.14	-0.16	0.06												
LCR	-0.21	-0.10	0.27	0.13											
SCR	-0.18	-0.00	-0.19	0.06	0.18										
IAR	-0.13	0.16	0.18	0.02	0.02	-0.08									
SAR	-0.03	0.22	-0.41	-0.04	0.31	0.03	0.11								
MAH	-0.04	0.25	-0.09	-0.00	0.11	-0.23	0.05	0.14							
IAI	-0.18	-0.04	0.12	0.02	0.10	0.08	-0.07	0.15	0.07						
ARI	-0.23	-0.07	0.32	0.21	0.07	0.34	0.10	0.41	0.20	0.19					
MFP	-0.18	-0.13	0.06	0.17	0.36	0.57	0.09	0.37	0.28	0.15	0.24				
LFP	-0.04	-0.02	0.29	0.21	0.23	0.27	0.19	0.41	0.29	0.11	0.07	-0.65			
SFP	-0.20	-0.09	0.21	0.21	0.29	0.50	0.20	0.45	0.38	0.18	0.18	-0.42	-0.70		
IFP	-0.10	-0.21	0.06	0.08	0.25	0.31	-0.03	0.27	0.19	-0.01	0.07	-0.63	-0.55	-0.70	

Axis 6:

	MAN	LAT	HEA	IAM	LCR	SCR	IAR	SAR	MAH	IAI	ARI	MFP	LFP	SFP	IFP
MAN															
LAT	-0.02														
HEA	0.11	0.16													
IAM	0.29	0.54	0.24												
LCR	-0.05	0.04	0.18	-0.15											
SCR	-0.07	-0.00	-0.05	-0.48	-0.01										
IAR	0.06	0.20	0.06	0.60	0.10	-0.08									
SAR	0.10	0.37	0.19	0.12	0.06	-0.27	0.01								
MAH	0.02	0.10	-0.03	-0.11	0.07	-0.05	-0.02	-0.20							
IAI	-0.05	0.20	0.25	0.10	-0.15	-0.18	0.20	0.13	0.15						
ARI	-0.09	0.06	0.22	-0.14	-0.26	0.04	0.07	0.08	0.11	-0.18					
MFP	-0.21	0.02	0.16	-0.39	-0.18	0.13	-0.17	-0.06	0.11	-0.27	-0.03				
LFP	-0.27	0.03	0.24	-0.07	-0.18	0.13	-0.13	0.08	0.15	-0.21	-0.02	0.02			
SFP	-0.23	-0.00	0.18	-0.33	-0.27	0.11	-0.25	-0.02	0.12	-0.32	-0.08	-0.03	0.04		
IFP	-0.27	-0.10	0.08	-0.41	-0.39	-0.02	-0.37	-0.16	0.01	-0.46	-0.22	-0.15	0.05	-0.16	

Axis 7:

	MAN	LAT	HEA	IAM	LCR	SCR	IAR	SAR	MAH	IAI	ARI	MFP	LFP	SFP	IFP
MAN															
LAT	-0.27														
HEA	-0.21	0.15													
IAM	-0.23	0.05	0.10												
LCR	-0.11	-0.09	-0.22	-0.04											

SCR	-0.21	-0.14	-0.41	-0.06	-0.04									
IAR	-0.36	-0.17	0.04	0.34	-0.15	-0.03								
SAR	-0.28	-0.25	-0.49	0.12	0.02	0.03	0.14							
MAH	-0.21	-0.07	-0.17	0.23	-0.03	-0.14	0.12	0.13						
IAI	-0.31	-0.10	-0.13	0.22	-0.09	-0.09	-0.09	0.08	0.04					
ARI	-0.14	-0.11	-0.20	-0.04	-0.12	-0.06	-0.15	0.04	-0.02	-0.07				
MFP	-0.13	0.01	-0.12	-0.02	0.15	-0.10	0.00	0.14	0.04	0.12	0.24			
LFP	-0.23	-0.07	-0.08	-0.00	0.28	0.08	-0.04	0.08	0.12	0.17	0.40	0.41		
SFP	-0.22	-0.11	-0.17	-0.09	0.20	-0.02	-0.11	0.05	0.05	0.10	0.29	0.44	0.16	
IFP	-0.22	-0.02	-0.08	-0.03	0.18	0.01	-0.04	0.16	0.11	0.13	0.27	0.38	0.34	0.29

Axis 8:

	MAN	LAT	HEA	IAM	LCR	SCR	IAR	SAR	MAH	IAI	ARI	MFP	LFP	SFP	IFP
MAN															
LAT	0.13														
HEA	-0.00	-0.26													
IAM	0.12	0.08	-0.07												
LCR	-0.13	-0.13	-0.01	-0.09											
SCR	-0.10	-0.22	0.01	-0.22	0.06										
IAR	0.16	-0.17	-0.16	-0.09	0.22	-0.06									
SAR	-0.01	-0.35	-0.18	-0.14	0.21	0.19	-0.12								
MAH	0.03	-0.16	0.01	-0.20	0.15	0.07	-0.07	0.09							
IAI	0.07	-0.20	-0.10	-0.23	0.16	-0.20	0.18	0.01	-0.02						
ARI	-0.13	0.00	0.16	0.02	0.35	0.12	0.34	0.37	0.23	0.31					
MFP	-0.22	-0.05	0.22	-0.17	-0.11	0.16	-0.00	0.35	0.23	0.03	-0.32				
LFP	-0.27	0.05	0.24	-0.05	-0.11	0.22	0.12	0.33	0.27	0.16	-0.31	0.12			
SFP	-0.19	-0.01	0.21	-0.15	-0.10	0.18	0.01	0.32	0.24	0.10	-0.32	0.07	0.17		
IFP	-0.26	-0.01	0.24	-0.12	-0.08	0.22	0.09	0.38	0.30	0.13	-0.31	0.19	0.00	0.11	

Axis 9:

	MAN	LAT	HEA	IAM	LCR	SCR	IAR	SAR	MAH	IAI	ARI	MFP	LFP	SFP	IFP
MAN															
LAT	-0.09														
HEA	0.26	0.27													
IAM	0.19	-0.26	-0.08												
LCR	0.20	-0.38	-0.37	-0.18											
SCR	0.15	0.08	-0.04	0.05	-0.38										
IAR	0.13	-0.23	-0.07	-0.10	-0.31	0.00									
SAR	0.13	0.14	0.06	-0.24	-0.56	-0.09	-0.17								
MAH	0.13	0.09	-0.15	-0.13	-0.19	0.16	-0.12	-0.13							
IAI	0.22	-0.21	-0.20	-0.08	-0.20	-0.08	-0.15	-0.28	-0.09						
ARI	0.12	-0.35	-0.21	-0.12	-0.26	-0.27	-0.23	-0.38	-0.09	-0.08					
MFP	-0.03	0.27	0.60	0.31	-0.05	0.03	0.34	0.60	0.42	0.43	0.10				
LFP	-0.30	0.05	0.51	0.13	-0.42	-0.01	0.13	0.43	0.33	0.19	-0.32	0.25			
SFP	-0.13	0.23	0.59	0.28	-0.44	-0.04	0.30	0.54	0.39	0.34	-0.27	-0.14	0.33		
IFP	-0.15	0.09	0.52	0.17	-0.32	-0.13	0.15	0.42	0.30	0.23	-0.18	-0.09	0.24	-0.33	

Axis 10:

	MAN	LAT	HEA	IAM	LCR	SCR	IAR	SAR	MAH	IAI	ARI	MFP	LFP	SFP	IFP
MAN															
LAT	0.10														
HEA	-0.18	-0.44													
IAM	0.01	-0.06	-0.03												
LCR	-0.12	-0.12	-0.09	-0.03											
SCR	-0.14	-0.29	0.02	-0.15	-0.03										
IAR	-0.18	-0.26	0.10	0.02	-0.26	-0.19									
SAR	-0.13	-0.37	0.08	-0.01	-0.06	-0.04	0.17								
MAH	-0.05	-0.36	-0.00	-0.12	0.06	0.10	-0.04	-0.07							
IAI	-0.10	0.04	0.17	0.25	-0.26	-0.45	-0.05	0.15	0.02						
ARI	-0.08	-0.06	-0.05	0.05	0.06	-0.12	-0.21	-0.02	0.04	-0.22					
MFP	-0.06	0.14	0.30	0.28	0.15	0.06	0.21	0.35	0.21	0.14	0.13				
LFP	-0.00	0.38	0.30	0.59	0.05	-0.05	0.42	0.33	0.16	0.28	0.09	-0.24			
SFP	-0.01	0.24	0.29	0.48	0.06	-0.08	0.35	0.30	0.13	0.22	0.08	-0.32	0.06		
IFP	-0.06	0.24	0.32	0.37	-0.02	-0.08	0.22	0.33	0.16	0.11	-0.01	-0.27	-0.05	0.19	

Axis 11:

	MAN	LAT	HEA	IAM	LCR	SCR	IAR	SAR	MAH	IAI	ARI	MFP	LFP	SFP	IFP
MAN															
LAT	-0.20														
HEA	-0.25	-0.13													
IAM	-0.11	0.60	0.12												
LCR	0.14	0.42	0.05	-0.14											
SCR	-0.01	0.19	-0.09	-0.28	-0.16										
IAR	-0.16	0.39	-0.06	0.12	0.14	0.04									
SAR	-0.22	0.06	-0.09	-0.05	-0.05	-0.17	-0.11								
MAH	-0.21	0.08	0.05	-0.19	-0.18	-0.28	-0.07	0.08							
IAI	-0.15	0.30	-0.08	-0.18	0.10	0.06	0.02	-0.08	-0.11						
ARI	0.07	0.40	0.07	-0.16	-0.10	-0.06	0.16	-0.01	-0.14	0.13					
MFP	0.16	0.39	0.26	-0.06	0.07	-0.12	0.36	0.15	0.03	0.28	0.13				
LFP	0.11	0.35	0.21	0.07	0.09	-0.20	0.31	0.09	0.00	0.14	0.08	-0.07			
SFP	0.12	0.37	0.23	0.00	0.04	-0.25	0.39	0.09	-0.02	0.21	0.09	-0.26	0.11		
IFP	0.11	0.28	0.19	-0.15	-0.17	-0.29	0.20	0.01	-0.09	0.04	-0.16	-0.14	0.02	0.06	

Axis 12:

	MAN	LAT	HEA	IAM	LCR	SCR	IAR	SAR	MAH	IAI	ARI	MFP	LFP	SFP	IFP
MAN															
LAT	-0.17														
HEA	-0.12	0.17													
IAM	-0.09	-0.06	-0.19												
LCR	-0.16	-0.02	-0.25	0.03											
SCR	-0.14	0.14	-0.14	0.08	0.12										
IAR	-0.08	0.50	-0.05	0.02	-0.19	-0.14									
SAR	-0.11	0.48	0.10	-0.03	-0.24	-0.25	0.01								
MAH	-0.09	0.36	0.06	0.05	-0.09	-0.18	0.04	-0.04							
IAI	-0.12	0.27	-0.09	0.01	-0.14	-0.03	-0.06	-0.04	0.03						
ARI	-0.08	0.16	-0.12	0.18	0.36	0.03	-0.09	-0.18	-0.08	-0.04					
MFP	-0.04	0.30	0.10	0.35	0.17	0.11	-0.01	-0.17	-0.06	0.02	-0.06				

LFP	-0.05	0.20	0.06	0.37	0.02	0.13	0.03	-0.13	-0.05	-0.00	-0.06	0.16		
SFP	-0.05	0.26	0.07	0.36	-0.07	-0.02	-0.09	-0.20	-0.12	-0.11	-0.27	-0.14	0.31	
IFP	-0.11	0.19	0.06	0.31	-0.04	0.07	-0.09	-0.21	-0.09	-0.09	-0.20	0.07	0.08	0.05

Axis 13:

	MAN	LAT	HEA	IAM	LCR	SCR	IAR	SAR	MAH	IAI	ARI	MFP	LFP	SFP	IFP
MAN															
LAT	-0.34														
HEA	-0.25	-0.07													
IAM	-0.11	0.03	-0.09												
LCR	0.21	0.10	0.01	0.08											
SCR	0.13	0.04	-0.04	0.04	-0.03										
IAR	-0.13	0.02	-0.05	0.02	0.06	0.03									
SAR	-0.15	0.07	0.10	-0.03	-0.01	-0.15	-0.00								
MAH	-0.10	-0.07	-0.09	0.02	0.12	0.13	0.12	-0.14							
IAI	-0.15	0.17	0.18	0.10	-0.12	-0.12	0.12	0.10	0.14						
ARI	0.19	0.10	-0.00	0.12	0.12	-0.03	0.08	-0.03	0.12	-0.07					
MFP	0.09	0.03	0.10	0.03	-0.25	-0.12	0.05	0.01	0.19	0.06	-0.31				
LFP	-0.06	0.13	0.19	0.13	-0.18	-0.06	0.18	0.15	0.24	0.21	-0.25	0.00			
SFP	-0.04	0.02	0.10	0.04	-0.22	-0.02	0.11	0.06	0.23	0.19	-0.29	0.22	-0.14		
IFP	-0.01	-0.04	0.05	-0.07	-0.40	-0.13	-0.06	-0.01	0.17	-0.02	-0.45	0.22	-0.25	-0.08	

Axis 14:

	MAN	LAT	HEA	IAM	LCR	SCR	IAR	SAR	MAH	IAI	ARI	MFP	LFP	SFP	IFP
MAN															
LAT	-0.02														
HEA	0.09	0.08													
IAM	-0.15	-0.18	0.21												
LCR	0.06	-0.13	-0.06	-0.10											
SCR	-0.08	-0.29	-0.26	-0.06	-0.18										
IAR	0.08	-0.18	0.00	-0.06	0.08	-0.16									
SAR	0.10	0.12	0.06	0.24	-0.03	-0.40	0.00								
MAH	-0.02	-0.04	0.08	0.03	-0.18	-0.44	-0.12	-0.02							
IAI	0.06	-0.10	0.05	-0.02	-0.08	-0.46	0.16	0.02	-0.11						
ARI	0.05	-0.13	-0.03	-0.06	0.05	-0.11	0.12	-0.01	-0.15	-0.02					
MFP	0.00	-0.12	-0.06	0.12	0.06	0.09	0.13	-0.01	0.04	0.06	0.02				
LFP	0.09	0.03	0.09	0.23	0.24	0.09	0.33	0.17	0.15	0.25	0.20	-0.06			
SFP	0.01	-0.13	-0.06	0.13	0.08	0.07	0.14	0.02	0.08	0.09	0.02	0.03	-0.10		
IFP	-0.00	-0.10	0.02	0.13	0.10	0.11	0.21	0.10	0.11	0.12	0.03	0.08	-0.18	0.11	

Axis 15:

	MAN	LAT	HEA	IAM	LCR	SCR	IAR	SAR	MAH	IAI	ARI	MFP	LFP	SFP	IFP
MAN															
LAT	-0.04														
HEA	-0.01	0.04													
IAM	-0.06	-0.16	-0.03												
LCR	0.09	0.13	0.18	0.28											
SCR	0.06	-0.12	-0.15	0.11	-0.05										

IAR	0.03	0.19	0.12	0.05	0.18	-0.10								
SAR	-0.00	-0.03	-0.07	0.01	0.16	-0.13	0.05							
MAH	-0.01	-0.10	-0.08	-0.02	0.10	-0.05	-0.00	-0.03						
IAI	0.05	0.05	0.02	0.08	0.15	-0.28	0.06	0.00	-0.01					
ARI	0.10	0.12	0.12	0.25	-0.07	-0.10	0.13	0.10	0.07	0.11				
MFP	-0.06	-0.08	-0.07	-0.07	-0.32	-0.01	-0.25	-0.04	0.01	-0.13	-0.27			
LFP	-0.09	-0.00	0.00	-0.21	-0.18	-0.04	-0.26	0.01	0.02	-0.05	-0.14	-0.09		
SFP	-0.06	0.02	0.01	-0.09	-0.23	-0.03	-0.22	0.03	0.04	-0.05	-0.18	-0.19	0.03	
IFP	-0.05	0.13	0.15	0.05	-0.16	0.05	-0.05	0.18	0.14	0.09	-0.09	-0.09	0.18	0.22

Axis 16:

	MAN	LAT	HEA	IAM	LCR	SCR	IAR	SAR	MAH	IAI	ARI	MFP	LFP	SFP	IFP
MAN															
LAT	-0.20														
HEA	-0.16	0.08													
IAM	-0.06	-0.11	-0.05												
LCR	-0.05	-0.10	0.04	0.02											
SCR	-0.12	-0.15	-0.01	-0.11	0.00										
IAR	0.01	0.06	-0.02	0.05	0.06	-0.21									
SAR	-0.14	-0.12	-0.08	-0.07	0.17	0.16	-0.07								
MAH	-0.03	0.00	0.01	0.04	0.14	0.09	0.01	0.10							
IAI	-0.07	-0.10	-0.00	-0.11	0.06	-0.13	-0.03	0.07	0.11						
ARI	0.02	-0.11	-0.04	-0.02	-0.00	-0.12	-0.01	0.09	0.08	-0.03					
MFP	0.08	0.05	-0.09	0.09	0.04	-0.02	0.07	0.12	0.09	0.05	0.08				
LFP	0.11	-0.05	-0.26	0.04	-0.02	-0.13	0.04	-0.13	-0.05	-0.08	0.08	0.04			
SFP	0.15	0.15	-0.06	0.26	0.26	-0.00	0.29	0.11	0.10	0.19	0.31	-0.03	0.05		
IFP	0.13	0.02	-0.19	0.10	0.04	-0.07	0.11	-0.01	0.03	0.00	0.13	-0.07	0.13	-0.03	

Axis 17:

	MAN	LAT	HEA	IAM	LCR	SCR	IAR	SAR	MAH	IAI	ARI	MFP	LFP	SFP	IFP
MAN															
LAT	0.12														
HEA	0.09	-0.13													
IAM	-0.00	-0.12	-0.08												
LCR	-0.01	0.02	0.02	-0.02											
SCR	-0.07	0.06	0.10	0.06	-0.14										
IAR	0.11	0.08	-0.05	0.02	-0.03	-0.11									
SAR	0.12	0.03	-0.08	-0.03	0.05	0.08	-0.07								
MAH	0.02	0.02	0.03	-0.05	-0.03	0.03	-0.16	0.01							
IAI	0.01	0.11	0.09	-0.04	-0.13	-0.15	0.01	0.10	0.04						
ARI	-0.01	0.10	0.15	0.07	-0.08	-0.11	0.10	0.15	0.06	-0.00					
MFP	0.05	0.03	0.07	0.12	0.20	-0.07	0.20	-0.03	0.03	0.02	0.21				
LFP	-0.01	-0.08	0.02	-0.02	-0.02	-0.10	0.21	-0.08	0.01	-0.09	0.03	0.04			
SFP	-0.04	-0.17	-0.06	-0.12	-0.15	-0.17	-0.00	-0.19	-0.07	-0.27	-0.09	-0.03	0.03		
IFP	-0.00	-0.08	0.00	0.01	0.01	-0.13	0.15	-0.13	-0.02	-0.12	0.02	-0.07	-0.04	-0.03	

Axis 18:

	MAN	LAT	HEA	IAM	LCR	SCR	IAR	SAR	MAH	IAI	ARI	MFP	LFP	SFP	IFP

MAN														
LAT	-0.12													
HEA	-0.06	-0.01												
IAM	0.02	-0.03	0.02											
LCR	-0.07	-0.10	-0.06	0.04										
SCR	0.01	-0.02	-0.03	0.01	0.24									
IAR	-0.00	-0.01	0.01	0.02	0.09	0.11								
SAR	-0.07	-0.03	-0.06	-0.03	-0.02	0.01	0.02							
MAH	-0.05	-0.04	-0.01	-0.03	0.04	-0.01	0.11	0.04						
IAI	-0.04	0.01	-0.02	-0.00	0.01	0.08	0.12	-0.00	0.01					
ARI	-0.01	-0.13	-0.12	0.01	-0.03	0.15	0.03	-0.11	-0.02	-0.05				
MFP	0.18	0.09	0.07	0.17	0.19	0.19	0.18	0.10	0.08	0.21	0.20			
LFP	0.07	-0.05	0.00	-0.01	-0.26	0.04	-0.09	-0.06	-0.04	-0.05	-0.28	-0.03		
SFP	0.09	-0.09	-0.06	-0.01	-0.16	0.07	-0.09	-0.09	-0.05	-0.04	-0.17	0.04	-0.00	
IFP	0.10	-0.07	-0.03	-0.00	-0.19	0.07	-0.08	-0.07	-0.04	-0.04	-0.17	-0.07	-0.10	0.13

Axis 19:

	MAN	LAT	HEA	IAM	LCR	SCR	IAR	SAR	MAH	IAI	ARI	MFP	LFP	SFP	IFP
MAN															
LAT	-0.01														
HEA	-0.02	0.05													
IAM	-0.04	0.01	-0.08												
LCR	0.03	0.03	-0.14	-0.09											
SCR	0.02	0.07	0.03	0.02	-0.01										
IAR	-0.00	0.08	-0.08	-0.03	-0.14	-0.00									
SAR	0.03	-0.03	0.05	-0.07	-0.06	0.01	-0.06								
MAH	0.05	0.08	0.04	0.03	-0.05	-0.13	0.00	0.07							
IAI	-0.02	0.05	0.02	-0.07	-0.10	0.14	-0.08	0.03	0.06						
ARI	-0.03	0.01	-0.12	-0.04	0.02	0.18	-0.06	0.03	0.02	-0.01					
MFP	0.01	-0.05	-0.27	-0.01	-0.08	0.08	-0.04	0.05	-0.07	-0.06	-0.11				
LFP	0.07	0.07	-0.14	0.07	0.06	0.13	0.14	0.19	0.08	0.05	-0.09	-0.08			
SFP	0.01	-0.05	-0.26	-0.03	-0.12	0.08	-0.03	0.10	-0.01	-0.08	-0.19	0.01	-0.10		
IFP	0.11	0.08	-0.18	0.12	0.14	0.14	0.15	0.22	0.06	0.10	0.03	0.00	0.00	-0.02	

Axis 20:

	MAN	LAT	HEA	IAM	LCR	SCR	IAR	SAR	MAH	IAI	ARI	MFP	LFP	SFP	IFP
MAN															
LAT	0.04														
HEA	0.06	-0.02													
IAM	-0.11	0.02	0.14												
LCR	0.03	0.05	0.02	-0.00											
SCR	-0.01	0.00	-0.03	0.10	-0.09										
IAR	-0.01	0.01	0.06	-0.02	0.07	0.09									
SAR	-0.05	-0.11	0.08	-0.03	-0.13	-0.08	-0.09								
MAH	-0.02	-0.02	-0.02	0.13	-0.03	-0.01	0.09	-0.04							
IAI	-0.04	-0.01	0.05	-0.01	-0.05	0.04	0.09	-0.06	0.03						
ARI	0.01	-0.01	-0.03	-0.05	0.05	-0.04	0.03	-0.14	-0.05	-0.07					
MFP	-0.03	0.01	0.03	0.07	0.06	0.05	0.07	0.10	-0.03	0.09	0.04				
LFP	-0.03	-0.07	-0.03	-0.09	0.02	-0.02	-0.09	-0.01	-0.10	-0.03	-0.01	0.02			

SFP	-0.03	-0.03	-0.00	-0.01	0.00	-0.02	-0.02	0.04	-0.08	0.00	-0.04	-0.02	0.04		
IFP	-0.03	-0.01	0.03	0.02	0.08	0.03	0.04	0.06	-0.05	0.05	0.05	-0.03	0.04	0.01	

Axis 21:

	MAN	LAT	HEA	IAM	LCR	SCR	IAR	SAR	MAH	IAI	ARI	MFP	LFP	SFP	IFP
MAN															
LAT	-0.20														
HEA	-0.05	0.04													
IAM	-0.05	0.01	0.01												
LCR	-0.02	-0.09	-0.02	-0.07											
SCR	-0.05	-0.01	0.07	-0.02	-0.09										
IAR	-0.06	-0.13	-0.01	-0.01	-0.02	0.08									
SAR	-0.03	0.07	0.04	-0.02	-0.06	0.01	-0.01								
MAH	-0.06	-0.00	-0.01	-0.10	-0.07	0.02	-0.07	-0.04							
IAI	-0.11	-0.08	0.05	-0.05	-0.07	0.12	0.03	0.02	-0.01						
ARI	-0.03	-0.03	0.06	0.02	0.03	-0.02	0.07	0.02	-0.01	0.03					
MFP	0.01	0.03	0.04	-0.04	-0.02	-0.01	0.02	-0.03	-0.04	-0.06	-0.06				
LFP	-0.01	0.04	0.05	-0.06	-0.05	-0.01	-0.04	0.00	-0.02	-0.12	-0.10	-0.02			
SFP	0.01	0.03	0.03	-0.05	0.04	0.04	0.02	-0.02	-0.02	-0.08	0.02	0.11	-0.02		
IFP	0.06	0.09	0.08	0.02	0.12	0.03	0.10	0.03	-0.01	0.00	0.06	-0.03	0.03	0.04	

Axis 22:

	MAN	LAT	HEA	IAM	LCR	SCR	IAR	SAR	MAH	IAI	ARI	MFP	LFP	SFP	IFP
MAN															
LAT	0.01														
HEA	-0.03	-0.01													
IAM	-0.03	-0.01	0.06												
LCR	0.03	-0.01	-0.05	-0.03											
SCR	0.07	-0.01	0.02	0.03	0.04										
IAR	-0.00	0.07	0.09	-0.08	-0.08	-0.05									
SAR	-0.03	-0.02	-0.04	0.06	-0.06	0.03	0.06								
MAH	-0.02	-0.11	-0.04	-0.05	-0.02	0.07	-0.06	-0.03							
IAI	0.00	0.04	0.03	-0.07	-0.05	0.08	-0.07	0.01	0.00						
ARI	0.03	0.06	0.01	0.04	-0.04	0.03	-0.03	-0.02	-0.01	0.00					
MFP	0.02	0.01	-0.09	0.09	0.02	0.04	-0.01	-0.15	-0.04	-0.04	0.00				
LFP	-0.03	0.05	-0.03	0.11	-0.02	0.08	0.03	-0.08	-0.01	-0.03	-0.01	-0.00			
SFP	-0.01	0.03	-0.04	0.15	0.04	0.10	0.05	-0.10	-0.01	-0.00	0.05	0.00	-0.04		
IFP	0.00	0.03	-0.06	0.09	-0.03	0.04	-0.02	-0.13	-0.04	-0.06	-0.04	-0.01	0.00	-0.05	

Axis 23:

	MAN	LAT	HEA	IAM	LCR	SCR	IAR	SAR	MAH	IAI	ARI	MFP	LFP	SFP	IFP
MAN															
LAT	0.01														
HEA	-0.02	-0.02													
IAM	0.01	0.01	0.02												
LCR	0.01	0.01	-0.02	0.03											
SCR	-0.02	-0.02	-0.01	-0.00	-0.03										
IAR	0.03	0.01	0.01	0.02	0.07	0.00									

SAR	0.03	0.03	0.01	0.08	0.02	-0.04	0.05							
MAH	-0.01	0.01	0.04	0.04	-0.01	-0.02	0.02	-0.01						
IAI	-0.01	-0.04	-0.02	0.01	0.03	0.07	0.05	0.01	0.02					
ARI	-0.04	-0.04	-0.04	0.01	0.01	0.09	0.06	0.02	0.03	0.03				
MFP	-0.01	-0.06	-0.08	0.06	-0.03	-0.01	0.04	-0.03	0.07	-0.02	-0.01			
LFP	-0.03	-0.11	-0.09	0.02	-0.06	-0.04	-0.00	-0.05	0.05	-0.09	-0.13	0.00		
SFP	0.01	-0.06	-0.06	0.10	0.02	-0.02	0.09	-0.01	0.07	-0.02	0.00	-0.02	0.07	
IFP	0.02	-0.07	-0.08	0.07	0.04	0.00	0.07	-0.02	0.08	-0.02	0.01	0.03	-0.00	-0.03

Axis 24:

	MAN	LAT	HEA	IAM	LCR	SCR	IAR	SAR	MAH	IAI	ARI	MFP	LFP	SFP	IFP
MAN															
LAT	-0.04														
HEA	-0.02	-0.01													
IAM	0.01	-0.00	-0.05												
LCR	0.03	-0.04	-0.01	-0.01											
SCR	0.06	-0.01	-0.06	-0.00	0.04										
IAR	0.04	0.04	-0.06	-0.05	0.02	-0.05									
SAR	0.00	0.01	0.04	-0.06	0.01	-0.04	-0.05								
MAH	-0.01	0.00	0.02	-0.02	-0.01	-0.03	-0.05	0.02							
IAI	0.01	-0.01	-0.03	-0.04	-0.00	-0.05	0.01	-0.01	-0.00						
ARI	0.01	-0.03	0.01	-0.01	-0.01	0.07	0.03	0.05	0.02	0.03					
MFP	-0.04	-0.03	0.02	0.01	-0.02	0.05	-0.04	0.08	0.02	-0.01	0.01				
LFP	-0.04	-0.05	-0.03	0.02	0.06	0.05	-0.01	-0.02	-0.03	0.01	0.11	0.04			
SFP	-0.00	-0.02	-0.01	0.01	0.03	-0.01	-0.05	0.01	-0.03	-0.00	0.07	0.03	0.07		
IFP	-0.06	-0.07	-0.03	-0.04	-0.03	0.02	-0.08	-0.01	-0.03	-0.05	0.00	-0.01	-0.02	0.04	

Axis 25:

	MAN	LAT	HEA	IAM	LCR	SCR	IAR	SAR	MAH	IAI	ARI	MFP	LFP	SFP	IFP
MAN															
LAT	0.01														
HEA	0.01	0.01													
IAM	0.00	0.01	0.00												
LCR	0.01	-0.00	-0.03	-0.02											
SCR	-0.00	0.00	-0.00	-0.02	0.00										
IAR	0.00	-0.01	-0.05	0.00	0.01	-0.02									
SAR	-0.02	-0.00	0.05	-0.02	-0.04	-0.04	-0.04								
MAH	-0.01	-0.01	-0.04	0.00	0.03	0.10	-0.00	-0.07							
IAI	-0.00	0.02	-0.00	-0.01	-0.01	-0.07	0.02	-0.01	0.01						
ARI	0.01	-0.00	-0.01	-0.01	0.04	-0.01	0.02	-0.02	0.03	0.01					
MFP	0.01	-0.05	-0.05	-0.02	0.00	0.00	-0.04	-0.05	-0.05	-0.04	-0.02				
LFP	-0.00	0.00	0.04	0.08	-0.00	0.02	0.08	-0.00	-0.04	0.03	-0.01	-0.01			
SFP	-0.01	-0.03	0.00	0.03	-0.02	0.01	0.02	-0.02	-0.05	-0.00	-0.05	-0.02	0.02		
IFP	0.01	-0.00	0.02	0.06	0.04	0.05	0.07	0.00	-0.02	0.04	0.03	0.03	-0.04	0.03	

4.3 - 16-landmark trial non-scaled correlations between distances and axis scores:

Axis 1:

	MAN	LAT	HEA	ART	IAM	LCR	SCR	IAR	SAR	MAH	IAI	ARI	MFP	LFP	SFP
IFP															
MAN															
LAT	0.79														
HEA	0.90	0.33													
ART	0.83	0.74	0.98												
IAM	0.94	0.58	0.79	0.62											
LCR	0.43	0.89	0.95	0.79	0.69										
SCR	0.83	0.78	0.90	0.71	0.73	0.90									
IAR	0.72	0.58	0.85	-0.15	0.52	0.70	0.86								
SAR	0.86	0.31	0.71	0.92	0.66	0.91	0.84	0.60							
MAH	0.91	0.43	0.50	0.76	0.93	0.86	0.64	0.85	0.35						
IAI	0.79	0.72	0.95	0.11	0.21	0.92	0.92	0.13	0.86	0.84					
ARI	0.40	0.91	0.94	0.85	0.73	0.35	0.89	0.77	0.92	0.88	0.97				
MFP	0.46	0.97	0.96	0.97	0.86	0.63	0.92	0.95	0.97	0.98	0.93	0.62			
LFP	0.32	0.99	0.95	0.96	0.88	0.62	0.94	0.96	0.95	0.97	0.95	0.67	0.69		
SFP	0.38	0.95	0.92	0.99	0.91	0.65	0.95	0.99	0.94	0.98	0.98	0.70	0.79	0.52	
IFP	0.42	0.98	0.97	0.96	0.87	0.69	0.94	0.96	0.97	0.97	0.94	0.69	0.73	0.41	0.53

Axis 2:

	MAN	LAT	HEA	ART	IAM	LCR	SCR	IAR	SAR	MAH	IAI	ARI	MFP	LFP	SFP
IFP															
MAN															
LAT	0.51														
HEA	0.33	-0.32													
ART	0.35	-0.45	0.07												
IAM	0.02	0.07	0.48	0.68											
LCR	0.06	0.02	0.09	0.17	-0.27										
SCR	0.18	-0.56	-0.36	-0.63	-0.25	0.32									
IAR	-0.12	-0.40	0.50	0.85	-0.71	-0.44	-0.28								
SAR	0.35	-0.82	-0.21	0.19	0.65	0.20	-0.39	0.74							
MAH	0.32	-0.89	-0.77	-0.43	0.33	0.45	0.62	0.51	-0.89						
IAI	0.07	-0.58	0.14	0.49	-0.36	0.05	0.23	-0.88	0.42	0.51					
ARI	0.09	-0.11	-0.00	0.08	-0.26	0.49	0.31	-0.44	0.12	0.39	0.01				
MFP	0.48	-0.06	-0.20	0.11	0.27	0.75	0.26	0.21	-0.07	0.15	0.30	0.70			
LFP	0.57	-0.00	-0.14	0.16	0.33	0.75	0.25	0.21	-0.00	0.07	0.24	0.72	0.40		
SFP	0.49	-0.26	-0.30	-0.05	0.18	0.68	0.14	0.07	-0.15	-0.02	0.13	0.63	0.50	0.32	
IFP	0.54	0.03	-0.11	0.18	0.29	0.71	0.27	0.20	0.02	0.15	0.26	0.63	0.39	0.62	0.70

Axis 3:

	MAN	LAT	HEA	ART	IAM	LCR	SCR	IAR	SAR	MAH	IAI	ARI	MFP	LFP	SFP
IFP															
MAN															
LAT	0.08														
HEA	-0.03	-0.81													
ART	0.20	0.02	-0.16												
IAM	0.11	0.55	0.01	-0.19											
LCR	0.90	0.36	-0.23	-0.26	-0.29										

SCR	0.53	0.12	-0.21	0.09	0.08	-0.28									
IAR	0.38	0.55	-0.16	-0.11	0.26	-0.08	-0.12								
SAR	0.15	0.20	-0.15	-0.08	0.23	-0.24	-0.26	-0.15							
MAH	0.16	-0.01	-0.03	0.39	0.18	-0.21	-0.21	-0.03	0.00						
IAI	0.47	0.32	-0.24	-0.44	-0.31	-0.09	0.04	-0.23	-0.22	-0.07					
ARI	0.91	0.29	-0.30	-0.31	-0.28	0.69	-0.31	-0.10	-0.32	-0.26	-0.08				
MFP	0.74	0.09	-0.17	0.08	0.01	0.07	-0.25	0.10	-0.24	-0.15	0.11	-0.20			
LFP	0.73	0.02	-0.22	-0.04	-0.09	0.21	-0.20	0.04	-0.25	-0.16	0.03	-0.02	0.01		
SFP	0.77	0.03	-0.23	-0.02	-0.06	0.16	-0.26	0.06	-0.29	-0.19	0.05	-0.16	0.04	0.09	
IFP	0.72	0.02	-0.18	-0.01	-0.11	0.00	-0.17	0.03	-0.22	-0.12	0.03	-0.27	0.39	-0.26	0.40

Axis 4:

	MAN	LAT	HEA	ART	IAM	LCR	SCR	IAR	SAR	MAH	IAI	ARI	MFP	LFP	SFP
IFP															
MAN															
LAT	-0.22														
HEA	-0.16	0.36													
ART	-0.35	0.15	0.08												
IAM	-0.29	-0.58	-0.28	-0.03											
LCR	-0.01	-0.11	-0.19	-0.50	0.33										
SCR	0.04	0.24	-0.05	0.13	0.61	-0.00									
IAR	-0.53	-0.31	0.04	-0.22	-0.22	-0.55	0.41								
SAR	-0.24	-0.14	-0.21	0.34	-0.15	-0.22	0.10	0.24							
MAH	-0.16	-0.12	-0.34	-0.22	0.06	-0.06	0.38	0.10	-0.21						
IAI	-0.28	0.04	-0.11	-0.74	0.79	-0.33	0.27	-0.41	-0.11	-0.06					
ARI	-0.03	-0.06	-0.16	-0.43	0.40	-0.15	-0.06	-0.45	-0.19	-0.06	-0.21				
MFP	0.01	0.24	0.09	0.13	0.43	0.19	-0.12	0.14	0.06	0.04	0.18	0.28			
LFP	-0.17	0.15	0.11	0.09	0.25	0.05	0.01	0.02	0.05	0.03	0.13	0.16	0.37		
SFP	-0.12	0.19	0.09	0.11	0.36	0.05	-0.05	0.08	0.04	0.02	0.15	0.17	0.27	0.29	
IFP	-0.08	0.19	0.09	0.08	0.32	0.10	-0.06	0.03	0.04	0.02	0.12	0.19	0.21	0.43	0.00

Axis 5:

	MAN	LAT	HEA	ART	IAM	LCR	SCR	IAR	SAR	MAH	IAI	ARI	MFP	LFP	SFP
IFP															
MAN															
LAT	0.26														
HEA	0.23	-0.08													
ART	0.18	-0.47	0.04												
IAM	0.15	-0.11	0.26	-0.34											
LCR	0.02	-0.24	-0.08	-0.19	-0.50										
SCR	0.02	-0.12	0.08	0.26	-0.18	-0.04									
IAR	0.18	-0.32	-0.00	-0.43	-0.33	-0.15	-0.02								
SAR	0.24	0.42	0.62	0.08	0.26	-0.14	-0.26	0.00							
MAH	0.12	-0.05	0.19	0.18	-0.01	-0.13	-0.13	-0.10	-0.17						
IAI	0.26	-0.21	0.03	0.02	-0.34	-0.17	-0.12	0.02	-0.13	-0.13					
ARI	-0.06	-0.25	-0.04	-0.06	-0.40	-0.38	0.06	-0.08	-0.08	-0.07	-0.05				
MFP	-0.04	0.02	0.07	0.16	0.10	-0.09	0.02	0.12	0.05	0.04	0.07	0.05			
LFP	-0.11	0.07	0.13	0.19	0.20	-0.10	0.15	0.20	0.15	0.14	0.16	-0.04	0.47		
SFP	-0.07	-0.04	0.04	0.09	0.10	-0.28	0.03	0.08	0.05	0.05	0.03	-0.22	0.23	0.73	

IFP	-0.07	0.08	0.12	0.21	0.20	-0.04	0.12	0.21	0.13	0.11	0.16	0.08	0.34	0.44	0.27

4.4 - 16-landmark trial correlations between SCALED distances and axis scores:

Axis 1:

	MAN	LAT	HEA	ART	IAM	LCR	SCR	IAR	SAR	MAH	IAI	ARI	MFP	LFP	SFP
IFP															
MAN															
LAT	-0.80														
HEA	-0.70	0.13													
ART	-0.53	0.74	0.09												
IAM	0.10	-0.00	-0.67	-0.81											
LCR	0.08	0.12	-0.09	-0.23	0.40										
SCR	-0.10	0.74	0.93	0.52	0.46	-0.59									
IAR	0.29	0.56	-0.79	-0.75	0.86	0.59	0.53								
SAR	-0.62	0.35	0.41	-0.14	-0.87	-0.32	0.77	-0.91							
MAH	-0.70	0.91	0.92	0.76	-0.67	-0.65	-0.79	-0.83	0.96						
IAI	0.04	0.75	-0.15	-0.40	0.37	0.01	-0.32	0.87	-0.62	-0.70					
ARI	0.04	0.37	0.15	-0.12	0.43	-0.51	-0.56	0.69	-0.15	-0.56	0.21				
MFP	-0.50	0.36	0.79	-0.07	-0.36	-0.91	-0.47	-0.49	0.42	-0.12	-0.62	-0.82			
LFP	-0.59	0.54	0.58	-0.22	-0.62	-0.93	-0.52	-0.41	0.23	0.09	-0.33	-0.88	-0.48		
SFP	-0.49	0.67	0.83	0.79	-0.22	-0.83	-0.21	0.33	0.52	0.29	-0.03	-0.73	-0.73	-0.31	
IFP	-0.56	0.23	0.61	-0.40	-0.49	-0.93	-0.54	-0.50	0.21	-0.11	-0.47	-0.81	-0.41	-0.61	-0.81

Axis 2:

	MAN	LAT	HEA	ART	IAM	LCR	SCR	IAR	SAR	MAH	IAI	ARI	MFP	LFP	SFP
IFP															
MAN															
LAT	-0.06														
HEA	0.15	0.36													
ART	-0.31	-0.07	0.45												
IAM	-0.31	-0.63	0.13	0.35											
LCR	-0.99	-0.69	0.66	0.25	0.29										
SCR	-0.98	-0.28	0.35	-0.26	-0.17	0.73									
IAR	-0.53	-0.65	0.46	0.09	-0.29	0.05	0.03								
SAR	-0.25	-0.28	0.19	0.30	-0.21	0.59	0.36	0.31							
MAH	-0.31	-0.14	-0.05	-0.54	-0.29	0.52	0.37	0.25	-0.08						
IAI	-0.77	-0.47	0.67	0.16	0.20	0.23	-0.14	0.10	0.53	0.32					
ARI	-1.00	-0.59	0.77	0.34	0.30	-0.70	0.75	0.08	0.74	0.60	0.35				
MFP	-0.85	-0.33	0.43	-0.37	-0.02	-0.03	0.71	-0.37	0.69	0.57	-0.18	0.23			
LFP	-0.74	-0.13	0.55	0.32	0.30	-0.19	0.72	0.03	0.66	0.52	0.11	0.06	-0.02		
SFP	-0.82	-0.20	0.45	0.05	0.12	-0.14	0.85	-0.46	0.66	0.57	0.02	0.18	0.05	-0.16	
IFP	-0.78	-0.17	0.52	0.13	0.28	0.06	0.61	0.02	0.67	0.49	0.11	0.35	-0.49	0.19	-0.37

Axis 3:

	MAN	LAT	HEA	ART	IAM	LCR	SCR	IAR	SAR	MAH	IAI	ARI	MFP	LFP	SFP
IFP															

MAN														
LAT	-0.17													
HEA	-0.20	-0.82												
ART	-0.43	-0.17	0.86											
IAM	-0.71	-0.26	0.31	-0.03										
LCR	0.09	-0.60	0.03	-0.77	-0.41									
SCR	0.10	-0.44	-0.01	-0.68	-0.03	0.14								
IAR	-0.18	-0.32	0.36	-0.60	0.04	-0.35	-0.40							
SAR	-0.22	-0.81	0.39	0.77	0.10	-0.03	-0.22	0.14						
MAH	0.05	-0.40	0.04	0.14	0.65	0.30	0.07	0.39	-0.02					
IAI	-0.25	-0.40	0.49	-0.85	-0.16	-0.45	-0.65	-0.33	0.25	0.43				
ARI	0.04	-0.63	0.05	-0.78	-0.32	0.07	0.19	-0.28	0.06	0.37	-0.01			
MFP	-0.15	-0.51	0.41	-0.27	-0.04	-0.32	0.17	-0.05	0.58	0.78	0.61	-0.35		
LFP	-0.28	-0.03	0.59	0.79	0.30	-0.29	0.38	0.76	0.70	0.83	0.91	-0.40	0.08	
SFP	-0.30	-0.50	0.33	0.12	-0.09	-0.46	0.29	0.33	0.52	0.72	0.93	-0.58	0.47	-0.07
IFP	-0.28	-0.41	0.59	0.40	0.07	-0.32	0.40	0.47	0.70	0.84	0.82	-0.38	0.56	-0.36

Axis 4:

	MAN	LAT	HEA	ART	IAM	LCR	SCR	IAR	SAR	MAH	IAI	ARI	MFP	LFP	SFP
IFP															
MAN															
LAT	0.44														
HEA	0.50	-0.43													
ART	0.61	-0.26	0.10												
IAM	0.55	0.72	0.62	0.12											
LCR	-0.03	0.11	0.62	0.51	-0.52										
SCR	-0.10	-0.42	0.14	-0.30	-0.86	0.17									
IAR	0.75	0.27	0.11	0.10	0.23	0.68	-0.74								
SAR	0.57	-0.15	0.41	-0.55	0.31	0.59	-0.20	-0.23							
MAH	0.62	0.00	0.37	0.30	0.02	0.28	-0.45	-0.02	0.19						
IAI	0.41	-0.18	0.49	0.29	-0.86	0.74	-0.67	0.34	0.36	0.30					
ARI	-0.01	-0.02	0.53	0.51	-0.63	0.23	0.30	0.64	0.55	0.31	0.83				
MFP	-0.07	-0.70	-0.12	-0.61	-0.90	-0.27	0.46	-0.63	0.05	0.16	-0.45	-0.37			
LFP	0.14	-0.79	-0.09	-0.12	-0.55	-0.08	0.19	0.18	0.10	0.17	-0.12	-0.24	-0.56		
SFP	0.07	-0.51	-0.09	-0.52	-0.93	-0.12	0.36	-0.62	0.08	0.20	-0.33	-0.27	-0.37	-0.40	
IFP	0.03	-0.81	-0.09	-0.24	-0.72	-0.15	0.40	0.04	0.12	0.22	-0.17	-0.27	-0.23	-0.49	0.09

Axis 5:

	MAN	LAT	HEA	ART	IAM	LCR	SCR	IAR	SAR	MAH	IAI	ARI	MFP	LFP	SFP
IFP															
MAN															
LAT	-0.37														
HEA	-0.45	-0.07													
ART	-0.26	0.59	0.18												
IAM	-0.30	0.14	-0.23	0.45											
LCR	-0.08	0.36	0.40	0.20	0.56										
SCR	-0.07	0.03	-0.05	-0.32	0.15	0.26									
IAR	-0.20	0.30	0.17	0.24	0.35	0.24	-0.06								
SAR	-0.42	-0.34	-0.69	-0.01	-0.29	0.45	0.44	0.05							

MAH	-0.19	-0.01	-0.13	-0.19	0.21	0.37	0.20	0.31	0.19						
IAI	-0.42	0.13	0.20	-0.08	0.23	0.45	0.10	-0.02	0.38	0.37					
ARI	-0.00	0.35	0.31	0.09	0.48	0.44	0.07	0.18	0.36	0.30	0.38				
MFP	-0.04	-0.13	0.00	-0.64	-0.23	0.06	0.16	-0.47	0.13	0.17	-0.08	-0.10			
LFP	0.04	-0.26	-0.09	-0.46	-0.38	0.09	-0.18	-0.47	-0.09	-0.05	-0.19	-0.00	-0.67		
SFP	-0.01	-0.01	0.06	-0.31	-0.25	0.27	0.18	-0.43	0.11	0.16	0.12	0.17	-0.32	-0.85	
IFP	-0.01	-0.31	-0.10	-0.78	-0.40	0.02	-0.06	-0.73	-0.04	0.00	-0.26	-0.12	-0.46	-0.47	-0.29